Enhancing T cell function in highly glycolytic tumors

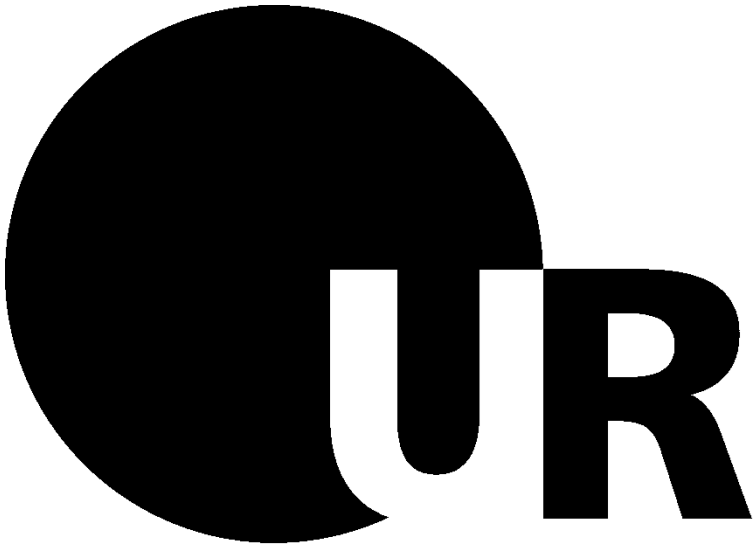

DISSERTATION ZUR ERLANGUNG DES
DOKTORGRADES DER NATURWISSENSCHAFTEN (DR. RER. NAT.)
DER FAKULTÄT FÜR BIOLOGIE UND VORKLINISCHE MEDIZIN
DER UNIVERSITÄT REGENSBURG

vorgelegt von

Sonja Decking

aus Ahaus

im Jahr 2021

The present work was carried out from January 2018 to November 2021 at the Clinic and Polyclinic of Internal Medicine III at the University Hospital Regensburg and the Regensburg Center for Interventional Immunology.

Die vorliegende Arbeit entstand im Zeitraum von Januar 2018 bis November 2021 an der Klinik und Poliklinik für Innere Medizin III des Universitätsklinikums Regensburg und dem Regensburger Zentrum für Interventionelle Immunologie.

Das Promotionsgesuch wurde eingereicht am: 19.11.2021
Die Arbeit wurde angeleitet von: Prof. Dr. Marina Kreutz

Unterschrift:

_____

To my parents

Table of contents

List of Figures

List of Tables

List of Abbreviations

2-DG	2-deoxy glucose
2-NBDG	2-(N-(7-Nitrobenz-2-oxa-1,3-diazol-4-yl)Amino)-2-Deoxyglucose
7-AAD	7-Actino aminomycin
ACT	Adoptive cell transfer therapy
AE	Anione exchanger
AKT	Protein kinase B
AMPK	5'AMP activated protein kinase
APC	Antigen presenting cell
APS	Ammonium peroxide sulfate
ASA	Aspirin
ATP	Adenoside triphosphate
BSA	Bovine serum albumin
CA	Carbonic anhydrase
CAR	Chimeric antigen receptor
CCR	Chemokine receptor
ccRCC	Clear cell renal cell carcinoma
CD	Cluster of Differentiation
cDNA	Complementary DNA
CFSE	Carboxyfluoresceinsuccinimidylester
CLB	Cell lysis buffer
CO_2	Carbon dioxide
CoA	Coenzyme A
COX	Cyclooxygenase
COXi	Inhibitor of Cyclooxygenase
CPTA1	Carnitine palmitoyl transferase 1
CS	Citrate synthase
CTL	Cytotoxic T Lymphocyte
CTLA-4	Cytotoxic T-Lymphocyte-Associated Protein 4
sCTLA-4	Soluble Cytotoxic T-Lymphocyte-Associated Protein 4
DC	Dendritic cell
Diclo	Diclofenac
DNA	Desoxyribonucleic acid
dNTPs	Deoxyribonucleosid-5'-triphosphates

DPBS	Dulbecco’s phosphate buffered saline
DTNB	5,5-dithio-bis-2-nitrobenzoic acid
ECL	Enhanced chemiluminescence
EDTA	Ethylene diamine tetraacetate
ETS	Electron transfer system
Exp	Experiment
FACS	Fluorescence-activated cell scanning
FAO	Fatty acid oxidation
FasL	Fas ligand
FCCP	Carbonyl cyanide-p-trifluoromethoxy phenylhydrazone
FCS	Fetal calf serum
FDA	Federal Drug Administration
FDG-PET	2-deoxy-2-[$_{18}$F] fluor-D-glucose positron emission tomography
FITC	Fluoresceinisothiocyanate
Foxp3	Forehead box protein 3
FSC	Forward scatter
GAPDH	Glyceralaldehyde-3-phosphate dehydrogenase
Glc	Glucose
GLUT	Glucose transporter
GNE	R-(+)-GNE-140
GPR	G-protein coupled receptor
GrzB	Granzyme B
H_2O	Water
H_2O_2	Hydrogen peroxide
H3K9Ac	Acetylation of lysine 9 in histone 3
HBSS	Hank’s buffered salt solution
HIF	Hypoxia inducible factor
HK	Hexokinase
HNSCC	Head-and-neck squamous cell carcinoma
HRE	Hypoxia responsive element
IFN	Interferon
IL	Interleukin
JAK	Janus kinase
Keto	Ketoprofen

Ki	Inhibitor constant
LA	Lactic acid
Lag-3	Lymphocyte activation gene 3
LDH	Lactate dehydrogenase
LDHi	NCI-737
LPS	Lipopolysaccharide
MACS	Magnetic activated cell sorting
MCT	Monocarboxylate transporter
MFI	Median fluorescence intensity
MHC	Major histocompatibility complex
M-MLV	Murine Moloney leukemia virus
mTOR	Mammalian target of rapamycin
mTORC	mTOR complex
NAD	Nicotinamide adenine nucleotide
NADP	Nicotine adenoside diphosphate
NFAT	Nuclear factor of activated T cells
NF-κB	Nuclear factor 'kappa-light-chain-enhancer' of activated B-cells
NGS	Next Generation Sequencing
NHE	Sodium proton exchanger
NK	Natural killer cell
NV	Naïve
O_2	Oxygen
ORR	Overall response rate
OXPHOS	Oxidative phosphorylation
PC	Pyruvate carboxylase
PCA	Principal component analysis
PCK	Phosphoenol-pyruvate carboxykinase
PCR	Polymerase chain reaction
PD-1	Programmed cell death protein 1
PDH	Pyruvate dehydrogenase
PDH	Pyruvate dehydrogenase
PDK	Pyruvate dehydrogenase kinase
PD-L1	Programmed cell death ligand 1
PE	Phycoerythrin

PGC	Peroxisome proliferator-activated receptor gamma coactivator
PI3K	Phosphoinositide-3 kinase
PKM	Pyruvate kinase
PlatA	Platinum-A cells
PTEN	Phosphatase and tensine homologue
PVDF	Polyvinylidenfluoride
qRT-PCR	Quantitative real-time polymerase chain reaction
RCI	Regensburg Center for Interventional Immunology
RNA	Ribonucleic acid
RNAseq	RNA sequencing
ROS	Reactive oxygen species
mROS	Mitochondrial reactive oxygen species
Rpm	Rounds per minute
S1PR1	Sphingosine-1-phosphate receptor
SCLC	Small-cell lung cancer
SDS	Sodium dodecyl sulfate
SEM	Standard error of the mean
siRNA	Small interfering RNA
SITS	4-Acetamido-4'-isothiocyanostilbene-2,2'-disulphonic acid
SNARF	Seminaphtharhodafluor
SSC	Side Scatter
STAT	signal transducer and activator of transcription proteins
TBS	Tris buffered saline
TCA	Tricarbolic acid cycle
TCIRG	T cell immune regulatory gene
Tcm	Central memory T cell
TCR	T cell receptor
Teff	Effector T cell
Tem	Effector memory T cell
TEMED	Tetramethylethyldiamin
TGF	Tumor growth factor
Th	T helper cell
TIL	Tumor infiltrating lymphocyte
TME	Tumor microenvironment

Tmem		Memory T cell
TNB		1,3,5-Trinitrobenzene
TNF		Tumor necrosis factor
Treg		Regulatory T cell
	nTreg	Natural regulatory T cell
	iTreg	Induced regulatory T cell
Trm		Tissue-resident memory T cell
Tscm		Stem cell memory T cell
UTR		Untranslated region
VEGF		Vascular endothelial growth factor
VHL		Von Hippel Lindau
β_2m		β-2-microglobuline

1. Introduction

1.1. The human immune system

The human immune system is formed by different organs, cell types and proteins, which all play their distinct role in the defense against pathogens. It can be divided in two different branches: The innate immune system, which represents a fast “first line of defense” against pathogens, and the adaptive immune system, driving a more specific immune response (Parkin and Cohen, 2001).

The innate immune response is mediated by physical barriers like the skin, the epithelial layer of the bronchial system and the mucosa of the digestive tract, proteins like antimicrobial peptides and the complement system and a cellular compartment composed by monocytes, dendritic cells (DCs), macrophages, granulocytes and natural killer (NK) cells (Turvey and Broide, 2010). Except for NK cells, which develop from the lymphoid lineage of hematopoiesis (Caligiuri, 2008), all cells of the innate immune system develop from myeloid precursor cells (Murphy and Weaver, 2017).

Cells of the innate immune system fulfill different specialized roles. Granulocytes, consisting of neutrophils, eosinophils, and basophils, secrete vesicles containing lysozymes and peptides lethal for microbes. NK cells directly kill target cells through different mechanisms and are tightly regulated by an interplay of activating and inhibiting receptors on their cell surfaces. Macrophages are primary phagocytotic cells, which internalize and destroy microbes in intracellular vesicles. Furthermore, together with DCs, they act as professional antigen presenting cells (APCs). They take up and process antigens and present them to cells of the adaptive immune system, thereby building a bridge between the innate and adaptive immune response (Murphy and Weaver, 2017).

The adaptive immune system is comprised of T cells and B cells, which both belong to the lymphoid lineage of differentiation (Murphy and Weaver, 2017). In contrast to the innate immune system, these cells react to a selected antigen, which they recognize via their specific surface receptors. Moreover, the adaptive immune system can create an immunological memory, leading to an accelerated and enhanced response upon re-infection. In addition, T cells play a major role in the anti-tumor defense and are therefore the target of many innovative therapies, which have taken route to the anti-cancer treatment regimens by now.

1.2. T cell differentiation and function

T cells can be separated into two major lineages according to their expression of the surface markers CD4 and CD8. Both lineages develop from a common lymphoid progenitor cell in the

bone marrow and undergo a maturation and selection process in the thymus, where auto-reactive and non-reactive T cells are eliminated. Finally, remaining cells form a pool of naïve T cells with different highly specific T cell receptors (TCRs) (Parkin and Cohen, 2001).

1.2.1. Activation and differentiation of T cells

A T cell becomes activated if its TCR binds to the specific antigen presented by major histo-compatibility complexes (MHCs), which can be separated in MHC class I (MHC-I) and MHC class II (MHC-II) molecules. In addition to TCR-binding to antigen-loaded MHC, the activation of T cells needs a sufficient co-stimulation by antigen-presenting cells (APCs). These signals act in a synergistic manner to activate a complex signaling cascade mediating the changes in the gene transcription and cellular remodeling crucial for the successful T cell response (Bhattacharyya and Feng, 2020).

TCRs are heterodimers build by either a pair of an α- and β-chain or a γ- and δ-chain. Both contain variable regions determining the antigen specificity and constant regions, which anchor the TCR to the plasma membrane. The CD3-molecule associates with the constant domains of the TCR. Furthermore, each TCR contains two constant ζ-chains, which together with CD3 mediate signal transduction upon ligation of the TCR-complex with the respective MHC-antigen-complex (Dopfer et al., 2014).

To initiate a T cell response, the TCR has to recognize and bind to its specific antigen presented by MHCs. MHC-I and MHC-II molecules have in common, that they consist of four different protein domains, but the overall structure is different (reviewed by Wieczorek et al., 2017). MHC-I molecules consist of three different α-chains, which are non-covalently associated with the invariant light chain β-2-microglobuline (β_2m). MHC-II molecules are composed by two α- and β-chains each. The two membrane-distant domains form a polymorphic cleft where the peptide presented as an antigen is bound (Kaliamurthi et al., 2018). Transmembrane helices anchor the membrane-close heavy chains to the membrane.

MHC-II molecules interact with CD4 T cells (Moss et al., 1992; Parkin and Cohen, 2001) and are expressed by professional APCs, which take up extracellular antigens in the periphery and afterwards migrate to the lymphoid organs, where the CD4 T cells can encounter the antigen loaded to MHC-II on the APC surface. Furthermore, T cell activation requires co-stimulatory signals, precisely by interaction of CD80/CD86 and CD40 expressed by APC and their respective counterpart CD28 and CD40L on T cell site. CD28 acts as a co-stimulator for T cells and is required for metabolic rewiring and to prevent anergy. Interaction of CD40 and CD40L in turn further stimulates APCs.

APCs play a crucial role in orchestrating the T helper cell response. Depending on various complex signals, activated CD4 T cells differentiate to several different T helper subsets with distinct roles and effector functions (Murphy and Weaver, 2017; Parkin and Cohen, 2001). Among CD4 T cells, one can distinguish between three major effector cell subsets: Th1 (T helper 1), Th2 (T helper 2) and Th17 (T helper 17) cells.

The classical model of T helper cell differentiation proposes that the different T helper subsets develop depending on the respective cytokine environment. The differentiation of Th1 cells is induced by interleukin (IL)-12, whilst Th2 cells are induced by the presence of IL-10 and IL-4 and Th17 cells develop in an environment, where tumor growth factor (TFG)-β, IL-6 and IL-23 are present (Wilson et al., 2009). However, this simple concept has been challenged, as it has been proposed that different subsets of DCs are responsible for the induction of Th1 and Th2 subsets and the T helper subset differentiation is orchestrated by a complex signaling network involving cellular, signaling pathway and microenvironmental factors (reviewed by Steinman and Banchereau, 2007).

T helper subsets are characterized by different cytokine profiles determining their functional characteristics (Zhu and Paul, 2008). Th1 cells secrete predominantly IFN-γ to activate NK cells (Okamura et al., 1998) and macrophages (Murphy and Weaver, 2017). In response to this stimulus, the latter increase the pathogen phagocytosis and lysis and upregulate MHC-II as well as costimulatory molecule expression, which in turn gives a positive feedback response to activated Th1 cells. Moreover, IFN-γ is an additional stimulator of CD8 T cell activity. Th2 cells secrete IL-4 and IL-5, which attracts eosinophils, basophils, and mast cells, as well as IL-13, which increases the strength of mucosal barriers, with the overall goal to enhance the immunity towards extracellular parasites and helminths. Th17 cells secrete IL-17 and IL-22, stimulating stromal and epithelial cells to secrete chemo-attractive molecules that conduct neutrophils to the site of inflammation and support the defense against extracellular bacteria. An additional subset of CD4 T cells are regulatory T cells (Treg) either developing in the thymus (natural Treg; nTreg) or induced by the stimulation of CD4 T cells in presence of TGF-β and IL-2 (induced Treg; iTreg). They are characterized by the expression of high levels of CD25, the α-chain of the IL-2 receptor, and the forehead box protein 3 (Foxp3) (Zhu and Paul, 2008). In contrast to the T helper subsets, Treg are not involved in the active defense against pathogens and the mediation of inflammation but are rather important in balancing the immune response. Presumably, their suppressive activity is mediated by the secretion of anti-inflammatory cytokines like IL-10 and TGF-β, which inhibit the response of pro-inflammatory T cells. In addition, Treg produce and secrete a soluble form of the Cytotoxic T-Lymphocyte-Associated Protein 4 (sCTLA-4), which binds to CD80/CD86 on APCs preventing co-stimulation of T cells (Ward et al., 2013). Moreover, Treg express surface molecules as CTLA-4 and Lag-3 (Lymphocyte activation gene 3) allowing a contact-dependent inhibition of T cell

activation and mediate a direct killing of target immune cells (Safinia et al., 2015; Sojka et al., 2008).

CD8 T cells interact with MHC-I molecules (Moss et al., 1992; Parkin and Cohen, 2001), which are expressed by platelets and all nuclear cells and present antigens synthesized and processed in the cell. When CD8 T cells get activated and receive sufficient co-stimulation either by DCs or through cytokines produced by Th1 cells, they differentiate into cytotoxic lymphocytes (CTL) with the capability to directly eliminate infected or altered cells (Murphy and Weaver, 2017). CTLs express Fas ligand (FasL) which binds to its receptor (Fas, CD95) expressed by many other kinds of cells, including other immune cells. The ligation of those receptors with its ligand induces the release of cytochrome *c* from mitochondria, which in turn starts the apoptotic cascade mediated by several caspases ending with the controlled death and collapse of the target cells (Waring and Müllbacher, 1999). Besides inducing apoptosis, CTLs can directly lyse their target cells by the release of cytotoxic granules containing perforin and granzymes. Upon secretion, perforin forms lytic pores in the plasma membrane of the target cell, through which granzymes can enter the cell and induce apoptosis by damaging mitochondria or directly activating caspases (Trapani and Smyth, 2002). Finally, CTLs secrete pro-inflammatory cytokines including IFN-γ and TNF. IFN-γ is known to activate macrophages and increases the expression of MHC-I and MHC-II on stromal cells by stimulating the janus kinase and signal transducer and activator of transcription proteins (JAK-STAT) pathway (Ilangumaran et al., 2002; Propper et al., 2003), which subsequently increases the chance of achieving a T cell response.

1.2.2. The formation of the immunological T cell memory

After a first encounter with a pathogen, the adaptive immune system forms an immunological memory persisting for a long time, sometimes even for lifetime. Beside memory B cells, which produce highly specific antibodies very fast upon re-infection, memory T cells (Tmem) developing from effector T cells (Teff) play the central role in the immunological memory formation. Among memory T cells, central memory (Tcm), effector memory (Tem) and tissue-resident memory cells (Trm) are distinguished. Recently, a subset of memory cells with stem-cell like properties and outstanding longevity, termed stem cell memory (Tscm) cells, has been described among murine and human CD8 memory T cells (Gattinoni et al., 2011; Lugli et al., 2013).

The different subsets can be distinguished by their expression profile of several surface proteins. Naïve T cells ($CD45RA^{+}CCR7^{hi}CD62L^{hi}$) are characterized by the expression of CD45RA and the homing receptors CCR7 and L-Selectin (CD62L), both important for the retention of lymphocytes in the secondary lymphoid organs as lymph nodes and the spleen.

The activation of a naïve T cells leads to a switch in the expression from CD45RA to CD45RO mediated by alternative splicing in the extracellular domain of CD45. Tem are defined as $CD45RO^{+}CCR7^{lo}CD62L^{lo}$, whilst Tcm keep the expression of the homing receptors CCR7 and CD62L and can consequently be defined as $CD45RO^{+}CCR7^{hi}CD62L^{hi}$. In contrast to Tcm and Tem cells, Trm do not circulate within the body but stay residual in the peripheral tissue. They express CXCR3, CXCR4 and CCR9 allowing them to enter distinct immunologically important peripheral tissues like the dermis or the lamina propria of the gut. In there, the cells express high levels of CD69 preventing the cells to exit the tissue by sequestration of the tissue-egress signal sphingosine-1-phosphate receptor (S1PR1; Szabo et al., 2019)

The lineage relationship of the different T cells subsets is still a matter of discussion and not fully understood (Raphael et al., 2020). According to the linear model of differentiation, naïve T cells activated by DCs give rise to a pool of effector and memory precursor cells, which then further differentiate to Tem and Tcm cells and eventually Trm cells. The asymmetrical model claims a connection between the relative distance of the T cell regarding the MHC-TCR interaction. It suggests that cells close to the immunological synapse develop to Tem cells, whilst more distal daughter cell develop to Tcm. In the self-renewal model, self-renewing effector T cells and Tcm cells are generated from the naïve T cells and then give rise to Tem cells. The simultaneous model applies to the generation of CD4 T cell memory and proposes, that naïve T cells first develop to the different Th subsets, and then each Th subset gives rise to a different memory subset: Th1 and Th17 cells differentiate to Tem cells, Th2 and Treg cells to Trm cells and follicular T helper cells to T cm cells.

1.3. Metabolism of human T cells – A link between metabolism and function?

In a quiescent state, T cells cover their energetic demands by oxidative phosphorylation (OXPHOS) and fatty acid oxidation (FAO) (Kareva and Hahnfeldt, 2013; van der Windt et al., 2012). Due to the increased energetic demands of T cells upon activation, the cellular metabolism of T cells undergoes changes characteristic for their respective functional and developmental stage (Krauss et al., 2001; Renner et al., 2015). Notably, this metabolic rewiring is mediated by the same signaling pathways as in cancer cells (see chapter 1.5.1).

Upon T cell activation and differentiation, changes regarding the amino acids and glucose metabolism as well as the mitochondrial activity have been observed. By applying a single-cell metabolic profiling technique, Hartmann and colleagues found three metabolic inflection points during T cell activation (Hartmann et al., 2020): First, the cells show a coordinated upregulation of various metabolic pathways, including glycolysis and glutamine metabolism. Second, the

cells initiate RNA synthesis and activate the cellular stress response. Furthermore, the cells downregulate the expression of the carnitine palmitoyl transferase I (CPT1A), a key enzyme in FAO. This inflection point coincides with the G0/G1 phase of the cell cycle. The third phase, in which cells stabilize the expression levels of key metabolic enzymes and reach the peak in translational activity, coincides with rapid cell division.

Several studies have shown that T cell metabolism is tightly connected to their effector functions, and that metabolic inhibition or restriction can lead to defective effector functions and proliferation. Moreover, tumor-infiltrating lymphocytes (TILs) often display a metabolically perturbed phenotype and modification of the T cell metabolism is a promising strategy to enhance anti-tumor immunity (Chang and Pearce, 2016; Leone and Powell, 2020; O'Sullivan and Pearce, 2015). Therefore, it is important to take a closer look into the connection of T cell metabolism and effector functions. Notably, most studies regarding the metabolism of T cells were conducted using murine T cells. To our knowledge, no study has systematically compared the metabolism of murine and human T cells so far, which makes it indispensable to carefully discriminate results according to the investigated species. As this work mostly focuses on processes related to glucose and mitochondrial metabolism of T cells and cancer cells, the focus of the following chapter shall be on these topics.

1.3.1. Glucose metabolism of T cells

In most healthy cells and under normal oxygen supply, adenoside triphosphate (ATP) is generated by the metabolization of glucose via the tricarbolic acid cycle (TCA) and oxidative phosphorylation (OXPHOS). Glucose is taken up by glucose transporters and metabolized via different intermediate steps to pyruvate, which can serve as substrate for TCA in mitochondria. This very effective metabolic pathway yields the generation of 36 mol ATP out of 1 mol glucose. Only under certain circumstances as for example in the working muscle or in certain tissues, energy is generated by anaerobic glycolysis followed by lactate fermentation, which means that pyruvate is not introduced to the mitochondrial bioenergetic pathways but instead metabolized directly to lactate, which is exported in co-transport with protons via monocarboxylate transporters (MCTs) into the cellular environment. Compared to the mitochondrial metabolization of glucose, lactate fermentation is rather ineffective as it results only in the generation of 2 mol ATP out of 1 mol glucose, but also it is much faster than OXPHOS and TCA intermediates can be provided to other biosynthetic pathways (Gatenby and Gillies, 2004). Furthermore, conversion of pyruvate to lactate is associated with $NADH/H^+$ oxidation, thereby regenerating cellular NAD^+ pools. Therefore, highly proliferative cells often switch their metabolism towards a glycolytic phenotype despite sufficient oxygen supply, which

was first described by Otto Warburg (Warburg et al., 1927) in cancer cells (see chapter 1.5.1.1).

The observation, that also human lymphocytes consume high amounts of glucose during clonal expansion, has been made already during the 1960s by Cooper and colleagues (Cooper et al., 1963). After stimulation, the T cells upregulate the expression of lactate dehydrogenase A (LDHA), hexokinase (HK) and monocarboxylate transporter 1 (MCT-1). This changes in transcription are detected between 15 minutes in murine (Menk et al., 2018) and 6 h in human T cells (Renner et al., 2015) after activation and the transcription peaks after 6 h to 48 h after activation. Accordingly, activated T cells show a strongly increased glucose consumption and lactate production beyond 24 h to 48 h of stimulation. Besides thereby allowing a fast energy generation and efficient glucose usage, the accumulation of glycolytic intermediates allows T cells to shunt these into other pathways as the pentose phosphate pathway (Wang et al., 2011), which is important to regenerate $NADP^+$ (nicotinamide adenoside diphosphate) to maintain the redox homeostasis in activated T cells (Leone and Powell, 2020). Moreover, Ho and colleagues found the accumulation of phosphoenolpyruvate, a glycolytic intermediate, to be important for sustaining murine T cells effector functions (Ho et al., 2015).

Several studies have shown that signaling cascades involving the 5'-AMP activated protein kinase (AMPK), protein kinase B (AKT), phosphoinositide-3 kinase (PI3K) and the mammalian target of rapamycin (mTOR) are involved in the metabolic switch of T cells. As these pathways are also involved in transmitting signals from the TCR and CD28, they also directly couple T cell activation to metabolic changes required to fulfil the metabolic needs of T cells. Several studies in murine and human T cells have shown that signals transmitted by CD28 promotes the glycolytic flux needed for full activation of T cells (Frauwirth et al., 2002; Jacobs et al., 2008; Macintyre et al., 2014). This underlines the importance of extracellular signals in mediating increased nutrient uptake. Signals transmitted by AKT, which is activated upon TCR ligation, are responsible for increased protein expression and membrane localization of GLUT-1 (Jacobs et al., 2008; Wieman et al., 2007). Xu and colleagues showed, that in murine T cells activation of PI3K by AKT induces the upregulation of Ldha on a transcriptional level (Xu et al., 2021).

The glycolytic metabolism of T cells and their function are tightly connected. It has been shown in both human and murine T cells, that the inhibition of glycolysis or the restriction of glucose as nutrient leads to a decreased proliferation of T cells (Cham et al., 2008; Jacobs et al., 2008; Wang et al., 2011). Macintyre and colleagues were able to show, that the deletion of GLUT-1, the main transporter for glucose in T cells, leads to defects in the proliferation of both human and murine CD4 and CD8 T cells (Macintyre et al., 2014). Similar results have been obtained using the glucose analog 2-deoxy glucose (2-DG; Bailis et al., 2019; Renner et al., 2015).

Surprisingly, the deletion of Ldha in murine T cells leads only to a slight delay, but not a complete blockade of T cell proliferation (Peng et al., 2016; Xu et al., 2021). Moreover, the replacement of glucose by galactose can restore the proliferative capacity of murine T cells by causing a switch towards OXPHOS (Chang et al., 2013). This suggests that lactate fermentation is not the only important metabolic pathway fueled by glucose uptake.

Regarding the relevance of glycolytic activity for cytokine production, studies led to contradictory results depending on whether the experiments were conducted with murine or human T cells. In murine T cells, effector cytokine production seems to be dependent on glycolytic activity as glucose limitation abolished the production of effector cytokines (Cham et al., 2008; Cham and Gajewski, 2005; Menk et al., 2018). Intriguingly, glucose limitation or treatment with 2-DG affected predominantly the production of inflammatory effector cytokines like IFN-γ and the effector functions of CD8 T cells, but not the production of anti-inflammatory cytokines (Ho et al., 2015) or IL-2 (Cham et al., 2008; Cham and Gajewski, 2005). Ho an colleagues were able to show that this was caused by an dampened Ca^{2+} flux and defective NFAT (nuclear factor of activated T cells) translocation to the nucleus (Ho et al., 2015). Moreover, different studies showed an effect on IFN-γ production already on transcriptional level. Under glucose deprivation, the rate-limiting enzyme of glycolysis glyceralaldehyde-3-phosphate dehydrogenase (GAPDH) binds to the 3' untranslated region (UTR) of the IFN-γ mRNA and thereby blocks the translation (Chang et al., 2013). Besides this, the deletion of LDHA in T cells leads to a decreased acetylation of lysine 9 in histone 3 (H3K9Ac) at the promoter of IFN-γ, which is normally promoting transcription (Peng et al., 2016). These data show that glucose metabolism regulates IFN-γ production on an epigenetic level.

In human T cells studies have come to different conclusions. The deletion of GLUT-1 in T cells did not affect the cytokine production of human T cells (Macintyre et al., 2014). Moreover, administration of MCT-inhibitors or the limitation of glucose availability did not abolish the effector functions of human CD4 or CD8 T cells (Gubser et al., 2013; Renner et al., 2015; Renner et al., 2019). Under these conditions, T cells upregulate the mitochondrial respiration to compensate for the missing glycolytic activity. Only by administration of high concentrations 2-DG the production of cytokines is completely abolished, as in those conditions also the respiratory activation is blocked (Renner et al., 2015).

1.3.2. Mitochondrial activity of T cells

Besides glycolysis, also mitochondrial activity is upregulated in activated T cells. The respiration of T cells in upregulated immediately after activation, although no upregulation in the transcription of key mitochondrial enzymes is detected (Renner et al., 2015). Different

reasons for the upregulation of mitochondrial respiration have been proposed. The ATP generated by mitochondrial respiration is important for the triggering the glycolytic machinery and is therefore important for the upregulation of the glycolytic activity (Chang et al., 2013; Renner et al., 2015). Furthermore, acetyl coenzyme A (acetyl-CoA) has been identified as an important molecule for the rapid recall activation of CD8 memory T cells upon re-infection (Balmer et al., 2016).

Several studies have highlighted the relevance of the mitochondrial metabolism for the normative development of T cell effector functions and proliferation. The inhibition of the ATP synthase by oligomycin during activation leads to a decreased proliferation rate and a defective upregulation of glycolysis in human T cells (Renner et al., 2015). However, oligomycin applied 24 h or 48 h after activation has no effect on T cell proliferation, underlining the relevance of mitochondrial ATP especially for the early phase of T cell activation. Similar, the relevance of mitochondrial ATP for T cell activation has been demonstrated in murine T cells (Ledderose et al., 2014).

The relevance of mitochondrial function for T cell activation goes far beyond ATP production, as several studies have also highlighted ATP-independent effects of mitochondrial metabolism on T cell activation. It has been shown that the development of a higher spare respiratory capacity mediated by the engagement of CD28 is important for the development of Tmem cells (Klein Geltink et al., 2017). Inhibition of glycolysis enhances the quality and quantity of differentiated Tmem cells (Sukumar et al., 2013), and the activity of the respiratory chain is critical for the development of T helper subsets (Bailis et al., 2019). Moreover, mitochondrial respiration is the source of mitochondrial reactive oxygen species (mROS). Sena and colleagues were able to show that murine T cells require ROS generated by complex III of the respiratory chain for T cells activation and IL-2 production *in vitro* and *in vivo* (Sena et al., 2013). Similar results were obtained with T cells which are defective in complex IV (Tan et al., 2017). Moreover, the acetyl-CoA provided by mitochondrial activity can be used as a substrate for the acetylation of histones, which is an important transcriptional activator and found at the promoter of the IFN-γ gene upon T cell activation (Mehta et al., 2017).

1.3.3. Subset-specific differences in T cell metabolism

During T cell activation and their development into different subsets, they undergo characteristic changes not only in their functional and metabolic profiles.

In a resting state, the energetic demands of T cells are relatively low and focused on maintaining the housekeeping functions. In contrast to activated T cells, which display an anabolic metabolism, the metabolic signature of quiescent T cells is catabolic. They largely

cover their energetic demands by OXPHOS activity, which is fueled by glucose, lipids or amino acid in an interchangeable manner (Jones and Thompson, 2007). Upon activation T cells upregulate various metabolic pathways, primarily aerobic glycolysis and mitochondrial respiration. Accordingly, quiescent T cells are almost unsensitive towards the deletion of GLUT-1 and the following decrease in glucose uptake (Macintyre et al., 2014), whilst depending on the chosen model and species glucose and mitochondrial deprivation can have dramatic effects on activated T cells. Regarding this, it has been reported that murine CD4 T cells show a stronger upregulation of OXPHOS, whilst CD8 T cells rely more on glycolytic activity, but are more resistant towards metabolic inhibition (Cao et al., 2014).

It is still a matter of discussion whether the metabolism of CD4 and CD8 Tmem cells is different (Chang and Pearce, 2016). It has been proposed that murine CD8 Tmem cells rely on FAO activity (O'Sullivan et al., 2014; Pearce et al., 2009). Treatment with etomoxir, an irreversible inhibitor of the carnitine palmitoyl transferase 1 (Cpta1), suppressed the restimulation of T cell *in vitro* (van der Windt et al., 2013). However, these findings are heavily discussed in the field, as they were working with very high concentrations of etomoxir inducing Cpta1-independent off-target effects as demonstrated by others (Raud et al., 2018). In line, it has been demonstrated that neither low-dose etomoxir treatment nor complete deletion of Cpt1a influenced Tmem differentiation of CD4 murine T cells (Raud et al., 2018). Nevertheless, mitochondrial activity and remodeling has been identified to be essential for Tmem generation, function and homeostasis. Buck and colleagues have shown that the molecule Opa1 mediates mitochondrial fusion upon activation, leading to the formation of a mitochondrial network critical for the metabolic shift towards FAO (Buck et al., 2016). Balmer et al. have identified acetate as a checkpoint molecule for Tmem rapid recall responses (Balmer et al., 2016). CD8 T cells use acetate for the expansion of their acetyl-CoA pools via ATP citrate lyase in mitochondria, which increases GAPDH acetylation and enhances T cell glycolytic activity. Furthermore, different studies have suggested a critical role of mTOR complex 1 (mTORC1) inhibition in the development of CD8 T cell memory (He et al., 2011; Pollizzi et al., 2015; Rao et al., 2010). In the end of effector phase, mTORC1 inhibition favors a switch from aerobic glycolysis towards higher mitochondrial activity.

Several studies have additionally shown that Treg have a metabolic phenotype distinct from Teff cells. In contrast to the high glycolytic activity detected in conventional T cells, Treg show a decreased expression of GLUT-1 and a decreased glucose uptake upon activation (Ho et al., 2015; Michalek et al., 2011) and their proliferation and survival is not affected by deletion of GLUT-1 (Macintyre et al., 2014). By now, several studies highlighted the higher relevance of OXPHOS compared to glycolysis in Treg subsets (Angelin et al., 2017; Beier et al., 2015; Gerriets et al., 2015; Leone and Powell, 2020). Foxp3, which is one of the main lineage determinants of Treg cells, binds to the MYC-related TATA box. Thereby, it prevents the

upregulation of MYC upon activation, inhibits the glycolytic switch and directly influences the expression profile of LDH to metabolize predominantly L-lactate, which also promotes an oxidative phenotype (Angelin et al., 2017).

1.4. The immunological anti-tumor response

The immune system is not only involved in the defense against pathogens but also plays an important role in the detection and elimination of cancer cells. Consequently, the overall immune infiltration of tumors can be predictive for disease outcome.

T cells assume a big part of the anti-tumor response. It has been shown that a high number of infiltrating T cells is associated with a better prognosis in a variety of tumor entities. Furthermore, even patients with a localized disease have a poor prognosis if the tumors are infiltrated by low numbers of T cells (Hadrup et al., 2013). As CD8 T cells get activated by MHC-I-antigen complexes expressed by all nuclear cells, they are often regarded as the T cell type mainly responsible for anti-tumor clearance. The transformation of a normal cell to a malignant cancer cell is often accompanied by accumulation of mutations leading to a number of changes in the transcriptional landscape of tumor cells (Hanahan and Weinberg, 2011). This includes not only the loss of tumor suppressors like p53 and the upregulation of oncogenes, but as well the expression of altered cellular antigens, the re-expression of embryonic genes normally silenced in adult cells or the enhanced translation of oncogenic proteins of viral origin. These are presented by MHC-I proteins on the cell surface, allowing the activation of CTLs with the subsequent lysis of the developing cancer cell via the same mechanisms also important in protection against viruses. Moreover, the secretion of IFN-γ by activated CTLs enhances the inflammatory reaction favoring the anti-tumor response.

Besides the obvious and well accepted role of CD8 T cells in the anti-tumor immunity, it has recently become clear that CD4 T cells are critical for the development and sustainment of an effective anti-tumor response. It has been demonstrated in murine tumor models (Antony et al., 2005; Bos and Sherman, 2010) and also in clinical studies (Fridman et al., 2012; Ossendorp et al., 1998; Toes et al., 1999; Tran et al., 2014) that CD4 T cells are of high relevance for developing and sustaining a successful anti-tumor immunity. The role of CD4 T cells has further been addressed with the development of so-called tumor vaccines using MHC-II restricted epitopes to induce tumor-targeted Th1 clones and CD4 CAR (chimeric antigen receptor) T cells (summarized by Tay et al., 2021).

CD4 T cells can support the anti-tumor response through several mechanisms. Activated CD4 T cells can provide direct help for CD8 T cells by secreting IL-2, which is needed by CD8 T cells for clonal expansion and full activation. Th1 polarized CD4 T cells secrete IFN-γ enhancing the

cytolytic functions of CTLs directly. Furthermore, IFN-γ acts on cross-presenting DCs stimulating the expression of co-stimulatory molecules and MHC-I needed for full activation of CD8 T cells (Borst et al., 2018). In addition, CD4 T cells express CD40L binding to CD40 on B cells, thereby supporting their maturation and consequently the production of tumor-specific antibodies (Gnjatic et al., 2003; Reed et al., 2015). What is more, CD4 T cells can show lytic activity and therefore also exhibit direct tumor-killing capacities (Cachot et al., 2021; Nakajima et al., 2002; Quezada et al., 2010).

As on one site the immune system owes several mechanisms to detect and kill developing tumor cells, a variety of mechanisms and properties of tumor cells that allow an evasion from immunosurveillance have been described in the past years. First, as described above, tumor cells often lose MHC-I expression making them somehow “invisible” for invading T cells and preventing tumor cell lysis mediated by CTLs (Algarra et al., 2004). Second, surface proteins with an inhibitory function towards immune cells, so-called “immune checkpoints”, have been shown to be expressed in several cancer entities. The programmed cell death ligand 1 (PD-L1) binds to its receptor programmed cell death protein 1 (PD-1), which is upregulated on T cells upon activation, and thereby inhibits T cell effector functions and effective cancer cell killing (Blank et al., 2004). Moreover, the cytotoxic T-lymphocyte-associated protein-4 (CTLA-4), which binds competitively to CD80/CD86 expressed by APCs and thereby hinders the co-stimulation of T cells upon activation, has been found to be upregulated on many tumor-infiltrating lymphocytes and prevents a successful anti-tumor response (Chambers et al., 2001). Beside these mechanisms, the tumor microenvironment (TME) plays an important role in shaping the immune response. Tumor cells often secrete TGF-β, inducing and favoring the accumulation of Treg within the tumor, which in turn inhibit invading T effector cells (Yang et al., 2010). In addition, the accumulation of suppressive tumor metabolites has turned out to play an important role in the immune evasion (see chapter 1.5.2) and therefore, the metabolism of tumor cells is widely accepted to display an own “metabolic immune checkpoint” nowadays (Renner et al., 2017; Singer et al., 2011).

1.5. Metabolic alterations of tumor cells as a “Hallmark of cancer”

The growth of a solid tumor within the body underlies a constant stress due to competition comparable to an evolutionary process. Therefore, a tumor cell needs to acquire features not only allowing to withstand this selective pressure, but also to supersede the surrounding healthy tissue. These features have been summarized by Hanahan and Weinberg as “Hallmarks of cancer” (Hanahan and Weinberg, 2011) and include, besides acquiring a high proliferative capacity, avoiding apoptosis and immune evasion, a dysregulation of the cell

metabolism. This has not only substantial effects on the tumor cells themselves, but also leads to major alterations in the tumor microenvironment (TME) characterized by nutrient depletion and the accumulation of metabolic side products, which can have strong impact on the anti-tumor immune response.

One of the earliest discoveries regarding the altered metabolism in tumor cells was made by Otto Warburg already in the 1920s. He described, that tumor cells often cover their energetic demands not by aerobic metabolization of glucose via the TCA, but rather use the more ineffective lactate fermentation (Warburg et al., 1927). Tumor cells are often characterized by a high consumption of glucose and lactate output, a phenotype today referred to as 'Warburg phenotype'. As this doctoral thesis focuses on modulating the negative consequences of this phenotype on immune cells, the molecular basis and its consequences on immune cell function shall be described here in more detail.

1.5.1. Glucose metabolism in cancer cells: The Warburg-effect

In cancer cells, the energy metabolism is often dysregulated as these cells mostly cover their energetic demands via glycolysis despite having sufficient oxygen supply (Figure 1-1). Warburg described that tumor cells often show a 10-fold higher glucose consumption compared to non-cancerous cells accompanied by an increased lactate secretion. Whilst Warburg contributed this phenotype to defective mitochondria it is known today that the mitochondrial function is intact in most cancer cells and that some tumors even depend on mitochondrial respiration (DeBerardinis and Chandel, 2020; Obre and Rossignol, 2015). Recently, it has been shown that cells engage aerobic glycolysis when the demand for NAD^+ to fuel cellular processes like aspartate and serine synthesis, histone deacetylation or maintenance of calcium homeostasis exceeds the demand for ATP (Luengo et al., 2021). High aerobic glycolysis in addition allows to feed non-mitochondrial pathways that contribute to macromolecular synthesis, including e.g. the pentose-phosphate pathway (PPP) producing ribose and NADPH for nucleotide and reductive biosynthesis, the serine-glycine-one-carbon metabolism or the glycerol synthesis for the production of complex lipids (DeBerardinis and Chandel, 2020).

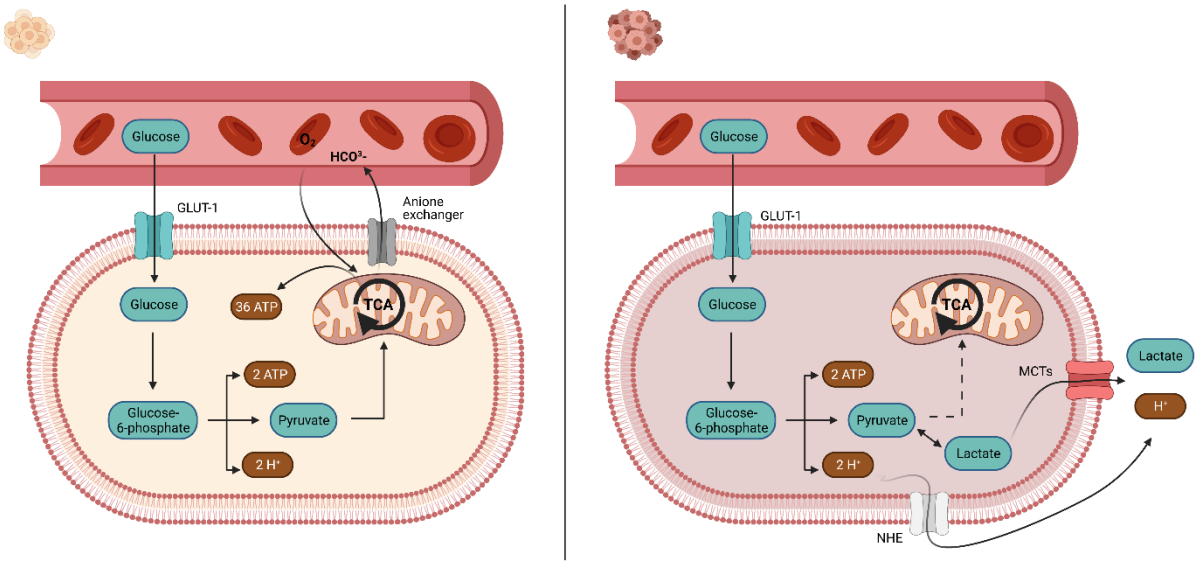

Figure 1-1: The Glucose metabolism in normal (left) and tumor cells (right) *(according to Cairns et al., 2011). ATP: Adenoside triphosphate; GLUT-1: Glucose transporter 1; MCTs: Monocarboxylate transporters; NHE: Sodium proton exchangers; TCA: Tricarbolic acid cycle. Created with BioRender.com.*

The Warburg phenotype is characterized by an elevated glycolytic flux. Tumor cells very often express elevated levels of the glucose transporters and the monocarboxylate transporters 1 and 4 (MCT-1, MCT-4), increasing the capability for glucose uptake and lactate secretion. The elevated glycolytic rate of tumor cells is used for diagnosis and staging of tumor patients in terms of FDG-PET (2-deoxy-2-[$_{18}$F] fluor-D-glucose positron emission tomography). FDG is taken up by the tumor cells, cannot be further metabolized and is therefore trapped in the cell. Using a special tomography method, this technique allows to detect tumors showing a high glucose uptake (Bensinger and Christofk, 2012).

1.5.1.1. Molecular basis of the Warburg effect

On molecular level, the Warburg effect is caused and maintained by overexpression of different key glycolytic enzymes such as PDK-1 (pyruvate dehydrogenase kinase 1), HK-2 (hexokinase 2), LDH-5 and proteins involved in glucose and lactate transport as GLUT-1, GLUT-3, MCT-1 and MCT-4 (Bensinger and Christofk, 2012). There are different reasons for the increase in aerobic glycolysis of tumor cells, the so-called glycolytic switch. On the one hand, it can be explained by an adaption of tumor cells to hypoxic conditions during tumor development (Gatenby and Gillies, 2004), on the other hand it can be directly connected to the activation of common oncogenes and the loss of tumor suppressors (Cairns et al., 2011; Gottfried et al., 2012).

A key molecule directly connecting the development of tumors and the glycolytic switch is the hypoxia-inducible factor-1α (HIF-1α) (Lu et al., 2002). HIF is a heterodimer build by an α- and β-subunit. Whilst the β-subunit is ubiquitously and stably expressed, the expression of the

α-subunit is strictly regulated and connected to cellular oxygen supply. Under normoxic conditions, the α-subunit is hydroxylated, allowing the interaction with the von Hippel Lindau-protein (pVHL) and subsequent proteasomal degradation. Under hypoxic conditions, the α-subunit is translocated to the nucleus, where it interacts with the β-subunit and binds to regulatory hypoxia responsive elements (HRE) in the DNA (Semenza, 2009, 2010). This mediates the increased expression of more than 70 genes including VEGF (vascular endothelial growth factor) and key glycolytic enzymes as GLUT-1, GLUT-3, MCT-4 and LDHA (Bensinger and Christofk, 2012; Cairns et al., 2011), which in turn enhances the glycolytic rate of the cells. An overexpression and increased stabilization of HIF-1 has been detected in several cancer entities, is correlated with cancer aggressiveness and a poor prognosis (Semenza, 2002; Unruh et al., 2003) and determines the chemosensitivity in gastric cancer patients by the modulation of tumor suppressor protein 53 (p53) and NF-κB (nuclear factor 'kappa-light-chain-enhancer' of activated B-cells) (Rohwer et al., 2010). Loss-of-function mutations in pVHL cause the von-Hippel-Lindau disease characterized by the development of sporadic hemangioblastomas in kidney, skin and spinal cord (Kim and Kaelin, 2004). Moreover, *VHL* is the most frequently mutated gene in clear cell renal cell carcinoma (ccRCC), and it's mutation or epigenetic silencing by promoter methylation comprises one of the hallmark events in ccRCC development (Comprehensive molecular characterization of clear cell renal cell carcinoma, 2013; Hsieh et al., 2017).

Besides stabilization of HIF-1 by hypoxia, several mutated oncogenes and tumor-suppressor genes can lead to an oxygen-independent stabilization of HIF-1 and subsequent activation of HIF-related transcription. Activation of PI3K and MYC can directly or indirectly lead to a stabilization of the HIF dimer (Cairns et al., 2011; Semenza, 2009). MYC is a central protein in the tumor development and dysregulated in a wide variety of cancers (Camarda et al., 2017). It can directly interact with HIF-1 to induce the transcription of the HIF-controlled genes (Dang, 2007) and itself targets several key enzymes of glycolysis, such as HK2, LDHA and GLUT-1 (Marinkovic et al., 2004; Osthus et al., 2000; Shim et al., 1997). In pancreatic cancer, concomitant dysregulation of MYC and LDHA regulate aerobic glycolysis and promote tumor progression (He et al., 2015). PI3K is activated by mutations in the tumor suppressor gene PTEN (phosphatase and tensine homologue) or in PI3K itself and causes a hyperactivation of mTOR, which in turn stimulates the HIF-induced gene expression (Cairns et al., 2011). Besides this, glycolytic end products such as lactate can directly lead to a stabilization of HIF-1, thereby acting as an auto- and paracrine feedback-loop promoting aerobic glycolysis (Gatenby and Gillies, 2004; Sonveaux et al., 2012).

Moreover, mutated oncogenes and tumor suppressor genes can directly enhance the glycolytic flux of cancer cells. Upon loss of p53, cells show a decreased oxygen consumption and a higher lactate secretion (Matoba et al., 2006). The activation of PI3K leads to the

activation of the AKT, one of the main regulators of glycolysis and mediating the expression of glucose transporters as well as the phosphorylation of glycolytic enzymes resulting in an increased activity of these enzymes (Xie et al., 2019). Besides this, many tumors express isoforms of key glycolytic enzymes with an enhanced drift towards the lactate fermentation (Bensinger and Christofk, 2012). For example, the M2 isoform of the pyruvate kinase (PKM2) is expressed by many cancer cells and its silencing leads to a reversion of the Warburg phenotype (Christofk et al., 2008). The pyruvate dehydrogenase kinase 1 (PDHK1) phosphorylates and thereby inactivates the pyruvate dehydrogenase (PDH), the enzyme responsible for the introduction of pyruvate into the TCA cycle (Porporato et al., 2011). Overall, these molecular and genetic changes build a complex network maintaining the Warburg phenotype of cancer cells.

1.5.1.2. The Lactate dehydrogenase (LDH)

The lactate dehydrogenase is the enzyme responsible for the interconversion of lactate and pyruvate. Until today, four different isoforms of the LDH encoded by separate genes (*LDHA* – *LDHD*) were identified. LDHC is predominantly expressed in embryonic tissue and testis (Li, 1989). LDHD is involved in the metabolism of D-Lactate (Monroe et al., 2019). In the following chapter, the role of *LDHA* and *LDHB* in adult cells shall be described in more detail.

The adult LDH is formed by two separately encoded subunits. The gene *LDHA* encodes for the subunit LDH-M (muscle), whilst *LDHB* encodes the subunit LDH-H (heart). Both subunits form homo- and heterotetramers resulting in five different LDH isoenzymes (LDH-1 to LDH-5, Figure 1-2). In the literature, the gene names are often used as synonyms for the encoded subunits, what shall be maintained in this work.

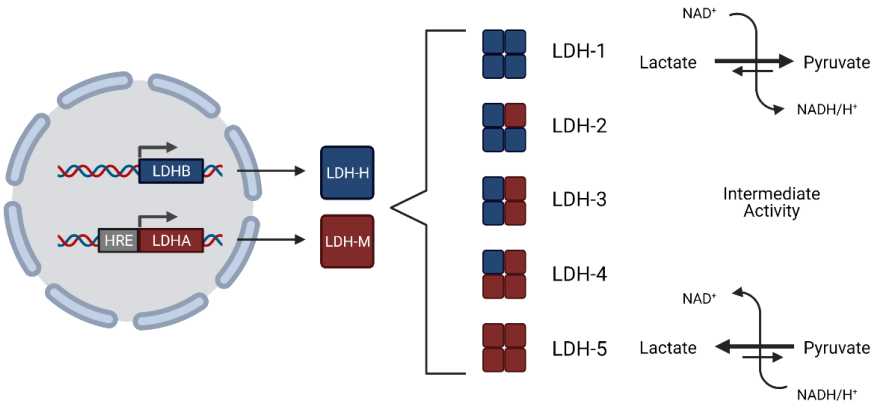

Figure 1-2: The assembly of the lactate dehydrogenase (LDH) *according to Porporato et al., 2011. Created with BioRender.com.*

It has been described that LDHA has a higher affinity towards pyruvate as a substrate whilst LDHB has a higher affinity towards pyruvate (Markert et al., 1975). These affinities influence the characteristics of the formed LDH isoenzymes: Whilst LDH-5 predominantly catalyzes pyruvate reduction, LDH-1 is responsible for lactate oxidation. The heterotetramers show an intermediate activity depending on their respective composition. However, this paradigm has been challenged recently, as several studies showed that only the deletion of both LDHA and LDHB led to a complete block of the lactate production in several tumor cell lines (Di Zhang et al., 2019; Mack et al., 2017; Ždralević et al., 2018). Moreover, the specificity of the different subunits was found to depend on the environmental pH and the temperature (Tang et al., 2017; Vesell, 1965) and post-translational phosphorylation of LDHB by the protein kinase Aurora-A switched its catalytic activity towards a glycolysis-promoting phenotype (Cheng et al., 2019).

1.5.2. Implications of the tumor-metabolism for the anti-tumor immune response

In the past decades it has become clear that the metabolic alterations of tumor cells are not only providing a biosynthetic and energetic advantage, but also shape the tumor microenvironment to suppress the anti-tumor immune response. Thereby, it connects two hallmarks of cancer, “altered energy metabolism” and “evading the immune response” (Hanahan and Weinberg, 2011). Several reports showed that T cells isolated from the tumor environment are metabolically and functionally impaired, as they show indicators of a decreased mitochondrial fitness (Siska et al., 2017; Zhang et al., 2017) and an impaired upregulation of glycolytic activity (Hartmann et al., 2020; Siska et al., 2017). This can be attributed to the intra-tumoral environment characterized by nutrient restriction and accumulation of toxic tumor metabolites. The relationship of the tumor metabolism and the anti-tumor immune response are discussed in more detail elsewhere (Guerra et al., 2020; Leone and Powell, 2020; Renner et al., 2017). As the presented thesis focuses on the link between glucose metabolism of tumor cells and the anti-tumor response of T cells, the following part will focus on this metabolic pathway.

1.5.2.1. Glucose restriction

The increased glycolytic flux of tumor cells causes a depletion of glucose in the tumor environment. Depending on the tumor entity, the interstitial fluid of solid tumors, the concentration of free glucose was found to be up to 10 fold lower than in the blood or the healthy tissue (Gullino et al., 1964; Ho et al., 2015).

As described above, glucose restriction affects the functionality of murine and human T cells distinctly (see chapter 1.3.1). Glucose has been shown to be essential for murine T cell effector functions in numerous studies. AMPK has been identified as a molecular sensor of murine T cells for metabolic stress, blocking Ifn-γ and increasing OXPHOS activity upon glucose starvation, thereby ensuring T cell persistence (Blagih et al., 2015). It has been proposed that TILs and tumor cells compete for the limited glucose in the TME and glucose limitation inhibits the secretion of pro-inflammatory cytokines in murine sarcoma models by limiting the mTOR-associated signaling (Chang et al., 2015; Ho et al., 2015). Moreover, low glucose levels suppress the generation of phosphoenolpyruvate, an glycolytic intermediate, disrupting the Ca^{2+}-dependent NFAT-signaling *in vitro* (Ho et al., 2015). However, another study suggests that upon glucose starvation or glycolytic inhibition T cells can switch towards an oxidative metabolic state and thereby maintain cytokine production (Salerno et al., 2016).

Human T cells seem to be less sensitive towards glucose restriction than murine T cells, however, the relevance of glucose fuel for human T cell functionality is still a matter of debate. Glucose restriction or glycolytic inhibition attenuated proliferation of human T cells but did not affect secretion of IFN-γ, TNF or IL-2 (Renner et al., 2015; Renner et al., 2019; Sanchez et al., 2020). However, it has been proposed by others that glucose restriction negatively affects the IFN-γ production of naïve T cells upon both initial stimulation and restimulation, but Tcm and Tem are more resistant to glucose restriction (Ecker et al., 2018). Moreover, Zhao et al. reported that inhibition of T cell function after incubation with tumor-conditioned supernatants could be reverted by adding additional glucose (Zhao et al., 2016).

1.5.2.2. Effects of lactate secretion

The high glycolytic activity of tumor cells is accompanied by the production of lactate, which also accumulates in the tumor environment. Several studies have shown a dramatic increase in lactate concentrations within solid tumors reaching levels of up to 40 mM (Brand et al., 2016; Holm et al., 1995; Walenta and Mueller-Klieser, 2004). High lactate levels within tumors revealed to be an important factor in the development of cancer cells and immune evasion. The accumulation of lactate correlates with a poor overall survival or tumor recurrence e.g. in cervix cancer and head-and-neck cancer (HNSCC) (Blatt et al., 2016; Walenta and Mueller-Klieser, 2004) as well as with the incidence of metastasis in cancer of the rectum, cervix and HNSCC (Brizel et al., 2001; Walenta et al., 1997; Walenta et al., 2000; Walenta and Mueller-Klieser, 2004). Moreover, high expression of glycolytic genes in tumors has been linked to the failure of adoptive T cell transfer (Cascone et al., 2018; Ho et al., 2015) and immune checkpoint inhibition therapy (Renner et al., 2019). These data already indicate a direct

immunomodulatory role of lactate and some have even proposed the lactate production as the “explanation and purpose” of the Warburg effect (San-Millán and Brooks, 2017).

The transport of lactate by MCTs is proton-coupled. Therefore, a high aerobic glycolysis of tumor cells leads to side-by-side accumulation of lactate and protons, hence designated as lactic acid accumulation. It is well accepted that an acidic microenvironment, as caused by proton accumulation, is unfavorable for a proper immune cell function. Acidity can activate HIF even under normoxic conditions, thus enhancing the glycolytic phenotype of tumor cells (Mekhail et al., 2004). A low tumor pH is associated with a poor outcome of patients receiving checkpoint inhibition therapy and decreases effector functions of T cells (Calcinotto et al., 2012; Zhang et al., 2019). In line, it has been reported that neutralization of the environmental pH increases T cell functionality *in vivo* (Uhl et al., 2020) and enhances the efficacy of immunotherapy (Pilon-Thomas et al., 2016).

However, it is still a matter of conflict whether high lactate levels at normal pH also have an inhibitory and modulatory effect on immune cells. Haas et al. showed that extracellular sodium lactate is taken up by T cells via the sodium-coupled transporter SLC5A12. This leads to a switch in cytokine profile and motility loss of CD4 T cells and loss of cytotoxicity of CD8 T cells (Haas et al., 2015). Another group has shown that accumulation of lactate in the environment of activated T cells leads to metabolic rewiring promoting the differentiation of Th17 cells (Pucino et al., 2019). Angelin et al. have conducted their studies on lactate sensitivity of Treg and Tconv using sodium lactate and described an inhibition of the proliferation of Tconv, but not Treg (Angelin et al., 2017). In contrast, in our hands only lactic acid, but not sodium lactate led to inhibition of T cell function (Brand et al., 2016; Fischer et al., 2007).

Several studies have investigated the influence of lactic acid on different entities of immune cells. Upon stimulation, T cells upregulate the expression of the lactate transporters MCT-1 and MCT-4, allowing a simultaneous import of lactate and protons. Consequently, lactic acid treatment leads to intracellular lactate accumulation and acidification, dose-dependently inhibits effector functions and proliferation and induces apoptosis in isolated TILs in higher concentrations (Brand et al., 2016; Fischer et al., 2007; Haas et al., 2015; Mendler et al., 2012). A similar effect has been described for NK cells (Brand et al., 2016; Harmon et al., 2019; Husain et al., 2013). The inhibitory effects on T cells is mainly mediated by a block of the cellular metabolism as the lactate produced by activated T cells cannot longer be secreted into the environment (Fischer et al., 2007). Mechanistically, high extracellular lactic acid concentrations lead to a decreased phosphorylation of p38 and JNK in CTLs (Mendler et al., 2012) and diminishes the NFATc1 level (Brand et al., 2016), which are key molecules in mediating the IFN-γ secretion. Similar inhibitory effects of lactic acid have been observed in myeloid cells. Lactic acid inhibits the proper differentiation of monocytes into dendritic cells,

limiting their antigen presentation and IL-12 production (Gottfried et al., 2006), and also inhibits the secretion of TNF of monocytes upon activation. However, these cells seem to be more resistant to lactic acid than T cells as they survive lactic acid at higher concentrations (Dietl et al., 2010).

Lactic acid not only directly inhibits important immune cell functions, but also contributes to the shaping of the TME towards a more immunosuppressive, anti-inflammatory environment. Lactic acid induces polarization of macrophages towards an tumor-promoting phenotype, which is mediated by the stabilization of HIF-1α (Colegio et al., 2014; Ohashi et al., 2017). HIF-1α upregulates the expression of VEGF, and in line is has been demonstrated that lactic acid treatment facilitates angiogenesis (Song et al., 2018). Furthermore, lactic acid leads to an increased production of IL-23 by tumor-associated macrophages, which in turn drives the differentiation of tumor-promoting Th17 cells (Shime et al., 2008). It has also been shown that Foxp3 expressed by Treg suppresses the activity of MYC, therefore favors the activity of OXPHOS and increases the resistance of Treg towards high lactate levels in the tumor environment (Angelin et al., 2017).

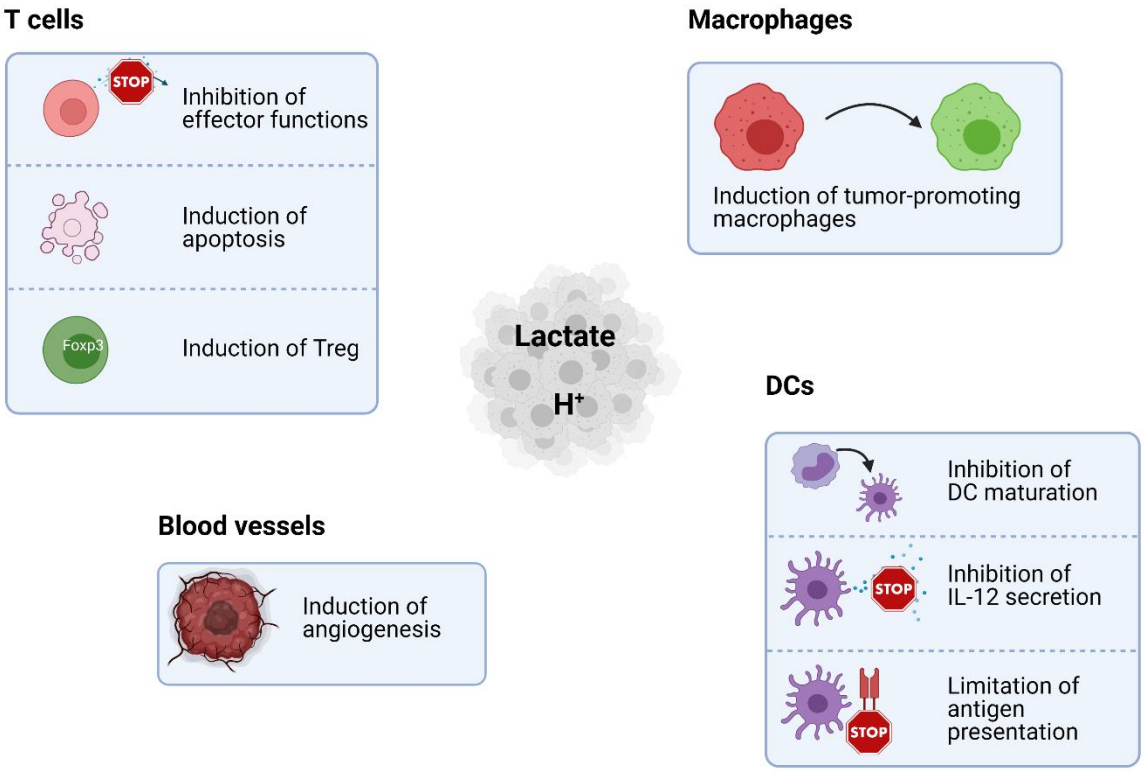

Figure 1-3: Effects of lactate and proton accumulation on cells in the tumor microenvironment. *DC: dendritic cells; Treg: Regulatory T cells. Created with BioRender.com.*

Thus, a high aerobic glycolysis of tumor cells affects the anti-tumor immune response at different important levels (summarized in Figure 1-3). Therefore, modulating the tumor and immune cell metabolism may be a promising strategy to enhance the anti-tumor immunity.

1.6. Metabolic manipulation as an emerging anti-cancer strategy

Modulating the cellular metabolism to enhance the anti-tumor immunity has raised increasing attention during the last years and is now accepted as an important component of tumor therapy. Hereby, two different strategies have been developed: First, the manipulation of the tumor cell metabolism itself by metabolic inhibitors and second, the genetic or pharmacological manipulation of the immune cell metabolism prior to adoptive cell transfer.

1.6.1. Manipulation of tumor cell glucose metabolism

Up to now, several different metabolic inhibitors with therapeutic potential have been developed and some are even tested in clinical trials (Leone and Powell, 2020). Among those, also several agents targeting glucose metabolism are in use. The glycolytic metabolism of tumor cells can be targeted on different levels. Inhibiting the glucose uptake and metabolism is a promising strategy to inhibit the glycolysis of tumor cells. The compounds WZB-117 (GLUT-1 inhibitor), dimethyl fumarate (GAPDH inhibitor), NCI-006 and NCI-737 (LDH inhibitors) or dichloroacetate (PDHK1 inhibitors) demonstrated substantial anti-tumor effects in pre-clinical studies. Dichloroacetate and dimethyl fumarate are currently tested in phase II clinical trials (Dunbar et al., 2014; Kornberg et al., 2018; https://clinicaltrials.gov/ct2/show/NCT02546440, 2019; Leone and Powell, 2020; Sanford Health, 2020; Xie et al., 2014; Yeung et al., 2019; Zhang et al., 2018). In addition, inhibition or siRNA-mediated silencing of LDHA have been shown to enhance the efficacy of an adoptive T cell transfer therapy or immune checkpoint inhibition therapy in the murine system (Cascone et al., 2018; Zhang et al., 2019).

Besides targeting glucose metabolism, inhibiting lactate secretion of tumor cells is an emerging strategy to modify the tumor metabolism and composition of the TME. To maintain the high glycolytic flux, lactate must be secreted into the cellular environment, which is mainly conducted by proton-coupled monocarboxylate transporters. MCTs are encoded by genes belonging to the SLC16 gene family including fourteen different members comprising five transporters with proven lactate transporting activity. The most abundant lactate transporter is MCT-1, which is encoded by the gene SLC16A1. In highly glycolytic cells, as tumor cells or activated T cells, the expression of MCT-4 (encoded by SCL16A3) is upregulated. In addition, MCT-2 and MCT-3 (encoded by SLC16A7 and SLC16A8) are described to have lactate-transporting activity. Whilst MCT-2 is expressed in different cells and tissues, including testis,

barin regions and T cells, MCT-3 is exclusively found in the retina (reviewed by Bosshart et al., 2021; Felmlee et al., 2020; Halestrap, 2012).

The inhibition of lactate secretion by blocking MCTs has been proven to enhance the anti-tumor immunity in different pre-clinical studies. The inhibition of MCT-1 led to an increased radiosensitivity of SCLC xenografts (Bola et al., 2014) and reduces cell proliferation and viability of human tumor cell lines (Doherty et al., 2014). Consequently, inhibitors for MCT-1 are currently tested in clinical trials (https://www.clinicaltrials.gov/ct2/show/NCT01791595, 2021). Recently, we were able to demonstrate that a combined inhibition of MCT-1 and MCT-4 by diclofenac increases the intra-tumoral pH and enhances the efficacy of immune checkpoint blockade therapy *in vivo* (Renner et al., 2019).

As a low environmental pH is an important characteristic of many solid tumors, neutralizing this pH is an additional strategy to increase the immune response *in vitro* and *in vivo*. As the lactate export via MCTs is proton dependent, one way to achieve this goal is blocking the lactate dehydrogenase or the MCT transporters itself. This has already been successfully demonstrated *in vitro* and *in vivo* (Cascone et al., 2018; Renner et al., 2019; Zhang et al., 2019). Besides, buffering the acidic pH by oral administration of bicarbonate or treatment with the proton-pump inhibitor esomeprazole has been demonstrated to be beneficial for the anti-tumor response *in vivo* (Calcinotto et al., 2012; Pilon-Thomas et al., 2016).

1.6.2. Manipulation of immune cell metabolism

Adoptive cell transfer therapy (ACT) has been developed several years ago to broaden the therapeutic possibilities in tumor patients. For this therapy, T cells are isolated from the patients' blood and either selected for tumor specific T cell clones or modified with a recombinant TCR or chimeric antigen receptor (CAR) specific for tumor epitopes. After an expansion phase, the T cells are transferred back to the patient, which in theory should lead to a robust T cell response against the tumor mediated by the specific T cells. By now, four different CAR T cell therapies are approved by the FDA for the treatment of hematological malignancies (Mullard, 2021) and several clinical studies using T cell therapeutics for the treatment of different cancer entities have entered a phase I or phase II clinical study (Met et al., 2019). Nevertheless, most studies demonstrate an overall response rate (ORR) below 50 % for most solid tumors (Met et al., 2019). Studies using TCR-engineered T cells directed against the tumor-testis antigen NY-ESO-1 have reached complete remission in 80 % of patients suffering from multiple myeloma (Rapoport et al., 2015), but only in 12 % of treated sarcoma and melanoma patients (Robbins et al., 2011). Similar, studies using T cells directed against glycoprotein 100 (gp100) or melan A (MART-1) for treatment of melanoma patients

achieved only 19 % or 13 % ORR, respectively (Johnson et al., 2009; Morgan et al., 2006). This failure of specific T cells could be a direct consequence of the suppressive TME: No matter how specific a T cell is, it must withstand the conditions within the tumor to mediate a successful anti-tumor response. Therefore, besides modulating the TME itself, modulating the T cell metabolism to resist the toxic conditions in solid tumors is a promising approach to increase the efficacy of ACT therapeutics.

Basically, the attempts to enhance the T cell fitness on a metabolic level can be separated in two different ways: First, the modification of the culture conditions during the expansion phase before ACT and second, the genetic modification of T cells themselves. Notably, none of these models has proceeded to the clinical use so far and were studied in mice models.

The quality of the transferred T cells plays a crucial role in the efficacy of ACT. During a long expansion phase or after initial immune response, T cells enter an exhausted, non-responding state and do not develop their full anti-tumor potential after transfer. Therefore, the timepoint as well as the subset composition of the transferred T cells is critical for ACT outcome. In line, it has been shown that the acquisition of full effector functions during the expansion dampens the anti-tumor efficacy *in vivo* (Gattinoni et al., 2005). Meanwhile, it has become clear that the anti-tumor effect after transfer of less differentiated Tcm or Tscm cells is superior compared to naïve or Tem cells (Gattinoni et al., 2011). Accordingly, expanding the cells with IL-15 instead of IL-2, which is known to generate more memory-like T cells, leads to an enhanced anti-tumor response after transfer (Klebanoff et al., 2004).

Several studies investigated the effects of modifying the nutrient conditions during the expansion phase before ACT and discovered, that this manipulation of the cellular metabolism shapes the T cell phenotype and increases the efficacy of ACT. Buck and colleagues were able to show that a pharmacological induction of mitochondrial fusion before ACT enhances the mitochondrial T cell metabolism, induces a memory-like phenotype and prolongs the survival of lymphoma bearing mice (Buck et al., 2016). Similarly, the inhibition of glycolysis either by glucose restriction, inhibition of the LDH or administration of 2-DG drove the T cells into a memory-like phenotype and increases their potential after ACT (Hermans et al., 2020; Klein Geltink et al., 2020; Sukumar et al., 2013). By contrast, the culture of T cells under hypoxic conditions causing a switch towards a more glycolytic phenotype, as well enhances their cytolytic function and increases efficacy of ACT in a B16 mouse melanoma model, showing that the mitochondrial metabolism is not the solely way to go in this direction (Gropper et al., 2017). Besides modifying glucose metabolism, culturing the cells with high levels of arginine has been discovered as a potential way to increase ACT efficacy (Geiger et al., 2016).

Another approach is, to manipulate the T cell metabolism on a genetic level by deletion or overexpression of proteins. This has the advantage, that these manipulations are stable and

therefore persist as a new T cell feature also when the cells face toxic TME conditions. Zhang and colleagues used T cells lacking HIF-1α and found increased fatty acid oxidation and enhanced anti-tumor effects in these cells (Zhang et al., 2017). Overexpression of PGC1α, a master regulator of mitochondrial biogenesis, increased T cell mitochondrial content and enhanced their anti-tumor efficacy (Scharping et al., 2016). Ho et al. demonstrated, that overexpressing the phosphoenol-pyruvate carboxykinase 1 (PCK1), an enzyme converting oxalacetate to phosphoenol-pyruvate, reprograms the metabolism of T cells and thereby rescues the T cell function in a low glucose environment and increases the anti-tumor response of the T cells after ACT.

These studies demonstrate that metabolic reprogramming of the TME or immune cells before ACT is as promising approach to enhance the efficacy of immune therapies in general and open exiting opportunities in addition to conventional therapies in clinical use.

1.7. Scientific question

The impact of the tumor microenvironment on immune cell function has raised emerging attention during the last years. Especially the consequences of the Warburg phenotype on the T cell-based anti-tumor immunity have been elucidated. It has become obvious, that aerobic glycolysis and lactic acid itself are important determinants of T cell function in the tumor environment and that the therapeutic outcome of an adoptive T cell transfer therapy is deeply affected by the glycolytic activity of the patients tumor (Cascone et al., 2018). As the tumor therapy with adoptively transferred T cells is more and more developing to a state-of-the-art option for a broad range of cancer entities, it is of strong interest to find ways to effectively manipulate the T cell metabolism to cope with high levels of lactic acid.

The aim of this study was to enhance the resistance of T cells towards lactic acid by genetic or pharmacological modification of their lactic acid metabolism.

2. Material

2.1. Equipment

Aria cell sorter	BD Biosciences, Franklin Lakes, NJ, USA
Autoclave	Systec,, Linden, Germany
Avanti J-20 XP centrifuge	Beckman Coulter, Brea, CA USA
CASY Cell Counter	Roche Innovatis, Bielefeld, Germany
Centrifuge 5424R	Eppendorf, Hamburg, Germany
CFX Connect	BioRad, Hercules, CA, USA
Evos Cell Imaging System	AMG, Thermo Fisher Scientific, Waltham, MA, USA
FACSCalibur™ Flow Cytometer	BD Biosciences, Franklin Lakes, NJ, USA
FACSCelesta™ Flow Cytometer	BD Biosciences, Franklin Lakes, NJ, USA
Forceps	Aesculap, Tuttlingen, Germany
Fusion Pulse	Vilber Lourmat, Eberhardzell, Germany
Hemocytometer	Marienfeld, Lauda-Königshofen, Germany
Incubators	Haereus, Osterode, Germany Thermo Fisher Scientific, Waltham, MA, USA
Laminar Flow cabinet	Haereus, Osterode, Germany and Thermo Fisher Scientific, Waltham, MA, USA
Light Cycler 480	Hoffmann-La Roche, Basel, Switzerland
LSRFortessa™ Flow Cytometer	BD Biosciences, Franklin Lakes, NJ, USA
MACSiMAG separator	Miltenyi Biotec, Bergisch Gladbach, Germany
Mastercycler nexus gradient	Eppendorf, Hamburg, Germany
Megafuge 16 R	Eppendorf, Hamburg, Germany
Microfuge	Haereus, Osterode, Germany
Microscopes	Zeiss, Oberkochen, Germany
Mini-Protean Tetra electrophoresis system	BioRad, Hercules, CA, USA
Multifuge X3 FR	Eppendorf, Hamburg, Germany
Multipette	Eppendorf AG, Hamburg, Germany
Nanodrop nd-1000	VWR International, Radnor, PA, USA
Oxygraph O2K	Oroboros instruments, Innsbruck, Austria
pH meter inolab 730	WTW, Weilheim, Germany
Picofuge	Haereus, Osterode, Germany

Pipetboy	Integra, Biebertal, Germany
Pipettes	Eppendorf AG, Hamburg, Germany
Power Supply EV1450	Consort, Turnhout, Belgium
PowerPac Power Supply	BioRad, Hercules, CA, USA
QuadroMACS™	Miltenyi Biotec, Bergisch Gladbach, Germany
Quickgel electrophoresis system	Helena Biosciences, Gateshead, UK
Repetitive Pipette HandyStep	Brand, Wertheim, Germany
SAS-MX electrophoresis system	Helena Biosciences, Gateshead, UK
SDR sensor dish reader	Presens, Regensburg, Germany
Sepatech Megafuge 3.0R	Haereus, Osterode, Germany
ShakerVibrax-VXR	IKA, Staufen, Germany
Sonorex Ultrasonic bath	Branson, Danbury, CT, USA
TapeStation	Agilent Technologies, Santa Clara, CA, USA
Tecan Spark 10M	Tecan, Männedorf, Switzerland
Thermomixer	Eppendorf, Hamburg, Germany
Vortexer	Scientific Industries, Bohemia, NY, USA
Water purification system	Millipore, Eschbach, Germany
Waterbath	Julabo, Seelstadt, Germany
Wellwash 4 M2K	Thermo Fisher Scientific, Waltham, MA, USA
Western Blot chamber	Biometra, Göttingen, Germany

2.2. Plastic materials and consumables

Casy Cups	OMNI Life Science, Bremen, Germany
Cell culture dish (96 well, U bottom)	BD Biosciences, Franklin Lakes, NJ, USA
Cell culture dishes, flat bottom	Eppendorf, Hamburg, Germany
Cell culture flasks	Eppendorf, Hamburg, Germany
Cell culture petri dish	Eppendorf, Hamburg, Germany
Cell scrapers	Sarstedt, Nümbrecht, Germany
Cell strainer (100 µm)	BD Biosciences, Franklin Lakes, NJ, USA
Combitips for Multipette	Eppendorf, Hamburg, Germany and Brand, Wertheim, Germany
Cryo tubes	Corning Costar, Corning, NY, USA
Falcon tubes (15 ml, 50 ml, 225 ml)	BD Falcon, Franklin Lakes, NJ, USA

Hard-Shell 96 well PCR plates, low profile, skirted, clear	BioRad, Hercules, CA, USA
Hydrodish HD24 plates	Presens, Regensburg, Germany
Immobilon-P PVDF membrane	Millipore, Eschbach, Germany
LS columns	Miltenyi Biotec, Bergisch Gladbach, Germany
Micro test tubes (1.5 ml, 2 ml)	Sarstedt, Nümbrecht, Germany
Micro test tubes, PCR-compatible (0.5 ml, 1.5 ml, 2 ml)	Sarstedt, Nümbrecht, Germany
Microseal B adhesive seal	BioRad, Hercules, CA, USA
Needles, disposable	BD Biosciences, Franklin Lakes, NJ, USA
Nunc™ Multidish (12 well) with UpCell surface	Thermo Fisher Scientific, Waltham, MA, USA
Oxodish OD24 plates	Presens, Regensburg, Germany
Petri dishes	Greiner, Kremsmünster, Austria
Pipette tips	Eppendorf, Hamburg, Germany
Polystyrene test tubes	BD Biosciences, Franklin Lakes, NJ, USA
Polystyrene test tubes with cell strainer cap	BD Biosciences, Franklin Lakes, NJ, USA
Scalpels, disposable	Feather safety razor, Ozaka, Japan
Serological pipettes	Greiner, Kremsmünster, Austria
Stericup vacuum filter bottles, 0.2 µm	Millipore, Eschbach, Germany
Stripwell microplates	Corning Costar, Corning, NY, USA
SurPhob SafeSeal® filter tips	Biozym Scientific, Hessisch Oldendorf, Germany
Syringe filters, sterile	Sartorius, Göttingen, Germany
Syringes, disposable	BD Biosciences, Franklin Lakes, NJ, USA
Whatman Chromatography Paper	GE Healthcare, Chicago, IL, USA

2.3. Media, buffers and solutions

Acrylamide/Bisacrylamide (30 %)	Carl Roth, Karlsruhe, Germany
RPMI1640, without L-Glutamine	Thermo Fisher Scientific, Waltham, MA, USA
RPMI1640, without Glucose, without sodium bicarbonate, powder	Sigma-Aldrich, St. Louis, MO, USA
RPMI1640, without Glucose, without L-Glutamine	neoFroxx, Einhausen, Germany
DMEM, with 4.5 g/l glucose, without L-Glutamine, Pyruvate	Thermo Fisher Scientific, Waltham, MA, USA

Isoton II	Beckman Coulter, Brea, CA USA
2-Mercaptoethanol, for cell culture	Thermo Fisher Scientific, Waltham, MA, USA
2-Mercaptoethanol, for analyses	Sigma-Aldrich, St. Louis, MO, USA
MEM Essential vitamins	Thermo Fisher Scientific, Waltham, MA, USA
MEM Non-essential amino acids	Thermo Fisher Scientific, Waltham, MA, USA
Penicillin/Streptomycin	Thermo Fisher Scientific, Waltham, MA, USA
L-Glutamine	PAN Biotech, Aidenbach, Germany
AB-serum, human	Bavarian Red Cross, München, Germany
Fetal calf serum (FCS)	Sigma-Aldrich, St. Louis, MO, USA
Bovine serum albumin	Sigma-Aldrich, St. Louis, MO, USA
Dimethlysulfoxide (DMSO)	Carl Roth, Karlsruhe, Germany
Ammonium persulfate (APS)	Sigma-Aldrich, St. Louis, MO, USA
RIPA buffer	Sigma-Aldrich, St. Louis, MO, USA
Cell Lysis Buffer	Cell Signalling Technology, Danvers, MA, USA
Sodium dodecyl sulfate (SDS)	Sigma-Aldrich, St. Louis, MO, USA
MEM Sodium Pyruvate	Thermo Fisher Scientific, Waltham, MA, USA
EDTA UltraPure	Thermo Fisher Scientific, Waltham, MA, USA
Trypsin/EDTA	Thermo Fisher Scientific, Waltham, MA, USA
Tween20	Sigma-Aldrich, St. Louis, MO, USA
Dulbecco's Phosphate Buffered Saline (DPBS)	PAN Biotech, Aidenbach, Germany
Hank's Balanced Salt Solution (HBSS)	PAN Biotech, Aidenbach, Germany
Casy Clean	Hoffmann-La Roche, Basel, Switzerland
H_2O_2	Sigma-Aldrich, St. Louis, MO, USA
H_2O_{bidest}	Braun, Kronberg im Taunus, Germany
PCR-H_2O	Thermo Fisher Scientific, Waltham, MA, USA
Glycine	Carl Roth, Karlsruhe, Germany
ε-Amino-n-capronic acid	Sigma-Aldrich, St. Louis, MO, USA
Hydrochloric acid	Merck, Darmstadt, Germany
Methanol	Merck, Darmstadt, Germany
Ethanol	Carl Roth, Karlsruhe, Germany
Acetic acid	Carl Roth, Karlsruhe, Germany
Trizma Base	United States Biological, Salem, MA, USA
Tetramethylethylendiamin	Merck, Darmstadt, Germany

FACS Flow	BD Biosciences, Franklin Lakes, NJ, USA
FACS Clean	BD Biosciences, Franklin Lakes, NJ, USA
FACS Rinse	BD Biosciences, Franklin Lakes, NJ, USA
Isopropanol, 70 %	Braun, Kronberg im Taunus, Germany
Gelatine solution 0.1 %	PAN Biotech, Aidenbach, Germany
Pancoll, human	PAN Biotech, Aidenbach, Germany
Glycerin	Merck, Darmstadt, Germany
Bromphenole blue	Sigma-Aldrich, St. Louis, MO, USA
Sodium chloride	Merck, Darmstadt, Germany

2.4. Enzymes, Kits and Reagents

10x Annexin V Binding buffer	BD Biosciences, Franklin Lakes, NJ, USA
2-NBD Glucose (2-NBDG)	Thermo Fisher Scientific, Waltham, MA, USA
5-(N-Ethyl-N-isopropyl)-amiloride (EIPA) in DMSO	Sigma-Aldrich, St. Louis, MO, USA
7-Amino-Actinomycin D (7-AAD)	BD Biosciences, Franklin Lakes, NJ, USA
Acetazolamide in DMSO	Selleckchem Chemicals, Houston, TX, USA
Acetyl salicylic acid (ASA) in medium	Fagron, Glinde, Germany
ATP determination kit	Thermo Fisher Scientific, Waltham, MA, USA
Bafilomycin in Medium	Sigma-Aldrich, St. Louis, MO, USA
BD Comp Beads	BD Biosciences, Franklin Lakes, NJ, USA
BD Cytofix/Cytoperm	BD Biosciences, Franklin Lakes, NJ, USA
BD GolgiStop (Monensin)	BD Biosciences, Franklin Lakes, NJ, USA
Bio-Rad DC Protein assay kit	BioRad, Hercules, CA, USA
Brilliant Stain Buffer	BD Biosciences, Franklin Lakes, NJ, USA
Carbonyl cyanide-p-trifluoro-methoxyphenylhydrazone in Ethanol	Sigma-Aldrich, St. Louis, MO, USA
Carboxy SNARF-1 AM acetate	Thermo Fisher Scientific, Waltham, MA, USA
Carboxyfluoresceinsuccimidylester (CFSE)	Sigma-Aldrich, St. Louis, MO, USA
CD4 (L3T4) MicroBeads, mouse	Miltenyi Biotec, Bergisch Gladbach, Germany
CD4 MicroBeads, human	Miltenyi Biotec, Bergisch Gladbach, Germany
CD8 MicroBeads, human	Miltenyi Biotec, Bergisch Gladbach, Germany
$CD8^+$ T cell Isolation Kit, mouse	Miltenyi Biotec, Bergisch Gladbach, Germany

CutSmart buffer	New England Biolabs, Frankfurt (Main), Germany
Cyclosporine A (Sandimmun®)	Novartis, Basel, Switzerland
D-Glucose in Medium	Sigma-Aldrich, St. Louis, MO, USA
Diclofenac sodium salt in Medium	Sigma-Aldrich, St. Louis, MO, USA
dNTP-Mix	Hoffmann-La Roche, Basel, Switzerland
DuoSet ELISA human IFNγ	R&D systems, Minneapolis, MN, USA
DuoSet ELISA human IL-10	R&D systems, Minneapolis, MN, USA
DuoSet ELISA human IL-17	R&D systems, Minneapolis, MN, USA
DuoSet ELISA human TNFα	R&D systems, Minneapolis, MN, USA
DuoSet ELISA mouse IFNγ	R&D systems, Minneapolis, MN, USA
DuoSet ELISA mouse TNFα	R&D systems, Minneapolis, MN, USA
Dynabeads™ Human T-Activator CD3/CD28	Thermo Fisher Scientific, Waltham, MA, USA
ECL™ Prime Western Blot Detection Reagent	GE Healthcare, Chicago, IL, USA
EcoRI	New England Biolabs, Frankfurt a.M., Germany
EndoFree Plasmid Maxi Kit	Qiagen, Hilden, Germany
FcR blocking reagent	Miltenyi Biotec, Bergisch Gladbach, Germany
Foxp3 staining kit	Thermo Fisher Scientific, Waltham, MA, USA
Glukose (HK) assay kit	Sigma-Aldrich, St. Louis, MO, USA
IL-15	PeproTech, Rocky Hill, NJ, USA
IL-2	PeproTech, Rocky Hill, NJ, USA
Intracellular pH Calibration Kit	Thermo Fisher Scientific, Waltham, MA, USA
Ionomycin	Enzo life sciences, Farmingdale, NY, USA
Ketoprofen	Sigma-Aldrich, St. Louis, MO, USA
Ligase	New England Biolabs, Frankfurt a.M., Germany
Ligase buffer	New England Biolabs, Frankfurt a.M., Germany
Lipopolysaccharide (LPS)	Enzo life sciences, Farmingdale, NY, USA
L-Lactic acid in Medium	Sigma-Aldrich, St. Louis, MO, USA
Lactic acid-13C3 solution	Sigma-Aldrich, St. Louis, MO, USA
LR Clonase II enzyme mix	Thermo Fisher Scientific, Waltham, MA, USA
Mitotracker Green FM	Thermo Fisher Scientific, Waltham, MA, USA
M-MLV Reverse Transcriptase	Promega, Madison, WI, USA
Myxothaizol in Ethanol	Sigma-Aldrich, St. Louis, MO, USA

NCI-737 in DMSO	Provided by Dr. Chi van Dang, Ludwig Institute for Cancer Research, Brussels, Belgium
Oligomycin in Ethanol	Sigma-Aldrich, St. Louis, MO, USA
Pantoprazole in Medium	Selleckchem Chemicals, Houston, TX, USA
Phenylmethylsulfonylfluoride (PMSF)	Hoffmann-La Roche, Basel, Switzerland
Phorbol-12-myristate-13-acetate (PMA)	Calbiochem, Merck Millipore, Burlington, MA, USA
Polybrene	Sigma-Aldrich, St. Louis, MO, USA
Precision Plus Protein Kaleidsokop protein standard	BioRad, Hercules, CA, USA
Protease Inhibitor Cocktail	Hoffmann-La Roche, Basel, Switzerland
QIAPrep Spin Miniprep Kit	Qiagen, Hilden, Germany
QuantiFast SYBR Green PCR Kit	Qiagen, Hilden, Germany
Qubit Protein Determination Kit	Thermo Fisher Scientific, Waltham, MA, USA
Quickgel LD Isoenzyme Kit	Helena Biosciences, Gateshead, UK
R-(+)-GNE-140 in DMSO	Selleckchem Chemicals, Houston, TX, USA
Random Decamer Primers	Thermo Fisher Scientific, Waltham, MA, USA
Reagent Diluent Concentrate	R&D systems, Minneapolis, MN, USA
ReBlot Plus Mild Antibody Stripping Solution	Merck, Darmstadt, Germany
Retronectine in PBS	Takara, Kyoto, Japan
RNeasy Micro Kit	Qiagen, Hilden, Germany
RNeasy Mini Kit	Qiagen, Hilden, Germany
Rotenone in Ethanol	Sigma-Aldrich, St. Louis, MO, USA
SAS-MX LD Vis Kit	Helena Biosciences, Gateshead, UK
Sodium bicarbonate	Merck, Darmstadt, Germany
Sodium L-Lactate in Medium	Sigma-Aldrich, St. Louis, MO, USA
Substrate Reagent Pack	R&D systems, Minneapolis, MN, USA
TransIT-293	Mirus Bio, Madison, WI, USA
TransIT-LT	Mirus Bio, Madison, WI, USA
Treg Expansion Kit	Miltenyi Biotec, Bergisch Gladbach, Germany
Trypan blue	Sigma-Aldrich, St. Louis, MO, USA
U13C-Glucose in glucose-free medium	Cambridge Isotope Laboratories, Saint-Aubin, France
XhoI	New England Biolabs, Frankfurt a.M., Germany
Zombie NIR Fixiable Viability Dye	Thermo Fisher Scientific, Waltham, MA, USA

2.5. Antibiotics

Ampicillin	Carl Roth, Karlsruhe, Germany
Puromycin dihydrochloride	Sigma-Aldrich, St. Louis, MO, USA

2.6. Oligonucelotides

2.6.1. DNA constructs and vectors for retroviral transduction

LDHB construct	Integrated DNA Technologies, Coralville, IA, USA
Ldhb construct	Thermo Fisher Scientific, Waltham, MA, USA
MSCV-Thy1.1	AG Feuerer, Regensburg Center for Interventional Immunology
pCL-Eco	AG Feuerer, Regensburg Center for Interventional Immunology
pCOLT-GALV	AG Thomas, Regensburg Center for Interventional Immunology
pHIT60	AG Thomas, Regensburg Center for Interventional Immunology
pMX-IRES-Puro	AG Thomas, Regensburg Center for Interventional Immunology

2.6.2. siRNAs

ON-TARGETplus Human LDHA	Dharmacon, Lafayette, CO, USA
ON-TARGETplus Non-targeting pool	Dharmacon, Lafayette, CO, USA

siRNAs were dissolved in PCR-grade H_2O to a final concentration of 1 µg/µl, aliquoted and stored at -20 °C.

2.6.3. Oligonucleotides used for quantitative real-time PCR

The listed oligonucleotides were designed as described below and synthesized by euorofins scientific, Luxemburg.

Gene	Sequence (Forward and Reverse)
18s rRNA	5’-ACCGATTGGATGGTTTAGTGAG-3’ 5’-CCTACGGAAACCTTGTTACGAC-3’
AE1 (SLC4A1)	5’-TTCAAGCCACCCAAGTATCACCC-3’ 5’-GGACTTCACCACCCACAGCA-3’
AE2 (SLC4A2)	5’-TGCTCACCCGTATCTTCACCGA-3’ 5’-ACACCCTCCCGCTCATCAAACAC-3’

CA12	5’-ATTCTTGGCATCTGTATTGTGGTGGT-3’
	5’-TGGTGGCTGGCTTGTAAATGACTC-3’
CA2	5’-AACAATGGTCATGCTTTCAACGTGGAG-3’
	5’-CCACAGTATGCTCTGAACCTTGTCC-3’
CA6	5’-CACTGAGAACGTCCACTGGTTTGTG-3’
	5’-GGGTCCTGCGGTAATCGTTGTG-3’
CA9	5’-GCCTTTGCCAGAGTTGACGAG-3’
	5’-CTCAGCGATTTCTTCCAAGCGAG-3’
GPR132	5’-CAGGAGCATCAAGCAGAGCATGG-3’
	5’-CGAAGCAGACTAGGAAGATGACAACCAC-3’
GPR4	5’-TGGACCACCTCTTTCCGCCA-3’
	5’-AGGTTCATCAGGTAGACGCCCAG-3’
GPR65	5’-GAAACAGTTGTTGAATATTGCGATGCCG-3’
	5’-GGTAGACTTTCCGGTTGCAGATCAG-3’
GPR68	5’-GAACCACCTTCTATAAACAGGATGGCG-3’
	5’-CAGGTAGCCGAAGTAGAGGGACAG-3’
LDHA	5’-GGTTGGTGCTGTTGGCATGG-3’
	5’-TGCCCCAGCCGTGATAATGA-3’
LDHB	5’-GATGGTGGTTGAAAGTGCCTATGAAGTC-3’
	5’-AGCCACACTTAATCCAATAGCCCA-3’
MCT-1 (SLC16A1)	5’-GCAGCTTCTTTCTGTAACACCGT-3’
	5’-GTCGCCTCTTGTAGAAATACTTGCC-3’
MCT-4 (SLC16A3)	5’-GGCCCTGCCAATGATTGCT-3’
	5’-GCATCAGAGGGACGAAGAAGAGGA-3’
NHE-1 (SLC9A1)	5’-GAGAGCCGCCCTGTTAATCATTCC-3’
	5’-AAACCTATCTTCATGAGGCAGGCC-3’
NHE3 (SLC9A3)	5’-AACCTGTTCGTCAGCACCACC-3’
	5’-GCTCCTCTTCACCTTCAGCCAC-3’
NHE8 (SLC9A8)	5’-GGGAGAAGATGGCGGAAGAGGA-3’
	5’-GGGAGCACCAGTTTCGTCGT-3’
TCIRG1	5’-ATCCGCACCAACCGCTTCAC-3’
	5’-CCCGAACATCACAGCAAACAGGA-3’

2.7. Antibodies

2.7.1. Antibodies for Western Blotting

Specificity	Source	Species reactivity	Molecular weight	Dilution	Company
α-Aktin	Rabbit	Human, animals	42 kDa	1:2000	Sigma-Aldrich
α-Ldha	Rabbit	Human, animals	36 kDa	1:1000	Cell Signalling Technology
α-Ldhb	Mouse	Human, animals	36 kDa	1:4000	Santa cruz biotechnology

2.7.2. Antibodies for FACS Staining

2.7.2.1. Anti-Human antibodies

Antigen	Function	Conjugate	Clone	Company
α-CCR7	Lymph node homing receptor	FITC	I50503	BD biosciences
α-CD25	Activity related marker for T cells	PE-Cy7	M-A251	BD biosciences
α-CD4	Part of the T cell co-receptor	PE	RPA-T4	BD biosciences
α-CD4	Part of the T cell co-receptor	BV711	RM4-5	BioLegend
α-CD45RA	Lymphocyte maker	PE	HI30	BD biosciences
α-CD45RA	Differentiation marker of T cells	PE-Cy7	REA	Miltenyi biotec
α-CD45RO	Differentiation marker of T cells	PE	UCHK1	BD biosciences
α-CD62L	Lymph node homing receptor	APC	DREG-56	BD biosciences
α-FoxP3	Transcription factor	PE	PCH101	eBioscience
α-Granzyme B	Cytolytic protein produced by T cells	FITC	GB11	BD biosciences
α-IFN-γ	Effector cytokine of T cells	FITC	B27	BD biosciences
α-Ki-67	Marker of proliferating cells	AlexaFluor647	B56	BD biosciences
α-Perforin	Cytolytic protein produced by T cells	BV421	B-D48	BioLegend

α-TNF	Effector cytokine of T cells	BV421	Mab11	BioLegend

2.7.2.2. Anti-Mouse antibodies

Antigen	Function	Conjugate	Clone	Company
α-CD3ε	Part of the T cell receptor	BB700	145-2C11	BD biosciences
α-CD4	Part of the T cell co-receptor	PE	RM4-5	BD biosciences
α-CD90.1	Glycoprotein, Selection marker used for murine transduction	APC	OX-7	BioLegend
α-Ifn-γ	Effector cytokine of T cells	PE-Cy7	XMG1.2	BioLegend
α-Tnf	Effector cytokine of T cells	FITC	MP6-XT22	BioLegend

2.7.2.3. Antibodies without dedicated species reactivity

Antigen	Function	Conjugate	Clone	Company
Annexin V	Marker for early apoptosis	FITC	145-2C11	BD biosciences
HIS	Selection marker used for human transduction	APC	GG11-8F3.5.1	Miltenyi Biotec

2.8. Cell lines

For transduction of human T cells, the packaging cell line Platinum-A was used. This cell line was derived from 293-T cells and contains genes encoding the viral proteins *gag*, *pol* and *env,* which enables a rapid and efficient production of retroviruses (provided by Prof. Dr. Simone Thomas, Regensburg Center for Interventional Immunology, Regensburg, Germany).

The transduction of murine T cells was performed using Phoenix-Eco cells for the viral packaging. Similar to Platinum-A cells, this cell line was derived from 293-T cells and genetically modified for the more rapid and efficient production of ectotrophic retroviruses (provided by Prof. Dr. Markus Feuerer, Chair for Immunology, Regensburg Center for Interventional Immunology, Regensburg).

The colon cancer cell line HCT-116 was available in our lab stock.

2.9. Bacteria

E. coli JM109-Blue	Provided by Prof. Dr. Simone Thomas, Regensburg Center for Interventional Immunology, Regensburg
TOP10	Provided by Prof. Dr. Markus Feuerer, Chair for Immunology, Regensburg Center for Interventional Immunology, Regensburg

2.10. Software and Platforms

CellQuest Pro	BD, Heidelberg, Germany
CFX Maestro Software	BioRad, Hercules, CA, USA
Citavi 6	Swiss Academic Software gmbH, Wädenswil, Switzerland
Enrichr	Icahn School of Medicine at Mount Sinai, NY, USA
Evolution-Capt	Vilber Lourmat, Eberhardzell, Germany
FACSDiva	BD, Heidelberg, Germany
FlowJo v9.9.6 or v10.6.2	FlowJo, LLC, Ashland, OR, USA
Graph Pad Prism	GraphPad Software, La Jolla, CA, USA
Microsoft Excel 2009/2010	Microsoft Deutschland GmbH
PerlPrimer	Marshall, 2004
SensorDish-Reader Software	Presens, Regensburg, Germany
UCSC genome browser	University of California, CA, USA
www.biorender.com	BioRender, Toronto, Canada

3. Methods

3.1. Cell culture methods

Cells were handled under a laminar air flow cabinet using sterile consumables and kept at 37 °C, 5 % CO_2, 95 % relative humidity. Unless otherwise indicated, centrifugation was performed at 300 g, 4 °C for 7 minutes.

3.1.1. Culture of Cell lines

Platinum-A (PlatA) cells were cultured in DMEM (4.5 g/L Glucose) supplemented with 10 % FCS, 2 mM L-Glutamine, 50 IU/ml Penicillin, 50 µg/ml Streptomycin, 1 µg/ml Puromycin and 10 mg/ml Blasticidin. Phoenix-ECO and HCT116 cells were cultured in RPMI-1640 supplemented with 10 % FCS and 2 mM L-Glutamine. For passaging, cells were rinsed with 10 ml DPBS and detached in 1 ml Trypsin/EDTA. Reaction was stopped by addition of 9 ml culture medium. Phoenix-ECO and PlatA cells were passaged every 3 – 4 days in a ratio of 1:4, 1:6 or 1:8, HCT116 in a ratio of 1:10 or 1:20 depending on pellet size.

3.1.2. Isolation and culture of human T cells

3.1.2.1. Isolation of CD4 and CD8 T cells

Human CD4 and CD8 T cells were isolated from MNCs of healthy donors. MNCs were obtained by proceeding thrombokegel, byproducts of a thrombocyte donation, via ficoll density gradient centrifugation. The thrombokegel was emptied into a 50 ml falcon and rinsed out with DPBS. Blood was diluted with DPBS to a final volume of 60 ml, and 30 ml of the diluted blood were layered onto 15 ml of Pancoll. Density gradient centrifugation was carried out at 700 g, 30 min, room temperature (RT) without break. The buffy coat was collected, cells were washed twice with DPBS and used for subsequent isolation of CD4 or CD8 T cells.

The enrichment of CD4 and CD8 T cells was carried out with the magnetic activated cell sorting (MACS) technology from Miltenyi Biotec. Therefore, CD4 and CD8 MicroBeads, respectively, were used after manufacturer's instructions. In brief, cells were washed with MACS washing buffer (DPBS + 1 % FCS + 2 mM EDTA) and stained with magnetically labeled antibodies against CD4 or CD8. After removal of unbound microbeads, labelled cells were loaded onto a LS column placed into the magnetic field of the MACS separator. Labelled cells were retained in the LS column, whilst unlabeled cells were washed out during the isolation. Remaining cells were flushed out of the column, centrifuged, and counted. Isolated T cells were adjusted to a

concentration of 10x10^6/ml in T cell medium (Table 3-3) and stored overnight under cell culture conditions or directly used for experiments.

3.1.2.2. FACS-based purification of T cell subsets

For the FACS-based purification of different memory-subsets, the CD4 T cells were harvested after the overnight storage and washed with sterile FACS washing buffer (DPBS + 2 % FCS). Afterwards, cells were labeled with four antibodies to distinguish between naïve (CD45RO$^-$, CD45RA$^+$, CCR7$^+$, CD62L$^+$), central memory (CM; CD45RO$^+$, CD45RA$^-$, CCR7$^+$, CD62L$^+$) and effector memory (EM; CD45RO$^+$, CD45RA$^-$, CCR7$^-$, CD62L$^-$) T cells (Table 3-1, Figure 3-1).

Table 3-1: Amounts of antibodies used for FACS-based purification of T cell subsets.

Antigen	Conjugate	Volume for 10x10^6 cells
CCR7	FITC	20 µl
CD45RA	PE-Cy7	15 µl
CD45RO	PE	90 µl
CD62L	APC	60 µl

The cells were incubated with the antibodies for 20 min at 4 °C in the dark, afterwards washed with sterile FACS washing buffer and suspended to a concentration of 20 – 30x10^6 cells/ml. The cell suspension was filtered through a 30 µm cell strainer into sterile FACS tubes and immediately sorted using the FACS Aria instrument. The sorted cells were collected in DPBS supplemented with 10 % FCS. To ensure the purity of the sorted cell subsets, a reanalysis was carried out directly after the sort.

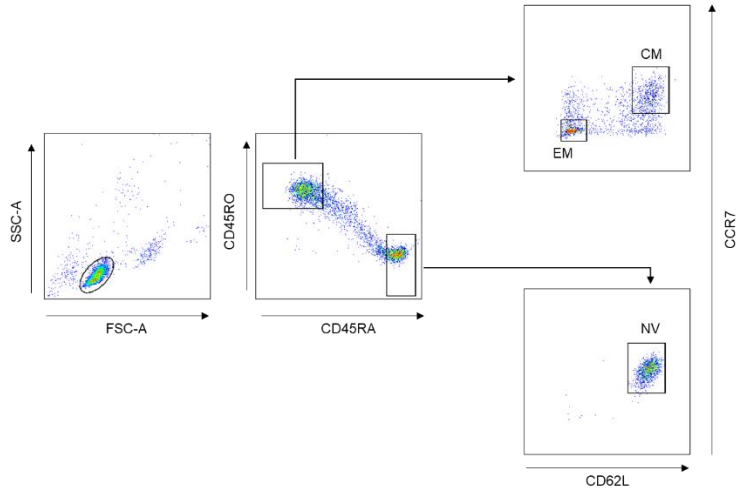

Figure 3-1: Gating strategy for the FACS-based purification of T cell subsets.

3.1.2.3. Electroporation of T cells with siRNA

The siRNAs were achieved from Dharmacon, dissolved in PCR-H_2O to a concentration of 1 µg/µl and stored at -20 °C.

T cells were isolated as described above and immediately used for the electroporation. $10x10^6$ cells per electroporation were washed first in RPMI1640 without phenole red and afterwards in 10 ml OptiMem. The cell pellet was resuspended in OptiMem to a concentration of $50x10^6$/ml.

A maximum of $10x10^6$ cells was electroporated at one shot. First, the siRNA was pipetted into the cuvette in a ratio of 1 µg/$1x10^6$ cells. Afterwards, the appropriate amount of T cells was added, mixed with the siRNA by tapping the cuvette, the cuvette directly placed into the electroporator and electroporated with the settings given in Table 3-2. Afterwards, T cells were transferred into 4 ml pre-warmed T cell medium and rested overnight before being subjected to the different experimental conditions.

Table 3-2: Settings for electroporation of T cells.

Setting	
Voltage application format	Square wave
Voltage	500 V
Pulse Counts	1
Interval	0
Cuvette width	0.4 mm

3.1.2.4. Experimental settings for human T cells

For experiments, $0.1x10^6$ cells/225 µl/well were seeded in round-bottom 96 well plates in T cell medium containing 25 IU/ml (T cells subsets) or 50 IU/ml (bulk T cells) IL-2. Cells were stimulated using anti-CD3/CD28 coated Dynabeads in a ratio of one bead/cell. If indicated, T cells were passaged in a ratio of 1:2 or 1:3 and fed after 72 h in culture.

For the determination of oxygen consumption and extracellular pH, the PreSens technology was used with a cell concentration of $0.8x10^6$ cells/ml/well.

For pre-stimulation before co-culture experiments, T cells were seeded into 24 well plates with $0.4x10^6$ cells/ml/well.

Table 3-3: Composition of the medium for human T cell culture.

Component	
AB-serum (heat-inactivated)	10 %
L-Glutamine	2 mM
Penicillin	50 IU/ml
Streptomycin	50 µg/ml
Sodium pyruvate	1 mM
Non-essential amino acids	1 %
MEM vitamins	0.4 %
2-Mercaptoethanol	0.05 mM
Filtered through a 0.22 µm filter	

3.1.3. Isolation and differentiation of human monocytes and macrophages

3.1.3.1. Isolation of monocytes by contraflow centrifugation

The elutriation, a method based on the principle of contraflow centrifugation, makes use of the balance between centrifugal force and counterflow drag force and thereby allows the separation of different cell types based on their size (summarized in Table 3-4).

In a first step, the elutriation chamber was assembled, connected to the rotor and the system sterilized by flushing with 6 % H_2O_2. Afterwards, the system was washed with DPBS and the

settings of the peristaltic pumps to achieve the required flow rates were determined by calibration with HBSS.

The monocytes were enriched from a lymphocyte donation obtained from volunteer donors in the transfusion medicine of the University Hospital Regensburg. The mononuclear cells (MNCs) were enriched by a gradient centrifugation as described in chapter 3.1.2.1 and injected to the elutriation chamber with a flow rate of 52 ml/min. The different cells were collected by applying different pump flow rates (Table 3-4) at a rotor speed of 2500 rpm at 4 °C temperature. To increase cell viability, the HBSS used as vehicle was supplemented with 6 % donor plasma.

Table 3-4: Settings acquired for elutriation

Cells	Cell size	Flow rate
B cells	7 µm	64 ml/min
T cells	8 – 9 µm	72 – 92 ml/min
Monocytes	10 µm	111 ml/min

The monocytes were collected in the last fraction. The purity of the cells was determined by flow cytometric analysis of the surface markers CD3, CD14 and CD20. To confirm the unstimulated state of the enriched monocytes, the cytokine IL-6 was measured in the supernatants of an overnight culture.

3.1.3.2. Culture of human monocytes

Human monocytes were cultivated in RPMI1640 supplemented with 2 % Human AB-serum, 2 mM L-Glutamine and 50 IU/ml Penicillin and 50 µg/ml Streptomycin. For the generation of RNA-lysates, $2.5x10^6$ cells were plated in 6 well plates with a culture volume of 4 ml. Cells were allowed to adhere in medium without serum for about 30 minutes. After adherence, AB-serum was added, and cells were stimulated with 100 ng/ml LPS.

3.1.3.3. Differentiation and culture of monocyte-derived macrophages

For the differentiation of monocyte-derived macrophages, monocytes were suspended in a concentration of $1x10^6$/ml in RPMI 1640 containing 2 % human AB-Serum, 2 mM L-Glutamine and 50 IU/ml Penicillin and 50 µg/ml Streptomycin. Cells were seeded in teflon-coated plastic bags and cultured for 6 – 7 days.

For harvesting, cells were incubated at 4 °C for about 30 minutes to detach them from the surface of the bag and poured into a 50 ml falcon tube. After centrifugation, cells were suspended in 3 – 5 ml culture medium without AB-Serum and counted.

3.1.3.4. Experiment settings for human monocytes and monocyte-derived macrophages

For generation of RNA and protein lysates, $2.5x10^6$ cells were seeded to 6 well cell culture plates. After adherence, human AB-serum was added to a final concentration 2 % and cells were stimulated by addition of LPS (100 ng/ml). Final culture volume was 4 ml.

To allow experiments with a subsequent flow cytometry analysis, $0.4x10^6$ cells were seeded in 500 µl culture medium without AB-serum in a 12 well UpCell plate and allowed to adhere. Afterwards, treatments and AB-serum (2 %) were added to a final volume of 1 ml. After 48 h incubation under cell culture conditions, culture plates were placed to 4 °C for about 1 h to induce a loss of cell adherence. Plates were placed onto ice bags and cells were harvested by intensive flushing.

3.1.4. Isolation and culture of murine T cells

For all experiments, C57BL/6N and Balb/c mice in the age of 12 – 20 weeks were used. Mice were provided by the central animal laboratories of the University Regensburg.

3.1.4.1. Preparation of murine splenocytes for T cell isolation

Mice were euthanized by CO_2 narcosis and cervical dislocation. The spleen was removed and kept in sterile DPBS on ice until further processing.

Spleens were scratched out in a petri dish containing 7 ml RPMI1640 containing 10 % FCS, 2 mM L-Glutamine, 50 IU/ml Penicillin and 50 µg/ml Streptomycin and the cell suspension filtered through a 100 µm cell strainer. Tissue remaining in the strainer was pressed though using the plug of a 2 ml syringe. Petri dish, plug and cell strainer were rinsed with 10 ml medium. Cells were centrifuged and the supernatant discarded. For erythrocyte lysis, pellet was diluted in 2 ml ACK buffer (Table 3-5) and incubated at room temperature for 3 minutes. Reaction was stopped by addition of 15 ml medium, and cells were centrifuged. The cell pellet was suspended in 1 ml medium and filtered through a 100 µm cell strainer. The falcon and cell strainer were rinsed with 19 ml medium, and cells were counted for subsequent isolation.

Table 3-5: ACK lysis buffer (6x).

Substance	Amount
NH_4Cl (Ammonium chloride)	49.64 g
$KHCO_3$ (Potassium bicarbonate)	6 g
EDTA disodium, dihydrate	0.222 g
H_2O_{dest}	Ad 1000 ml
pH adjusted to 7.4	
Filtered through a 0.22 µm filter	

3.1.4.2. Isolation of murine T cells

For isolation of CD4 T cells, the CD4 T cell isolation Kit (mouse, L3T4) was used according to manufacturer's instructions and as described in chapter 3.1.2.1. To increase purity of the cells, an additional washing step of the MACS LS columns was included. CD8 T cells were isolated from the throughflow collected during CD4 T cell isolation using the CD8a T cell isolation Kit (mouse) according to manufacturer's instructions. To increase yield of the cells, an additional washing step of the MACS LS columns was included.

3.1.4.3. Experimental settings used for murine T cells

Murine T cells were cultivated in murine T cell medium (Table 3-6) containing 100 IU/ml IL-2 and 50 ng/ml IL-15. In the primary stimulus, cells were seeded in 96 well round bottom plates with a density of $0.2x10^6$ cells/200 µl/well and stimulated using the Treg Expansion Kit with ratio of one Bead/Cell.

For the determination of apoptosis and intracellular cytokine production after retroviral transduction, cells were seeded with $0.1x10^6$ cells/200 µl/well without adding fresh beads.

For the determination of oxygen consumption, the PreSens technology was used with a cell concentration of $1.2x10^6$ cells/ml/well.

Table 3-6: Composition of T cell medium used for murine T cell cultures

Component	
FCS	10 %
L-Glutamine	2 mM
Penicillin	50 IU/ml
Streptomycin	50 µg/ml
Sodium Pyruvate	1 mM
Non-essential amino acids	1 %
MEM vitamins	0.4 %
2-Mercaptoethanol	0.05 mM

3.1.5. Cell freezing and thawing

PlatA cells and Phoenix-Eco cells were frozen in a solution of 90 % FCS and 10 % DMSO. HCT116 cells were frozen in a solution of 50 % cell culture medium, 40 % FCS and 10 % DMSO. Cells were counted, centrifuged and suspended to a concentration of 1.2 – 2x10^6/ml in freezing medium. 1 ml of cell suspension was transferred to Nunc freezing tubes, slow-frozen in cryo freezing containers and transferred to liquid nitrogen for long term storage.

Cells were thawed at room temperature, directly transferred to 10 ml cell culture medium, centrifuged and transferred to a T75 cell culture flask containing prewarmend fresh culture medium.

3.1.6. Cell counting

Concentration of cell suspensions from PlatA and Phoenix-Eco cells were determined using 0.1 % trypan blue and a hematocytometer.

For all other cells, the CASY cell counter was used to determine cell count, viability and cell size.

3.1.7. Test for mycoplasma contamination

All cell lines were routinely tested for mycoplasma contamination. Cell were kept in antibiotics-free medium to a confluency of 100 % and tested using the MycoAlert™ Mycoplamsa detection kit after manufacturer's instructions.

3.1.8. Retroviral transduction of human CD4+ T cells

3.1.8.1. Generation of retrovirus-containing supernatants using PlatA cells

Only freshly thawed cells were used for virus generation. Cells were thawed three days in advance and cultured in culture medium without selection antibiotics. One day before transfection, cells were harvested, and $1.5x10^6$ cells were seeded in T75 flaks containing 15 ml medium without selection antibiotics.

For transfection, a mix containing TransIT-LT reagent, OptiMem and the required plasmid DNAs (Table 3-7) was prepared and incubated for 20 minutes at room temperature. Afterwards, 5 ml medium was removed from the cells and the transfection mix was added dropwise under constant pivoting. Cells were incubated overnight under cell culture condition. On the next day, culture medium was replaced by 8 ml fresh antibiotics-free medium, and cells again incubated under cell culture conditions. Virus supernatant was harvested on day 2 and day 3 after transfection and either used directly or stored at -80 °C.

Table 3-7: Transfection mix used for PlatA cells

Component	
DNA (Gene of Interest)	11.5 µg
pCOLT-GALV	6.5 µg
pHIT60	6.5 µg
OptiMEM	2 ml
TransIT-LT	60 µl

3.1.8.2. Infection and selection of human T cells

Human CD4 T cells were stably retrovirally transduced via spin transduction. T cells were isolated as described in chapter 3.1.2.1 and stimulated for 48 h as described in chapter 3.1.2.3. For spin transduction, wells of a 12 well plate were coated with 2 ml retronectin (25 µg/ml in

DPBS) over night at 4 °C. Retronectin was used up to five times. Before transduction, plates were blocked 30 minutes at room temperature using 2 % BSA and washed twice with DPBS.

T cells were harvested, the stimulation beads removed and up to $4x10^6$ cells/well seeded in 500 µl total volume to the retronectin coated wells. The virus supernatant was harvested, shortly centrifuged to remove cell debris and 3.5 ml of the virus supernatant was added to the T cells. IL-2 was added to a final concentration of 50 IU/ml. The plate was centrifuged for 90 min, 2000 rpm at 30 °C without break. Afterwards, the plate was incubated overnight under cell culture conditions. On the next day, the procedure was repeated replacing 3 ml of the supernatant by fresh virus supernatant and adding IL-2 and after centrifugation again incubated overnight.

After the second infection period, T cells were harvested for expansion. Then, T cells were seeded in 24 well plates with $0.3x10^6$ cells/ml/well, using a total volume of 2 ml per well and stimulated with anti-CD3/CD28 coated Dynabeads in a ratio of one bead per three cells. IL-2 was added to a final concentration of 50 IU/ml. T cells were subcultured in a ratio of 1:3 and fed 48 h after restimulation.

The selection process was started 72 h after the end of the viral infection. Therefore, stimulation beads were removed, and cells were seeded into 24 well plates in a concentration of $1x10^6$ cells/ml with a total volume of 2 ml per well in medium containing 50 IU/ml IL-2. Cells were treated for 72 h with 50 ng/ml puromycin.

After selection, cells were expanded for experiments. Cells were harvested and restimulated as after viral infection. Cells were subcultured and feeded after 48 h. Experiments were performed on day 3 or 4 after end of selection.

To assess the transduction efficacy and purity of the transduced cells, a staining against the His-Tag fused to LDHB was performed after transduction, after selection and on the day of experiments, respectively.

3.1.9. Retroviral transduction of murine $CD4^+$ T cells

3.1.9.1. Generation of retrovirus-containing supernatants using Phoenix-Eco cells

Phoenix-Eco cells were cultured as described in chapter 3.1.1. For generation of virus supernatants, $0.9x10^6$ cells/2 ml were seeded into 6 well plates coated with 0.1 % gelatin solution. Transfection of cells was performed 6 h later. Therefore, DNA was centrifuged at full speed for 5 min and transfection mix was prepared according to Table 3-8. The mix was incubated at room temperature for 30 minutes and afterwards dropwise pipetted onto the

seeded cells. On the next day, medium was replaced by 2 ml fresh medium. Virus supernatant was harvested 2 days after transfection and immediately used.

Table 3-8: Transfection mix used for Phoenix-Eco cells

Component	
DNA (Gene of Interest)	6 µg
pCL-Eco	1 µg
OptiMEM	250 µl
TransIT-293	12 µl

3.1.9.2. Infection of murine T cells

Murine CD4 T cells were isolated as described in chapter 3.1.4. Cells were stimulated using the Treg activation and expansion kit in a bead-to-cell ratio of 1:1, seeded into 96 well round bottom plates with $0.04x10^6$ cells/100 µl/well and treated with 100 IU/ml IL-2 and 50 ng/ml IL-15. On the next day, cells were infected with the virus. Therefore, virus supernatant was harvested, centrifuged to remove cell debris and supernatant was transferred to a fresh tube. Polybrene (final concentration 6 µg/ml), IL-2 and IL-15 were added to the supernatants, and T cells treated with 100 µl supernatant per well. Cells were incubated at cell culture conditions for 6 h. Afterwards, 140 µl medium were replaced by 150 µl murine cell culture medium containing IL-2 and IL-15 and cells were expanded for additional 72 h before performing experiments.

Transduction efficacy and purity of the cells was assessed by staining against the surface marker CD90.1 included into the used vector.

3.1.10. Spheroid Co-Culture

Tumor cell spheroids can be generated from a tumor cell line by preventing the cell adherence to a plastic surface. If the cells can't adhere to a surface, they adhere to each other, thereby forming three-dimensional aggregates which well mimic an *in vivo* tumor environment.

Tumor cell spheroids were generated from HCT116 cell with the hanging-drop method. $0.01x10^6$ cells/30 µl were brought on the insight of a lid of a treated cell culture petri dish. The lower part of the dish was filled with DPBS. The cells were incubated for 4 – 5 days under cell culture conditions to allow spheroid assembly.

After assembly, spheroids were harvested, and the culture medium was replaced. A 96 well flat-bottom plate was coated with a 1 % agarose solution and one spheroid per well transferred with a final volume of 200 µl. Spheroids were allowed to grow for 8 – 10 days.

For co-culture, T cells were pre-stimulated for 24 h using α-CD3/CD28 coated Dynabeads at a bead-to cell-ratio of 1:1. 100 µl/well were removed from the spheroid culture, and $0.1x10^6$ T cells/well were applied in 100 µl T cell medium containing 50 IU/ml IL-2.

After 48 h, the co-cultures were treated with monensin for 3 h to allow flow cytometric analysis of cytokine production. Spheroids were harvested and washed in DPBS to remove remaining immune cells. Afterwards, spheroids were dissembled by incubation with trypsin/EDTA. Reaction was stopped by addition of 1 ml cell culture medium and flow cytometric staining was performed as described in chapter 3.4.

3.2. Biochemical methods

3.2.1. Preparation of proteins

Preparation of proteins was conducted on ice using pre-chilled chemicals and equipment. To prevent protein degradation, one tablet protease-inhibitor cocktail was dissolved in 10 ml of protein isolation buffer before use. Samples were stored at -80 °C. Lysates were centrifuged at 13.000 g for 15 minutes at 4 °C and protein concentration was determined by either using the RC DC protein assay or the Qubit protein assay kit, both after manufacturer's instructions.

3.2.1.1. Preparation of RIPA-lysates

For isolation of proteins from adherent cells, $2.5x10^6$ cells were seeded into 4 ml medium in 6 well plates and kept under cell culture conditions. On the next day, medium was removed, and cells washed two times with DPBS. Cells were scraped down in 50 µl of RIPA buffer and transferred in a fresh sample tube. In case of suspension cells, $2.5x10^6$ cells were washed directly twice with DPBS and the cell pellet was suspended in 50 µl of RIPA buffer. The lysate was vortexed for one minute, incubated at -20 °C for 5 minutes, again vortexed for on minute and snap-frozen in liquid nitrogen. The lysates were stored at -80 °C.

3.2.1.2. Preparation of zymography lysates

For isolation of proteins from adherent cells, $1x10^6$ cells were seeded into 4 ml medium in 6 well plates and kept under cell culture conditions. On the next day, medium was removed, and

cells washed two times with DPBS. Cells were scraped down in 50 µl of CLB buffer and transferred in a fresh sample tube. In case of suspension cells, $2.5x10^6$ cells were washed twice with DPBS and the cell pellet was suspended in 50 µl of CLB buffer. The lysate was incubated on ice for 15 minutes and directly stored at -80 °C.

3.2.1.3. Preparation of zymography-tissue-lysates

For protein isolation from tissue, the tissue samples were snap-frozen in liquid nitrogen and stored at -80 °C until further processing. For generation of lysates, tissue was cut down and weight of the tissue was determined. The tissue was homogenized in 1 ml tissue lysis buffer (Table 3-9) per 1 mg tissue and further lysed using 20 G syringes. The lysate was centrifuged first at full speed for 10 minutes, the supernatant transferred to a fresh cup, again centrifuged for 20 minutes at full speed and the supernatant stored at -80 °C.

Table 3-9: Composition of the tissue lysis buffer

Component	
Cell Lysis Buffer	2 x
Phenylmethylsulfonylfluoride (PMSF)	1 mM
Protease Inhibitor Cocktail	1 tablet
H_2O_{bidest}	Ad 7 ml

3.2.2. LDH zymography analysis

The LDH zymography analysis is used to determine the LDH isoenzyme pattern of cells. For this, protein lysates of cells are separated in a native setting and afterwards, the isoenzymes are visualized by an enzymatic staining. Therefore, a mixture of lactate, NAD, phenazine methosulfate (PMS) and nitro tetrazolium blue chloride (NBT) is used. LDH converts lactate to pyruvate, thereby reducing NAD to NADH. In a next step, NADH reduces PMS, which then in turn reacts with NBT to form blue formazan crystals enriching at the enzyme side. Then, each band presented on the gel represents one isoenzyme. While LDH-1, the homotetramer of LDHB, migrates fast and is located close to the cathode, the homotetramer of LDH-5 migrates slower and stays at the anode. The bands in between represent heterotetramers composed by LDHA and LDHB.

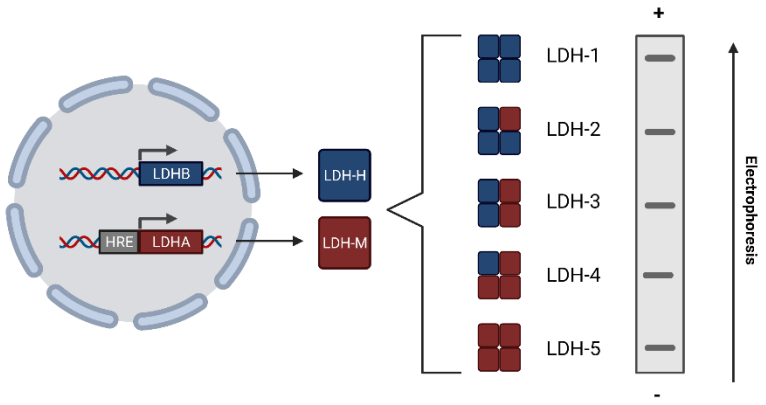

Figure 3-2: Principle of an LDH isoenzyme analysis. *Graphic created with BioRender.com.*

For the LDH zymography analysis, two different systems were used (the systems had to be switched due to discontinuation, but the principle of the two systems was the same).

LDH zymography analysis using the SAS-MX system was carried out using the SAS-MX LD Vis Kit and the SAS-MX LD Vis Reagent. Handling of the gels and detection of LDH isoenzymes was performed according to manufacturer's instructions. Protein samples were thawed on ice and diluted with PBS to equal concentration. 3 µl of the protein dilution was loaded onto the gel. For human samples, electrophoresis was carried out at 100 V for 15 minutes. For murine samples, electrophoresis was carried out for 25 minutes.

LDH zymography analysis using the Quickgel system was carried out using the Quickgel LD isoenzyme Kit. Handling of the gels and detection of LDH isoenzymes was performed according to manufacturer's instructions. Protein samples were prepared as described above. For human samples, electrophoresis was carried out at 400 V for 5 minutes. For murine samples, electrophoresis was carried out for 8 minutes. Gels were destained in 1 M acetic acid.

3.2.3. Western blot analysis

The western blot technique is used to detect specific proteins in a whole cell lysate. For this purpose, the proteins are separated according their size using SDS (sodium dodecyl sulfate)-polyacrylamide gel electrophoresis and afterwards transferred to a PVDF membrane, where they can be visualized using specific antibodies and immunohistochemical detection methods.

3.2.3.1. SDS-polyacrylamide gel electrophoresis

For the separation of the proteins, a 12 % separation gel and a 5 % stacking gel were poured. The running gel was prepared as described below (Table 3-10, Table 3-11), immediately filled

into the prepared glass plates in the casting frames and covered with isopropanol. After polymerization, the isopropanol was removed, the glass plates rinsed with water and the 5 % stacking gel solution was filled in. The comb was placed into the solution and the gel was allowed to polymerize. The prepared gels were stored at 4 °C until electrophoresis.

Table 3-10: Formulation of the SDS-polyacrylamide gels

Component	Running gel (12 %)	Stacking solution (5 %)
Running gel solution	11 ml	-
Stacking gel solution	-	5 ml
Tetramethylethyldiamin (TEMED)	11 µl	5 µl
APS (10 %)	55 µl	40 µl

Table 3-11: Formulation of the SDS-polyacrylamide gel solutions

Component	Running gel solution	Stacking gel solution
Running gel buffer (1.5 M Tris, pH 8.8)	25 ml	-
Stacking gel buffer (0.5 M Tris, pH 6.8)	-	25 ml
Acrylamide/Bis-Acrylamide (30 %)	40 ml	16.65 ml
SDS (10 %)	1 ml	1 ml
H_2O_{bidest}	Ad 100 ml	Ad 100 ml

For analysis, 10 – 20 µg protein were loaded per lane. The protein was diluted to an appropriate concentration with DPBS, mixed with one volume of 2x SDS sample buffer (Table 3-12) and boiled for 10 minutes at 95 °C. The gels were briefly rinsed with water and placed into the running chamber filled with 1x Laemmli's running buffer (**Table 3-13**). Afterwards, the protein mix and the protein standard were loaded onto the gel. Electrophoresis was performed according to Table 3-14.

Table 3-12: 2x SDS sample buffer

Component	Concentration
Glycerin	20 %
1.25 M Tris-HCl, pH 6.8	125 mM
SDS	4 %
2-Mercaptoethanol	10 %
Bromphenole blue	0.02 %
H_2O_{bidest}	Ad 50 ml

Table 3-13: Laemmli's running buffer (4x)

Component	Concentration
Glycine	0.95 M
Tris	40 mM
SDS	0.5 %
H_2O_{bidest}	Ad 3 L

Table 3-14: Phases of the SDS polyacrylamide gel electrophoresis.

Voltage	Electrophoresis phase	Estimated time
80 V	Running in of samples	20 min
100 V	Migration through the stacking gel	30 min
120 V	Migration through the separation gel	90 min

3.2.3.2. Western Blotting

For the transfer of the separated proteins to the PVDF membrane, a semi-dry blotting technique was used. The membrane was activated in 70 % isopropanol and stored in buffer B until further usage. First, three sheets of whatman paper soaked with buffer A were placed onto the electrophoresis area and next, papers soaked in buffer B were placed on top. Next, the membrane was placed, air bubbles and protruding borders removed. The gel was placed onto the membrane and again the air bubbles carefully removed. Last, the gel was covered

with three sheets of whatman paper soaked with buffer C. Air bubbles were removed from the blotting sandwich. The electrophoresis chamber was closed, and the electrophoresis carried out at 11 V for 1 h. The formulation of the used buffers is given in Table 3-15.

Table 3-15: Buffers used for western blotting

Component	Concentration
Buffer A	
Tris	0.3 M
Methanol	20 %
H_2O_{bidest}	Ad 1 L
Buffer B	
Tris	25 mM
Methanol	20 %
H_2O_{bidest}	Ad 1 L
Buffer C	
ε-Amino-n-Capronsäure	4 mM
Methanol	20 %
H_2O_{bidest}	Ad 1 L
Tris-Buffered Saline (TBS; 2X)	
Tris/HCl	20 mm
NaCl	150 mM
H_2O_{bidest}	Ad 2 L

After blotting, the whatman papers were removed and the membrane directly transferred into 10 ml washing buffer (1x TBS + 0.1 % Tween; TBS-T). The membrane was washed two times (10 minutes each). Afterwards, unspecific antibody binding sites were blocked by incubation in a 5 % skimmed milk solution in TBS-T for 1 h at room temperature under constant shaking. Afterwards, the primary antibody was diluted in 5 % skimmed milk and the blot incubated overnight at 4 °C in the antibody solution. On the next day, blot was incubated for 30 min in the primary antibody solution at room temperature and afterwards washed three times in

TBS-T. Next, the secondary antibody was applied in 5 % skimmed milk in TBS-T and the blot incubated for 1 h at room temperature. Afterwards, the blot was again washed three times in TBS-T.

For the immunohistochemical detection, the enhanced chemiluminescence (ECL) detection solution was prepared according to manufacturer's instructions. The membrane was carefully dried, placed on a plastic foil, layered with the ECL solution, and incubated at room temperature for 5 minutes. Afterwards, ECL was removed, and the signal was detected using the fusion pulse instrument.

For the detection of further proteins, the antibodies were removed by membrane stripping. Therefore, the membrane was washed after the immunochemical signal detection step two times in TBS-T and afterwards incubated for 15 minutes under constant shaking in 1x mild stripping solution. Next, membrane was washed again three times in TBS-T and blocking and protein detection was performed as described above.

3.3. Molecular biology techniques

3.3.1. Preparation of Ribonucleic acids (RNA)

Preparation and handling of RNA samples was conducted on ice using RNase free plastic material and consumables. RNA lysates and samples were stored at -80 °C.

3.3.1.1. RNA-Isolation

For generation of RNA lysates from adherent cells, 1 – 2.5x10^6 cells were seeded into 4 ml cell culture medium in 6 well plates and incubated at cell culture conditions. On the next day, medium was removed, cells scraped down in RLT-buffer supplemented with β-meracptoethanol according to manufacturer's instructions and the further lysed using a 20 G needle and syringe.

For the generation of RNA-lysates from suspension cells, up to 5x10^6 cells were pelleted, suspended in RLT-buffer supplemented with β-meracptoethanol according to manufacturer's instructions and the further lysed using a 20 G needle and syringe.

For the isolation of RNA, the RNeasy Mini Kit was used according to manufacturer's instructions. To isolate RNA from a small number of cells, the RNeasy Micro Kit was used.

The RNA concentration was assessed using the NanoDrop instrument.

3.3.1.2. RNAseq analysis

The RNAseq was conducted and analyzed by the NGS core facility of the Regensburg Centrum for Interventional Immunology (RCI).

3.3.2. Quantification of gene expression

The quantification of gene expression was performed by quantitative real-time polymerase chain reaction (qRT-PCR). In this technique, the RNA content of a cell is first translated into the complementary DNA (cDNA) by reverse transcription. In a next step, a PCR for specific genes is performed. To assay the expression level of the gene, a fluorescent dye (SYBR Green) is included in the PCR mix, which needs to bind double stranded DNA to emit fluorescent signals. Within the framework of the PCR, more double strands of the respective gene of interest are synthesized, which leads to an increase of the fluorescent signal and can be detected by real-time PCR instruments. At one timepoint, called Cq, the specific fluorescence exceeds the background fluorescence. The higher the abundance of the RNA encoding for the respective gene in the sample was, the earlier this happens. By means of a standard curve included in every experiment, the absolute expression of the gene can be calculated and referred to the expression of a housekeeping gene.

3.3.2.1. Primerdesign

The primers used for the qRT-PCR were designed using the open-source software PerlPrimer following the criteria below (Table 3-16). The coding and genomic sequences of the genes were obtained from the UCSC database. The specificity of the primers was checked using the 'in-silico PCR' and the 'BLAT' function provided by the UCSC.

Table 3-16: Criteria for primer design

Criterium	
GC content	40 – 60 %
Melting temperature (Tm)	65 – 68 °C
Primer length	20 – 28 bp
Amplicon length	70 – 150 bp
Position	On 2 different exons

3.3.2.2. Reverse Transcription

To transcribe the RNA into the corresponding cDNA, a reverse transcription was conducted using a reverse transcriptase derived from the murine Moloney leukemia virus (M-MLV), 2'-deoxyribonucleosid-5'-triphosphates (dNTPs) and random decamer primers. The total reaction volume was 20 µl. The reaction was carried out in a thermocycler following the protocol described below (Table 3-17).

Table 3-17: Protocol for Reverse Transcription

Reagent	**Volume/Reaction**
Total RNA	≡ 500 ng
Random Decamer Primers (10 µM)	1 µl
dNTPs (10 mM)	1 µl
PCR-H_2O	Ad 15 µl
Incubation: 5 minutes at 65 °C	
5x Reverse Transcription buffer	4 µl
Incubation: 2 minutes at 42 °C	
M-MLV Reverse Transcriptase	1 µl
Incubation: 50 minutes at 42 °C	
Incubation: 15 minutes at 70 °C	

3.3.2.3. Quantitative real-time PCR

For the qRT-PCR, a reaction mix was prepared in 96 well plates according to Table 3-18. In each well, 9 µl of the reaction mix were mixed with 1 µl of the respective standard or sample dilution. The samples were pipetted in triplicates, and each point of the standard row was pipetted in duplicates. The plates were sealed with a PCR plate seal, briefly centrifuged and the reaction was carried out in the BioRad CFX instrument following the protocol shown in Figure 3-3. Afterwards, the data were analyzed using the CFX maestro software.

Table 3-18: Reaction mix for qRT-PCR (1x)

Component	
cDNA (diluted)	1 µl
QuantiFast SYBR Green PCR Kit	5 µl
Primer (10 pMol)	0.5 µl each
PCR-H_2O	3 µl

The specific amplification of the PCR product was controlled by the pattern of the melting curve. By means of the standard curve, the amounts of specific mRNA present in the sample were calculated.

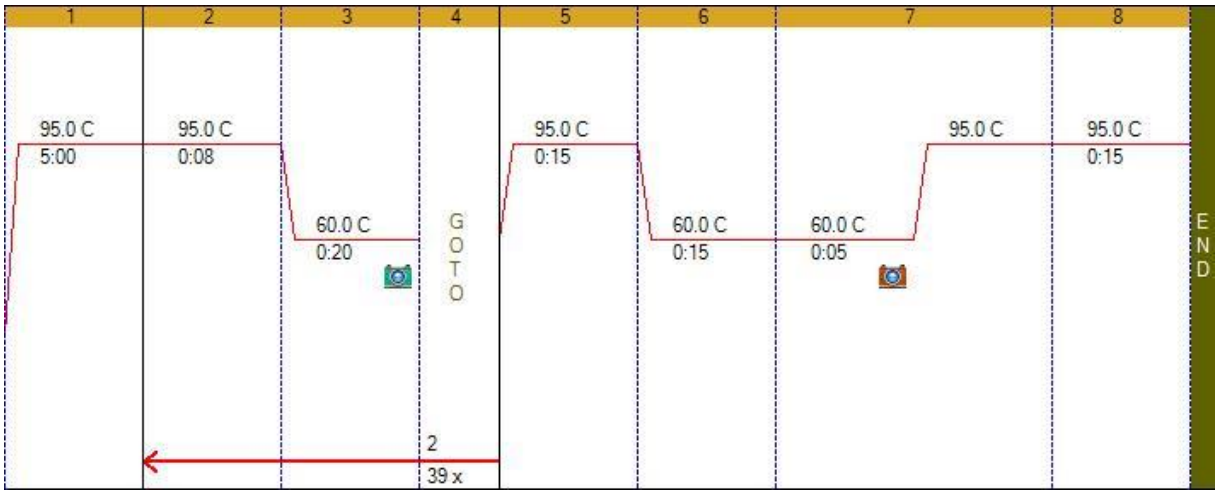

Figure 3-3: PCR-Program for quantitative real-time PCR.

3.3.3. Generation of DNA for retroviral transduction

3.3.3.1. Generation and cloning of the pMX-IRES-Ldhb vector

The sequence for the human LDHB was cloned into the commercially available vector pMX-IRES-Puro provided by Prof. Simone Thomas/ Regensburg Center for Interventional Immunology. To allow an easy detection of the overexpressed LDHB in the transduced cells, LDHB was tagged with an HIS-tag.

The gBlock DNA Fragment encoding the HIS-tagged LDHB was ordered from Integrated DNA Technologies. Upon arrival, the fragment was dissolved in PCR-grade H_2O to a final concentration of 10 ng/µl. To lay bare the cloning sites of the fragment and revive the insert DNA, it was digested with the cloning enzymes EcoRI and XhoI at 37 °C overnight (Table 3-19).

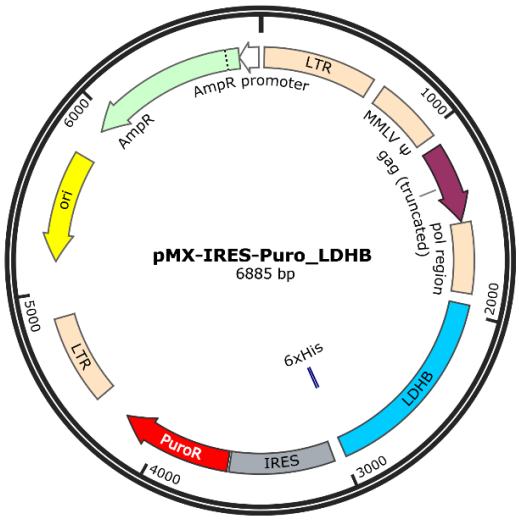

Figure 3-4: Plasmid map of pMX-IRES-Puro_LDHB. *This vector was used for the overexpression of LDHB in human T cells after viral infection. To allow a detection of the exogenous LDHB, the sequence was equipped with a HIS-Tag. A resistance gene for puromycin allowed an antibiotics selection after viral transduction.*

Table 3-19: Components for the template digestion.

Component	Amount
Template DNA	100 ng
CutSmart Buffer	2 µl
Cutting enzymes	0.5 µl each
H_2O	Ad 7 µl

On the next day, the DNA was purified using the PCR QIAQuick PCR Purification Kit after manufacturer's instructions. Afterwards, the template was cloned into the pMX-IRES-Puro vector by a ligation reaction (Table 3-20).

Table 3-20: Components for the vector-insert ligation.

Component	Amount
Insert DNA	15 µl
Vector DNA	1 µl
Ligase buffer	2 µl
Ligase	1 µl
H_2O	1 µl

3.3.3.2. Generation and cloning of the MSCV-Thy1.1-Ldhb vector

The sequence for the murine Ldhb was cloned into a modified MSCV-Thy1.1 provided by Prof. Markus Feuerer/Institute for Immunology/University of Regensburg. The vector was modified beforehand to be compatible with the “Gateway-System” provided by Thermo Fisher Scientific, which allows a more simple and effective one-step cloning procedure.

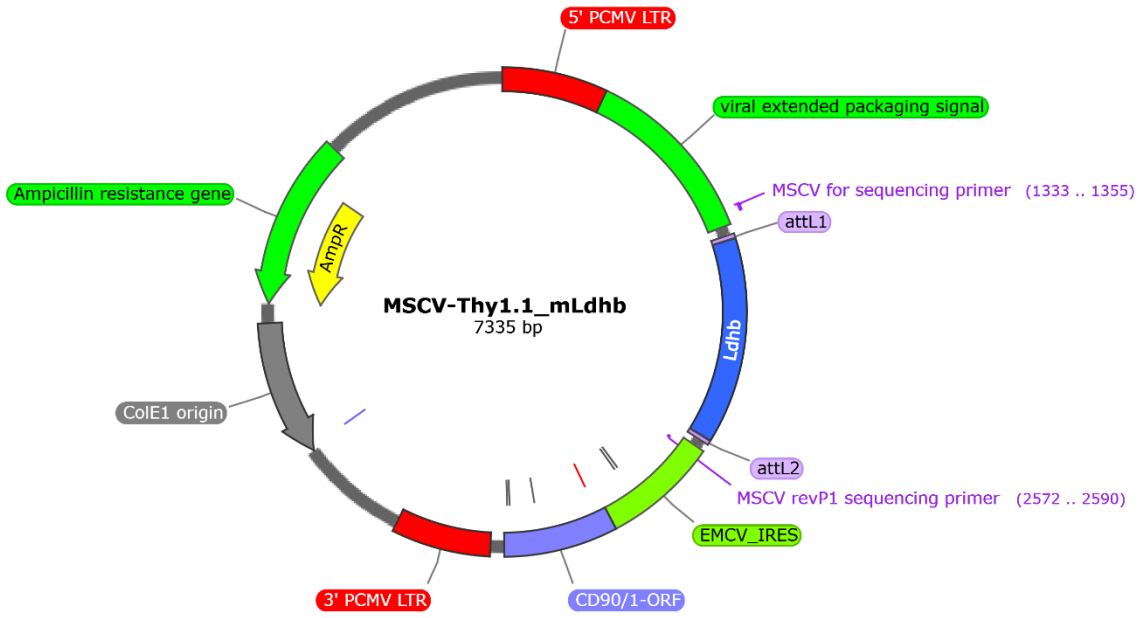

Figure 3-5: Plasmid map of MSCV-Thy1.1_Ldhb. *Plasmid used for the overexpression of Ldhb in murine T cells after viral infection.*

The Ldhb donor vector was synthesized by Thermo Fisher Scientific. Upon arrival, the DNA was reconstituted in PCR-H_2O. 150 ng of the donor and receiver vector were mixed with 2 µl LR Clonase, filled up with H_2O to a final volume of 8 µl and incubated for 1 h at 25 °C. To stop the reaction, 1 µl of proteinase K was added and the mixture incubated for 10 min at 37 °C.

3.3.3.3. Transformation of bacteria

To allow a multiplication of the prepared DNA, a bacteria transformation protocol was used.

The pMX-IRES-Puro-LDHB construct was introduced into the *JM109 E. coli* strand provided by Prof. Simone Thomas/Regensburg Center for Interventional Immunology. 2 µl of the ligation product was carefully mixed with 100 µl of bacteria and incubated on ice for 30 minutes followed by a heat-shock at 42 °C for 45 seconds. The bacteria were cooled down for one minute on ice, transferred to 1 ml LB-Medium and shaked for 60 minutes at 37 °C for 280 rpm. Afterward, this culture was used to inoculate LB-plates supplemented with 100 µg/ml ampicilline and incubated over night at 37 °C. On the next day, the plate was checked for clones and further used for the inoculation of a small-scale bacteria culture.

The MSCV-Thy1.1-Ldhb construct was introduced into the *TOP10 E. coli* strand provided by Prof. Markus Feuerer/Institute for Immunology/University Regensburg. 2 µl of the ligation product was carefully mixed with 50 µl of bacteria and incubated on ice for 30 minutes followed by a heat-shock at 42 °C for 30 seconds. The bacteria were cooled down for one minute on ice, transferred to 250 µl SOC-Medium and shaked for 45 minutes at 37 °C for 280 rpm. Afterward, this culture was used to inoculate LB-plates supplemented with 100 µg/ml ampicilline and incubated over night at 37 °C. On the next day, the plate was checked for clones and further used for the inoculation of a small-scale bacteria culture.

Table 3-21: Formulation of the LB medium.

Component	Amount
Yeast extract	5 g
Tryptone	10 g
Sodium chloride	5 g
H_2O	Ad 1 L
Sterilized at 121 °C	

3.3.3.4. Isolation of plasmid DNA from small-scaled bacterial culture (Mini-Prep)

From positive clones obtained after transformation, an overnight culture was grown in 3 ml LB medium supplemented with 0.1 mg/ml ampicillin (LB-Amp). 2 ml of this culture were used to isolate plasmid DNA using the QIAfilter Plasmid Mini Prep Kit according to manufacturer's instructions. The DNA concentration was determined using the NanoDrop instrument. Sequencing of the introduced DNA fragment was performed by GeneArt.

3.3.3.5. Endotoxin-free isolation of plasmid DNA from large-scaled bacterial culture (Maxi-Prep)

The remaining culture from the Mini-Prep culture (see chapter 3.3.3.4) was plated again on an ampicilline-agar-plate. One of the clones was picked and grown in 2 ml LB medium supplemented with 0.1 mg/ml ampicilline (LB-Amp) for one day at 37 °C, 280 rpm shaking. This culture was diluted 1:250 in 100 ml LB-Amp and incubated over night at 37 °C, 280 rpm shaking. From this culture, plasmid DNA was isolated using the EndoFree Plasmid Maxi Kit according to manufacturer's instructions. The DNA concentration was determined using the NanoDrop instrument.

3.4. Flow cytometry analyses

All centrifugation steps were carried out at 1600 rpm, 4 °C. In case of staining murine cells, the cells were incubated with 1 µl Fc receptor blocking reagent for 10 minutes at 4 °C before further staining. When using BV-conjugated antibodies, the antibodies were preincubated in BV staining buffer (1 µl antibody/10 µl buffer) for 30 minutes at room temperature before the staining was performed. The acquisition of stained cells was performed with the BD FACS Calibur, BD FACS Fortessa or the BD FACS Celesta instrument.

3.4.1. Staining of surface markers

For the staining of surface markers, 0.5 – 1x10^6 cells per staining were used. Cells were washed one in FACS washing buffer (DBPS + 2 % FCS) and the supernatant discarded. In case of staining murine cells, the cells were incubated with 1 µl Fc blocking reagent for 10 minutes at 4 °C and afterwards washed with FACS washing buffer. Afterwards, the cells were incubated with the antibodies for 20 minutes at 4 °C, washed in FACS washing buffer, resuspended in 300 µl FACS washing buffer and measured.

3.4.2. Intracellular staining

3.4.2.1. Staining for cytokines

To analyze intracellular cytokine production of human and murine T cells, 0.1x10^6 cells/96 well were pre-incubated with the respective treatments and without additional stimulus overnight. On the next day, cells were stimulated with 12-myristate-13-acetate (PMA, 0.018 µg/ml) and Ionomycin (0.89 µM) and additionally treated with Golgi-Stop for 2 – 4 h.

Cells were harvested and stainings for live-dead discrimination and surfaces markers were performed as described in chapters 3.4.1 and 3.4.3. Afterwards, the cells were washed in DPBS and lysed using the BD Cytofix/Cytoperm Kit according to manufacturer's instructions. Incubation with the respective antibodies was performed at 4 °C for 30 minutes. Afterwards, cells were washed twice with FACS washing buffer, resuspended in 300 µl FACS washing buffer and immediately measured.

3.4.2.2. Staining for nuclear markers

For staining nuclear markers, cells were harvested and staining for live-dead discrimination and surface markers was performed as described in chapter 3.4.1 and 3.4.3. Afterwards, cells were washed in DPBS and lysed using the Foxp3 staining Kit according to manufacturer's instructions. Incubation with the respective antibodies was performed at 4 °C for 30 minutes. Afterwards, the cells were resuspended in 300 µl FACS washing buffer and immediately measured.

3.4.3. Staining for live/dead discrimination

For live/dead discrimination, cells were stained using the Zombie NIR fixable viability dye before the surface staining. Therefore, cells were washed twice with DPBS and afterwards, cells were incubated in 80 µl of the diluted Zombie dye (1:650 in DPBS) for 10 minutes at room temperature. Thereafter, antibodies for surface staining were directly added to the cells without additional washing step and staining was performed according to chapter 3.4.1.

3.4.4. Determination of cell viability by staining with Annexin V/7-AAD

The staining of cells with 7-AAD and Annexin V is a method to discriminate between living cells and cells undergoing different states of apoptosis. Annexin V binds to phosphatidylserine, which is part of the cell membrane normally facing the intracellular compartment. Upon apoptosis, the membrane is flipped, phosphatidylserine is presented on the cellular surface and can be bound by Annexin V. The dye 7-AAD is membrane-impermeable and consequently does not stain living cells. In the late phases of apoptosis, the cell membrane gets leaky, so that 7-AAD can stain the cytosol of the cells. Therefore, in this staining, double negative cells are assigned as "living cells", Annexin$^+$ 7-AAD$^-$ cells mark early apoptosis and double positive cells are assigned as late apoptotic cells.

0.5 – 1x10^6 cells were subjected to this staining. The cells were washed with DPBS, suspended in 300 µl 1x Annexin Binding Buffer and stained with 5 µl Annexin V-FITC and 10 µl 7-AAD. The cells were incubated at room temperature in the dark for 15 minutes and subsequently measured.

3.4.5. Flow-cytometric determination of the cellular mitochondrial mass

The determination of the cellular mitochondrial mass was performed using the dye Mitotracker Green FM. For this, 0.5x10^6 cells/staining were washed with DPBS and resuspended in 1 ml cell culture medium without serum. Cells were treated with 1.5 µM Cyclosporine A and 10 nM Mitotracker Green FM and incubated for 1 – 2 h under cell culture conditions. Afterwards, cells were washed in FACS washing buffer and surface staining was performed as described in chapter 3.4.1.

3.4.6. Flow-cytometric determination of cellular glucose uptake

To assess the cellular glucose uptake, the cells were stained with the fluorescent glucose analog 2-NBDG. For this, 0.5x10^6 cells/staining were washed with HBSS and resuspended in 200 µl of a 50 µM 2-NBDG solution in HBSS. Cells incubated for 45 min under cell culture conditions. Afterwards, surface staining was performed as described in chapter 3.4.1.

3.4.7. Determination of the intracellular pH

Intracellular pH was assessed by flow cytometry using the pH-sensitive dye carboxy SNARF-1 AM acetate. Macrophages were incubated with indicated treatments for 24 h. Cell were harvested, and the supernatants kept under cell culture conditions for the later measurement. Cells were washed once with HBSS and stained with 10 µM Carboxy SNARF-1 AM acetate for 30 minutes under cell culture conditions. Afterwards, cells were again washed with HBSS and the respective culture supernatant added to re-adjust the intracellular pH. The cells were kept under cell culture conditions until the measurement. For calibration, cells were incubated with pH-controlled buffers (pH Intracellular Calibration Kit). To ensure a proper adjustment of the intracellular pH, valinomycin and nigericin were added. For analyses, ratios of emission wavelength λ1, transmitted by a 550LP BP filter and wavelength λ2, transmitted by a 670LP filter, were calculated.

3.4.8. CFSE-Staining of T cells

Carboxyfluoresceinsuccinimidylester (CFSE) is a cell-permeable fluorescent dye used for proliferation studies. After the staining, it remains in the cytosol of a cell and can be detected by flow cytometry. Upon proliferation, the dye equally distributes to the daughter cells, which leads to a decrease of the fluorescence in those cells. The more divisions a cell undergoes, the more the fluorescence declines. This allows to directly retrace the number of proliferation cycles of distinct cells and to discriminate between proliferating and non-proliferating cells.

Staining and handling of the cells was performed under sterile conditions in a laminar flow cabinet. To prevent photobleaching, direct light irradiation was avoided. For staining of T cells, $10x10^6$ cells each were stained in 15 ml Falcons. Cells were washed twice with DPBS. Afterwards, cells were incubated in a solution of 2.5 µM CFSE in 1 ml PBS for 4 minutes at room temperature. Afterwards, cells were washed with 10 ml DPBS containing 10 % FCS and again with 10 ml complete culture medium. The stained cells were merged and subjected to experiments.

3.4.9. Compensation

Compensation for antibodies was performed using the BD Compensation Particles according to manufacturer's instructions. Hereby, single conjugates were compensated using generic antibodies and tandem conjugates were compensated using the specific antibody. For the compensation of fluorescent dyes, single-stained cells of the respective origin were used.

3.5. Cell-culture based techniques for metabolic analysis

3.5.1. Determination of lactate secretion

The lactate secretion of cells was assessed by enzymatic determination of the lactate concentration in the cell culture supernatants. This analysis was carried out by the department of clinical chemistry of the University Hospital Regensburg.

3.5.2. Measurement of the cellular oxygen consumption and extracellular pH

The oxygen consumption and extracellular pH of cells was measured using the Presens technology. For the determination of oxygen levels in cell culture medium, cells were seeded into OD24 Oxodish plates. For the measurement of extracellular pH, HD24 Hydrodish plates

were used. The cells were kept under normal cell culture conditions and measurements performed using the SDR sensor dish reader system.

3.5.3. Determination of cellular glucose consumption

The glucose levels in cell culture supernatants were assessed using the HK glucose assay kit after manufacturer's instructions. The absorbance was measured using the TECAN Spark microplate reader.

3.5.4. 13C-Tracing analysis

Carbon-13 (C13) is a natural, stable isotope of carbon (C12) often used for metabolic flux assays. Instead of having 6 protons and 6 neutrons in the atomic core, it has 6 protons and 7 neutrons. This makes it possible to detect 13C using common techniques, e.g. NMR spectroscopy or mass spectrometry. If a cell is incubated with a 13C-labelled substrate as for example U13C-glucose, all metabolites in the downstream metabolization pathway can in turn enrich the 13C label and can be detected and identified by the mentioned techniques. This allows to draw conclusions regarding the preferentially used metabolization pathway and the turnover of the respective substance in the cellular metabolism.

For the tracing analyses of the LDHB overexpressing cells, the cells were plated in a concentration of $0.8x10^6$/ml in 24 well plates and stimulated with anti-CD3/CD28 coated Dynabeads in a ratio of 1:5 (glucose tracing) or 1:1 (lactate tracing). To analyze the glucose metabolism, the cells were beforehand washed and then cultivated in glucose-free medium, which was supplemented with 10 mM U13C-labelled glucose. For the lactate tracing, cells were treated with 13C-labelled lactic acid (13C3 lactic acid).

After 6 h and 24 h, respectively, the cells were harvested, and the stimulation beads removed. Cells were washed two times in DPBS and afterwards, the pellet was snap-frozen in liquid nitrogen and stored and -80 °C until further analysis.

The 13C enrichment analysis was conducted by the Institute for Functional Genomics, University Regensburg.

3.5.5. High-Resolution Respirometry of human and murine T cells

Respiratory profiles of T cells were determined by high-resolution respirometry using the Oxygraph O2-k. This technique allows to determine the oxygen consumption rate in whole

cells. As the systems owes closed chambers, absolute values can be measured and directly compared. Through injection ports into the chamber, chemicals modulating the respiratory function can be applied.

All measurements were carried out in the respective cell culture medium. Before starting, cell culture medium was filled into the chambers and air calibration of the medium was performed, which can vary from day to day. Cell suspension was filled into the chambers, a sub-sample taken for cell number determination, and the chamber was closed without inclusion of any air bubbles. The cell number was used to calculate the exact oxygen flux per cell. After a stabilization phase around 10 minutes, basic respiration (ROUTINE) was determined. Afterwards, oligomycin, an inhibitor of the ATP synthase, was applied, thereby LEAK respiration was measured. The amount of oxygen related to ATP production can by calculated by subtracting LEAK from ROUTINE respiration. Subsequently, the respiratory chain was uncoupled by applying Carbonyl cyanide-p-trifluoromethoxy phenylhydrazone (FCCP). FCCP was titrated in 1 – 5 µl steps until no further increase in the oxygen consumption rate was observed. The uncoupling of the respiratory system by FCCP allows to draw conclusions regarding oxygen consumption when the electron transfer system (ETS) operates at its maximal capacity. Rotenone was added to inhibit complex I of the respiratory chain. Finally, myxothiazol was used to inhibit the complex III activity and thereby the whole respiratory system, thus allowing measurement of residual oxygen consumption (ROX). ROX was subtracted from all respiratory parameters. The concentrations and functions of the applied substances are given in Table 3-22.

Table 3-22: Substances used to modulate the oxygen consumption.

Substance	Concentration	Function
Oligomycin	2 µg/ml	Inhibitor of the ATP synthase
FCCP	Up to 30 µM	Uncoupling of the ETS
Rotenone	0.5 µM	Inhibitor of complex I
Myxothiazol	0.5 µM	Inhibitor of complex III

3.5.6. Determination of Citrate Synthase activity in T cells

Specific activity (pmol/s) of the mitochondrial enzyme citrate synthase (CS) was measured photometrically at 412 nm using an established protocol (Bergmeyer, 1974). In brief, citrate synthase (CS) activity was determined in the same specimen analyzed by High-Resolution Respirometry. After finishing the respirometry protocol, the total volume of cell suspension was retrieved directly from the oxygraph chamber, shock frozen, and stored at -80 °C. After

repeated freezing and thawing cycles, specific CS activity (IU/ml) was quantified photometrically. CS catalyzes the reaction of acetyl-CoA and oxalacetate to citrate and CoA-SH, which further reacts with DTNB to TNB and CoA-S-S-TNB. TNB has an intense absorption at 412 nM, which increases linearly over the whole measuring period of 200 s. For photometry, a NanoDrop 2000c was used.

3.5.7. Determination of cytokine secretion using ELISA

The determination of cytokine concentrations in cell culture supernatants was performed using sandwich-ELISA. In this technique, the molecule of interest is caught in a “sandwich” of two specific antibodies, of which the “lower” one is bound to the surface of a 96 well plate and “upper” one is biotinylated and can be labelled with a horseradish-peroxidase, which catalyzes a colorimetric reaction and allows a subsequent absorbance measurement. By means of a standard curve, the absolute concentration of the molecule of interest in test material can be calculated.

For the quantification of cytokine levels, the respective DuoSet ELISA Kits provided by R&D systems were used according to manufacturer’s instructions.

3.6. Graphics and Statistics

Graphics were created with the GraphPad Prism software or by licensed BioRender.com. Statistical analyses were performed using GraphPad Prism software.

4. Results

4.1. Effects of lactic acid on human CD4 T cells

As a consequence of their highly glycolytic phenotype, tumor cells are often characterized by high lactate secretion (Cairns et al., 2011; DeBerardinis and Chandel, 2020; Semenza, 2008). This is also reflected in patients, where solid tumors often show an increased intra-tumoral concentration of lactate compared to normal tissue (Holm et al., 1995; Walenta and Mueller-Klieser, 2004). Lactate is exported from tumor cells in co-transport with protons by monocarboxylate transporters (MCTs), which leads to an enrichment of lactate and protons in the tumor environment (lactic acid accumulation). It has been reported that lactic acid has a strong inhibitory effect on murine CD4 and CD8 T cells as well as human CD8 T cells (Brand et al., 2016; Fischer et al., 2007; Mendler et al., 2012). However, this work mainly focuses on investigating and modulating the lactic acid effects in human CD4 T cells, as data regarding the sensitivity of human CD4 T cells towards the effects of lactic acid are sparser. Therefore, in a first step the effects of lactic acid treatment on CD4 T cells shall be elucidated.

4.1.1. Lactic acid induces apoptosis and inhibits effector functions of human CD4 T cells

CD4 T cells were isolated from MNCs of healthy donors and a purity of more than 98 % was confirmed by flow cytometry analysis (data not shown). To investigate the effects of lactic acid on T cell function, T cells were stimulated using α-CD3/CD28 coated beads in the presence of different concentrations of lactic acid.

Similar to what has been described for murine and human T cells before, high concentrations of lactic acid showed a strong negative impact on the viability of human CD4 T cells (Figure 4-1 A). After 72 h of treatment with 20 mM lactic acid, the median viability of CD4 T cells was significantly reduced to 21.9 %. Lower levels of lactic acid showed only a slight effect, as 10 mM and 15 mM lactic acid reduced the viability to 83.9 % and 79.3 %, respectively.

Next, the effect of non-lethal lactic acid concentrations on effector functions and proliferation of CD4 T cells was investigated (Figure 4-1 B - F). Already low concentrations of lactic acid inhibited proliferation of CD4 T cells starting 72 h after α-CD3/CD28 stimulation (Figure 4-1 B). The secretion of the effector cytokines IFN-γ and TNF was assessed after 48 h of treatment (Figure 4-1 C, D). Both cytokines were significantly reduced upon lactic acid treatment, although TNF secretion was slightly more resistant. In line, also the upregulation of the activation-marker CD25 was significantly diminished in T cells treated with 15 mM lactic acid

(Figure 4-1 E, F). Interestingly, 10 mM lactic acid led to a slight increase in the upregulation of CD25, but still strongly inhibited the cytokine response.

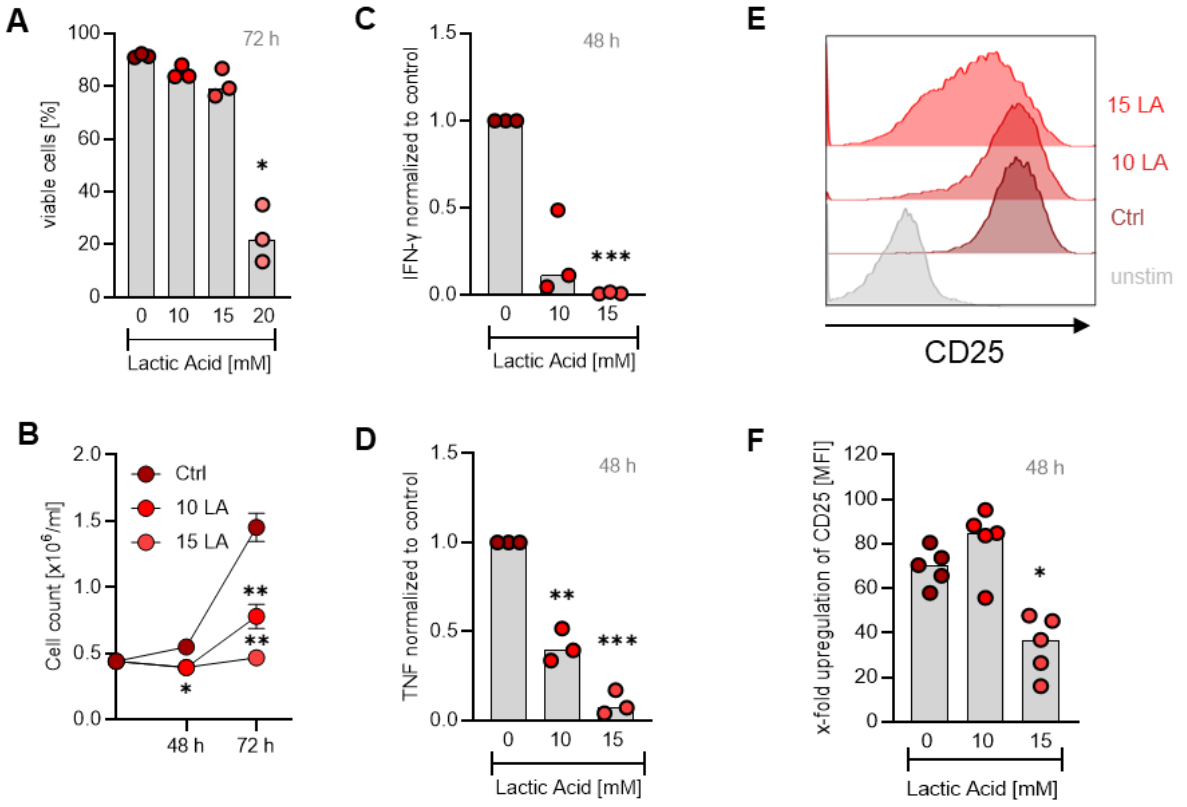

Figure 4-1: Lactic acid induces cell death, inhibits proliferation and effector functions of human CD4 T cells. *T cells were isolated from MNCs of healthy donors, stimulated with α-CD3/CD28 beads at a cell-to-bead ratio of 1:1 in the presence of IL-2 and treated with the indicated concentrations of lactic acid. (A) Viability of the cells was assessed after 72 h treatment by an Annexin V/7-AAD staining and subsequent flow cytometric analysis. Viable cells were designated as Annexin V⁻ 7-AAD⁻. (B) To assess the proliferation, cells were counted using the CASY cell counter system. (C, D) Cytokine levels in the cell culture supernatants were measured with ELISA after 48 h treatment and normalized to the respective control. (E, F) The expression of the activation marker CD25 after 48 h was assessed by means of flow cytometry. (E) Shown is a representative histogram, (F) and the summary of the increase in median fluorescence intensity (MFI) upon stimulation. (B) Shown are mean values with SEM (n = 3) or (A, D - E) median levels with and single data points. Asterisks give the significance levels between treatments and control. The significance levels were determined using (B) 2-way ANOVA or (A, D - E) one-way ANOVA and post-hoc Bonferroni multiple comparison test (* p < 0.05, ** p < 0.01, *** p < 0.001).*

In summary, lactic acid inhibited the proliferation and effector functions of human CD4 T cells in lower concentrations (10-15 mM) and reduced the viability of T cells in higher concentrations (20 mM).

4.1.2. Lactic acid blocks mitochondrial respiration and glycolytic activity of human CD4 T cells

Sustaining a highly efficient energy metabolism fueled by both oxidative phosphorylation (OXPHOS) and glycolysis is of critical importance for a proper T cell activation. Thus, lactate generated as a consequence of aerobic glycolysis needs to be exported from the cytosol to maintain the glycolytic activity. High intracellular levels of lactate block glycolysis and, thereby,

the consumption of glucose and OXPHOS activity as well. Therefore, in a next step, the effects of non-lethal doses of lactic acid on the T cell metabolism were analyzed.

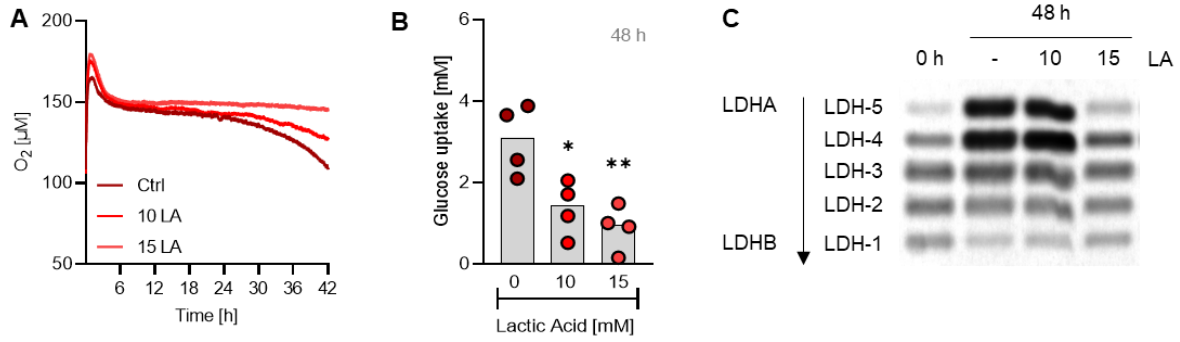

Figure 4-2: Lactic acid blocks mitochondrial and glycolytic activity of human CD4 T cells and dampens LDHA upregulation. *T cells were isolated from MNCs of healthy donors, stimulated with α-CD3/CD28 coated beads at a cell-to-bead ratio of 1:1 in the presence of IL-2 and treated with the indicated concentrations of lactic acid. (A) The respiration of the cells was assessed with the PreSens technology (mean values from n = 3 independent healthy donors). (B) To assess glucose uptake of the T cells within 48 h of culture, the glucose remaining in the culture supernatants was measured and subtracted from the initial glucose concentration. Summarized data are displayed as median, each symbol represents one donor. Asterisks give the significance levels between treatments and control. The significance levels were determined by one-way ANOVA and post-hoc Bonferroni multiple comparison test (* p < 0.05, ** p < 0.01). (C) The LDH isoenzyme pattern of cells before and after 48 h stimulation was analyzed by LDH zymography analysis applying 3 µg total protein loaded per lane. A representative example out of three independent experiments is shown.*

The respiratory activity of CD4 T cells upon lactic acid treatment was assessed with the PreSens technology (Figure 4-2 A). CD4 T cells started to consume oxygen upon stimulation and even more pronounced after 24 h, indicating an upregulation of their mitochondrial metabolism. The consumption of oxygen was lowered by lactic acid treatment and almost completely blocked by the addition of 15 mM lactic acid, indicating that lactic acid inhibits the mitochondrial activity of T cells in a concentration-dependent manner.

To assess the glycolytic activity of CD4 T cells, cellular glucose uptake was calculated by subtracting the glucose remaining in the culture supernatant after 48 h of treatment from the initial glucose concentration in the T cell medium (Figure 4-2 B). Glucose uptake of the T cells was decreased with increasing concentrations of lactic acid, indicating a block in the glycolytic activity. In line, an isoenzyme analysis of lactate dehydrogenase (LDH) revealed that the upregulation of LDHA in the T cells, which is necessary to enhance glycolytic activity, is dampened by lactic acid treatment (Figure 4-2 C).

Taken together, the results show that lactic acid causes a metabolic blockade by inhibiting both mitochondrial and glycolytic activity of T cells.

4.1.3. Lactic acid sensitivity of T cell memory subsets

As a result of the immune cell differentiation in the course of an immune response, the total T cell population can be separated into different memory subtypes with diverging proliferative

capacity, effector functions and cellular metabolism. Different studies have shown that success of an adoptive T cell transfer therapy depends on the differentiation state of the transferred T cells, even though results regarding a superior subtype are not consistent. Therefore, we questioned whether the outcome of an adoptive cell transfer therapy (ACT) after the transfer of a specific memory subtype might be related to a higher resistance of one subset towards lactic acid and tested the sensitivity different memory subtypes.

Naïve (NV), central memory (CM) and effector memory (EM) T cells were isolated by specific surface marker staining and cell sorting with the FACSAria. Re-analysis of the sorted cells revealed a purity of > 98 % (data not shown). Cells were stimulated with α-CD3/CD28 coated beads, treated with different concentrations of lactic acid and analyzed for their survival, effector functions and cellular metabolism in the presence of lactic acid.

Cell viability was assessed 72 h and 6 d after stimulation. As the antibodies used for the sorting approach remain bound to the cells for quite a long time, an analysis of the viability by Annexin V/7-AAD staining is difficult in sorted cells. Instead, viability was assessed by means of forward- and side-scatter (FSC/SSC), the light scattered by cells in flow cytometry analysis. FSC intensity is a measure for cell size, SSC provides information on the granularity of the analyzed cells. Dead T cells are smaller compared to their living counterparts, causing a decrease in the FSC, and as a consequence of the formation of apoptotic bodies and budding of the cells, the SSC start to increase. This modulation of the parameters allows an estimate of the portion of living cells in a culture.

As observed in bulk T cells cultures (Figure 4-1), sorted memory and naïve T cells did not survive 72 h treatment with 20 mM lactic acid, except for one more resistant donor (Figure 4-3 B). Interestingly after 6 days the “lactic acid resistance” of this donor was no longer found in naïve and CM T cells but maintained in EM cells. Notably, EM cells showed the lowest proliferation during the observation time (Figure 4-4 A) indicating that proliferation drives naïve and CM T cells into a more vulnerable state. Overall, the viability of the different T cells subsets against long-term exposure to lactic acid was not different compared to the short-term condition.

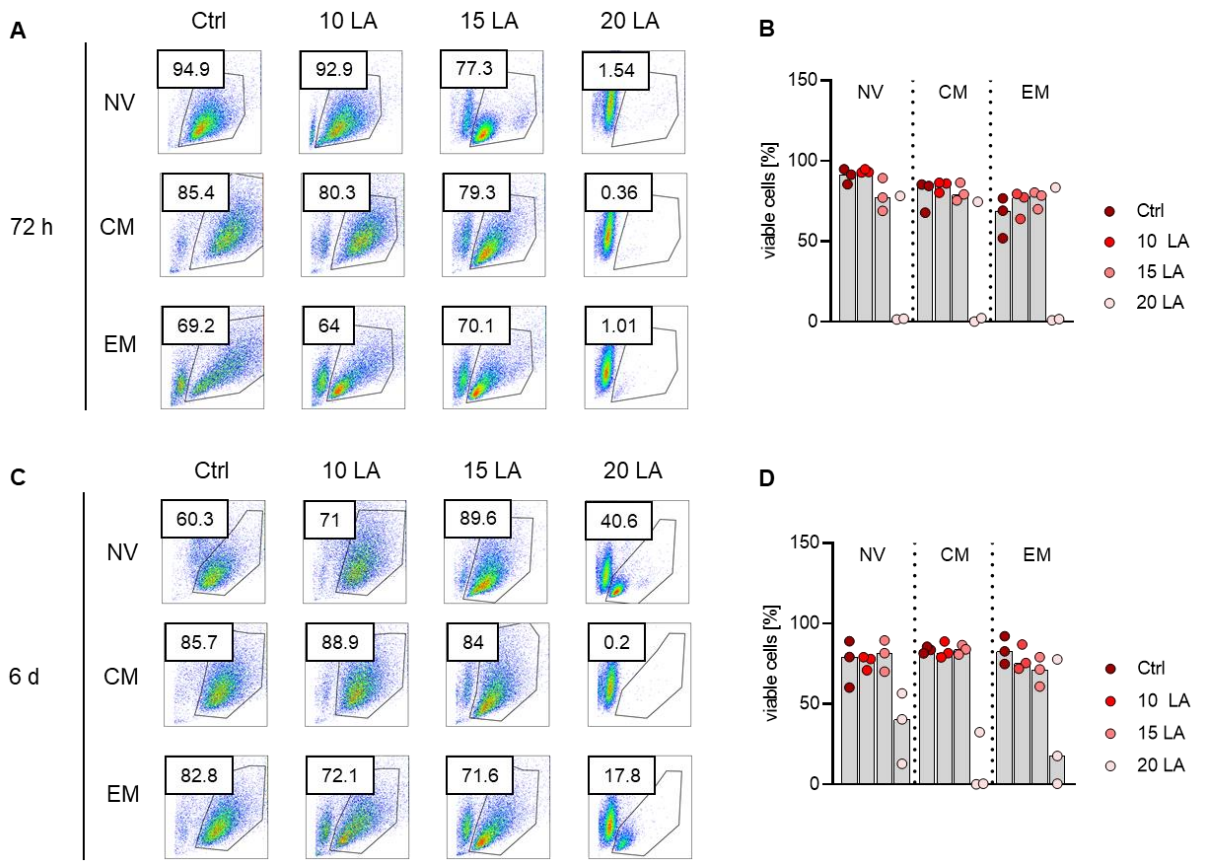

Figure 4-3: No survival advantage of a T cell subtype upon treatment with high levels of lactic acid. *CD4 T cells were isolated from MNCs of healthy donors and naïve (NV), central memory (CM) and effector memory (EM) cells purified by flow cytometry cell sorting. The cells were stimulated with α-CD3/CD28 coated beads in a bead-to-cell ratio of 1:1 in the presence of IL-2 and treated with indicated concentrations of lactic acid. The viability of the cells was analyzed after (A, B) 72 h and (C, D) 6 d incubation time by means of flow cytometry. Displayed are (A, C) one representative example (X-axis: FSC; Y-axis: SSC) and (B, D) median viability levels with single values. The significance levels were determined by one-way ANOVA and post-hoc Bonferroni multiple comparison test (no significance detected).*

To assess the functionality of the T cell subsets in the presence of lactic acid, cells were counted at different time points and cytokine secretion measured after 48 h of culture (Figure 4-4). Lactic acid treatment significantly inhibited the proliferation in all three T cell subsets. Cytokine secretion was assessed by measurement of IFN-γ and TNF in cell culture supernatants. 10 mM lactic acid did not significantly suppress IFN-γ secretion and even led to a 2-fold increase in naïve T cells of two donors. A similar trend was observed analyzing TNF secretion of EM T cells. Upon treatment with 15 mM lactic acid, the IFN-γ secretion was significantly decreased in CM cells and in three of four analyzed donors in naïve T cells. Interestingly, EM T cells seemed to be slightly less sensitive, but still showed a pronounced decrease in IFN-γ secretion. In contrast, TNF secretion was more susceptible in all T cell subtypes and significantly decreased after treatment with 15 mM lactic acid.

Interestingly, one donor seemed more resistant towards lactic acid treatment and was able to maintain production of both IFN-γ and TNF despite treatment with 15 mM lactic acid. Importantly, this donor also survived treatment with 20 mM lactic acid (Figure 4-3). Based on

this finding that some donors may have an intrinsic capacity to resist higher lactic acid concentrations, we performed a RNAseq analysis to define “resistance parameters” (see chapter 4.6.2).

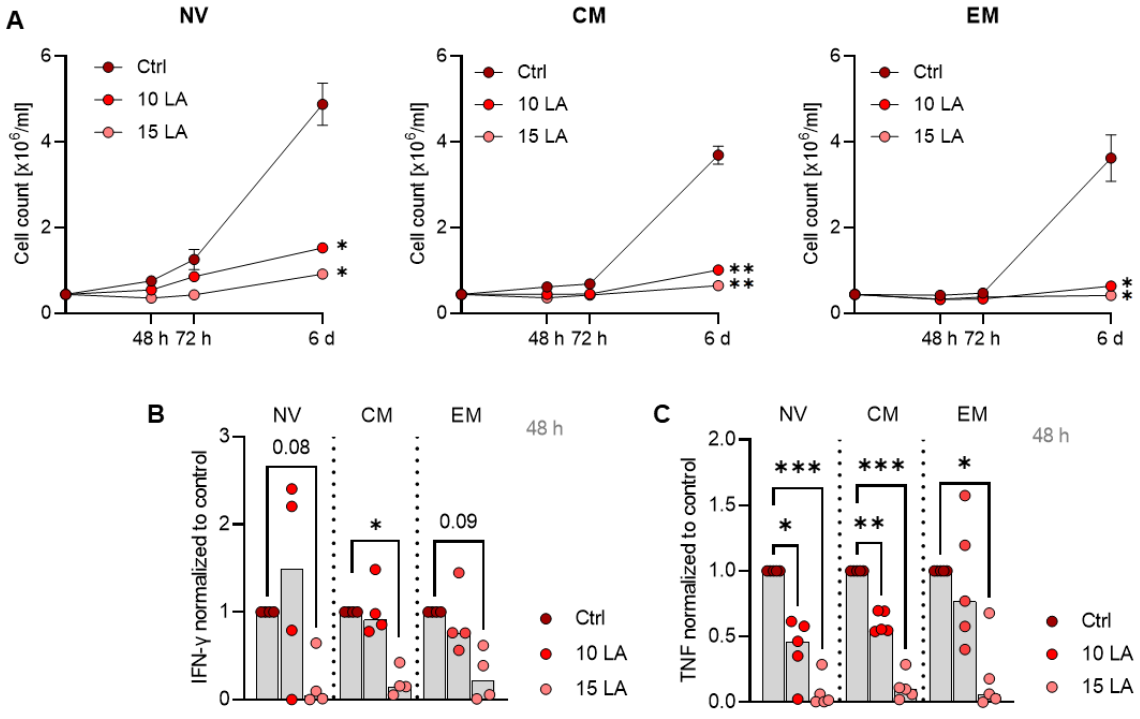

Figure 4-4: The functionality of different T cell subsets is inhibited by lactic acid to a similar degree. *CD4 T cells were isolated from MNCs of healthy donors and naïve (NV), central memory (CM) and effector memory (EM) cells purified by flow cytometry cell sorting. The cells were stimulated with α-CD3/CD28 coated beads at a bead-to-cell ratio of 1:1 in the presence of IL-2 and treated with the indicated concentrations of lactic acid. (A) Cells were counted at the indicated time points using the CASY Cell counter (n = 3). (B, C) The levels of (B) IFN-γ and (C) TNF were measured after 48 h in the culture supernatants using ELISA. Depicted are (A) mean values with SEM and (B, C) median levels with single data points. Asterisks show significant differences between control and treatments. Statistical difference was calculated using (A) two-way ANOVA with Dunnet's multiple comparison test or (B, C) one-way ANOVA and post-hoc Bonferroni multiple comparison test (* p < 0.05; ** p < 0.01; *** p < 0.001; numbers give exact p values)*

Last, we assessed the influence of lactic acid on mitochondrial metabolism and LDH isoenzyme distribution in the different T cell subsets (Figure 4-5). Naïve T cells showed the strongest respiratory activity, followed by CM T cells, whilst EM T cells showed a reduced respiratory activity. In both CM and naïve T cells, 15 mM lactic acid almost completely abolished the respiratory activity, whilst 10 mM lactic acid either had no effect (CM T cells) or even slightly increased the respiratory activity (NV T cells). In a similar manner, upregulation of LDHA and the corresponding shift in the LDH isoenzyme pattern was not influenced by 10 mM lactic acid in naïve T cells, but severely affected in CM and EM T cells. However, treatment with 15 mM lactic acid completely abolished the LDH isoenzyme shift in all three analyzed T cell subsets.

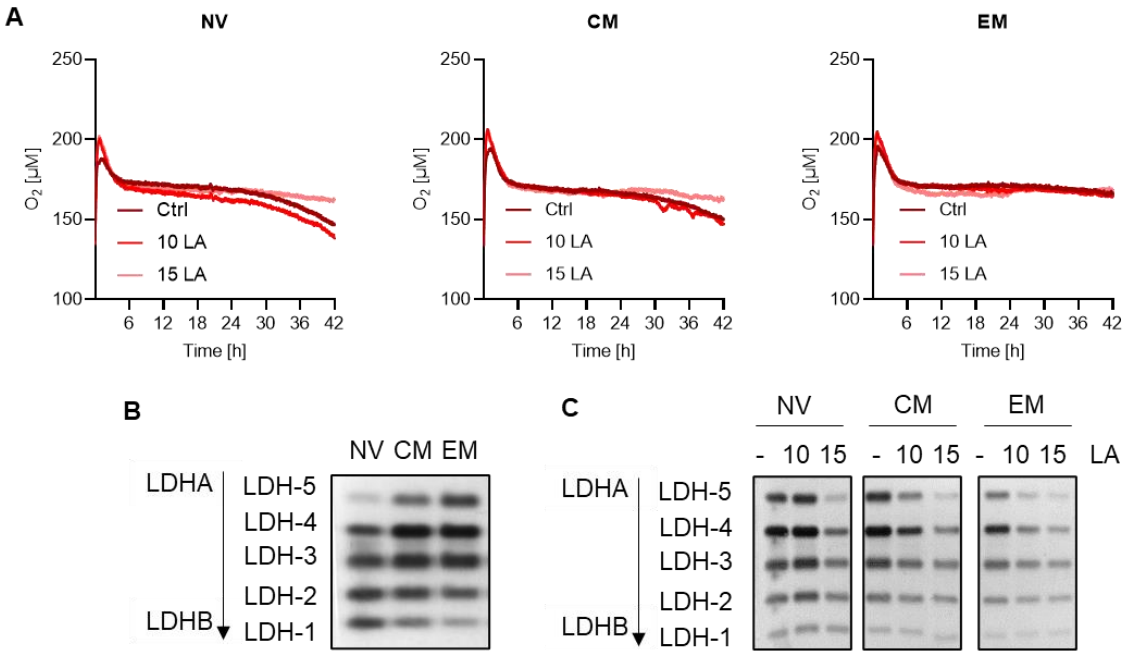

Figure 4-5: Naïve T cells show a higher metabolic resistance towards low, but not high, levels of lactic acid. *CD4 T cells were isolated from MNCs of healthy donors and naïve (NV), central memory (CM) and effector memory (EM) cells purified by flow cytometry sorting. Cells were stimulated with α-CD3/CD28 coated beads at a bead-to-cell ratio of 1:1 in the presence of IL-2 and treated with indicated concentrations of lactic acid. (A) The respiration of the cells was measured using the PreSens technology (n = 2). (B, C) The LDH isoenzyme profile of (B) unstimulated and (C) 48 h stimulated and lactic acid treated cells was assessed by LDH zymography analysis. Depicted is one representative example each (n = 2 for unstimulated and LA treated, n = 3 for stimulated cells).*

Taken together, we were not able to identify a single T cells subset with a higher resistance towards lactic acid. Overall, the suppression in proliferation, cytokine response and metabolism were similar in bulk T cell cultures and subsets.

4.2. Buffering of the extracellular pH strengthens T cell metabolism, survival and cytokine secretion

Due to the co-transport of lactate and protons via MCTs, enrichment of lactate in a tumor is associated with a decrease in the environmental pH, which has been described to affect the anti-tumor activity of most immune cells, including T cells (Erra Díaz et al., 2018). Therefore, we investigated whether buffering the extracellular pH would compensate the negative impact of high extracellular lactic acid levels.

To assess effects of the low pH caused by lactic acid on the T cell functionality, human T cells were isolated, stimulated and treated with lactic acid as described above whilst cultured in normal RPMI or RPMI which displayed a higher buffering capacity. The general composition of the different media was the same, but in case of the buffered medium, sodium bicarbonate necessary for the buffering capacity was added freshly, enhancing its buffering properties. Consequently, after the addition of lactic acid the pH dropped less in buffered culture medium

resulting a difference of up to 0.6 units at 20 mM lactic acid, resembling the pH in the presence of 15 mM lactic acid in standard medium.

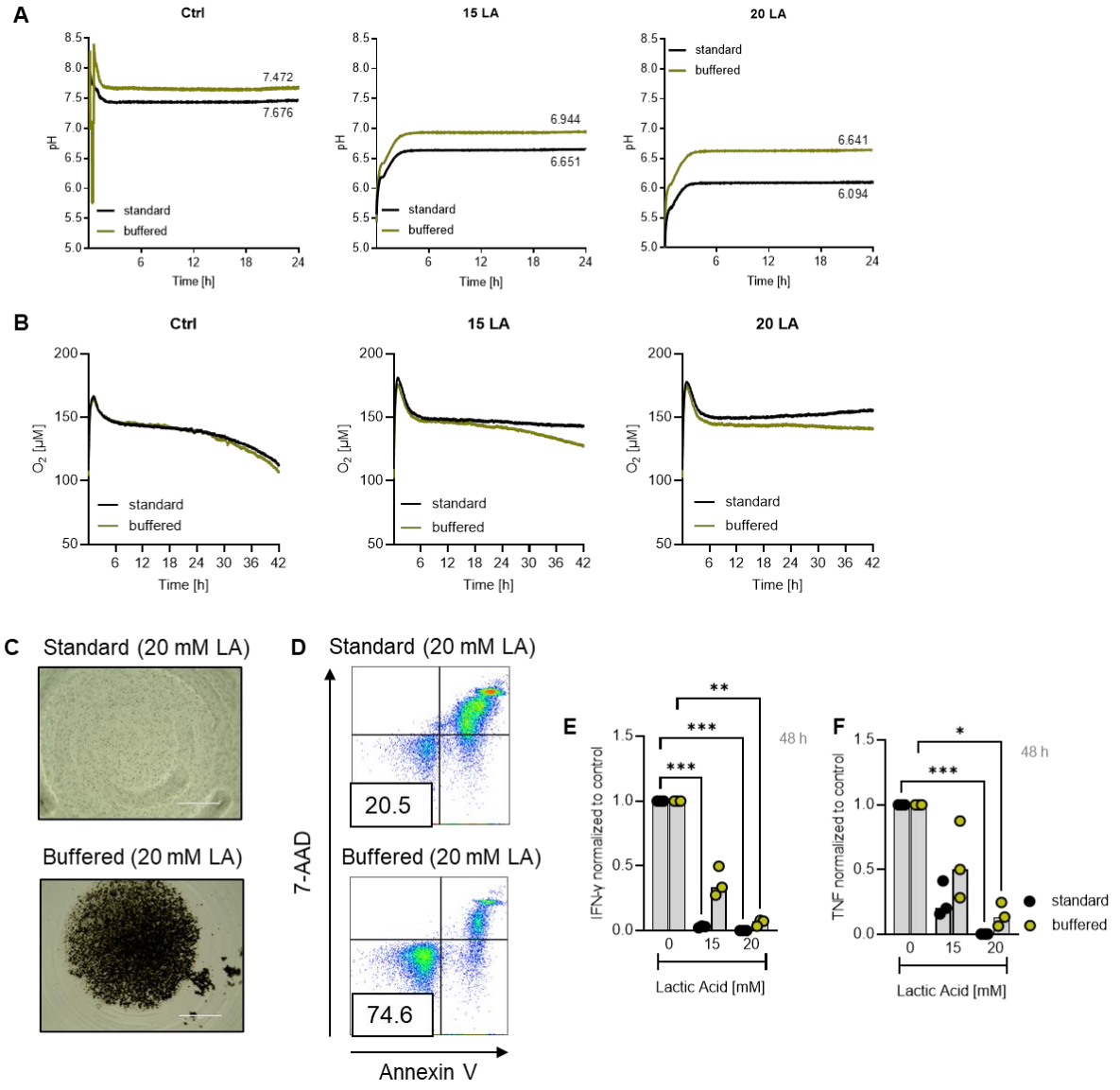

Figure 4-6: Buffering of the extracellular pH mitigates effects of lactic acid treatment. *CD4 T cells were isolated from MNCs of healthy donors, stimulated with α-CD3/CD28 coated beads at a bead-to-cell ratio of 1:1 in presence of IL-2 and treated with the indicated concentrations of lactic acid while cultured in standard RPMI (standard) or RPMI with a higher buffering capacity (buffered). (A) The pH of the cell-free medium was determined using the PreSens technology. (B) Cellular respiration was measured using the PreSens technology (n = 3). (C) The morphology of T cells treated with 20 mM lactic acid was judged after 48 h treatment and pictures recorded with the EVOS system. Shown is a representative example. (D) The viability of the cells after 72 h treatment was assessed by an Annexin V/7-AAD staining after 72 h and a subsequent flow cytometric analysis. Viable cells were designated as Annexin V$^-$/7-AAD$^-$ (X-Axis: Annexin V, Y-Axis: 7-AAD). Depicted is one representative example out of three independent experiments. (E, F) The levels of (E) IFN-γ and (F) TNF in the cell culture supernatants were measured by ELISA after 48 h treatment and normalized to the respective control. Shown are (A, B) mean values and (E, F) median levels with single data points. Asterisks give the significance levels between treatments and control. Significance was determined using one-way ANOVA and post-hoc Bonferroni multiple comparison test (* $p < 0.05$, ** $p < 0.01$, *** $p < 0.001$).*

We analyzed whether extracellular buffering would affect the lactic acid effect on the cellular mitochondrial metabolism, and found that extracellular buffering enhanced, but not completely normalized T cell respiration upon lactic acid treatment. In presence of 20 mM lactic acid,

clustering and on blast formation as a sign for T cells activation were only observed in buffered medium. Strikingly, buffering the extracellular pH prevented the lactic acid-induced cell death (Figure 4-6 D) and enhanced cytokine secretion of lactic acid treated T cells. Therefore, extracellular buffering can mitigate lactic acid triggered effects on T cells.

4.3. Pharmacological and metabolic intervention to enhance T cell resistance

Many different approaches have been attempted to increase the anti-tumor capacity of T cells after ACT. Among them, modifying the culture conditions of T cells before transfer by modulating the metabolic conditions or applying pharmacological substances influencing the cellular metabolism have led to promising results. We hypothesized, that this would also be a reasonable approach to enhance T cell resistance towards lactic acid. Enhancing the respiratory activity of T cells could lead to an increased metabolism of lactate, thereby reducing its intracellular concentration and enhance the T cell function at last.

4.3.1. Culture under glucose restriction

As described above, treatment of T cells with lactic acid blocking their mitochondrial and glycolytic activity rooted in a metabolic blockade of glucose metabolism itself. Therefore, we hypothesized that glucose restriction, which would force T cells to increase their mitochondrial metabolic activity instead, would pose a way to rescue T cell metabolism and thereby also the T cell function in high lactic acid conditions.

In a first step, the influence of glucose restriction and lactic acid treatment were analyzed in primary stimulated T cells. For those experiments, cells were cultivated in T cell medium without the addition of sodium pyruvate. Glucose restriction did not affect cellular respiration or LDH isoenzyme profile (Figure 4-7 A, B). Cell proliferation was inhibited in correlation with the applied glucose concentration (Figure 4-7 C), most likely because of glucose restriction over time as it was not replenished. Absolute cytokine secretion was not influenced by glucose restriction (data not shown). 15 mM lactic acid completely abrogated respiratory activity of T cells independently of the glucose concentration and the glucose concentration did not alter the impact of the lactic acid on the LDHA upregulation, cell proliferation, or cytokine production. Therefore, glucose restriction during lactic acid exposure does not enhance T cell resistance.

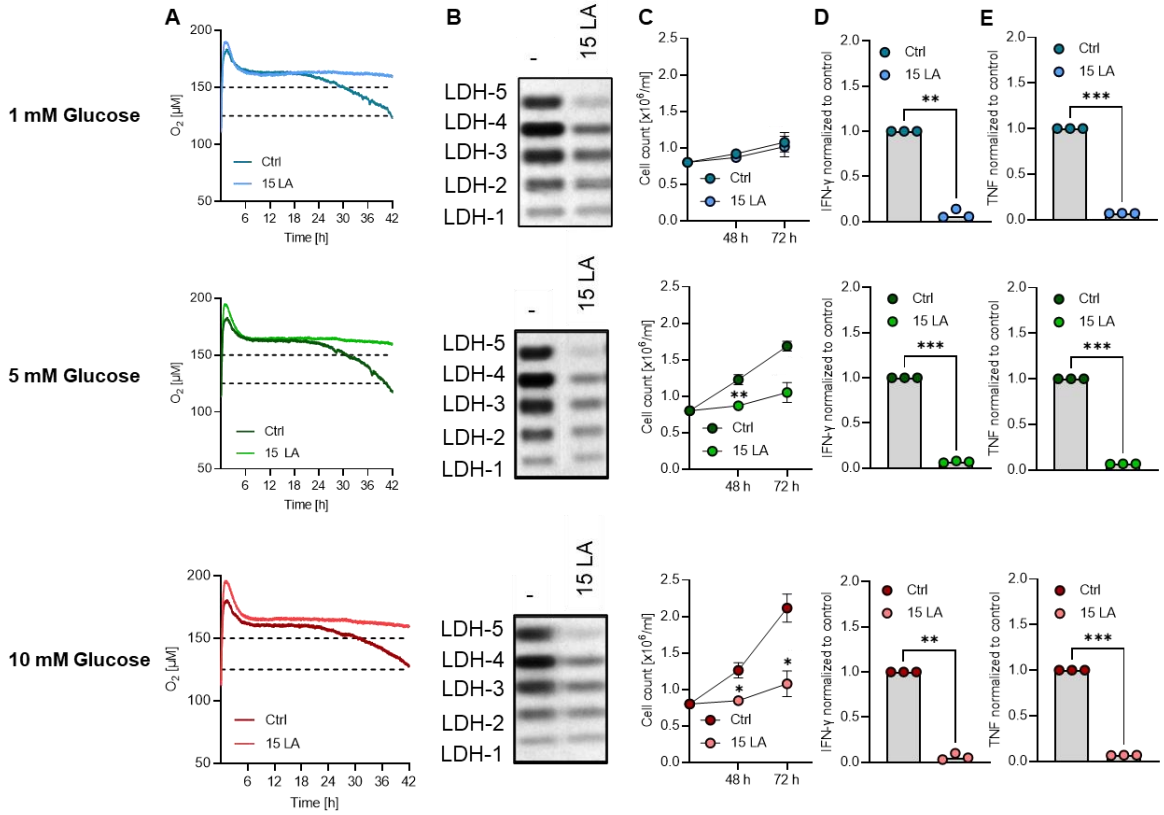

Figure 4-7: Effects of glucose restriction on the lactic acid sensitivity of T cells. *CD4 T cells were isolated from MNCs of healthy donors, stimulated with α-CD3/CD28 coated beads at a bead-to-cell ration of 1:1 in the presence IL-2 and treated with 15 mM lactic acid while cultured with 1 mM, 5 mM or 10 mM glucose (normal RPMI concentration 11 mM). (A) The oxygen consumption of the cells was measured using the PreSens technology (mean values of n = 3). Dotted lines at 150 µM and 120 µM O_2 are given for better orientation. (B) The LDH isoenzyme profile of T cells was analyzed after 48 h in culture by LDH zymography applying 7 µg total protein per lane. Depicted is a representative example of n = 3 experiments. (LA = Lactic acid) (C) The cells were counted after 48 h and 72 h treatment using the CASY Cell Counter. (D, E) The levels of the effector cytokines (D) IFN-γ and (E) TNF were measured in the supernatants of 48 h cultures by means of ELISA. (C) Depicted are mean values with SEM (n = 3) or (D, E) median values and single data points. Asterisks give the significance levels between treatments and the respective controls. Significance was calculated using (C) two-way ANOVA or (D, E) one-way ANOVA and post-hoc Bonferroni multiple comparison test (* p < 0.05; ** p < 0.01; *** p < 0.001).*

4.3.2. LDH inhibition

The inhibition of the LDH could represent another way to pharmacologically enhance the respiratory activity of T cells, as many available LDH inhibitors have a higher affinity for LDHA than for LDHB and should therefore target the lactate-producing, not the lactate metabolizing subunit of the LDH.

Hermans et al. described, that LDH inhibition in combination with IL-21 increases oxygen consumption of murine T cells and enhance their *in vivo* anti-tumor functions (Hermans et al., 2020). The alteration of the cellular metabolism by IL-21 has been confirmed in human CD8 T cells (Loschinski et al., 2018). However, in our hands, IL-21 failed to increase respiration or alter glycolytic activity of T cells (data not shown). Nevertheless, we investigated how LDH inhibition would affect the human T cell metabolism.

First, the LDH inhibitor R-(+)-GNE-140 (referred to as GNE) was applied to T cells. Cells were isolated from MNCs of healthy donors, stimulated with α-CD3/CD28 coated beads in the presence or absence of 30 µM GNE. After 48 h, cells were counted, and lactate secretion was determined (Figure 4-8).

As expected, LDH inhibition led to a strong increase in the respiratory activity of CD4 T cells, whilst the cell proliferation up to 48 h was not or only slightly affected by GNE treatment. Lactate secretion of T cells was only slightly diminished by GNE treatment. Similar results were obtained investigating CD8 T cells (data not shown).

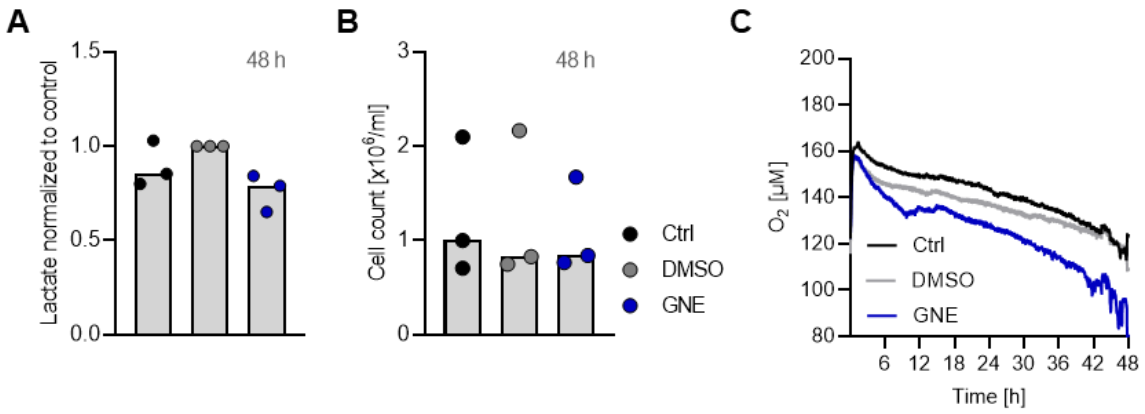

Figure 4-8: Treatment with the LDH inhibitor R-(+)-GNE-140 enhances respiratory activity and slightly diminishes lactate secretion of CD4 T cells. *T cells were isolated from MNCs of healthy donors and stimulated with α-CD3/CD28 coated beads at a bead-to-cell ratio of 1:1 in the presence of IL-2 and treated with 30 µM R-(+)-GNE-140 (GNE). DMSO served as a control. (A) Lactate concentrations in the culture supernatants were measured after 48 h in culture and normalized to the vehicle control. (B) After 48 h, cells were counted using the CASY Cell Counter. (c) Cellular respiration was monitored using the PreSens technology. Depicted are (A, B) median levels and single data points or (C) mean values (n = 3). Significance was determined using one-way ANOVA and post-hoc Bonferroni multiple comparison test (no significance detected).*

GNE treatment did not significantly affect lactic acid secretion of T cells. As an alternative, we used NCI-737 (referred to as LDHi), which has a much lower K_i for LDH compared to GNE.

In contrast to GNE treatment, LDHi decreased lactate secretion of T cells at a concentration of 3 µM, which was accompanied by a minor delay in proliferation. Surprisingly, treatment with LDHi did only slightly increase T cell respiration under control conditions, and only when applied in the highest concentration. Again, similar observations were made regarding CD8 T cells (data not shown).

However, when applied together with low levels of lactic acid, LDHi slightly increased respiratory activity of T cells at lower concentrations. Nevertheless, 15 mM lactic acid still led to a complete block in respiratory activity regardless of LDH inhibition.

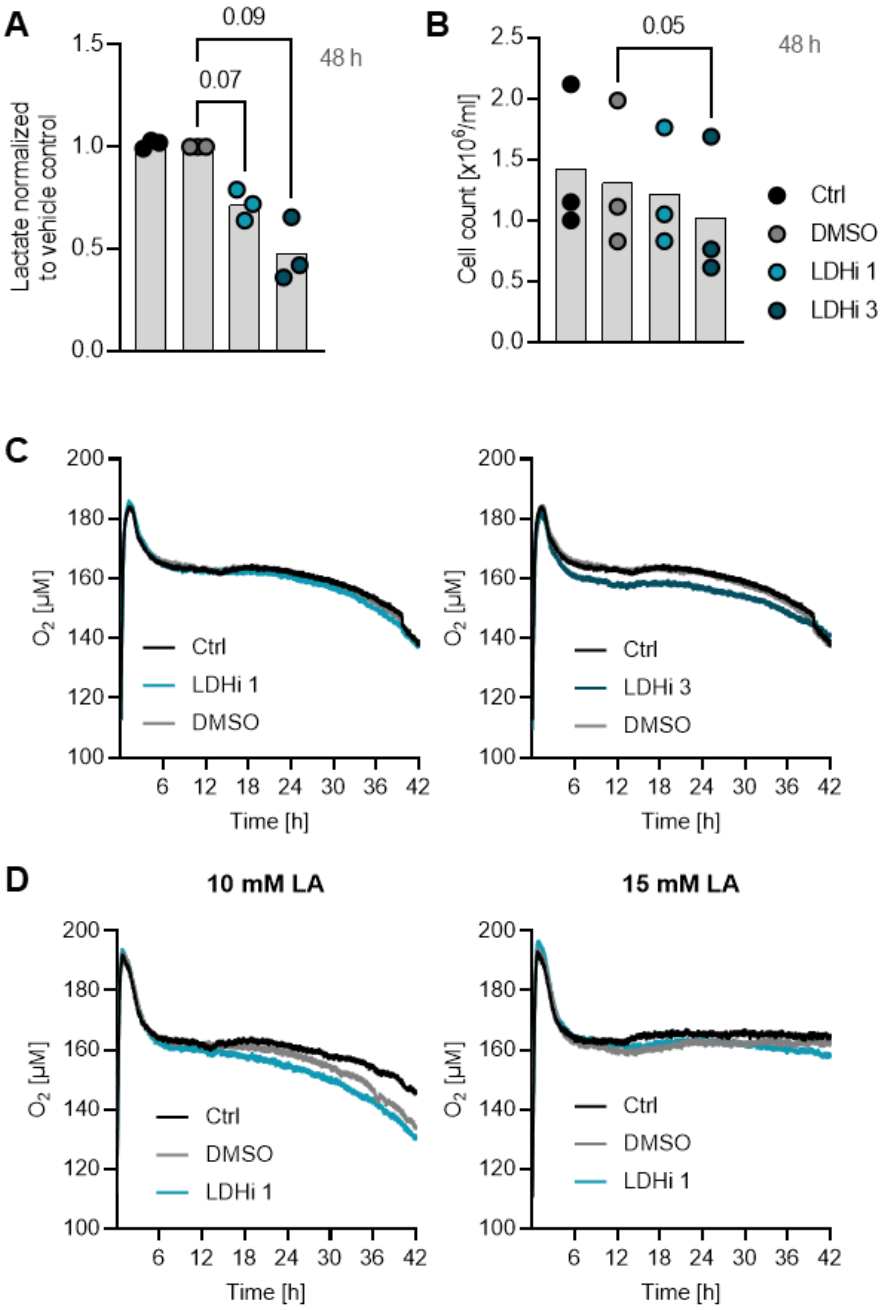

Figure 4-9: Treatment with NCI-737 impacts glycolysis but fails to increase cellular respiration. *T cells were isolated from MNCs of healthy donors and stimulated with α-CD3/CD28 coated beads at a bead-to-cell ratio of 1:1 in the presence of IL-2 and treated with NCI-737 (LDHi) in the indicated concentrations [µM]. DMSO served as a vehicle control. (A) Lactate concentrations in the culture supernatants after 48 h were measured by the department for Clinical Chemistry of the University Hospital Regensburg and normalized to the vehicle control. (B) After 48 h, cells were counted using the CASY Cell Counter. (C, D) Respiration of the cells was monitored using the PreSens technology. (D) Cells were treated with the indicated concentrations lactic acid. Depicted are (A, B) median levels and single data points or (C, D) mean values of (C) n = 3 and (D) n = 2 experiments. (A, B) Significance was determined using one-way ANOVA and post-hoc Bonferroni multiple comparison test. Numbers give exact p values.*

4.4. Genetic manipulation of T cells

Genetic manipulation of T cells offers the possibility to permanently alter T cell metabolism and thereby equip the cell with the ability to resist toxic metabolic conditions in the tumor

environment. This has, in the context of ACT, the advantage, that beneficial properties of the transferred cells are maintained for a longer time, whilst the modulation of the expansion conditions only has temporary effects.

As lactate is one of the metabolites contributing to the LDH reaction, it stands to reason to manipulate the balance between LDHA and LDHB and thereby shift the LDH isoenzyme-pattern towards a more LDHB-containing, lactate metabolizing phenotype. In a high lactic acid environment, lactate is taken up by T cells and accumulates in the cytosol, which causes a metabolic blockade associated with decreased metabolic activity and effector functions. By manipulating the LDH isoenzyme balance towards a more LDHB-containing phenotype, T cells shall gain the ability to metabolize the lactate to pyruvate, thereby resolving the metabolic blockade and restoring their effector functions. We hypothesized, that this would enable the T cells to metabolize the up taken lactate to pyruvate, which could be channeled into the tricarbolic acid cycle in mitochondria. Thereby, the metabolic blockade caused by lactate could be resolved and the T cell metabolism restored (Figure 4-10).

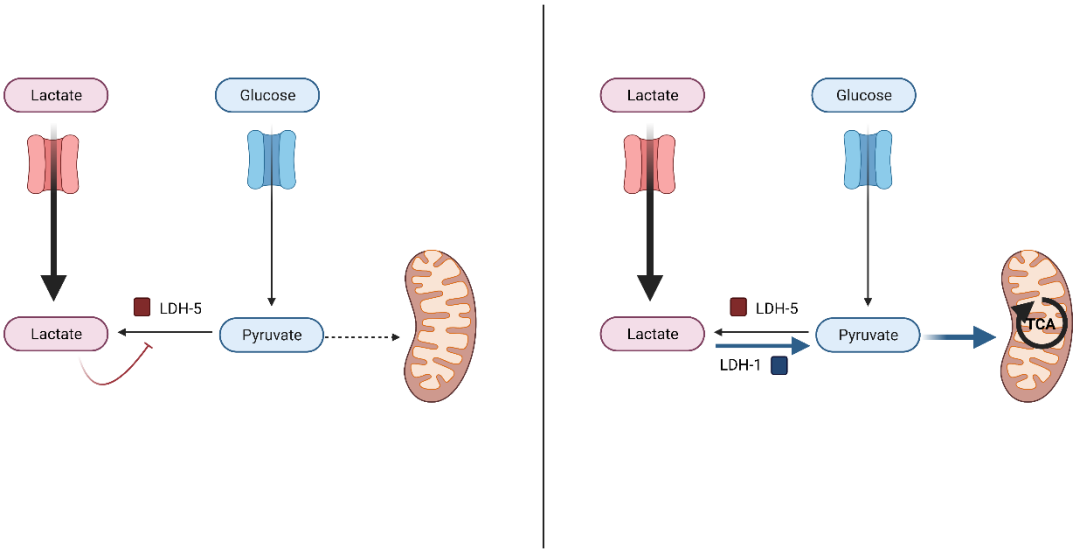

Figure 4-10: Underlying concept of the genetic manipulation to increase the lactic acid resistance of T cells. *Graphic created with BioRender.com.*

In this work, the shift in the LDH isoenzyme pattern was induced by two different methods: First, the siRNA-mediated knockdown of LDHA leading to a transient shift in the LDH isoenzyme pattern and second, the stable overexpression of LDHB in T cells by retroviral gene delivery.

4.4.1. Knockdown of LDHA in human T cells

The knockdown of LDHA in human CD4 T cells was achieved by electroporation of unstimulated T cells with a siRNA-Pool targeting LDHA ($LDHA^{low}$). The mixture of four different

siRNAs in one pool enhances knockdown efficacy and reduces the off-target effects of the siRNA electroporation. As a control, T cells were electroporated with a pool of scrambled siRNAs. To elucidate the effect of the electroporation itself on T cell metabolism, non-electroporated cells were included as experimental control. After electroporation, T cells were rested overnight and stimulated at the following day. Importantly, viability of the cells was not affected by the electroporation and the procedure did not cause CD25 upregulation or IFN-γ secretion, indicating no pre-stimulation (data not shown).

The electroporation of the T cells with the LDHA-specific siRNA caused a shift in the LDH isoenzyme pattern upon stimulation, which persisted for at least 48 h after stimulation. 6 d after stimulation, the LDH isoenzyme pattern was comparable in all treatment groups, thus the knockdown was only transient. Interestingly, the knockdown of LDHA did not cause a complete shift of the pattern to LDHB, but rather prevented the upregulation of LDHA and induced a LDH pattern more similar to unstimulated T cells.

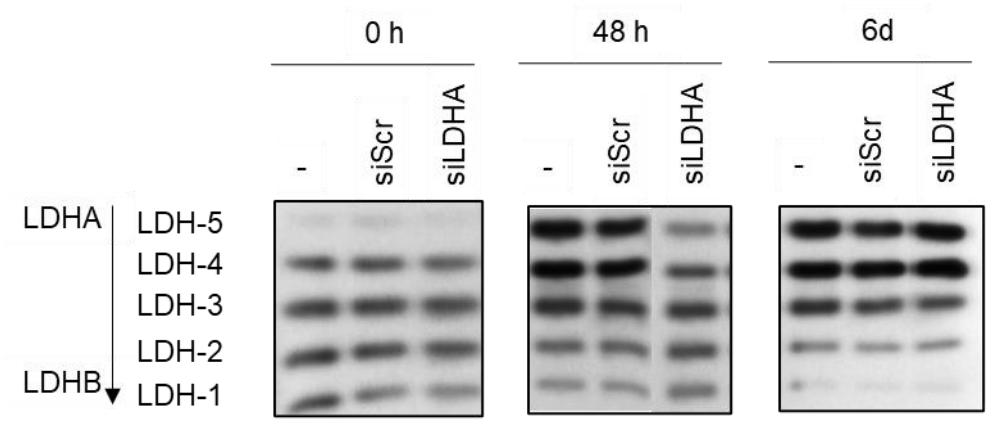

Figure 4-11: The electroporation of T cells with siRNA against LDHA prevents LDH-5 upregulation in the first 48 h after stimulation*. T cells were isolated from MNCs of healthy donors and electroporated with either a scrambled siRNA-Pool (siScr) or a siRNA-Pool against LDHA (siLDHA). Non-electroporated cells (-) were included as an additional control. After an overnight storage, the cells were stimulated for the indicated times with α-CD3/CD28 beads in a ratio of 1:1. Cells without electroporation were used as a control. The LDH isoenzyme profile was analyzed after LDH zymography applying 5 µg total protein per lane. Depicted is a representative example (n = 1 for 6 d, n = 3 for 0 h and 48 h).*

Next, we sought to investigate the influence of the LDHA knockdown on the metabolism of activated CD4 T cells. Surprisingly, neither oxygen consumption nor lactate production of T cells was affected by the altered LDHA expression (Figure 4-12 A, B), and two of the three analyzed donors even showed an increased lactate production of the $LDHA^{low}$ T cells compared to the T cells receiving the scrambled control siRNAs. $LDHA^{low}$ T cells also didn't show a decreased cytokine production or proliferation (data not shown) compared to the electroporation control, however, the electroporation procedure itself caused a decrease in the cytokine production and respiration (Figure 4-12 A, C, D).

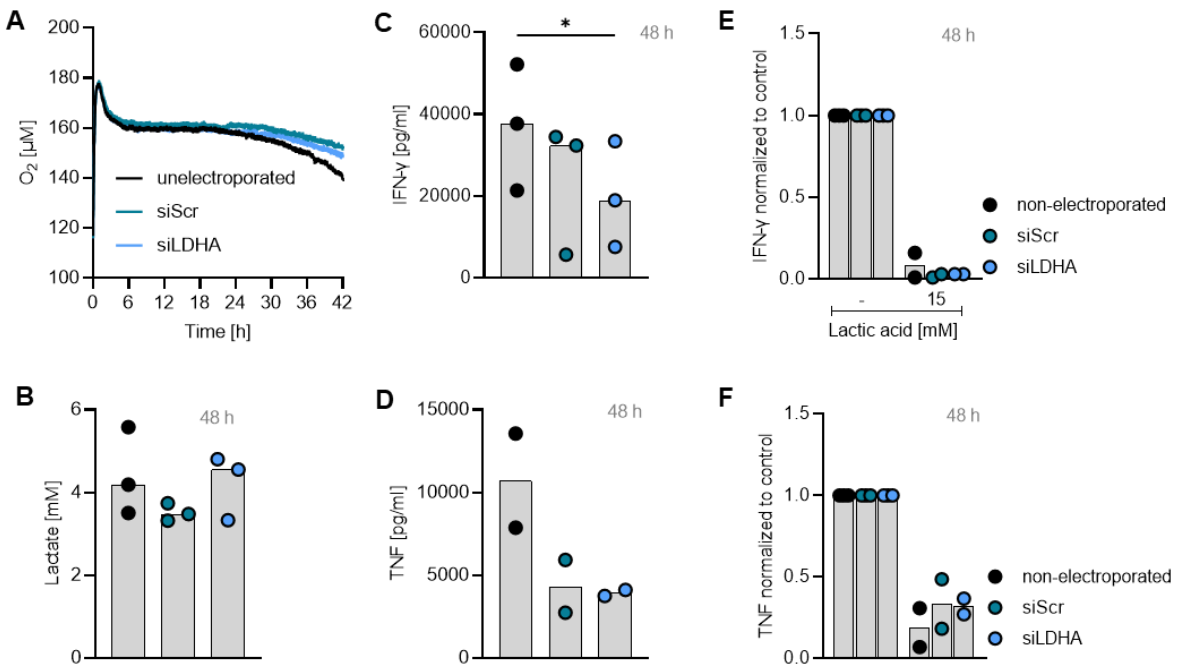

Figure 4-12: Knockdown of LDHA does not influence metabolic activity of CD4 T cells and does not increase lactic acid resistance. *T cells were isolated from MNCs of healthy donors and electroporated with either a scrambled siRNA-Pool (siScr) or a siRNA-Pool against LDHA (siLDHA). Non-electroporated cells were included as an additional control. After an overnight storage, the cells were stimulated for 48 h with α-CD3/CD28 coated beads at a bead-to-cell ratio of 1:1 in the presence of IL-2. (A) The oxygen consumption of the T cells was monitored using the PreSens technology (mean values, n = 3). (B) The accumulation of lactate in the cell culture supernatants was measured by the department for clinical chemistry of the university hospital Regensburg. (C - F) The concentrations of the effector cytokines IFN-γ and TNF in the cell culture supernatants was measured by means of ELISA. (E, F) Levels were normalized to the respective controls. (B – F) Shown are median levels and single data points. Asterisks give the significance levels between the non-electroporated control and siRNA-electroporated cells. The statistical significance was determined by a one-way ANOVA and post-hoc Bonferroni multiple comparison test (* p < 0.05).*

Lastly, cells were treated with 15 mM lactic acid and effects of the lactic acid on LDHA^{low} T cells investigated. Addition of 15 mM lactic acid completely blocked the respiration of the control cells and LDHA^{low} CD4 T cells (data not shown). In line, also cytokine secretion of CD4 T cells was inhibited by lactic acid regardless of the LDHA expression (Figure 4-12 E, F). Therefore, the knockdown of LDHA surprisingly seems to have no effect on the activation or metabolism of T cells and is not beneficial in a high lactic acid containing environment.

4.4.2. LDHB overexpression in human T cells

The overexpression of LDHB in human CD4 T cells was achieved by retroviral gene delivery (schematic overview over the protocol depicted in Figure 4-13 A). The viral transduction process led to an overexpression of LDHB in up to 66 % of the T cells as estimated by staining against the HIS-Tag fused to the exogenous LDHB, followed by a flow cytometric analysis (Figure 4-13 B). After the selection step, the purity of the LDHB overexpressing T cells (LDHB cells) was up to 97 % (Figure 4-13 C).

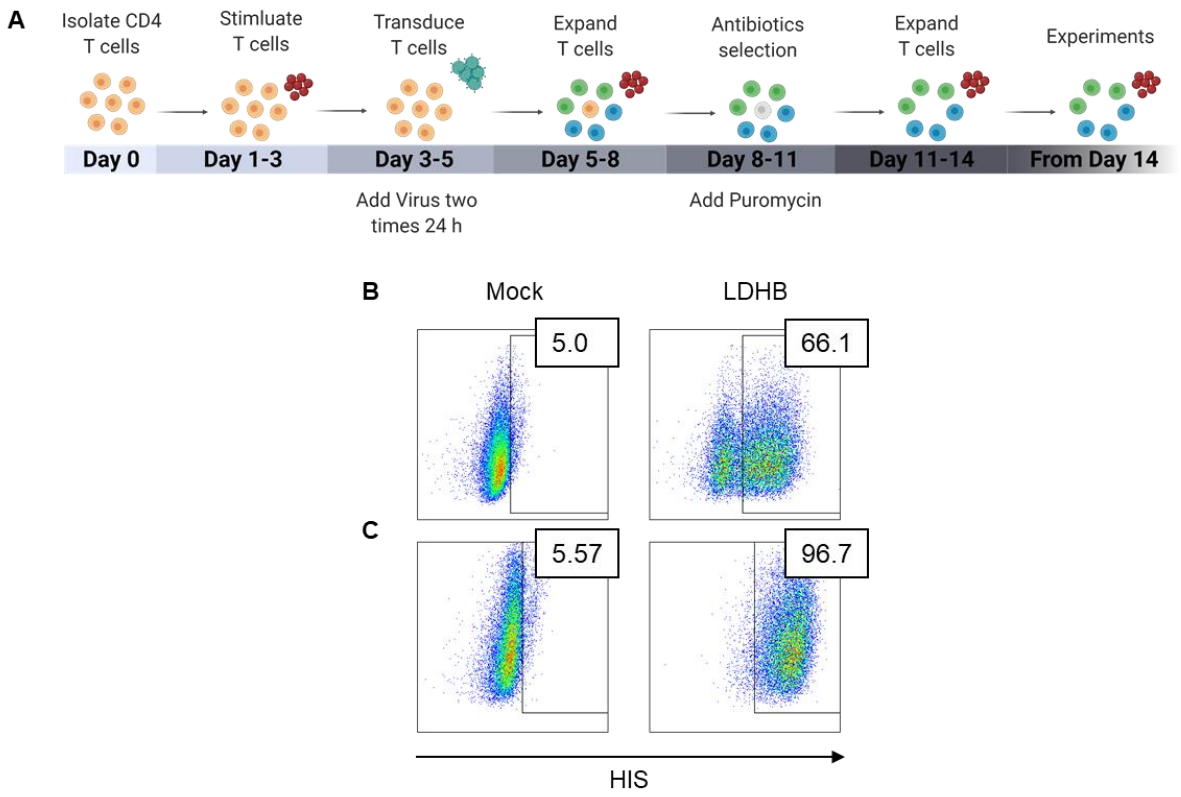

Figure 4-13: Protocol for retroviral transduction of T cells. *(A) Schematic overview of the transduction protocol. Red dots represent the presence of αCD3/CD28 Dynabeads. (B, C) The expression of the exogenous LDHB was assessed by staining for the HIS-Tag and subsequent flow cytometric analysis (B) three days after infection and (C) three days after end of the selection process. Given are representative FACS plots of n = 12 experiments.*

4.4.2.1. LDHB overexpression in human CD4 T cells leads to a clear shift in the LDH isoenzyme pattern

The overexpression of LDHB in CD4 T cells was controlled on mRNA levels by qRT-PCR and on protein level by western blot and LDH isoenzyme analysis (Figure 4-14). In empty vector transduced (Mock) cells, the relative LDHB mRNA expression normalized to the housekeeping gene was 0.07, whilst it was increased to 1.9 in the LDHB overexpressing T cells. Western blot analysis revealed expression of LDHB in Mock cells but LDHB was strongly overexpressed in retrovirally infected cells. In contrast, expression of LDHA was not altered in the LDHB cells neither on mRNA nor on protein level. Most importantly, the retroviral gene delivery induced a distinct shift in the LDH isoenzyme pattern. In LDHB cells, the expression of LDH-5 was reduced, but the fraction of LDH-1 and LDH-2 was increased compared to Mock cells.

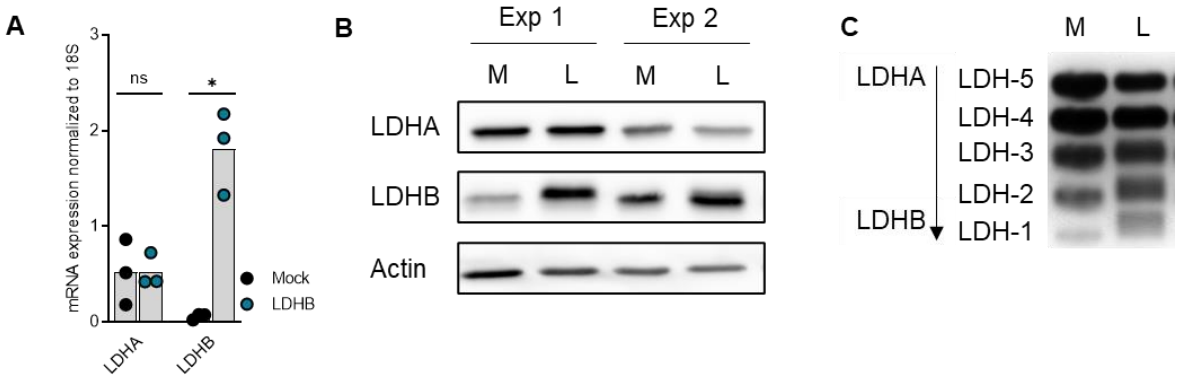

Figure 4-14: Overexpression of LDHB in human CD4 T cells leads to a redistribution of LDHA subunits and a shift in the LDH isoenzyme pattern. *LDHB was overexpressed in human CD4 T cells as described in chapter 3.1.8. All analyses were carried out three days after end of the selection process. (A) The expression of the LDH subunits LDHA and LDHB was assessed on mRNA level by means of qRT-PCR. Depicted are the median gene expression levels and single data points. Significance was calculated using one-way ANOVA and post-hoc Bonferroni multiple comparison test (* $p < 0.05$). (B) The expression of the LDH subunits LDHA and LDHB was assessed on protein level by a western blot analysis. Actin served as a loading control. Shown are two representative examples out of n = 8 experiments. (C) The LDH isoenzyme pattern was analyzed by a LDH zymography analysis with 6 µg total protein loaded per lane. One representative example out of n = 5 experiments is given. (B, C) M: Mock; L: LDHB.*

Altogether, this suggests that in LDHB overexpressing T cells the LDHA subunits are redistributed and pair more often with the LDHB subunits, which leads to a detectable shift in the LDH isoenzyme pattern of LDHB cells.

4.4.2.2. Basic characterization of LDHB overexpressing T cells

The overexpression of LDHB in T cells might have a direct influence on the cellular metabolism. Not only effector functions of CD4 T cells are directly related to their metabolic state, but many reports have also additionally stated that different CD4 T cell subsets show distinct metabolic characteristics related to their lactate and mitochondrial metabolism. Therefore, the cellular metabolism of LDHB overexpressing T cells as well as their functional differentiation were characterized.

First, we analyzed whether the overexpression of LDHB would alter the differentiation and activation of the cells. CD4 T cells can differentiate into several T helper subsets as well as into induced regulatory T cells (Treg). As these subsets all display different metabolic and functional characteristics, we analyzed the cytokine profile of the modified T cells as well as the amount of Tregs in our culture. Between Mock and LDHB cells, no changes in the cytokine profile upon stimulation with PMA/Ionomycin were detected (Figure 4-15 A). In addition, the percentage of Treg ($FOXP3^+$ $CD25^{high}$) cells was not significantly increased in the LDHB overexpressing cells, although a slight increase in the percentage of Treg was detectable (Figure 4-15 B). Furthermore, proliferation was not different between Mock and LDHB cells

(Figure 4-15), confirming that the LDHB overexpression had no influence on the basic functional characteristics of the T cells.

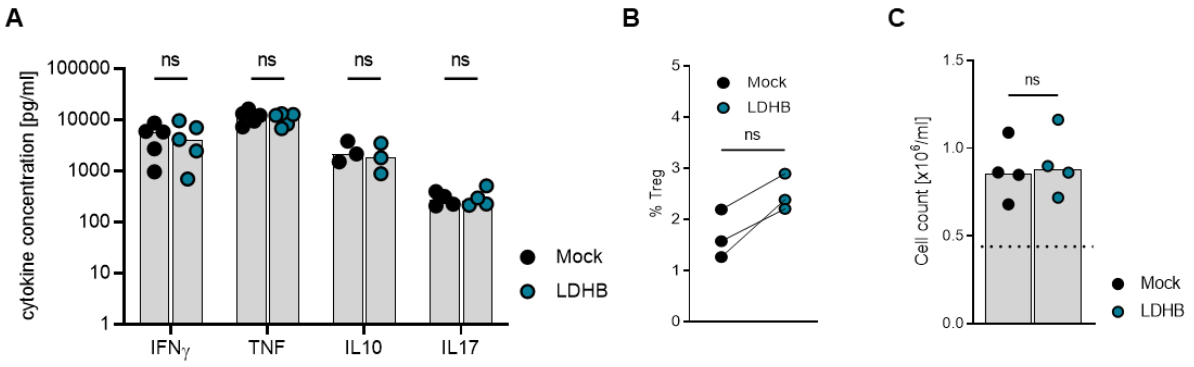

Figure 4-15: The differentiation and functional characteristics of CD4 T cells are not altered by LDHB overexpression. *LDHB was overexpressed in human CD4 T cells as described in chapter 3.1.8. (A) T cells were stimulated with PMA/Ionomycin for up to 3 h and the cytokine levels in the supernatants measured by means of ELISA. Shown are median levels and single data points. (B) The percentage of Treg (FOXP3⁺ CD25^{high}) among all cells was assessed by flow cytometry analysis. Shown are single data points, the lines connect paired values. (C) T cells were stimulated with α-CD3/CD28 coated beads at a bead-to-cell ratio of 1:1 in the presence of IL-2 and counted after 24 h using the CASY cell counter system. The dashed line represents the seeded cell number. (A – C) Shown are median levels and single data points. Significance levels were calculated using Wilcoxon's matched-pair signed rank test (ns: not significant).*

Next, metabolic characteristics of LDHB overexpressing T cells were investigated. We concentrated on glucose usage and mitochondrial metabolism of the modified cells.

First, we analyzed glucose uptake and metabolism of the LDHB overexpressing cells in comparison to Mock cells. Neither glucose uptake (Figure 4-16 A), nor lactate secretion (Figure 4-16 B) of LDHB cells were significantly altered compared to Mock cells. In line, the lactate transporters MCT-1 and MCT-4 were not differentially expressed (Figure 4-16 C, D).

Next, we aimed to analyze the mitochondrial metabolism of the LDHB T cells (Figure 4-16 E – G). First, cellular oxygen consumption was monitored using the PreSens technology. LDHB cells showed a slightly increased oxygen consumption compared to the Mock cells starting 6 h after activation. This higher mitochondrial respiratory activity could be caused either by a general increase in mitochondrial activity or an increase in mitochondrial mass of the cells. To elucidate this, we analyzed the mitochondrial content by staining with the mitochondrial dye Mitotracker Green, followed by a flow cytometry analysis. No changes in the mitochondrial mass between Mock and LDHB cells were detected, suggesting that the higher respiration and mitochondrial metabolism of the cells is the result of a higher mitochondrial activity.

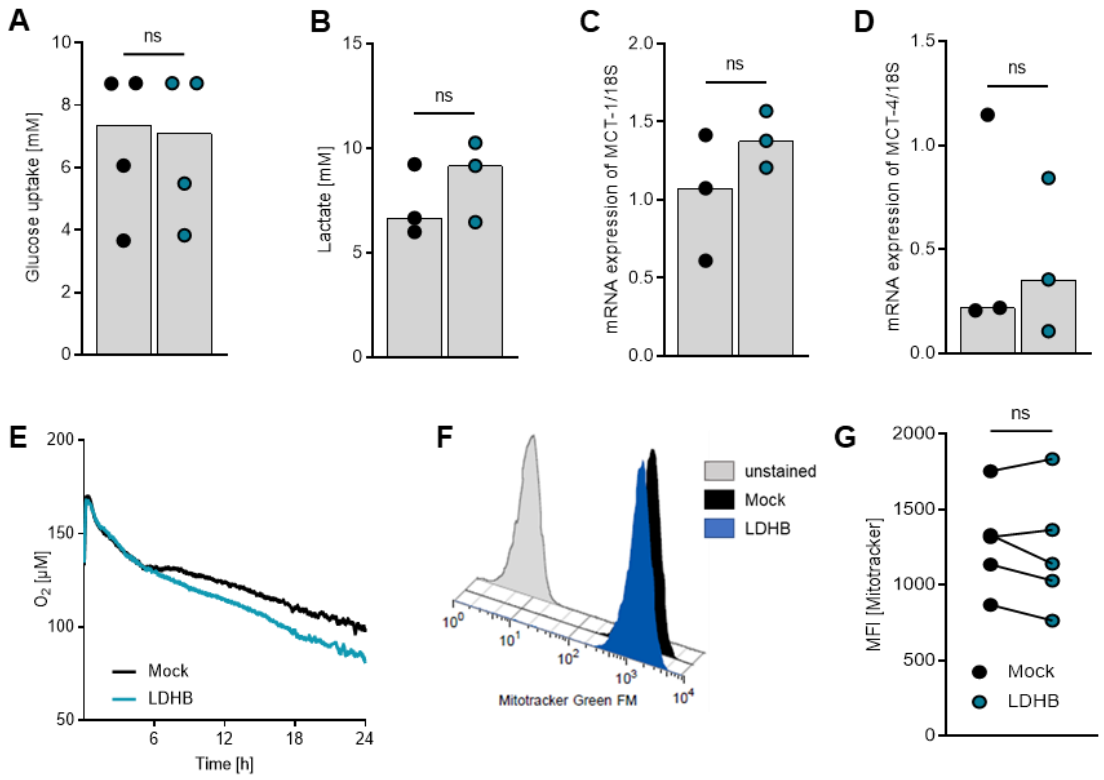

Figure 4-16: Glucose and mitochondrial metabolism in LDHB overexpressing CD4 T cells. *LDHB was overexpressed in human CD4 T cells as described in chapter 3.1.8. (A, B) T cells were stimulated with α-CD3/CD28 coated beads at a bead-to-cell ratio of 1:1 in the presence of IL-2 and analyzed after 24 h. (A) To calculate the glucose uptake, glucose remaining in the supernatants was measured and subtracted from the initial glucose concentration in the RPMI. (B) Lactate in culture supernatants was measured by the department for Clinical Chemistry (University hospital Regensburg). (C, D) Expression of (C) MCT-1 and (D) MCT-4 in the cells three days after the end of the selection was assessed by means of qRT-PCR analysis. (E) T cells were stimulated with α-CD3/CD28 coated beads at a bead-to-cell ratio of 1:1 in the presence IL-2 and oxygen consumption was monitored using the PreSens technology (n = 4). (F, G) The mitochondrial content of the cells was assessed by staining by with the fluorescent dye Mitotracker Green FM, followed by flow cytometric analysis. Shown are (F) a representative example and (G) the median fluorescence intensity for single data points. The lines connect paired data points. (A – D, G) Significance was calculated with Wilcoxon's matched-pair signed rank test (ns: not significant).*

In summary, the overexpression of LDHB in human CD4 T cells did not influence the differentiation or basic functional characteristics but increased mitochondrial respiratory activity of the cells.

4.4.2.3. LDHB overexpressing cells show no distinct alterations in glucose or lactate metabolism

The higher basic respiratory activity of LDHB T cells suggested that T cells could have altered their mitochondrial metabolism. To address this question, Mock and LDHB cells were stimulated with α-CD3/CD28 coated beads and treated with non-lethal concentrations of lactic acid. As already observed in primary stimulated cells, lactic acid treatment severely affected glucose uptake of T cells regardless of LDHB expression (Figure 4-17 A). Interestingly, lactic acid treatment increased the initial respiration of LDHB compared to Mock cells up to 24 h

(Figure 4-17 B). Therefore, we sought to closer investigate the glucose and lactate metabolism of lactic acid treated LDHB overexpressing cells.

After generation from lactate or glucose, pyruvate can take two different ways into the TCA cycle (schematic depiction in Figure 4-17 C). Most commonly, oxidative decarboxylation by pyruvate dehydrogenase (PDH) leads to generation of acetyl-CoA, which is afterwards converted into citrate. As an alternative, a carboxyl group can be added to pyruvate by the enzyme pyruvate carboxylase (PC) generating oxalacetate.

In first instance, we analyzed how the glucose metabolism of LDHB overexpressing cells was affected by lactic acid treatment. Cells were stimulated with α-CD3/CD28 coated beads and incubated with 10 mM uniformly labeled glucose with or without 10 mM and 15 mM lactic acid. After 6 h, cells were harvested, lysed and the enrichment of the 13C label in the metabolic intermediates was analyzed (Figure 4-17 C). The short incubation time was chosen on basis of the cellular respiration upon lactic acid treatment, which started to be substantially different after 6 h treatment.

Interestingly, glucose tracing analysis showed that glucose flux into pyruvate was only slightly affected by lactic acid treatment. In contrast, lactic acid treatment significantly reduced 13C incorporation in lactate compared to control (15 mM LA, one-way ANOVA with post-hoc Bonferroni multiple comparison test, $p < 0.05$) in both Mock and LDHB cells and by trend also in TCA metabolites, indicating that pyruvate metabolism via LDH, PDH and PC was blocked by lactic acid. Notably, the 13C enrichment in different metabolites was not different between Mock and LDHB cells, indicating that the overall glucose metabolism was not altered in LDHB overexpressing cells. It should be noted that unlabeled lactate uptake from the medium will result in the measurement of lower 13C mean enrichment in intracellular lactate.

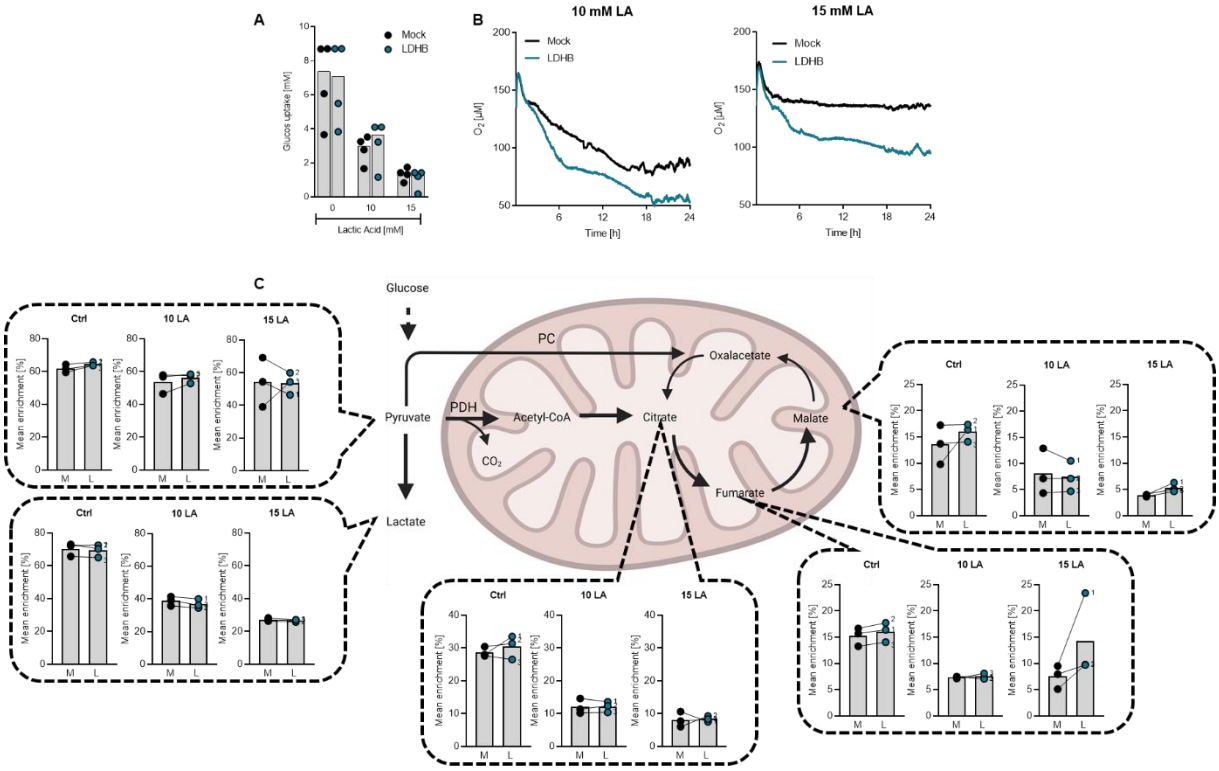

Figure 4-17: LDHB overexpressing cells show higher respiration upon lactic acid treatment but no alterations in glucose flux. *LDHB was overexpressed in human CD4 T cells as described in chapter 3.1.8. T cells were stimulated with α-CD3/CD28 coated beads at a bead-to-cell ratio of (A, B) 1:1 or (C) 1:5 in the presence of IL-2 and treated with the indicated concentrations of lactic acid. (A) To assess glucose uptake of the T cells within 24 h of culture, glucose remaining in the culture supernatants was measured and subtracted from the initial glucose concentration. (B) Cellular oxygen consumption was measured with the PreSens technology (mean values; n = 4). (C) Mock (M) and LDHB overexpressing (L)T cells were incubated with 10 mM uniformly labeled glucose and with and without 10 mM or 15 mM lactic acid for 6 h. Subsequently, cells were lysed and 13C incorporation in the different metabolites measured by the Institute for Functional Genomics, University of Regensburg. (A, C) Shown are median levels and single data points. Lines connect paired data; numbers correspond to the analyzed donors. Significance within one treatment was calculated using Wilcoxon's matched-pair signed rank test (no significance detected). Graphic depicting glucose metabolism was created with BioRender.com; PDH: Pyruvate Dehydrogenase; PC: Pyruvate Carboxylase; LA: Lactic acid.*

To closer trace the metabolic flux of lactate, we performed a 13C3 lactic acid tracing analysis (Figure 4-18). Cells were stimulated with α-CD3/CD28 coated beads and treated with 10 mM and 15 mM 13C3 lactic acid. After 6 h and 24 h, cells were harvested, lysed and the enrichment of the 13C label in the metabolic intermediates was analyzed.

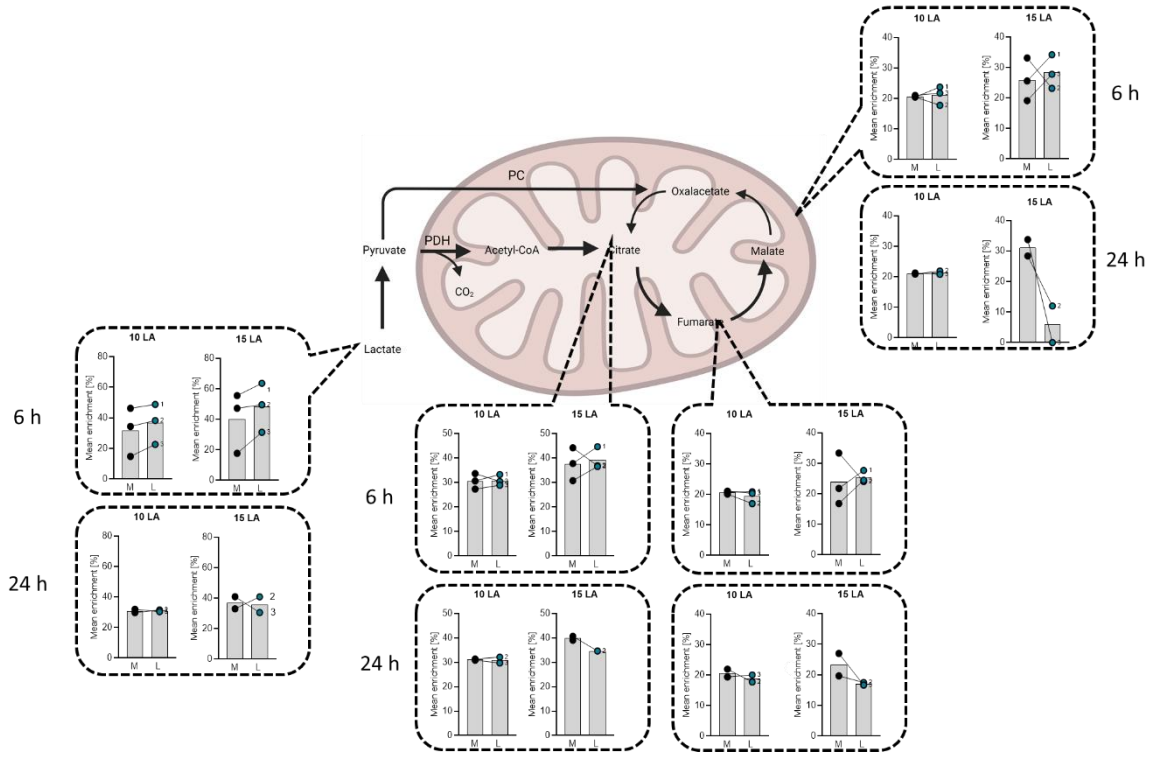

Figure 4-18: Lactate metabolism of LDHB overexpressing CD4 T cells. *LDHB was overexpressed in human CD4 T cells as described in chapter 3.1.8. T cells were stimulated with α-CD3/CD28 coated beads at a bead-to-cell ratio of 1:1 in the presence of IL-2 and treated with 10 mM and 15 mM uniformly labeled lactic acid (13C3 lactic acid) for 6 h and 24 h. Subsequently, cells were lysed and 13C enrichment in the different metabolites measured by the Institute for Functional Genomics, University of Regensburg. Mean enrichment of labeled lactate, citrate, malate and fumarate are given. M: Mock; L: LDHB overexpressing cells. Significance was calculated using Wilcoxon's matched-pair signed rank test (no significance detected). Graphic depicting lactate metabolism was created with BioRender.com; PDH: Pyruvate Dehydrogenase; PC: Pyruvate Carboxylase.*

Tracing lactate metabolism, no 13C labeled pyruvate was detected in the cell pellets after 6 h, which can have instrumental reasons as pyruvate signals were low in general but can also indicate that pyruvate serves as an intermediate step in lactate metabolism and is immediately further metabolized to clear the pyruvate pool for further LDH and glycolysis reaction. Surprisingly, in both Mock and LDHB cells 13C-labeled components of the TCA cycle were detected, indicating that also cells with normal LDHB expression have the ability to metabolize external lactic acid to a certain degree. Moreover, mean enrichment of the 13C label in TCA metabolites was not significantly altered in LDHB overexpressing cells, indicating no substantial changes in the lactate metabolism. Instead, we found a slightly, but not significantly higher enrichment of 13C labeled lactate within the cell pellet of LDHB cells. After 24 h, this difference was even more pronounced in one donor (donor 3) upon treatment with 15 mM lactic acid, whilst in the other donor (donor 2) the enrichment even decreased. Notably, this was consistent with the measured respiration upon lactic acid treatment (data not shown). Donor 2 showed a consistently higher respiratory activity during the whole observation time, whereas respiratory activity of donor 3 was only slightly increased during the first 6 h of treatment. This indicates that the higher respiration of LDHB cells might be fueled by higher

lactate uptake. However, more studies investigating more donors and later time points are necessary.

Interestingly, in the lactate tracing analysis we found a slightly higher enrichment of m + 3 citrate in LDHB cells compared to Mock cells (data not shown). When incubating cells with 13C labeled lactic acid, m + 3 citrate can either originate from TCA cycle activity or from pyruvate metabolism by PC. This could indicate, that LDHB cells upregulate the PC pathway. However, further studies are necessary to confirm the origin of m+3 citrate in PC metabolism and to elucidate its role in LDHB T cells.

Taken together, the present glucose and lactate tracing data did not give an explanation for increased respiratory activity of LDHB cells upon lactic acid treatment. Therefore, further studies are necessary to elucidate this phenomenon.

4.4.2.4. Influence of LDHB overexpression on T cell function and viability upon lactic acid treatment

In a next step, we investigated the effect of LDHB overexpression on lactic acid sensitivity of T cells. First, we analyzed the viability of T cells upon treatment with lactic acid. In both Mock and LDHB cells, addition of 20 mM lactic acid significantly reduced the survival of the T cells, with no difference between LDHB overexpressing and Mock cells. In addition, the cell proliferation upon lactic acid treatment was not rescued by LDHB overexpression (Figure 4-19 A, B).

To assess the influence of LDHB overexpression on cytokine production upon lactic acid treatment, we pre-treated the cells over night with lactic acid and then stimulated the cells for 2 – 3 h with PMA/Ionomycin to induce a strong cytokine response. For the analysis of the intracellular cytokine production, the cells were additionally treated with monensin, followed by intracellular IFN-γ and TNF staining and subsequent flow cytometry analysis.

Analyzing the cytokine secretion, no significant differences between Mock and LDHB cells were observed regarding TNF or IFN-γ secretion. However, upon treatment with 10 mM lactic acid less inhibition was detected in some donors in LDHB cells, indicating that in those donors LDHB overexpression positively influenced lactic acid resistance.

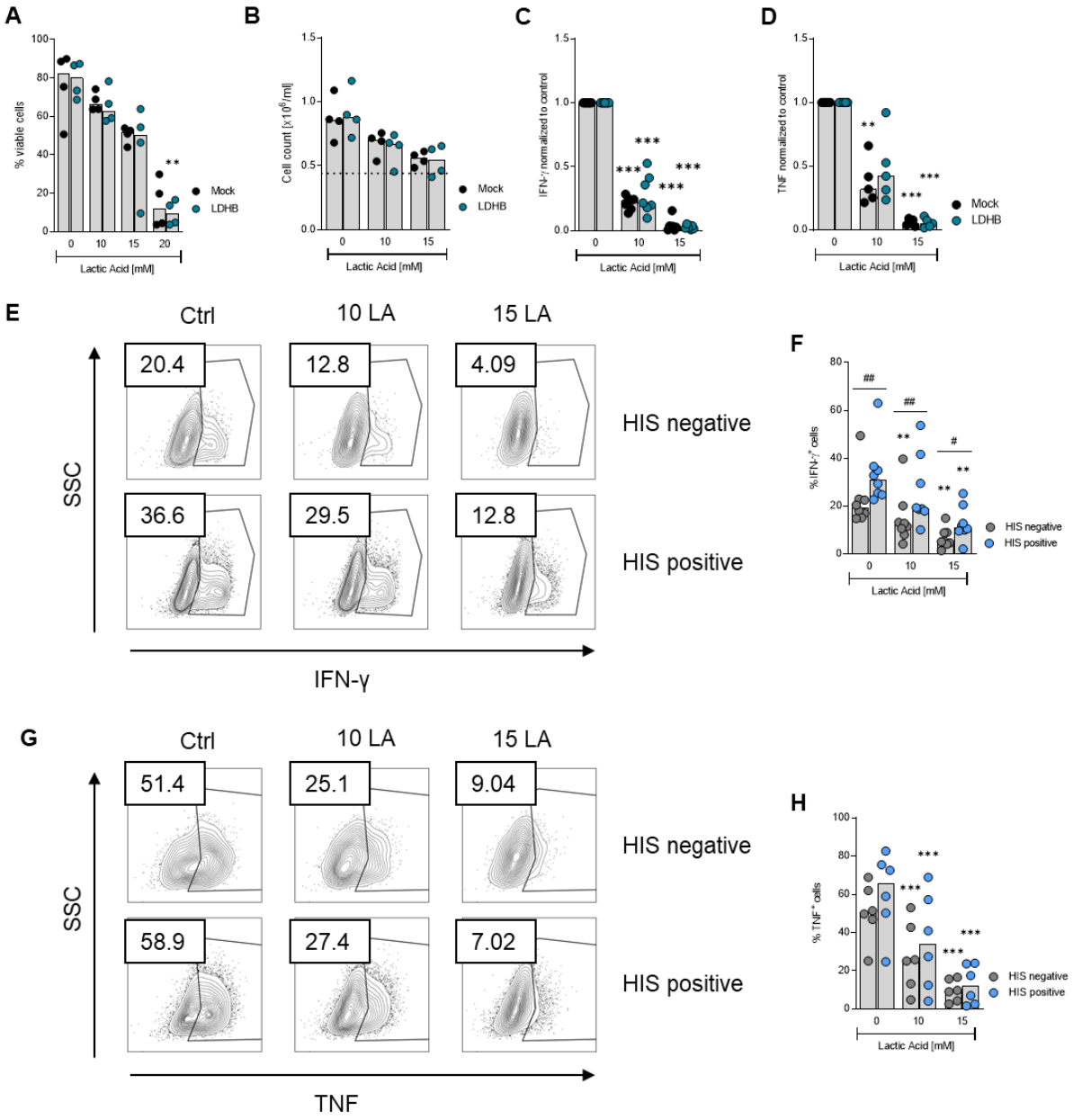

Figure 4-19: LDHB overexpression improves intracellular cytokine production upon lactic acid treatment but has only slight effects on cytokine secretion. *LDHB was overexpressed in human CD4 T cells as described in chapter 3.1.8. (A, B) T cells were stimulated at α-CD3/CD28 coated beads at a bead-to cell ratio of 1:1 in the presence of IL-2 and treated with the indicated concentrations of lactic acid. (A) The viability of the T cells was assessed after 48 h of treatment by an Annexin V/7-AAD staining. (B) To assess the proliferation, cells were counted using the CASY cell counter system. (C – G) Cells were pre-treated with lactic acid overnight and stimulated with PMA/Ionomycin. (C, D) The levels of (C) IFN-γ and (D) TNF in the supernatants of the PMA/Ionomycin stimulated cells were measured with ELISA and normalized to the respective control. (E – H) The amount of (E, F) IFN-γ or (G, H) TNF cytokine producing cells was assessed by a FACS staining after monensin treatment. Cells were separated into cells with high and normal LDHB expression within LDHB transduced cells by gating on HIS expression and distinguished in HIS negative and HIS positive cells. (E, G) Shown are representative FACS Plots, numbers indicate the percentage of positive cells. (F, H) Summary of cytokine positive cells among the HIS populations. Shown are median levels and single data points, except for E and G. Asterisks give significant differences between the treatment and the respective controls, hashes mark differences within the treatments between the groups. The significance levels were determined using one-way ANOVA and post-hoc Bonferroni multiple comparison test (* p < 0.05; ** p < 0.01; *** p < 0.001; same for #).*

In our case, the expression of the HIS-Tag as detected in the FACS analysis declined by up to 15 % during the PMA/Ionomycin stimulus. We hypothesized, that the donor-dependent

change in cytokine secretion could be related to the number of LDHB overexpressing cells within the bulk T cell population and analyzed the intracellular cytokine expression taking into consideration LDHB expression. Thereby, we made use of the HIS-Tag to distinguish between LDHB overexpressing (HIS^+) and cells with normal LDHB expression (HIS^-) within the LDHB transduced cells. We found a significantly increased proportion of IFN-γ^+ cells among the HIS^+ compared to the HIS^- population not only under control conditions, but also under lactic acid treatment. Analyzing TNF production, three of the analyzed donors showed more TNF producing cells among LDHB overexpressing cells, in three other donors this was not observed. This suggests a beneficial effect of LDHB on the cytokine expression upon lactic acid treatment at least in 50 % of the donors.

4.4.2.5. Extracellular buffering enhances the protective effects of LDHB overexpression

Buffering the extracellular pH increases T cell viability and function upon lactic acid treatment and has been shown to augment the anti-tumor response *in vivo* (Calcinotto et al., 2012; Pilon-Thomas et al., 2016). As shown above, buffering the extracellular pH partially rescued T cell survival and mitigated lactic acid effects on cytokine secretion (see chapter 4.2). Therefore, we aimed to combine two approaches, extracellular buffering and LDHB overexpression, to determine whether they act in a synergistic manner and enhance the T cell function in the presence of lactic acid.

LDHB was overexpressed in CD4 T cells as described above. The genetic modification and all experiments were performed in T cell medium with enhanced buffering capacity (see chapter 4.2).

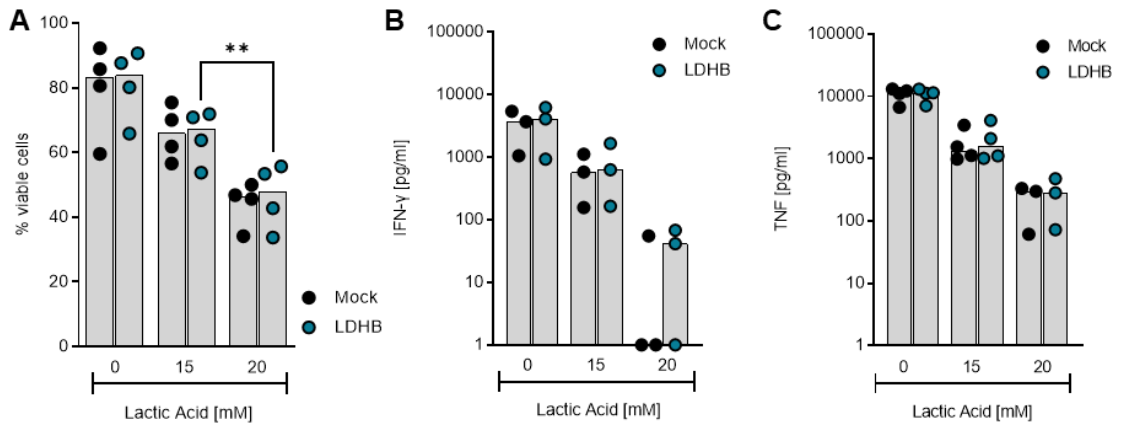

Figure 4-20: Extracellular buffering combined with LDHB overexpression enhances LDHB effect under high concentrations of lactic acid. *LDHB was overexpressed in human CD4 T cells as described in chapter 3.1.8. For the genetic modification and all experiments, culture medium with a higher buffering capacity was used. (A) T cells were stimulated with α-CD3/CD28 coated beads at a bead-to-cell ratio of 1:1 in the presence of IL-2 and were treated with the indicated concentrations of lactic acid. (A) Cell viability was assessed after 48 h treatment by Annexin V/7-AAD staining. (C, D) Cells were pre-treated with lactic acid overnight and stimulated with PMA/Ionomycin for up to 3 h. The levels of (C) IFN-γ and (D) TNF in the supernatants of the PMA/Ionomycin stimulated cells were measured by ELISA. Shown are median levels and single data points. Asterisks give significant differences between treatment and the respective controls. Significance levels were determined using one-way ANOVA and post-hoc Bonferroni multiple comparison test (** $p < 0.01$).*

As already observed in primary stimulated T cells (Figure 4-6), the higher buffering capacity of the culture medium enhanced the viability of T cells treated with lactic acid independently of LDHB overexpression. (Figure 4-20 A). We measured cytokine secretion and found, that upon treatment with 20 mM lactic acid two of three donors still showed a weak secretion of IFN-γ, which was detectable in only one donor among the Mock cells. No effect was observed regarding TNF secretion. This emphasizes the potential of extracellular buffering to enhance T cell function and suggests, that multiple manipulations are required to increase lactic acid resistance of T cells.

4.4.2.6. LDHB overexpressing cells show slightly increased cytotoxic activity in tumor spheroid co-cultures

Finally, we aimed to investigate, whether LDHB overexpression supports T cell function in a co-culture model of T cells and tumor spheroids. Tumor spheroids are clusters of tumor cells forming three-dimensional aggregates. *In vitro*, they can be used to mimic a tumor environment (TME). Comparable to solid tumors, spheroids display inwardly decreasing gradients of oxygen and nutrients and increasing lactate concentrations. This makes them a suitable intermediate step for the transfer of *in vitro* concepts to the *in vivo* situation.

We tested the anti-tumor capacity of LDHB overexpressing T cells using spheroids of the colon cancer cell line HCT116. To get as close as possible to the patient situation, where you would

not find a pure population of modified cells, we decided to use transduced T cells without puromycin selection for these experiments.

Spheroid were allowed to assemble for 14 days. Transduced T cells 3 d after end of transduction were stimulated with α-CD3/CD28 coated beads for 24 h and subsequently co-cultured with the spheroids for 48 h. Afterwards, non-infiltrated immune cells were washed away, the spheroids were dissolved by incubation with trypsin/EDTA and infiltrated immune cells analyzed by flow cytometry (for schematic representation see Figure 4-21).

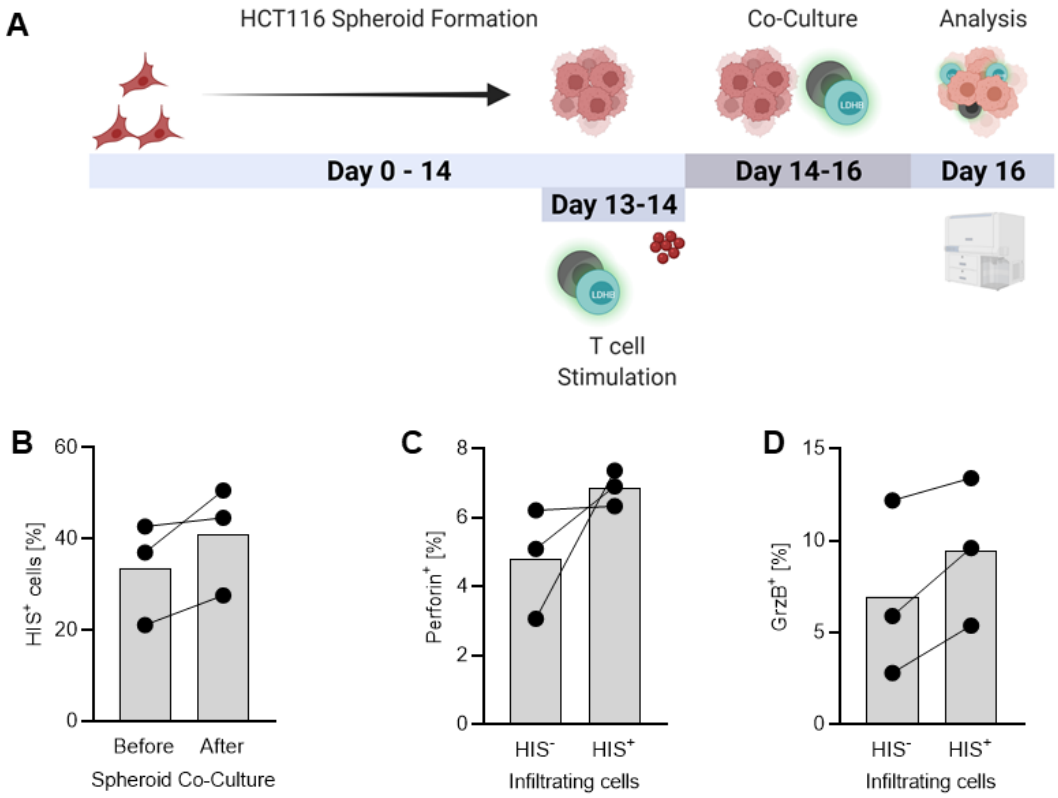

Figure 4-21: LDHB overexpressing cells preferentially infiltrate into HCT116 spheroids and show slightly increased cytotoxicity. *HCT116 tumor spheroids were assembled for 14 days as described in 3.1.8. LDHB T cells were generated as described in chapter 3.1.8 and used at day 3 after end of transduction. T cells were stimulated with α-CD3/CD28 coated beads at a bead-to-cell ratio of 1:1. After 24 h, 0.1x10^6 T cells/spheroid were added. Infiltrated immune cells were analyzed after 48 h co-culture by means of flow cytometry. (A) Schematic overview over the co-culture protocol. (B) Amount of HIS$^+$ T cells before co-culture and among infiltrated T cells. (C, D) Infiltrating T cells were separated into cells with high and normal LDHB levels by means of HIS expression. Amount of (C) perforin and (D) granzyme B (GrzB) expressing cells among the total populations were analyzed. (B – D) Lines connect paired data points. Statistical significance was assessed by Wilcoxon's matched-pair signed rank test (no significance detected).*

Before and after co-culture, the amount of LDHB overexpressing cells among the T cell population was analyzed by flow cytometric analysis of the HIS-Tag. In two of the three analyzed donors, the number of HIS$^+$ T cells was higher among the infiltrated T cells compared to the population before co-culture, indicating that LDHB T cells preferentially infiltrated into HCT116 spheroids compared to cells with normal LDHB expression. To assess the cytotoxic activity of T cells in co-culture, we separated cells with high and normal LDHB levels by means of HIS expression and analyzed the amount of perforin and granzyme B expressing cells

among the two populations. Intriguingly, again two of the analyzed donors showed increased expression of perforin and granzyme B, indicating increased cytotoxicity of LDHB overexpressing cells. These results indicate an enhanced functional fitness of LDHB overexpressing cells within a spheroid mimicking a TME.

4.5. Transfer the genetic manipulation into the mouse model

To test the anti-tumor capacities of LDHB overexpressing cell *in vivo*, we next aimed to establish and test the genetic manipulation in murine T cells.

4.5.1. Ldhb overexpression in murine T cells

The overexpression of Ldhb in murine CD4 T cells (C57BL/6N) was achieved by retroviral gene delivery. The transduction efficacy was up to 98 % as evidenced by flow cytometric analysis of the co-transduced marker CD90.1 (Figure 4-22).

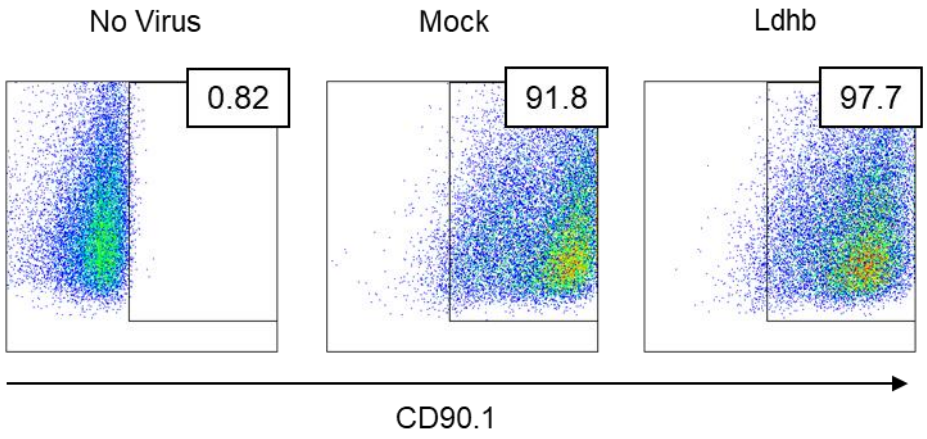

Figure 4-22: Efficacy of the retroviral gene delivery of the Ldhb overexpression protocol for murine T cells. *The expression of the selection marker CD90.1 was assessed three days after viral transduction by flow cytometric analysis. Given are representative FACS plots out of n = 5 experiments.*

4.5.1.1. Ldhb can be overexpressed in murine T cells and induces a shift in the Ldh isoenzyme pattern

The overexpression of Ldhb in murine CD4 T cells was confirmed on protein level by western blot and LDH zymography analysis (Figure 4-23). Ldhb was strongly overexpressed in the retrovirally infected cells, whilst the expression of Ldha was not altered. Compared to human T cells, Ldhb overexpression was even stronger in the murine T cells. Importantly, the retroviral gene delivery induced a strong shift in the Ldh isoenzyme pattern. In contrast to human T cells,

the proportion of Ldh-5 was not distinctly reduced by Ldhb overexpression, but a clear shift towards the more Ldhb containing isoforms was visible. Overall the isoenzyme pattern was clearly different in murine T cells with a dominant Ldh-5 expression.

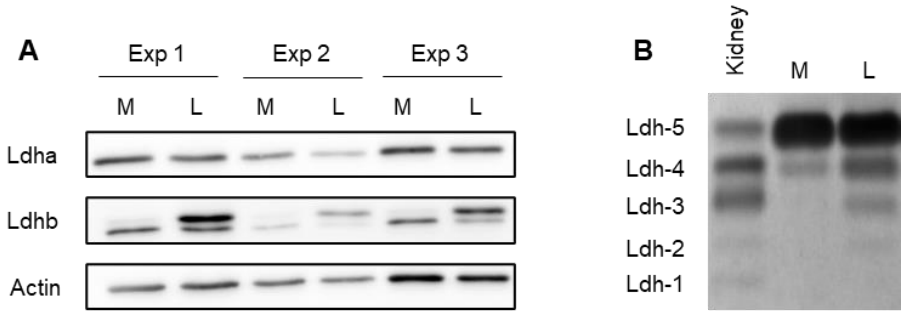

Figure 4-23: The overexpression of Ldhb in murine CD4 T cells leads to a redistribution of Ldha subunits and a shift in the LDH isoenzyme pattern. *Ldhb was overexpressed in murine CD4 T cells as described in chapter 3.1.9. Analyses were carried out three days after viral infection. (A) The expression of the Ldh subunits Ldha and Ldhb was assessed on protein level by a western blot analysis. Actin served as a loading control. Shown are three representative examples out of n = 4 experiments. (B) The Ldh isoenzyme pattern was analyzed by a Ldh zymography analysis with 4.5 µg total protein loaded per lane. One representative example out of n = 4 experiments is given. M: Mock; L: Ldhb T cells.*

Altogether, these data show that Ldhb can be overexpressed in murine CD4 T cells. The overexpression of Ldhb leads to a redistribution of Ldha subunits and in consequence to a shift in the Ldh pattern, although the pure Ldhb tetramer Ldh-1 was not detected.

4.5.1.2. Basic characterization of Ldhb overexpressing murine T cells

Again, in a first step, we characterized the Ldhb overexpressing murine CD4 T cells (Figure 4-24).

Similar to what was observed in LDHB overexpressing human T cells, Ldhb overexpression in murine T cells did not alter the differentiation of T cells, as the proportion of Treg among the total cell population was very small and did not increase due to Ldhb overexpression. Monitoring the cellular respiration in culture, we observed that the transduced murine cells barely showed any respiration activity, and Ldhb overexpression did not increase the basic respiration, which was different to the results obtained with human T cells. Furthermore, Ldhb overexpression did not influence lactate secretion or cell proliferation within 48 h of culture, although we observed a big heterogeneity between the different experiments (Figure 4-24).

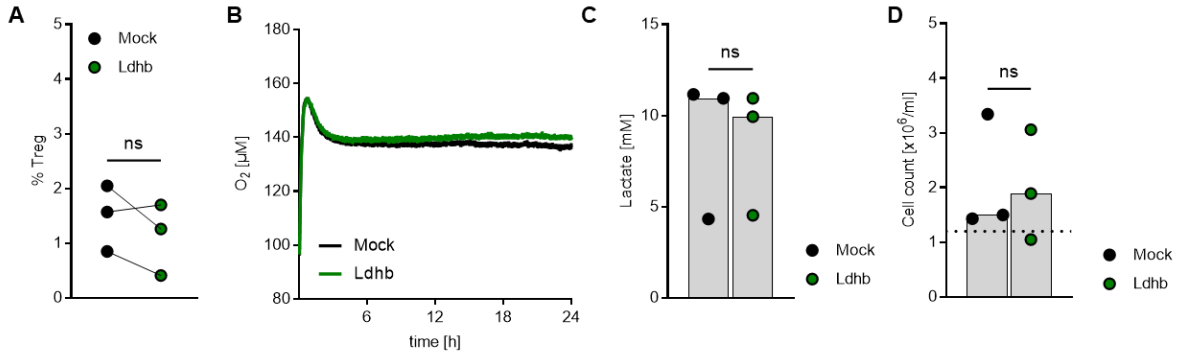

Figure 4-24: Ldhb overexpression does not influence basic differentiation and metabolic characteristics of murine CD4 T cells. *Ldhb was overexpressed in murine CD4 T cells as described in chapter 3.1.9. (A) The percentage of Treg (CD25^{high} Foxp3^{+}) in the culture was assessed by flow cytometric analysis three days after viral transduction. Lines connect paired data points. (B - D) The T cells were stimulated with α-CD3/CD28 coated beads at a bead-to cell ratio of 1:1 in the presence of IL-2 and IL-15. (B) Cellular oxygen consumption under cell culture conditions was monitored using the PreSens technology (n = 3). (B, C) After 48 h, (B) lactate concentration in the supernatants was measured and (C) cells were counted with the CASY cell counter system. Shown are (A) single data points, (B) mean values and (C, D) median levels and single data points. Significance levels were determined using Wilcoxon's signed-rank test (ns: not significant).*

Together, Ldhb overexpression did not influence the basic differentiation or metabolic characteristics of murine CD4 T cells.

4.5.1.3. Ldhb overexpression does not induce a switch in cellular metabolism or increase resistance towards lactic acid

Next, we investigated the effect of the Ldhb overexpression upon lactic acid treatment.

First, we analyzed the viability of the T cells upon treatment with lactic acid. Similar to human T cells, Ldhb overexpression had no effect on survival of murine T cells upon lactic acid treatment. Unlike human LDHB overexpressing T cells, Ldhb failed to increase the respiratory activity of murine T cells in the presence of lactic acid.

For analysis of cytokine expression, cells were pre-treated with lactic acid over night, stimulated with PMA/Ionomycin and treated with monensin for subsequent intracellular cytokine staining. Due to the very high and constant expression of the transduction marker CD90.1, separating cells with high and normal Ldhb expression was not possible in this system. Again, no effect of Ldhb on the cytokine expression or secretion in the presence of lactic acid was found (Figure 4-25).

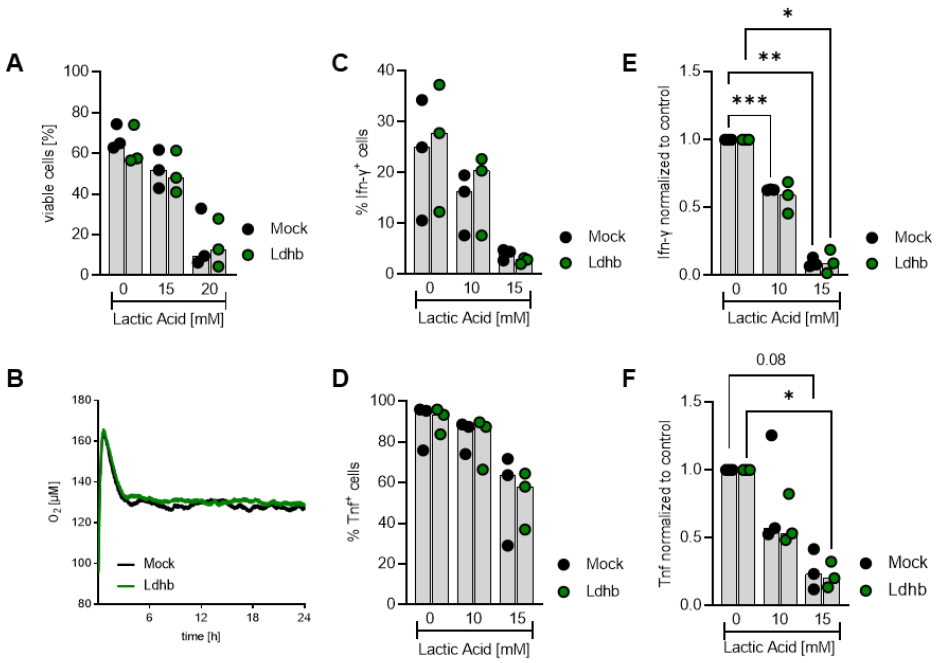

Figure 4-25: Ldhb overexpression fails to increase respiration, survival or cytokine expression of murine T cells in the presence of lactic acid. *Ldhb was overexpressed in murine CD4 T cells as described in chapter 3.1.9. The cells were either (A) treated with the indicated concentrations of lactic acid after change of culture medium and re-adjusting the seeded cell number, (B) restimulated with α-CD3/CD28 coated beads in a bead-to-cell ratio of 1:1 in the presence of IL-2 and IL-15 and treated with 15 mM lactic acid or (C – F) incubated with the indicated concentrations of lactic acid overnight and stimulated with PMA/Ionomycin. (A) Viability of the cells was assessed after 48 h in culture by an Annexin V/7-AAD staining and subsequent flow cytometric analysis. (B) The oxygen consumption of the cells was monitored using the PreSens technology (n = 3). (C - F) The cells were pre-treated with the indicated concentrations of lactic acid over night and stimulated with PMA/Ionomycin. (C, D) The percentage of (C) Ifn-γ and (D) Tnf producing cells was assessed by flow cytometric analysis after treatment with monensin. (E, F) The concentration of cytokines in the cell culture supernatants were measured by ELISA and levels normalized to the respective controls. Shown are (B) mean values or (A, C – F) median levels with single values. Significance was calculated with one-way ANOVA and post-hoc Bonferroni multiple comparison test (digits give exact p value, * p < 0.05; ** p < 0.01; *** p < 0.001)*

Therefore, in contrast to the human T cells, Ldhb overexpression showed no beneficial effect on lactic acid treated murine T cells, which excludes the usage of mouse models for the *in vivo* testing.

4.5.2. Human and murine T cells are metabolically distinct

The overexpression of LDHB in CD4 T cells led to different results in human and murine T cells. Whilst in human T cells the overexpression of LDHB resulted in increased respiration and an enhanced intracellular cytokine production upon lactic acid treatment, these effects were not observed in the murine system despite an even stronger overexpression of Ldhb and shift in the Ldh isoenzyme pattern. We hypothesized, that this might be reasoned in a distinct cellular metabolism of murine and human T cells. Therefore, we analyzed crucial metabolic parameters of CD4 and CD8 T cells isolated from human MNCs or splenocytes from C57BL/6N (depicted by black mouse symbols) or Balb/c mice (white mouse symbols)

.

For the metabolic comparison, T cells were isolated and cultivated as described in chapters 3.1.2 and 3.1.4. The T cells were stimulated with α-CD3/CD28 coated beads in a bead-to-cell ratio of 1:1. To improve the viability of murine T cells, IL-15 was added to the culture, which was not necessary in the human cultures, as the viability of T cells was good at the analyzed time points.

Glucose taken up by a cell is phosphorylated to glucose-6-phosphate in a first step. Afterwards, it can be shunt into different metabolic pathways: The pentose-phosphate-pathway, the mitochondrial TCA cycle and the generation of lactate from pyruvate. Whilst the TCA cycle and the glycolysis are both involved in energy provision, the pentose-phosphate pathway is mainly responsible for the regeneration and production of the redox equivalent NADPH. As for this work only the mitochondrial and glycolytic metabolism of glucose are most relevant, we focused our comparison on these two compartments.

Before and after 72 h of stimulation, the mitochondrial content of the T cells was analyzed by staining with the fluorescent dye Mitotracker Green FM. Whilst there was no difference between CD4 and CD8 T cells of either strain and species, comparing human and murine T cells revealed striking differences. In murine T cells, the mitochondrial content was upregulated by about three-fold upon stimulation and finally matched that of stimulated human T cells. Unstimulated human T cells had a much higher mitochondrial content than murine T cells and displayed only a slight upregulation upon stimulation (Figure 4-26).

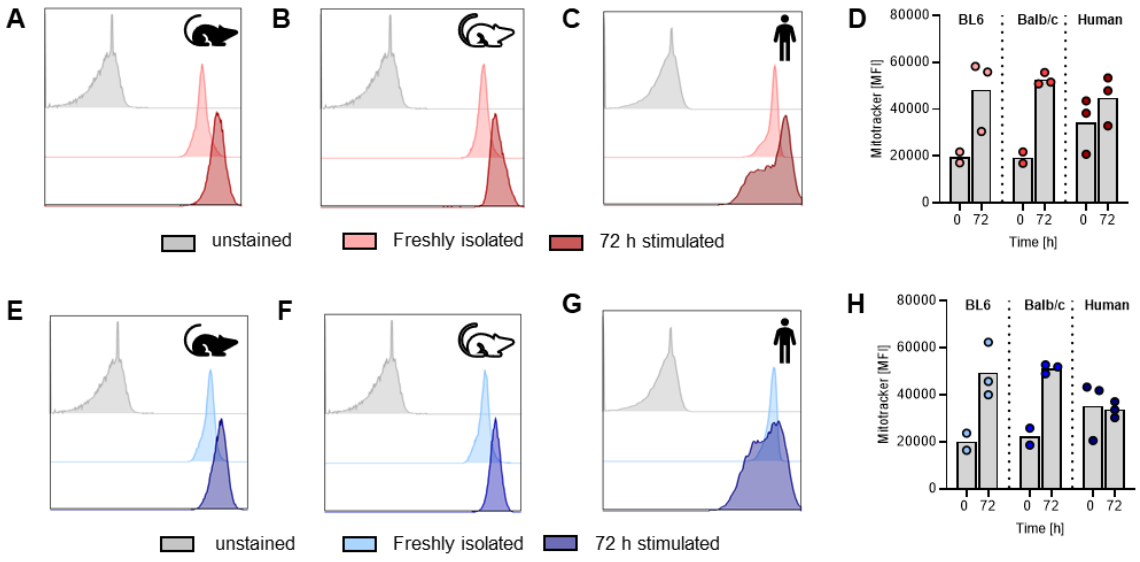

Figure 4-26: Murine and human T cells show a different regulation of the mitochondrial content upon stimulation. *Murine and human (A-D) CD4 and (E-H) CD8 T cells were stimulated with α-CD3/CD28 coated beads at a bead-to cell ratio of 1:1. Before and after 72 h stimulation, the mitochondrial content was assessed by a staining with Mitotracker Green FM and subsequent flow cytometric analysis. Representative FACS plots of (A, E) CD57BL/6, (B, F) Balb/c and (C, G) human T cells and (D, H) summarized median fluorescence intensities (MFI; median levels and single data points) are given.*

To gain deeper inside in the kinetics of the respiratory phenotype, we aimed to analyze the respiratory activity of murine and human T cells. As the distinct proliferation kinetics could influence and adulterate the results obtained using the PreSens technology, we decided to analyze the mitochondrial function by High-Resolution Respirometry. This technique allows to draw direct conclusions regarding the exact oxygen usage per cell and is therefore not biased by distinct proliferation behavior. What is more, High-Resolution Respirometry offers the possibility to apply different modulatory chemicals and therefore allows the analysis of not only the basic respiration (ROUTINE), but also the calculation of the amount of oxygen used for ATP production and the maximal capacity of the electron transport system in an uncoupled state (ETS, oxygen consumption of complex I to IV).

ROUTINE respiration of the cells was measured after an equilibration phase before the application of any chemical. To calculate the amount of oxygen used to fuel ATP production, cells were treated with oligomycin, inhibiting the ATP synthase, and the remaining oxygen consumption was subtracted from basic respiration. The maximal capacity of the ETS was measured after stepwise uncoupling with FCCP. All values were corrected for residual oxygen consumption, measured after inhibition of complex I and III with rotenone and myxothiazol, respectively.

Murine and human T cells displayed major differences in their respiratory profile in both T cell populations. In unstimulated cells, the ROUTINE respiration was lowest in human T cells but increased strongly upon stimulation in CD4 and CD8 T cells. In contrast, ROUTINE respiration of murine T cells showed no (CD57BL/6) or only a modest increase (Balb/c) upon stimulation and even decreased beyond 24 h of stimulation in CD8 T cells. Although ROUTINE respiration was significantly higher in unstimulated murine CD4 T cells, after 48 h of stimulation, murine T cells exhibited a lower respiratory activity compared to human T cells. A similar kinetics was observed regarding the ATP-related respiration, which also was found to be significantly lower in human CD4 and CD8 T cells before, but significantly higher after a 48 h period of stimulation.

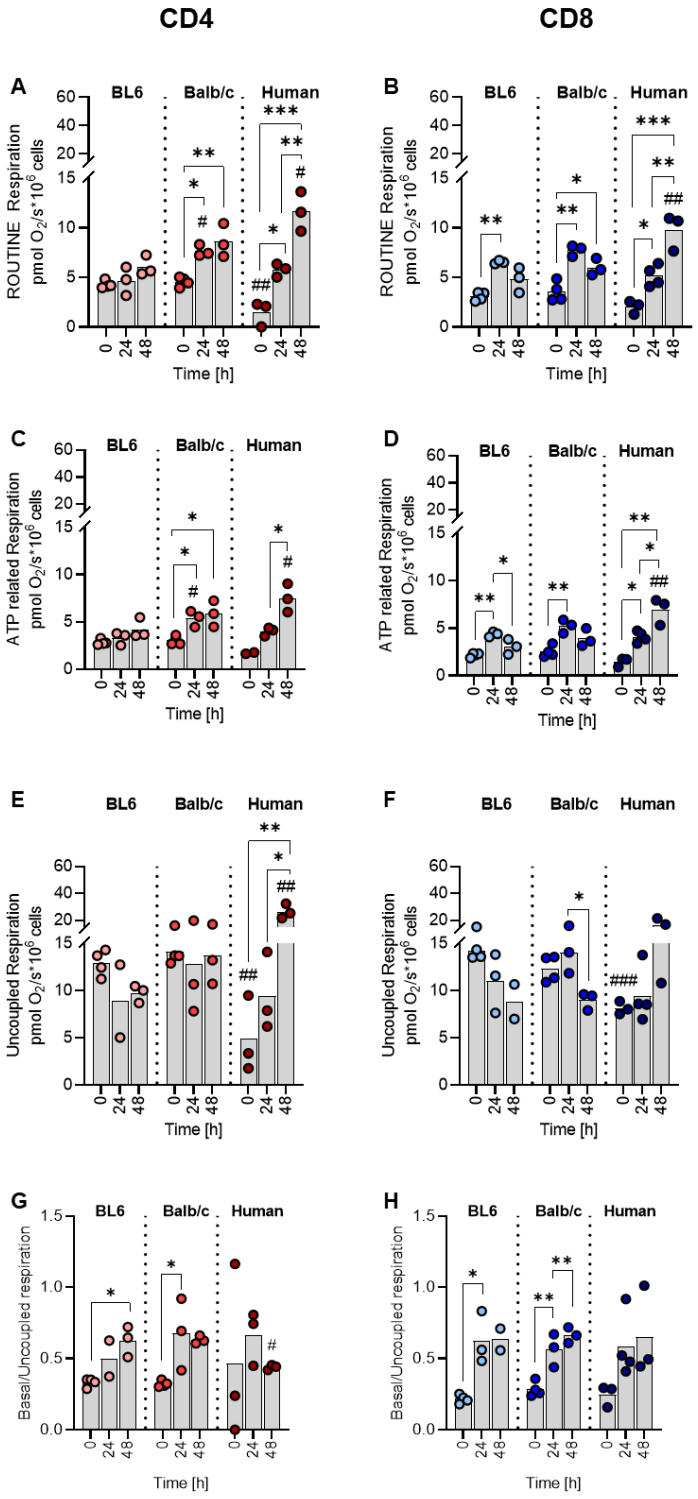

Figure 4-27: Respiratory profiles display major differences between murine and human T cells. *Murine and human CD4 (red) and CD8 (blue) T cells were isolated from C57BL/6 (BL6) and Balb/c splenocytes and human MNCs, respectively, and mitochondrial function analyzed by High-Resolution Respirometry in unstimulated cells (0 h) or after 24 h and 48 h stimulation with α-CD3/CD28 coated beads at a ratio of 1:1. All respiratory parameters were measured in culture medium. (A, B) Basal respiratory capacity was measured in normal cell culture medium. (C, D) ATP production was calculated after treatment with oligomycin and subtracting remaining oxygen consumption from ROUTINE respiration (Δ Routine-Oligomycin). (E, F) Capacity of the electron transfer system was determined after stepwise titration with FCCP. (G, H) To calculate the degree of respiratory capacity utilization, basal respiration was normalized to uncoupled respiration. (A-H) Given are median levels and single data points. Significance within the different measuring timepoints and species was separately calculated by ordinary one-way ANOVA and post-hoc Bonferroni multiple comparison test. Asterisks give significance levels within one species, hashes within different timepoints compared to C57BL/6 (* p < 0.05, ** p < 0.01, *** p < 0.001; same for #).*

The maximal ETS capacity again was significantly lower in unstimulated human compared to murine CD4 and CD8 T cells. However, whilst the uncoupled respiratory activity of human T cells strongly increased in the course of stimulation, the maximal respiratory capacity of murine CD4 and CD8 T cells even decreased upon stimulation and was significantly lower 48 h after the first stimulation.

Both murine and human CD4 and CD8 T cells increased the degree of respiratory capacity utilization in the course of stimulation. However, in CD4 T cells, this increase was more pronounced in murine than in human T cells. Stimulated human CD4 T cells used only 50 % of their maximal ETS capacity for basic respiration, whereas this percentage was significantly higher in murine CD4 T cells.

Taken together, we detected major differences in the mitochondrial function of murine and human T cells in the course of stimulation.

An important indicator of the mitochondrial function is the activity of the citrate synthase (CS). This enzyme is located in the mitochondrial matrix and catalyzes the condensation reaction of acetyl-CoA and oxalacetate to citrate, thus regenerating coenzyme A. CS activity is most commonly used as quantitative marker for intact mitochondria within a cell. To be able to directly correlate the measured respiratory activity to the mitochondrial cell content, we measured the citrate synthase activity in the same samples analyzed before and with High-Resolution Respirometry (Figure 4-28).

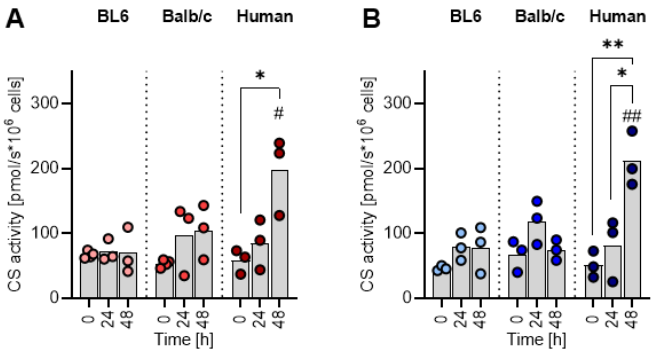

***Figure 4-28**: **Citrate synthase activity increases upon stimulation in human, but not in murine T cells.** Murine and human (A) CD4 and (B) CD8 T cells were isolated from C57BL/6 (BL6) and Balb/c splenocytes and human MNCs, respectively, and citrate synthase activity was measured in the same samples respiratory activity was determined in using a spectrophotometric assay. Given are median levels and single data points. Significance within the different measuring timepoints and species was separately calculated by ordinary one-way ANOVA and post-hoc Bonferroni multiple comparison test. Asterisks give significance levels within one species, hashes give significance levels within different timepoints compared to C57BL/6 (* $p < 0.05$, ** $p < 0.01$, *** $p < 0.001$; same for #).*

The analysis revealed that in murine CD4 and CD8 T cells the citrate synthase activity was only barely upregulated upon stimulation, whereas in human T cells CS activity was strongly

upregulated beyond 48 h of stimulation. Overall, the observed kinetics correlates well with changes in basic respiratory activity in the different sample sets (Figure 4-27). Interestingly, the citrate synthase activity of human T cells was upregulated only beyond 48 h of stimulation, but the respiratory activity already increased within the first 24 h of stimulation, indicating the initial upregulation of the respiratory activity is based on a higher nutrient influx into mitochondrial respiration.

Besides mitochondrial metabolism of glucose via the TCA cycle, glucose can as well be converted to lactate, a process often referred to as aerobic glycolysis in the context of malignant or highly proliferating cells. Different studies have highlighted the relevance of the aerobic glycolysis for T cell function but have led to conflicting results depending on whether murine or human T cells were analyzed (Cham and Gajewski, 2005; Chang et al., 2013; Renner et al., 2015; Renner et al., 2019). Therefore, we aimed to closer characterize the activity of this metabolic pathway in murine and human T cells.

First, we analyzed the glucose uptake of murine and human T cells using the fluorescent glucose analog 2NBDG and found an opposed pattern to what has been observed regarding mitochondrial content. Unstimulated murine CD4 and CD8 T cells displayed a higher 2NBDG uptake compared to human T cells. Upon stimulation, the 2NBDG uptake remained constant in murine T cells, but was increased in human T cells, and beyond 72 h of stimulation human T cells displayed a higher 2NBDG uptake compared to murine T cells (Figure 4-29).

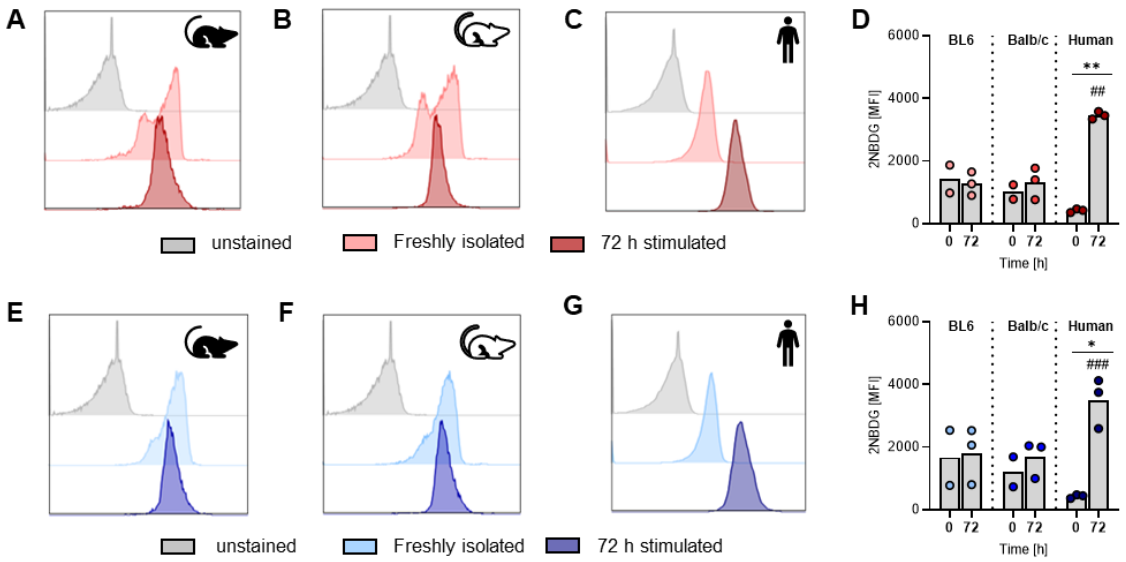

Figure 4-29: Murine and human T cells show a distinct glucose uptake pattern. *Murine and human (A-D) CD4 and (E-H) CD8 T cells were stimulated with α-CD3/CD28 coated beads at a bead-to-cell ratio of 1:1. Glucose uptake was assessed by a staining with 2NBDG and subsequent flow cytometric analysis before and beyond 72 h of stimulation. Representative histograms of (A, E) CD57BL/6, (B, F) Balb/c and (C, G) human T cells and (D, H) median levels and single data points are given. (D, H) Significance within a timepoint was calculated by ordinary one-way ANOVA and post-hoc Bonferroni multiple comparison test; significance in the course of stimulation within*

one species by paired t-test. Asterisks give significance upon stimulation, hashes within one timepoint compared to C57BL6 (p < 0.05, ** p < 0.01, *** p < 0.001; same for hashes).*

A key enzyme for aerobic glycolysis is the LDH, which catalyzes the rate limiting conversion of pyruvate and lactate. As the two subunits of the LDH may have different affinities for catalyzing either of the reaction, the composition of the LDH may pose a major determinant for the glycolytic or mitochondrial activity of a cell. Therefore, we compared the LDH isoenzyme distribution in murine and human T cells before and after stimulation and found major differences between both species (Figure 4-30). Unstimulated human T cells displayed a LDHB shaped phenotype, and upregulated LDHA upon stimulation, but kept an isoenzyme pattern including all five different isoenzymes. In contrast, unstimulated murine T cells mainly expressed the Ldha homologue Ldh-5 and only a small portion of Ldh-4. Upon stimulation, the isoenzyme pattern even shifted towards a more Ldha containing phenotype, and the cells lost their expression of Ldh-2. Therefore, not only the mitochondrial, but also the glycolytic metabolism reveals major differences between murine and human T cells.

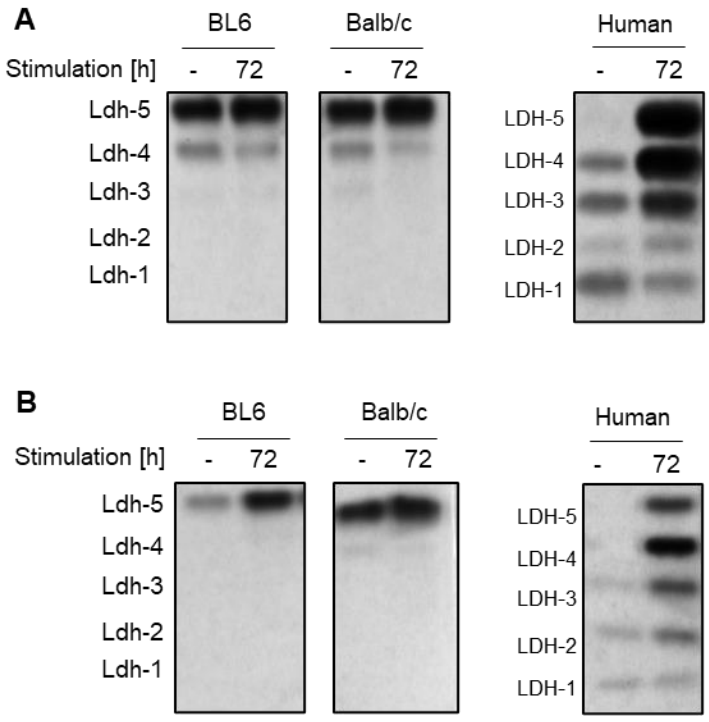

Figure 4-30: Murine and human T cells show major differences in their LDH isoenzyme pattern and regulation. *(A) CD4 and (B) CD8 T cells were isolated from splenocytes of C57BL/6 (BL6) and Balb/c mice and human MNCs. The LDH isoenzyme pattern was analyzed by LDH zymography before and after 72 h of stimulation with α-CD3/CD28 coated beads at a bead-to-cell ratio of 1:1.*

We asked, which consequences these metabolic differences could have on the outcome of studies focusing on the interplay of tumor- and immunometabolism. The inhibition of the LDH is an emerging strategy to inhibit the glycolytic tumor metabolism and currently tested in different *in vivo* studies. We questioned whether the inhibition of the LDH would lead to distinct results in murine and human T cells. Therefore, we stimulated the human and murine CD4 T

cells for 48 h and 72 h, respectively, while treating them with the LDH inhibitor NCI-737 and assessed the impact on lactate and cytokine secretion.

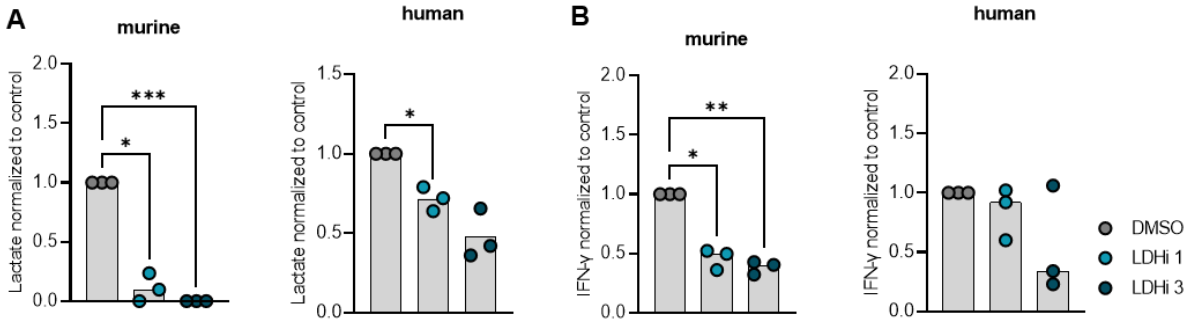

Figure 4-31: LDH inhibition lowers lactate and cytokine secretion of murine, but not human CD4 T cells. *Murine CD4 T cells were isolated from splenocytes of C57BL/6 mice. Human CD4 T cells were isolated from MNCs of healthy donors. Cells were stimulated with α-CD3/CD28 coated beads in a bead-to-cell ratio of 1:1 and treated with NCI-737 (LDHi) in the indicated concentrations [µM] for 48 h. DMSO served as a control. (A) Lactate concentrations in the culture supernatants were measured by the Department for Clinical Chemistry of the University Hospital Regensburg. (B) IFN-γ levels in the supernatants were measured by means of ELISA. Statistical significance was determined by one-way ANOVA and post-hoc Bonferroni multiple comparison test (* $p < 0.05$; ** $p < 0.01$; *** $p < 0.001$).*

Surprisingly, treatment with the LDH inhibitor significantly lowered the lactate release rate of the murine T cells (Figure 4-31 A) already at low concentrations but had a reduced effect on the lactate secretion of human T cells. A similar trend was observed regarding IFN-γ secretion, which was diminished by treatment with 1 µM LDHi in murine T cells but not affected at this concentration in human T cells. Notably, high-dose LDH inhibitor led to a distinct decrease in IFN-γ in two human T cell donors as well, indicating that human T cells as well can be negatively affected by LDHi treatment depending on donor susceptibility. Together, this shows that metabolic manipulation may affect human and murine T cells in different ways, which has to be considered for evaluation of treatment strategies in animal models.

4.6. Learning lessons from cells resistant towards lactic acid

To increase lactic acid resistance of T cells by manipulating their LDH isoenzyme pattern or glucose metabolism itself stands to reason. But as shown so far, none of the taken approaches in this work led to a striking success. Therefore, more target structures have to be identified to increase T cell lactic acid resistance, and it seems feasible to analyze the phenotype of cells that cope better with lactic acid treatment.

4.6.1. Learning lessons from macrophages

Regarding functionality, almost all types of immune cells are affected by lactic acid treatment in some way. But not all immune cell populations are affected as drastic in their viability as

T cells and NK cells. For example, it has been shown that monocytes are severely affected in their effector function development, but survive the treatment with 20 mM lactic acid (Dietl et al., 2010), which is the lethal to T cells.

In the human system, macrophages differentiate from monocytes after their invasion into peripheral tissue. They belong to the innate immune system and are phagocytic cells, which, among other functions, phagocyte bacteria and cell debris at a site of acute inflammation. Here, macrophages often face with a very acidic pH (Menkin, 1956). Therefore, it seems feasible to analyze why monocyte-derived macrophages have the capability to survive in high lactic acid concentrations

4.6.1.1. Macrophages survive high-dosage lactic acid treatment and show reduced intracellular acidification

Monocytes were isolated from the MNCs of healthy donors and differentiated to macrophages by the addition of 2 % human AB serum to culture medium for 6 – 7 days. Then, the cells were harvested and seeded into UpCell culture dishes. These cell culture dishes have a temperature-sensitive surface, which turns hydrophobic upon cooling, but enables cell attachment at cell culture conditions (37 °C). This allowed detachment and harvesting of macrophages after prolonged culture for flow cytometric analysis.

To test the survival of macrophages upon lactic acid treatment, cells were seeded into UpCell culture dishes and treated with 20 mM lactic acid for 48 h. Afterwards, the viability was assessed by Annexin V/7-AAD staining and a subsequent flow cytometric analysis.

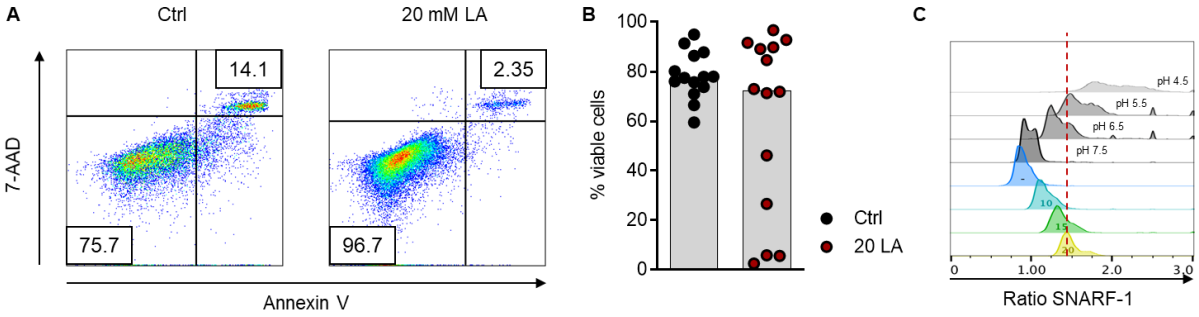

Figure 4-32: Macrophages survive treatment with 20 mM lactic acid and show limited intracellular acidification. *Monocyte-derived macrophages were generated as described in chapter 3.1.3.3. (A, B) The cells were seeded into UpCell culture dishes, treated with 20 mM lactic acid for 48 h and the viability of the cells was analyzed by an Annexin V/7-AAD staining, followed by subsequent flow cytometric analysis. Given is (A) one representative example of the experiments summarized in (B), plotting the median viability and single data points. The significance was calculated with Wilcoxon's matched-pair signed rank test (no significance detected). (C) To assess the intracellular acidification, the macrophages were loaded with the pH-sensitive dye SNARF-1 acetate and afterwards treated with lactic acid (different colors). To allow a pH determination, a standard curve using buffers with a fixed pH (depicted in grey) was recorded. Shown is a representative histogram (n = 3). The red dashed line marks the signal peak of the 20 mM lactic acid treated cells. This work was conducted by Nathalie Babl.*

As shown in Figure 4-32 A and B, most of the analyzed macrophage cultures survived the treatment with 20 mM lactic acid. A few cultures displayed poor survival, suggesting a donor-dependent mechanism. This makes macrophages a suitable cell type to investigate resistance mechanisms towards lactic acid.

Keeping in mind that extracellular buffering rescued T cell survival, we hypothesized that the intracellular buffering system of macrophages could be the key for their increased lactic acid resistance. Indeed, compared to T cells, which presented an intracellular pH of 4.5 upon treatment with 20 mM lactic acid (data not shown), macrophages showed a less pronounced intracellular acidification, maintaining a pH of approximately 5.5 upon lactic acid treatment (Figure 4-32 C, experiments performed by Nathalie Babl).

Therefore, we attempted to characterize the buffering system of macrophages analyzing the expression of known key pH regulators in comparison to monocytes, natural regulatory (nTreg) and conventional CD4 and CD8 T cells by means of qRT-PCR. Monocytes and conventional CD4 and CD8 T cells were isolated from the MNCs of healthy donors. Natural Treg were isolated by flow cytometric cell sorting and expanded by the group of Prof. Matthias Edinger and PD Dr. Petra Hoffmann of the University Hospital of Regensburg. Conventional T cells were stimulated with α-CD3/CD28 coated beads at a ratio of 1:1 as indicated. Monocytes (Mo) and Macrophages (Mac) stimulated with 100 ng/ml LPS. In addition, when specific inhibitors for the analyzed regulators were available, we tested the effect of inhibiting several components of the pH regulation machine on the lactic acid resistance of macrophages.

4.6.1.2. The expression of pH-sensing receptors in immune cells

First, we analyzed the expression of proton-sensing G protein coupled receptors (GPRs) in different cell types. Currently, four different GPRs with pH sensing activity are known: GPR4 , GPR65 (also known as TDAG8), GPR68 (also known as OGR1) and GPR132 (also known as G2A) (Justus et al., 2013; Yang et al., 2015), and all of them play important roles in mediating immune responses.

Concerning all four analyzed pH-receptors, monocytes showed the highest mRNA expression compared to T cells or macrophages, although a considerable donor heterogeneity was found in all four analyzed genes. Interestingly, only monocytes showed a strong expression of *GPR4*, whilst all other analyzed immune cells showed either a lower or nor expression (Figure 4-33). Macrophages as well expressed all four pH-receptors, but to a much lesser extent compared to Monocytes. In T cells, the expression of the receptors was the lowest compared to the myeloid cells, and no big differences were found between nTreg and normal CD4 T cells. The expression of the other receptors appeared to be tightly connected to their activation state.

GPR65 was downregulated 48 h after initial activation in both CD4 and CD8 T cells but upregulated after 6 d again. In contrast, the expression of *GPR68* was upregulated 48 h and 6 d after activation, and the expression of *GPR132* was downregulated upon activation. This could indicate that macrophages, due to their higher levels of proton sensors, can sense and respond more flexible to extracellular acidification than T cells and better adapt to low extracellular pH.

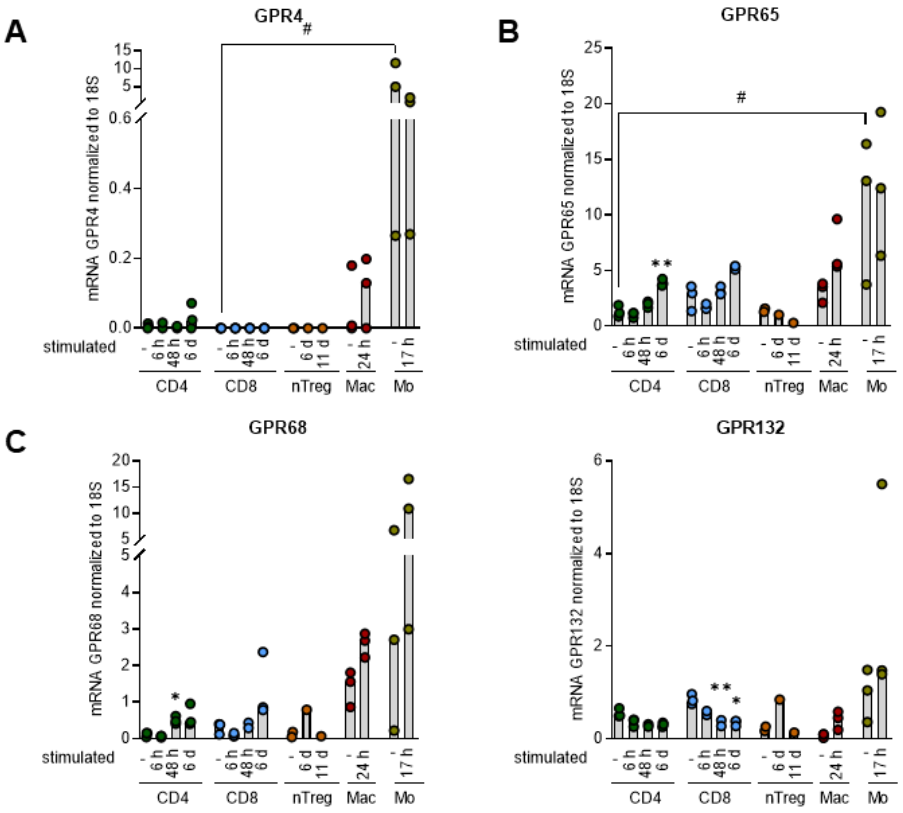

Figure 4-33: Expression of pH-sensing G protein coupled receptors in different immune cells. *Cells were isolated and stimulated for the indicated times as described above (see page 106). The mRNA expression of (A) GPR4, (B) GPR65, (C) GPR68 and (D) GPR132 was analyzed by means of qRT-PCR. Depicted are median expression levels and single data points. Statistical significance was calculated within the different immune cell upon stimulation (T cells: One-way ANOVA and post-hoc Bonferroni multiple comparison test; Monocytes and Macrophages: Wilcoxon's matched-pair signed rank test) and comparing the expression levels of unstimulated immune cells (Kruskal-Wallis test). Asterisks give significant differences of expanded compared to unstimulated cells, hashes give significant differences in between different immune cell populations (* p < 0.05, ** p < 0.01; same for #).*

4.6.1.3. Role of carbonic anhydrases in macrophage resistance

Carbonic anhydrases (CAs) are a family of metalloenzymes that catalyze the interconversion of HCO_3^- and CO_2, thereby binding protons and contributing to intracellular buffering of many cells. Of the 15 known isoforms of carbonic anhydrases, 12 are catalytically active (Aggarwal et al., 2013). In this work, the expression of four of those isoenzymes was analyzed: *CA-II*, the

isoform which is most broadly expressed among different cell types, *CA-VI*, which is the only known secreted isoform of the CAs, *CA-IX* and *CA-XII*, which both have been described to play an important role in pH maintenance of cancer cells.

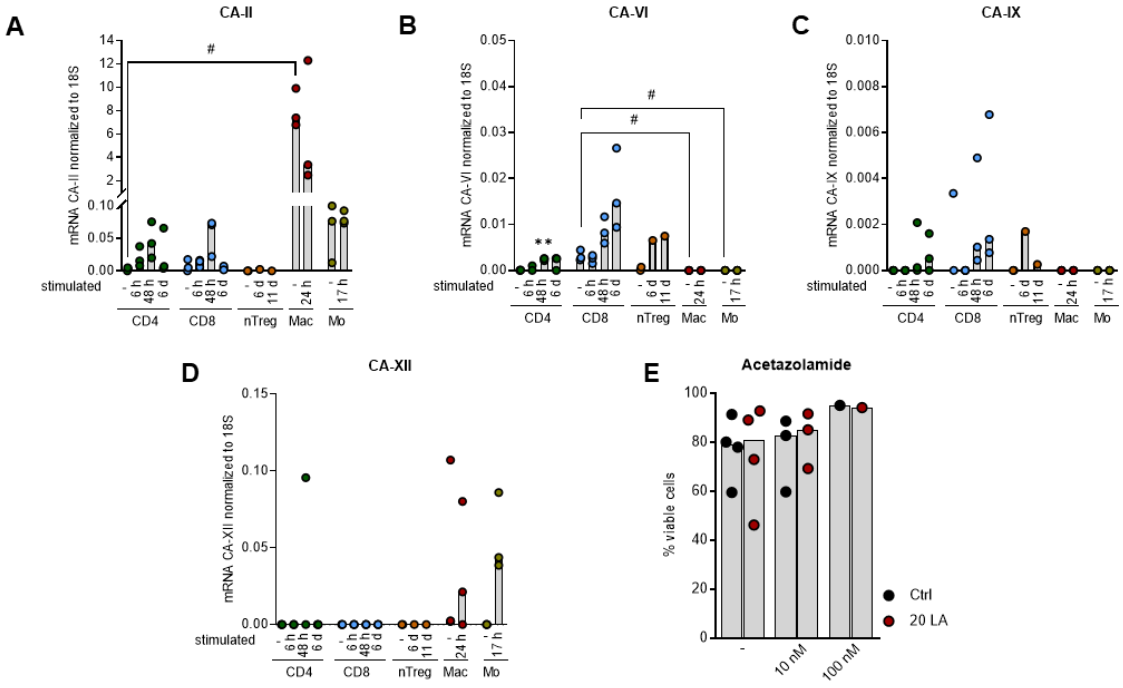

Figure 4-34: Expression of different carbonic anhydrase isoforms in immune cells and their influence on the lactic acid resistance of macrophages. *(A – D) Cells were isolated and stimulated for the indicated times as described above (see page 106). The mRNA expression of (A) CA-II, (B) CA-VI, (C) CA-IX and (D) CA-XII was analyzed by qRT-PCR. Depicted are median expression levels and single data points. Statistical significance was calculated within the different immune cell upon stimulation (T cells: One-way ANOVA and post-hoc Bonferroni multiple comparison test; Monocytes and Macrophages: Wilcoxon's matched-pair signed rank test) and comparing the expression levels of unstimulated immune cells (Kruskal-Wallis test). Asterisks give significant differences of expanded compared to unstimulated cells, hashes give significant differences in between different immune cell populations (* $p < 0.05$, ** $p < 0.01$; same for #). (E) Monocyte-derived macrophages were seeded into UpCell dishes and treated with 20 mM lactic acid for 48 h in the presence or absence of acetazolamide in the indicated concentrations. Viability was determined with an Annexin V//-AAD staining. Viable cells were designated as Annexin V^-/7-AAD^-. Depicted are median viability and single data points. Significance was calculated by one-way ANOVA and post-hoc Bonferroni multiple comparison test (no significance detected).*

The most abundant isoform of the carbonic anhydrases in immune cells was *CA-II*, which was on a very high level expressed in macrophages, on lower levels in monocytes and even less in T cells. Interestingly, macrophages downregulated the expression of the *CA-II* upon LPS-treatment, whilst in both CD4 and CD8 T cells *CA-II* transcription was induced upon activation and peaked after 48 h.

Th expression of *CA-VI* was only detected on a very low level in T cells and nTreg, in which the transcription was induced by stimulation and constantly increased during the observation time. No transcription of *CA-VI* was detected in myeloid cells. The same was found for *CA-IX*, which peaked 6 days after the activation of effector T cells or nTreg. In contrast, the transcription of *CA-XII* was only induced in myeloid cell after LPS stimulation, but in T cells except for one donor at a specific time point no expression in T cells was detected.

To closer investigate the role of carbonic anhydrases for lactic acid resistance of macrophages, monocyte-derived macrophages were treated with 20 mM lactic acid and acetazolamide, a pan-carbonic anhydrase inhibitor, was administered for 48 h and viability was assessed. Treatment with acetazolamide did not sensitize macrophages towards lactic acid, indicating that carbonic anhydrases play a minor role in the protection against lactic acid or can be substituted by other pH regulatory enzymes,

4.6.1.4. Role of H^+-pumps for macrophage resistance

Proton pumps play a major role in several physiological processes. They actively transport protons against concentration gradients by either ion-coupled co-transports or use ATP as energetic source.

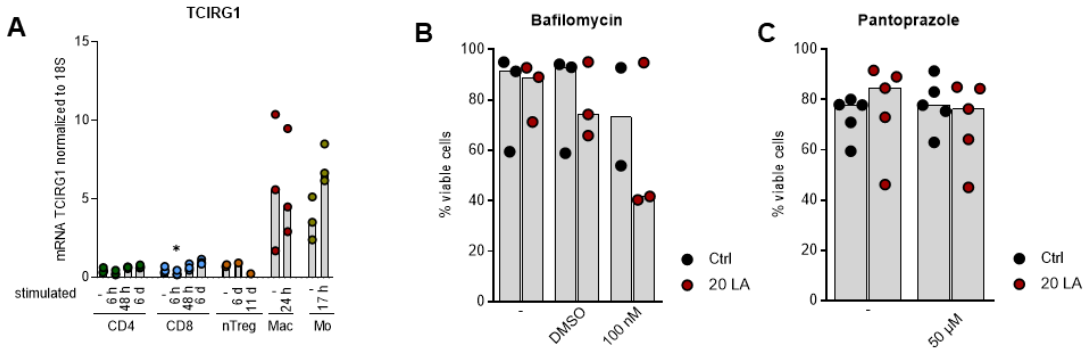

Figure 4-35: Expression of TCIRG1 in immune cells and the influence of proton pumps on lactic acid resistance of macrophages. *(A) Cells were isolated and stimulated for the indicated times as described above (see page 106). The mRNA expression of TCIRG1 was analyzed by means of qRT-PCR. Depicted are median expression levels and single data points. Statistical significance was calculated within the different immune cell upon stimulation (T cells: One-way ANOVA and post-hoc Bonferroni multiple comparison test; Monocytes and Macrophages: Wilcoxon's matched-pair signed rank test) and comparing the expression levels of unstimulated immune cells (Kruskal-Wallis test). Asterisks give significant differences of expanded compared to unstimulated cells (* p < 0.05). (B, C) Monocyte-derived macrophages were seeded into UpCell dishes and treated with 20 mM lactic acid and (B) bafilomycin or (C) pantoprazole in the indicated concentrations for 48 h. (B) DMSO served as a vehicle control. Viability was determined by an Annexin V//-AAD staining. Depicted are the median viablity and single data points. Significance was calculated by one-way ANOVA and post-hoc Bonferroni multiple comparison test (no significance detected).*

TCIRG1 (T cell immune regulator gene 1) encodes a beta-subunit of vacuolar ATPases, which uses ATP to either pump protons into intracellular vesicles, which is for example essential for the acidification of lysosomes after phagocytosis, or if located at the plasma membrane also to transport protons to the extracellular space. Our expression analysis revealed, that the gene *TCIRG1* is much higher expressed in monocytes and macrophages than in T cells (Figure **4-35** A). In monocytes, the expression of *TCIRG1* was upregulated upon LPS stimulation, which was not the case in macrophages, in which the expression remained more or less constant.

To test the contribution of proton pumps to lactic acid resistance of macrophages, cells were treated with 20 mM lactic acid and with and without 100 nM bafilomycin (Figure 4-35 B), which is an inhibitor of vacuolar ATPases, or 50 µM pantoprazole (Figure 4-35 C), which is an inhibitor of potassium-proton ATPases, which are mainly located in the gastric mucosa important to maintain the acidic pH in the stomach. Pantoprazole had no effect on the viability of macrophages in the presence of lactic acid. Treatment with bafilomycin reduced the viability of lactic acid treated macrophages in two of three donors, suggesting a role of vacuolar ATpases in lactic acid resistance of macrophages.

4.6.1.5. Role of NHEs for macrophage resistance

Sodium hydrogen exchangers (NHEs) are antiporters that exchange protons for sodium ions. The nine different NHE isoforms are encoded by genes of the SLC9 family and are expressed in almost all tissue types across the body. Here, we analyzed the expression of *NHE1* and *NHE8.*

NHE1 was found to be expressed in both T cell populations and myeloid cells, although the expression in macrophages and monocytes was up to ten times higher compared to unstimulated or stimulated T cells. Compared to *NHE1*, *NHE8* was expressed to a much lesser extent in myeloid cells, but on a similar level in T cells. Whilst the *NHE1* expression levels was independent from the respective activation state of the cells, the transcription level of *NHE8* increased upon LPS stimulation of macrophages and monocytes.

To closer investigate the role of NHEs in lactic acid resistance of macrophages, the cells were treated with cariporide, a selective inhibitor for NHE1, and 5-(N-ethyl-N-isopropyl)-Amiloride (EIPA), which is an unspecific inhibitor of NHEs. For both, DMSO served as a vehicle control. Again, the effect of the inhibitors was donor dependent. The inhibition of NHE1 by cariporide sensitized two of the three analyzed donors towards lactic acid treatment. The application of EIPA sensitized one out of two macrophage donors towards lactic acid treatment in lower concentrations. This indicates, that rather NHE1, but not NHEs may contribute to lactic acid resistance of macrophages.

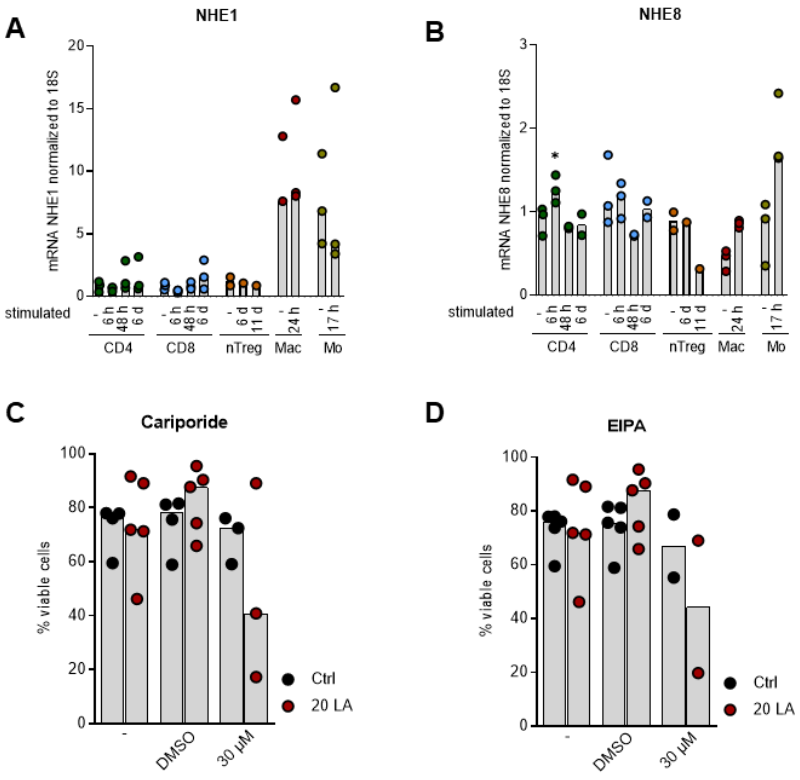

Figure 4-36: Expression of NHE1 and NHE3 in immune cells and the influence of NHEs on lactic acid resistance of macrophages. *(A, B) Cells were isolated and stimulated for the indicated times as described above (see page 106). The mRNA expression of (A) NHE1 (SLC9A1) and (B) NHE8 (SLC9A8) was analyzed by means of qRT-PCR. Depicted are median expression levels and single data points. Statistical significance was calculated within the different immune cell upon stimulation (T cells: One-way ANOVA and post-hoc Bonferroni multiple comparison test; Monocytes and Macrophages: Wilcoxon's matched-pair signed rank test) and comparing the expression levels of unstimulated immune cells (Kruskal-Wallis test). Asterisks give significant differences of expanded compared to unstimulated cells, hashes give significant differences in between different immune cell populations (* p < 0.05). (C, D) Monocyte-derived macrophages were seeded into UpCell dishes and treated with 20 mM lactic acid and (C) cariporide or (D) EIPA at the indicated concentrations for 48 h. DMSO served as a vehicle control. Viability was determined with by Annexin V/7-AAD staining, followed by flow cytometric analysis. Depicted are the median viability and single data points. Significance was calculated by one-way ANOVA and post-hoc Bonferroni multiple comparison test (no significance detected).*

4.6.1.6. Role of AEs for macrophage resistance

Anion exchangers (AEs) exchange extracellular HCO_3^- for intracellulaur Cl^-, thereby transporting bicarbonate ions into the cell, which can serve as substrate for the carbonic anhydrases (see 4.6.1.3) to bind protons. In humans, all anion exchangers belong to the *SLC4* family, which includes 10 members, of which three encode anion exchangers.

The most famous member of this group is AE1, also known as band 3 protein, which plays a major role in erythrocyte physiology. As our analyses showed, *AE1* is not expressed in T cells or myeloid cells (data not shown). Instead, the qPCR analysis revealed that T cells and macrophages express *AE2* on a low to moderate level.

To closer assess the importance of AEs for the lactic acid resistance of macrophages, the cells were treated with 20 mM lactic acid and SITS, which is an unspecific inhibitor of anion

exchangers. After 48 h, the viability of the cells was assessed by flow cytometry analysis. Again, this analysis revealed donor dependency, as three out of five donors displayed a moderate to strongly decreased viability upon lactic acid treatment in the presence of SITS, whereas two donors showed no effect.

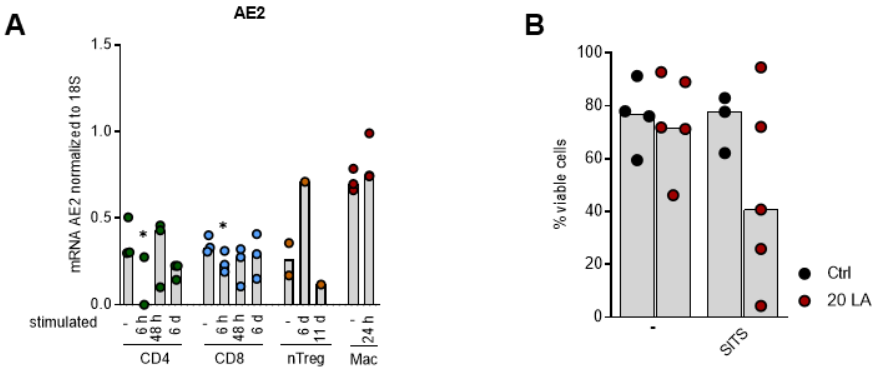

Figure 4-37: Expression of AE2 in immune cells and the influence of AEs on lactic acid resistance of macrophages. *(A) Cells were isolated and stimulated for the indicated times as described above (see page 106). The mRNA expression of AE2 (SCL4A2) was analyzed by means of qRT-PCR. Depicted are median expression levels and single data points. Statistical significance was calculated within the different immune cell upon stimulation (T cells: One-way ANOVA and post-hoc Bonferroni multiple comparison test; Monocytes and Macrophages: Wilcoxon's matched-pair signed rank test) and comparing the expression levels of unstimulated immune cells (Kruskal-Wallis test). Asterisks give significant differences of expanded compared to unstimulated cells, hashes give significant differences in between different immune cell populations (* $p < 0.05$). (B) Monocyte-derived macrophages were seeded into UpCell dishes and treated with 20 mM lactic acid and SITS for 48 h. Viability was determined with an Annexin V/7-AAD staining, followed by flow cytometric analysis. Viable cells were designated as Annexin $V^+/7\text{-}AAD^-$. Depicted are the median viability levels and single data points. Significance was calculated by one-way ANOVA and post-hoc Bonferroni multiple comparison test (no significance detected).*

4.6.1.7. Role of MCTs for macrophage resistance

Last, the impact of the lactate transporters themselves on the lactic acid resistance of macrophages was analyzed. Lactate is mainly exported form the intracellular space by monocarboxylate transporters (MCTs) in co-transport with a proton. These transporters are encoded by genes of the *SLC16* gene family including 14 members, of which 4 have been described to act as lactate transporters.

MCT-1 and MCT-4 are the most abundant lactate-transporting MCTs. It has been demonstrated before that MCT-1 is expressed in macrophages (Jha et al., 2021) as well as T cells (Renner et al., 2015). MCT-4 expression has been demonstrated to be essential for the response of macrophages to LPS stimulation (Tan et al., 2015). We focused our analyses on MCT-4 expression. In T cells, expression of *MCT-4* was tightly connected to their activation state, as in both CD4 and CD8 T cells the transcription was upregulated upon activation and peaked 6 d after activation. In unstimulated monocytes, *MCT-4* was expressed on a similar level as in stimulated T cells, but the transcription was strongly upregulated by LPS stimulation.

The transcription level of *MCT-4* in macrophages was up to 20-fold higher compared to stimulated T cells and was not regulated by LPS stimulation.

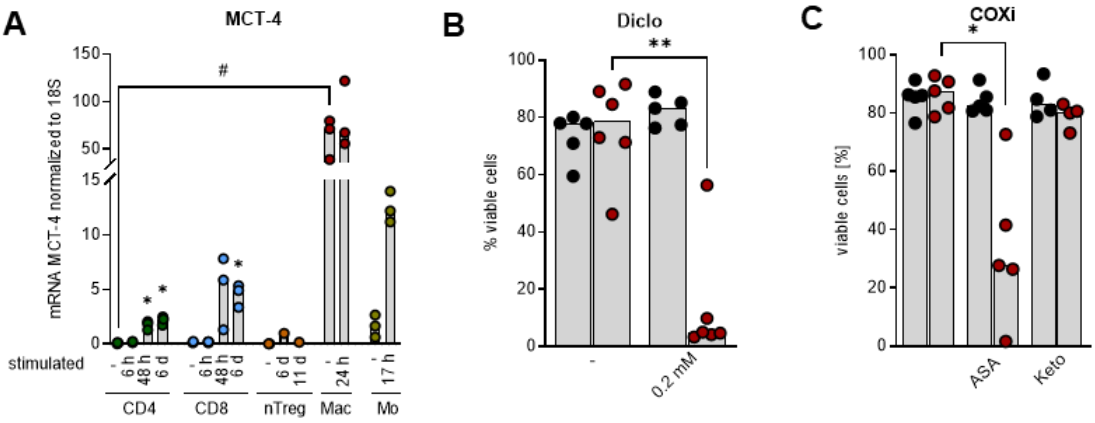

Figure 4-38: Expression of lactate transporters in immune cells and the influence of MCT inhibition on the lactic acid resistance of macrophages. *(A) Cells were isolated and stimulated for the indicated times as described above (see page 106). The mRNA expression of MCT-4 (SLC16A3) was analyzed by means of qRT-PCR. Depicted are median expression levels and single data points. Statistical significance was calculated within the different immune cell upon stimulation (T cells: One-way ANOVA and post-hoc Bonferroni multiple comparison test; Monocytes and Macrophages: Wilcoxon's matched-pair signed rank test) and comparing the expression levels of unstimulated immune cells (Kruskal-Wallis test). Asterisks give significant differences of expanded compared to unstimulated cells, hashes give significant differences in between different immune cell populations (* $p < 0.05$, ** $p < 0.01$; same for #). (B, C) Monocyte-derived macrophages were seeded into UpCell dishes and treated with 20 mM lactic acid and (B) 0.2 mM diclofenac or (C) 1 mM aspirin (ASA) or 0.2 mM ketoprofen (Keto) for 48 h. Viability was determined with an Annexin V/7-AAD staining, followed by flow cytometric analysis. Depicted are the median viability levels and single data points. Significance was calculated by one-way ANOVA and post-hoc Bonferroni multiple comparison test (* $p < 0.05$, ** $p < 0.01$).*

To investigate the role of lactate transporters in lactic acid resistance of macrophages, cells were treated with 20 mM lactic acid while applying diclofenac as MCT inhibitor. Diclofenac, a non-steroidal anti-inflammatory drug (NSAID) was originally described as an inhibitor for cyclooxygenases (COX), but has been described as a potent inhibitor of MCT-1 and MCT-4 by our group (Renner et al., 2019). The application of 0.2 mM diclofenac sensitized all analyzed donors towards lactic acid treatment but did not influence the viability of the cells under control conditions.

Besides being a potent MCT inhibitor, diclofenac is a well-known non-steroidal inflammatory drug (NSAID) inhibiting cyclooxygenases (COX), and it's not possible to distinguish whether the diclofenac effect on macrophages is mediated by MCT or COX inhibition. Therefore, the macrophages were treated with 20 mM lactic acid and in the presence or absence of aspirin (ASA) or ketoprofen, both NSAIDs inhibiting COX but not MCTs (Renner et al., 2019). Surprisingly, treatment with 1 mM ASA and 20 mM lactic acid had a similar effect on macrophage viability as diclofenac treatment, but ketoprofen treatment failed to induce cell death upon lactic acid treatment. This indicates that the induction of cell death in lactic acid treated macrophages is neither mediated by MCT nor by COX inhibition. Therefore, a third mechanism still to be elucidated must be involved in mediating the lactic acid resistance of

macrophages, and more research is needed in this area to gain deeper insights into this mechanism.

4.6.2. Learning lessons from lactic acid-resistant T cells

The response of immune cells towards lactic acid can be very heterogenous among a T cell culture and varied between donors (see chapter 4.1.3). Using CFSE, a fluorescent dye which dilutes on cell division, we found that proliferative activity of most cells within a culture was abrogated upon lactic acid treatment. However, a population of cells still showed CFSE dilution and Ki-67 upregulation, although the proliferation was delayed, and the number of cell cycles within 6 days was diminished (Figure 4-39 A).

Based on those observations, we aimed to analyze the transcriptional profile of T cells proliferating on lactic acid treatment. We hypothesized that those cells manage to express target genes turning them resistant towards lactic acid influence. Therefore, we stained cells with CFSE prior to stimulation and lactic acid treatment. Subsequently, we sorted for proliferating and non-proliferating cells (Figure 4-39 B) and performed an RNAseq analysis. In addition, we included unstimulated cells (d 0) as control. Both RNAseq and data analysis were conducted by the NGS core facility of the Regensburg Institute for Interventional Immunology (RCI).

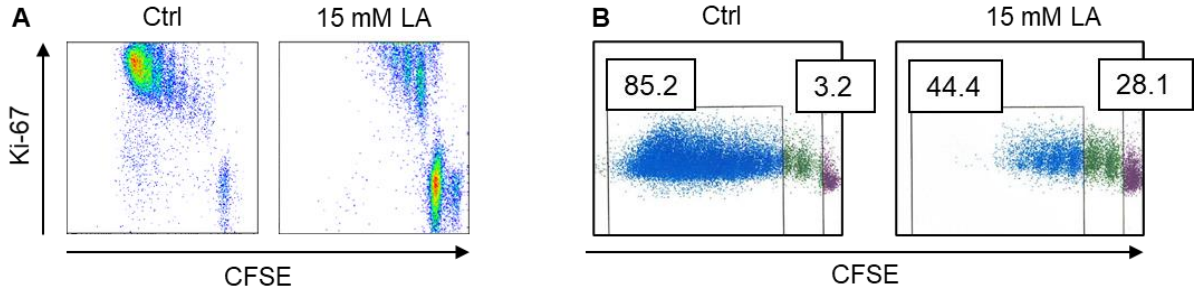

Figure 4-39: CD4 T cells are heterogeneously inhibited in their proliferation by lactic acid treatment. *CD4 T cells were labelled with CFSE, stimulated with α-CD3/CD28 coated beads in a bead-to-cell ratio of 1:10 and treated with lactic acid as indicated. Shown is one representative example each. (A) After 6 d, a flow cytometric analysis of Ki-67 expression was performed (n = 2). (B) Sorting strategy used for the generation of RNAseq samples (n = 3).*

First, a principal component analysis (PCA) was performed. Unstimulated, proliferating, and non-proliferating cells separated regardless of lactic acid treatment along principal component 1 (PC1) covering 76 % variance (data not shown). Proliferating cells separated according to their treatment along PC3 which includes 25 genes given in Figure 4-40 B. In contrast, non-proliferating cells only separated slightly along PC3.

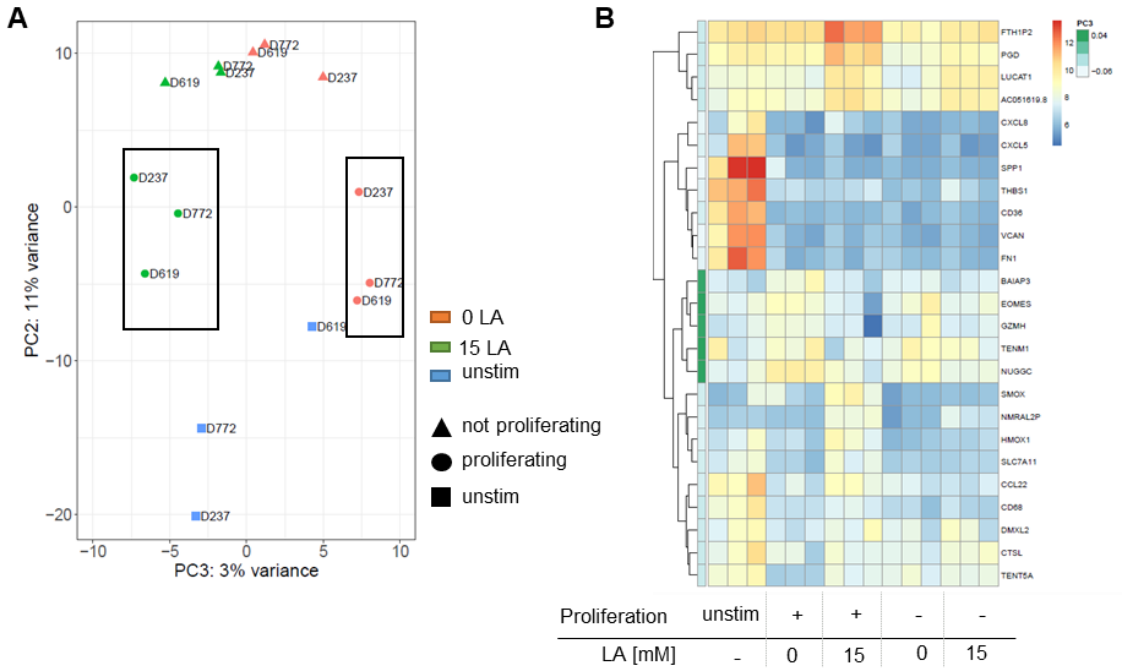

Figure 4-40: Proliferating cells separate along Principal Component 3 according to their respective lactic acid treatment. *CD4 T cells were labelled with CFSE, stimulated with α-CD3/CD28 coated beads in a bead-to-cell ratio of 1:10 and treated with lactic acid as indicated. Cells were sorted into proliferating (CFSE decreased) and not proliferating (CFSE stable) cells by flow cytometric cell sorting and subjected to RNAseq analysis. (A) Principal Component Analysis of the RNAseq data. Numbers denote corresponding donors. (B) Heatmap showing the genes determining PC3.*

We hypothesized, that in cells proliferating upon lactic acid the lactic acid treatment induced genes responsible for the higher resistance and compared the gene expression profiles of proliferating cells with and without lactic acid treatment. The direct comparison of the expression profiles of lactic acid treated cells with control cells revealed 436 differentially upregulated genes (|log2 Fold Change| > 0; FDR < 0.05). From these, 7 distinct clusters were deduced (Figure 4-41).

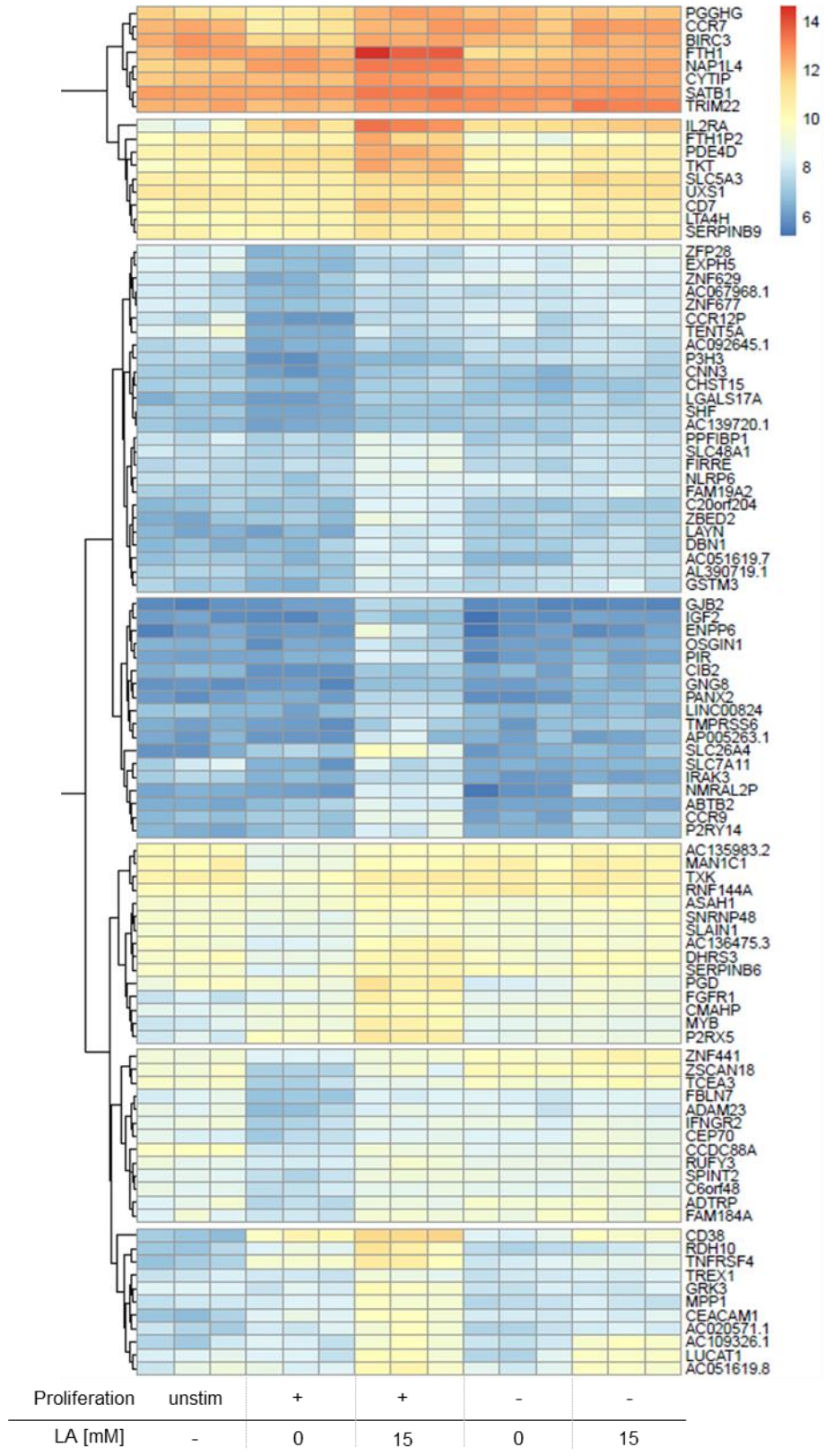

Figure 4-41: Impact of lactic acid on gene expression profiles of CD4 T cells. *CD4 T cells were labelled with CFSE, stimulated with α-CD3/CD28 coated beads in a bead-to-cell ratio of 1:10 and treated with lactic acid as indicated. Cells were sorted into proliferating (CFSE decreased) and not proliferating (CFSE stable) cells by flow cytometry cell sorting and subjected to RNAseq analysis. Shown is a heatmap of the TOP100 genes upregulated in lactic acid treated proliferating compared to control proliferating cells (FDR < 0.05).*

The genes up- and downregulated in lactic acid treated proliferating T cells compared to control proliferating T cells were subjected to a gene set enrichment analysis (Chen et al., 2013;

Kuleshov et al., 2016; Xie et al., 2021). Shown in Figure 4-42 is a bar graph of significantly enriched cell type gene signatures from EnrichR for the differentially up- and downregulated genes. One of the highest signatures enriched for upregulated genes was *CD14+ monocytes*. Monocytes are lactic acid resistant cells. This strengthens monocytes and macrophages as suitable model cell types to investigate lactic acid resistance. In line, the signature for *CD56+ NK cells*, which are lactic acid sensitive, was highest enriched within the differentially downregulated genes.

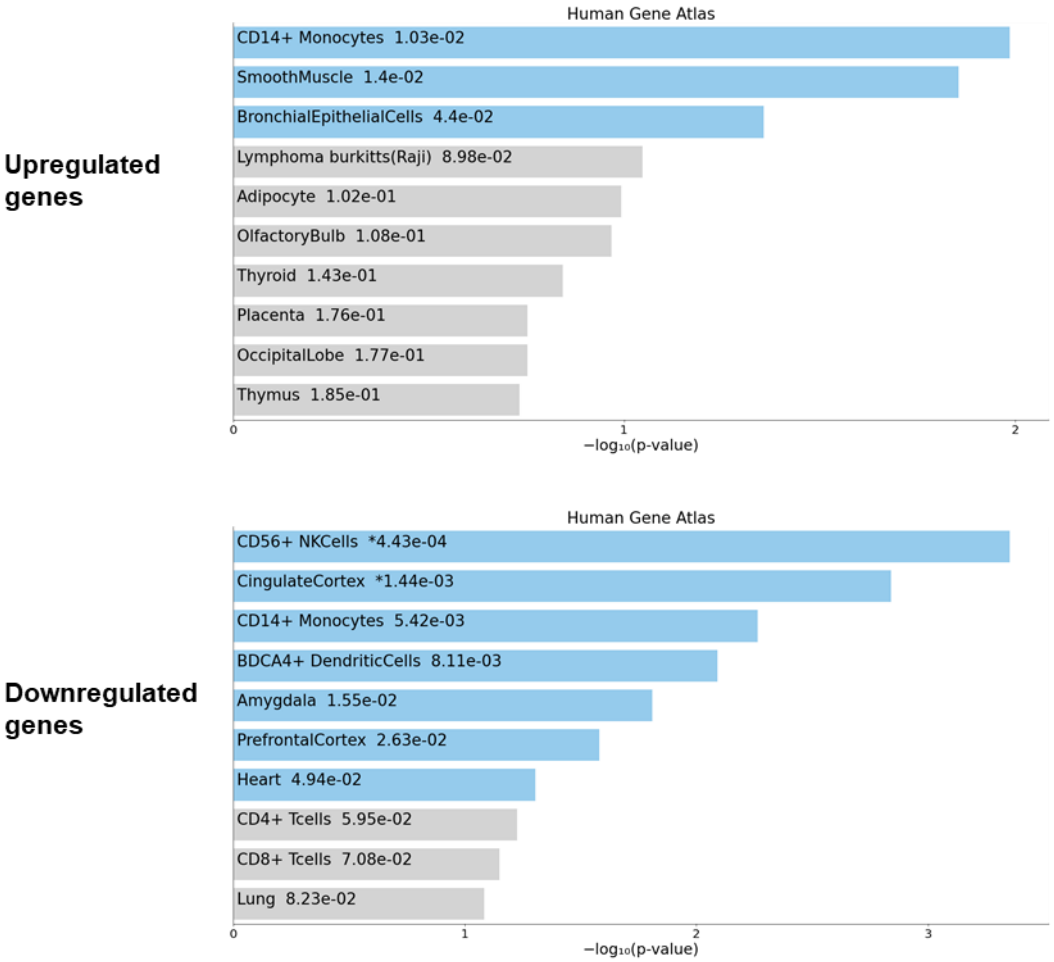

Figure 4-42: EnrichR analysis of enriched cell type specific gene signatures in genes up- and downregulated by lactic acid. *Gene sets derived from the analysis shown in Figure 4-41 were subjected to an EnrichR analysis. Shown are the Top10 hits from the human gene atlas enriched in the genes up- and downregulated by lactic acid. Digits give the respective p values.*

We used the KEGG 2021 database and EnrichR to screen for enriched signaling pathways within the genes up- and downregulated by lactic acid treatment (Figure 4-43). The pathway *Th17 differentiation* was enriched in both data sets, suggesting an interference of lactic acid treatment with this pathway. The *pentose phosphate pathway* (PPP), which is important for redox homeostasis, was enriched in the upregulated gene set, which suggests that lactic acid resistant cells might compensate the redox stress induced by acidification via an increased NADPH generation following PPP activity. Interestingly, also the *JAK-STAT pathway* enriched in the upregulated by lactic acid treatment gene set. This pathway is one of the central

pathways in T cell activation and differentiation. It regulates a wide variety of cellular processes, including metabolic pathways. This suggests a link between the lactic acid resistance of T cells and an adapted cellular metabolism.

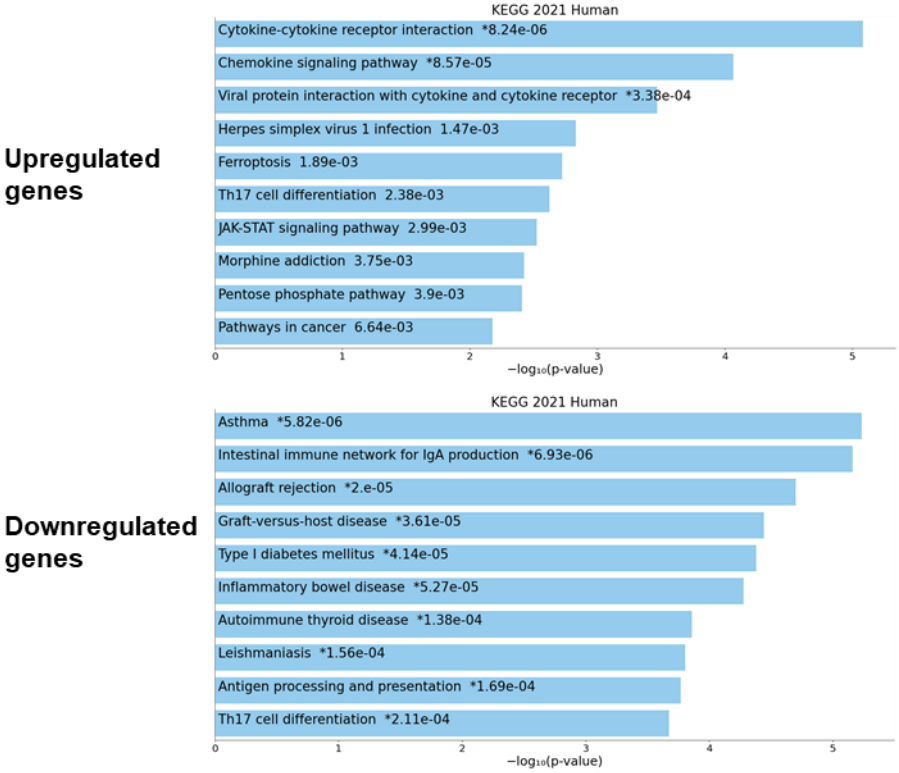

Figure 4-43: EnrichR analysis of enriched pathways in genes up- and downregulated by lactic acid. *Gene sets derived from the analysis shown in Figure 4-41 were subjected to an EnrichR analysis. Shown are the Top10 hits from KEGG 2021 enriched in the genes up- and downregulated by lactic acid. Digits give the respective p values.*

The RNAseq approach showed, that lactic acid treatment causes major changes on the transcriptional level of T cells. More and deeper studies are required to find similarities between myeloid cells and resistant T cells, identify resistance mediators and therefore new targets to enhance the T cell fitness for cell transfer therapy.

5. Discussion

5.1. Increasing the lactic acid resistance of T cells

Besides an abnormal and accelerated cell division and the ability to form metastases, a dysregulated cellular metabolism is one of the most important functional characteristics of cancer cells. Among different known metabolic alterations in cancer cells, the Warburg effect, representing the shift from an oxidative to a glycolytic metabolism in cells, is found in the majority of human tumors. It goes along with an enhanced glucose consumption and increased secretion of lactate and protons, accumulating in the tumor environment as lactic acid. Several studies have shown a link between an enhanced glycolytic metabolism, high intra-tumoral lactate levels and a worse anti-tumor immune response, associated with a poor overall survival (Cascone et al., 2018; Liu et al., 2018; Liu et al., 2021; Ottensmeier et al., 2016; Singer et al., 2011; Walenta and Mueller-Klieser, 2004). Therefore, metabolic characteristics of tumor cells and their influence on invading immune cells have aroused more interest in the past years.

The adoptive transfer of (modified) T cells (ACT) is an emerging anti-cancer strategy already applied in treatment of leukemic diseases (Mullard, 2021), however, the response rates in treatment of solid tumors are still low. Cascone and colleagues have demonstrated a negative correlation between the expression of glycolytic genes in melanoma and patients response to ACT (Cascone et al., 2018). They explained their findings by the fact that high glycolytic activity inhibits the development of effector functions of T cells as anti-glycolytic treatment enhanced ACT. This is in line with *in vitro* data showing that T cells and NK cells are suppressed by lactic acid and higher concentrations lactic acid even lead to cell death (Brand et al., 2016; Fischer et al., 2007; Haas et al., 2015; Mendler et al., 2012). Consequently, it stands to reason to enhance the fitness of T cells towards lactic acid to help them coping with the toxic tumor environment.

5.1.1. Lactic acid and T cells: A fatal combination

In the past years, it has become clear that lactate and protons (lactic acid) secreted by glycolytic tumor cells are not only a ‘waste product’ but rather have dramatic effects on invading immune cells within the tumor environment. The negative impact of lactic acid on CD8 T cells and NK cells has been demonstrated by us and others in both human and murine CD8 T cells (Brand et al., 2016; Fischer et al., 2007; Husain et al., 2013; Mendler et al., 2012). Data regarding the inhibitory function of lactic acid on CD4 T cells are also limited. Analyzing murine CD4 T cells, it was shown that treatment with increasing concentrations of sodium lactate or lactic acid inhibited their proliferation (Angelin et al., 2017; Quinn et al., 2020). Regarding

human CD4 T cells, Haas and colleagues analyzed the influence of lactic acid on human CD4 T cells with regards to its role in rheumatoid arthritis and found that lactic acid treatment inhibited the migration of CD4 T cells (Haas et al., 2015). Moreover, they have shown that treatment of CD4 T cells with sodium lactate leads to an altered cytokine secretion profile shifting the cells towards a Th17 phenotype, a finding confirmed by others (Pucino et al., 2019).

To characterize the effects of lactic acid on CD4 T cells more precisely, in a first step viability and functionality of lactic acid treated human CD4 T cells were analyzed. Similar as already demonstrated for human and murine CD8 T cells (Brand et al., 2016; Fischer et al., 2007), treatment with 20 mM lactic acid was lethal for human CD4 T cells. Both proliferation and cytokine secretion of CD4 T cells were decreased by 10 mM and 15 mM lactic acid treatment in a dose dependent manner. In line, the upregulation of the activation marker CD25 was severely diminished by 15 mM lactic acid treatment. Interestingly, treatment with 10 mM lactic acid increased the CD25 expression. This could be a hint for a possible compensation mechanism, in which T cells upregulate CD25, the α-chain of the IL-2 receptor, to increase their endogenous IL-2 signaling and compensate for the functional limitation by lactic acid.

Naturally, the accumulation of lactic acid is associated with accumulation of protons and consequently with a lowered pH. MCTs, which are responsible for the transport of lactate, are proton dependent and therefore contemporaneously transport both lactate and protons. MCT-1 and MCT-4 are upregulated during T cell activation (Renner et al., 2015; Renner et al., 2019) and can therefore be considered as the main ‘entry port’ for lactate into T cells under acidic conditions. Sodium lactate is transported by sodium coupled monocarboxylate transporters (SLC5A8 and SLC5A12), of which only SLC5A12 was shown to be expressed in both human and murine T cells (Haas et al., 2015; Pucino et al., 2019). However, publicly available data sets suggest a higher RNA expression of the proton-coupled transporters in human T cells, and SLC5A12 is considered to be expressed on a lower level (Uhlen et al., 2019).

In the literature, conflicting results were reported regarding the role of the acidification for the lactic acid effects on T cells. Whilst some authors report an inhibition of T cell functions by sodium lactate (Angelin et al., 2017; Haas et al., 2015), others have reported conflicting results stating that only lactic acid but not sodium lactate has suppressive effects on T cells (Brand et al., 2016; Fischer et al., 2007; Quinn et al., 2020).

The low pH itself is a major inhibitor of T cell function and the anti-tumor response. Different reports state that a low environmental pH leads to intracellular acidification (Pilon-Thomas et al., 2016) and suppresses T cell functions (Calcinotto et al., 2012; Zhang et al., 2019). It has been reported that T cells build up an acidic environment in lymph nodes repressing their own effector functions and preventing over-activation (Wu et al., 2020). In this study, acidic compartments in the lymph nodes showed a pH of 6.3 to 6.7, corresponding to the pH achieved

by treatment with 10 mM and 15 mM lactic acid, respectively. This suggests that the pH sensitivity of T cells could have a physiological background taking a turn for the worse in the pathophysiological situation in the tumor environment.

We treated T cells with increasing concentrations of lactic acid while cultivating them in normal RPMI or RPMI with a higher buffering capacity. In freshly buffered RPMI, the effects of lactic acid were mitigated in relation to the achieved pH increase. For example, treatment with 20 mM lactic acid in buffered RPMI led to a decrease in pH similar to the treatment with 15 mM in normal RPMI, thus reverting the lethal effect of the high lactic acid dose and leading to a similar degree of effector function repression as treatment with 15 mM lactic acid in standard RPMI. Our results are in accordance with a report by Uhl et al., who showed that lactic acid derived by acute myeloid leukemia (AML) cells hampers the T cell metabolism and inhibits their effector functions, which could be reverted by sodium bicarbonate addition (Uhl et al., 2020). This underlines the strong pH dependency of the lactic acid inhibitory effects and suggests that the pH regulatory system of both tumor cells and immune cells could be a target to enhance the lactic acid resistance of T cells within ACT. In line, it has been shown that treatment of tumor bearing mice with oral bicarbonate administration or the proton pump inhibitor esomeprazole increases the intra-tumorous pH and thereby as well the anti-tumor response (Pilon-Thomas et al., 2016; Zeng et al., 2016) and enhances the graft-vs-leukemia effect in a model of murine AML (Uhl et al., 2020), giving *in vivo* evidence for the crucial role of the acidic tumor pH in immune evasion and underlining the relevance of the pH regulatory system as target for the modulation of the anti-tumor immune response.

The glucose and mitochondrial metabolism of T cells are tightly connected with their functional development. The availability of glucose fuels the proliferation of T cells, while only the combined inhibition of both glycolysis and oxidative phosphorylation (OXPHOS) activity blunts cytokine production of T cells (Renner et al., 2015). As the transport of lactate via MCTs is gradient dependent, high extracellular lactate levels block its export, and even lead to lactate and proton import into T cells. This has two main consequences: First, the accumulation of lactate in the cells, and second, the acidification of the T cell cytoplasm, interfering with different aspects of T cell function and metabolism as the enzymatic function of several enzymes is pH-dependent (Even et al., 2003; Halperin et al., 1969; van Leemputte et al., 2020).

Extra- and intracellular acidification were reported to increase the ROS production of T cells and induce a hyperpolarization of the mitochondrial membrane potential in HEK293T cells (Teixeira et al., 2018), thereby interfering the respiratory chain activity and the mitochondrial ATP production. Mitochondrial dysfunction and increased oxidative stress is associated with immune dysfunction in HIV patients (Younes et al., 2018) and we have recently demonstrated a key role of high cellular ROS levels and metabolic imbalance in T cell dysfunction of patients

suffering from severe COVID-19 (Siska et al., 2021). Furthermore, it has been demonstrated that lactic acid derived by AML cells causes a metabolic unfitness of human CD8 T cells (Uhl et al., 2020). This is in accordance with our experiments showing that the respiration of CD4 T cells is blocked by lactic acid in a dose dependent manner, explaining in part the reduced cytokine production of lactic acid treated T cells. Increasing the pH of the culture medium partially mitigated the effects of lactic acid on the mitochondrial respiration, thereby underlining the role of the acidic pH. The decreased mitochondrial activity of T cells upon lactic acid treatment has some physiological relevance with regards to the anti-tumor immune response.

It has been proposed that independent of the acidic pH, lactate accumulation in the cytoplasm can shift the NAD:NADH ratio towards a more reduced state, thereby limiting the GAPDH forward reaction and glycolysis (Quinn et al., 2020) and impairing T cell proliferation. In our hands, treatment of T cells with lactic acid led to a reduced glucose consumption and impaired upregulation of LDHA, pointing to a reduced glycolytic activity of lactic acid treated T cells. As glucose availability is especially important for the proliferative capacity in human T cells, this could explain their reduced proliferation upon lactic acid treatment.

Different studies demonstrate that T cells isolated from human tumors display a decreased mitochondrial fitness (Siska et al., 2017; Zhang et al., 2017), which could also be related to the disturbed mitochondrial membrane potential due to acidification. What is more, it was shown that the decrease in response of CLL (chronic lymphatic leukemia) patients to CAR T cell therapy is related to degree of mitochondrial impairment of the infused CAR T cells (van Bruggen et al., 2019). This demonstrates that mitochondrial function is a determinant of T cell functionality in the tumor environment and suggests the cellular metabolism represents a potential target to increase the lactic acid resistance of T cells.

5.1.1. Metabolic manipulation of the culture conditions does not increase the lactic acid resistance of CD4 T cells

One way to increase the metabolic resistance of T cells used in ACT is to manipulate the culture conditions of T cells beforehand, thereby trying to prime the cellular metabolism to withstand the toxic conditions in the tumor environment. Different approaches involved changing the cytokines applied for expansion, manipulating the glucose concentration in the culture medium, or using drugs to manipulate the cell metabolism (Hermans et al., 2020; Klein Geltink et al., 2020). Up to now almost all studies have in common that they have been conducted using murine T cells, as most of them include syngeneic *in vivo* models. With respect to the differences in the cellular metabolism of murine and human T cells demonstrated in this work and in the published literature, we tested some of the published strategies with

regards to their effects on human T cell metabolism and whether the described strategies could increase lactic acid resistance.

5.1.1.1. Culture with IL-21 to increase cellular respiration

The cytokine IL-21 has pleiotropic effects on several immune cells and is considered to increase the anti-tumor response *in vivo*. It has been reported, that IL-21 increases the respiratory capacity of both human and murine CD8 T cells (Hermans et al., 2020; Loschinski et al., 2018) as demonstrated using the Seahorse approach. Moreover, compared to IL-2 cultivated cells the extracellular acidification rate was reduced upon IL-21 treatment, suggesting a metabolic shift towards a respiratory phenotype. However, in our investigation, we were not able to detect the described shifts in the cellular metabolism neither in human CD4 nor in human CD8 T cells. One explanation for these contradictory results could be the methods used for the detection of the metabolic changes. In both publications mentioned above, the major changes upon IL-21 treatment were detected in the spare respiratory capacity, which can be assessed during after FCCP treatment while measuring the oxygen consumption rate in the Seahorse system. As we were using the PreSens system, we measured the basic oxygen consumption, which was also not influenced by IL-21 in both publications. Nevertheless, we tested the lactic acid resistance of IL-21 cultured human T cells and found no difference to IL-2 cultured cells (data not shown).

5.1.1.2. Culture under glucose restriction does not increase lactic acid resistance

In the tumor microenvironment (TME), besides the accumulation of metabolites, T cells also compete with tumor cells and other stroma cells for available nutrients, including glucose (Chang et al., 2015; Ho et al., 2015; Leone and Powell, 2020). It is controversially discussed whether glucose restriction itself leads to impaired T cell functionality and murine T cells seem to be more dependent on glucose supply than human T cells. Upon activation, T cells upregulate glycolysis and develop a Warburg phenotype. Under glucose starvation, T cells are expected to upregulate their oxidative metabolism to compensate for the lack of substrate for glycolysis. Therefore, we hypothesized that upon glucose starvation, when T cells are forced to shut down glycolysis and lactate production, the metabolic blockade by lactic acid would be mitigated.

Surprisingly, glucose restriction did not increase cellular respiration and the LDH isoenzyme profile of the T cells. Regardless of glucose availability, treatment with 15 mM lactic acid still prevented upregulation of LDHA and the shift to LDH-5, both markers for high glycolytic

activity, and led to a complete block in cellular respiration, accompanied by inhibition in effector cytokine secretion

Based on these results, glucose restriction during lactic acid treatment does not increase the lactic acid resistance of T cells.

5.1.1.3. LDH inhibition as pharmacological way to increase respiration, but not lactic acid resistance

A pharmacological way to enhance the T cell resistance towards lactic acid would have several advantages. At first, administration before the therapy during T cell expansion would be very easy. Second, using orally available therapeutics would offer the possibility to not only treat T cells in culture before ACT but as well using it during and after ACT as co-treatment. By this, one could try to simultaneously harm tumor cells while fitting T cells for the challenges in the TME. A possible substance class, that could match this profile are LDH inhibitors. Angelin et al. already demonstrated *in vitro*, that treatment with an LDH inhibitor can rescue murine T cells from sodium lactate induced inhibition (Angelin et al., 2017) and Hermans and colleagues showed that the simultaneous application of IL-21 and LDH inhibition during murine T cell culture before ACT enhanced the efficacy of the anti-tumor response after T cell transfer (Hermans et al., 2020).

To date, no specific LDHA inhibitor has been developed, but most commercially available inhibitors have a higher affinity for LDHA than for LDHB. Tumor cells often rely on aerobic glycolysis, therefore, treatment with an LDH inhibitor would severely influence the tumor cell metabolism, thereby on the one hand restricting their ATP production and on the other hand limiting their lactic acid production mitigating the toxic effects within the TME. A similar approach using the MCT inhibitor diclofenac has already been published by our group (Renner et al., 2019).

On the other hand, the systemic application of metabolic inhibitors would also target the invading immune cells. This could have both positive and negative consequences. On the one hand, activated T cells rely on aerobic glycolysis to fuel their proliferative capacity (Renner et al., 2015), which could be blunted by LDH inhibition, leading to a hampered clonal expansion. On the other hand, the application of LDH inhibitors targeting LDHA over LDHB could shift the LDH activity in a direction favoring OXPHOS, thereby increasing T cell respiration. By this, imported lactate could fuel the TCA cycle thereby resolving the metabolic blockade. As some reports state, that the mitochondrial activity is crucial for the development of effector cytokines, this could help the T cells start a cytokine response despite the presence of lactic acid.

To elucidate whether LDH inhibition could pose a way to increase the lactic acid resistance of T cells, we treated T cells with the commercially available LDH inhibitor R-(+)-GNE-140 and measured cell respiration, proliferation, and lactate secretion. In primary activated human CD4 T cells, the treatment with a high dose of R-(+)-GNE-140 led to a remarkable increase in the respiratory activity, whilst lactate secretion was only slightly diminished by this treatment. This suggests that T cells can flexible modulate their cell metabolism to compensate for the inhibited aerobic glycolysis, as already described by our group earlier (Renner et al., 2015). The increased respiratory activity could indeed help the T cells to resist at least lower lactic acid concentrations, but more investigations are needed to address this question. Notably, the concentration of the LDH inhibitor necessary to achieve this effect was three times as high as the concentration leading to a significant reduction of lactate secretion in tumor cells (Boudreau et al., 2016; Ždralević et al., 2018). This indicates that LDH inhibition indeed seems to preferably target tumor cells over T cells and therefore might pose a valuable anti-tumor treatment.

Currently, different LDH inhibitors are under development. The overall goal is to increase the affinity for LDHA to reduce side effects and decrease the concentration necessary for LDH inhibition. Treatment with R-(+)-GNE-140 altered T cell lactate secretion only at high concentrations (30 µM). Therefore, we compared how treatment with NCI-737, another LDH inhibitor, would affect T cell metabolism. Intriguingly, NCI-737 reduced lactate secretion at lower concentrations (1 µM) than R-(+)-GNE-140 but did not increase respiratory activity. An increase in oxygen consumption was only observed when T cells were additionally treated with 10 mM lactic acid. This indicates that lactate is converted to pyruvate by LDH even in the presence of an LDH inhibitor. Most likely both LDH inhibitors have a preference for LDHA and still allow LDHB to convert lactate to pyruvate. However, 15 mM lactic acid still led to a complete block in mitochondrial respiration, indicating no increased lactic acid resistance of LDH inhibitor treated T cells.

5.1.2. Modification of the LDH isoenzyme profile as an approach to increase metabolic T cell resistance

The genetic modification of T cells before ACT with the overall goal to enhance their anti-tumor efficacy is already applied in the clinics in terms of CAR (chimeric antigen receptor) T cell therapy (Rad S M et al., 2021). Furthermore, metabolic manipulation of immune cells by genetic modification can enhance the anti-tumor efficacy of transferred T cells in murine tumor models and many of those attempts targeted the glucose and mitochondrial metabolism of the investigated cells. Scharping and colleagues demonstrated that overexpression of Pgc1a in murine T cells leads to enhanced mitochondrial biogenesis associated with an increased

survival of tumor-bearing mice after ACT (Scharping et al., 2016). Aside, it was demonstrated that the deletion of Hif1a in T cells before transfer leads to an enhanced FAO activity and increases the anti-tumor activity of T cells (Zhang et al., 2017). Notably, HIF1a also upregulates the expression of key glycolytic enzymes, including LDHA. Therefore, it can be presumed that the deletion of HIF1a could have had a similar effect as we aimed by directly manipulating the balance between LDHA and LDHB.

The approach tested here was to equip T cells with an LDH enzyme pattern allowing them to metabolize lactate taken up in the tumor environment, which otherwise would have toxic effects on T cells. This was achieved by on the one hand inducing a knockdown of LDHA and on the other hand overexpressing LDHB, both shifting the LDH isoenzyme pattern towards a pattern with higher lactate metabolizing activity.

First, we attempted to shift the LDH isoenzyme pattern by a transient knockdown of LDHA in human unstimulated T cells. This did not induce a shift of the LDH isoenzyme pattern in direction of LDHB but rather prevented the upregulation of LDHA upon stimulation.

Analyzing the effects of the LDHA knockdown on the cellular metabolism and the functionality of T cells, we saw that neither the metabolic activity nor the T cell functions were affected by the blocked LDHA upregulation, and lactate secretion was not affected. These results suggest that LDHB is taking over the tasks of LDHA in regards of lactate production. It has been demonstrated in different murine and human tumor cell lines, that only a deletion of both LDHA and LDHB completely abrogates lactate secretion of tumor cells (Di Zhang et al., 2019; Mack et al., 2017; Ždralević et al., 2018) and that Aurora A mediated phosphorylation of LDHB enhances their glycolytic activity (Cheng et al., 2019). However, our results are contradictory to other studies suggesting a crucial role for Ldha expression in the cytokine production of T

cells. Working with $Ldha^{-/-}$ T cells, Peng and colleagues showed that Ldha activates the transcription of Ifn-γ by an epigenetic mechanism, leading to significantly lower Ifn-γ production of the LDHA-lacking cells (Peng et al., 2016). Moreover, they demonstrated that due to the decreased Ifn-γ secretion $Ldha^{-/-}$ cells fail to clear an infection with *L. monocytogenes* (Xu et al., 2021). In our hands, LDHA was not determining the production of IFN-γ and lactate. Of note, the studies of the group around Peng were carried out using murine T cells. Therefore, the observed differences are most likely based on metabolic differences between murine and human T cells. We show here that the LDH isoenzym pattern is completely different in mice and men. Mice have a much stronger expression of the Ldh-5 enzyme which indicates a stronger dependance on Ldha. In line, LDH inhibition had a stronger impact on murine T cell lactate secretion and cytokine response. As $LDHA^{low}$ human T cells still have the capacity to perform glycolysis on a normal level, it was no surprise that lactic acid treatment of $LDHA^{low}$ T cells still impaired cytokine secretion.

The other approach used in this work to induce a shift towards better lactate metabolism was the overexpression of LDHB in human T cells, which was conducted in activated CD4 T cells. Here, the LDH isoenzyme analysis revealed a clear shift in the LDH isoenzyme patter towards more LDHB containing isoforms of the LDH.

Beyond its role as end product of glycolysis, lactate itself can serve as substrate for TCA. In fasted mice, available glucose is converted to lactate, which is turn shared by tissues all across the body to main TCA activity (Hui et al., 2017), thereby decoupling glycolysis from ATP production. Lactate has even been suggested as “universal fuel” for cellular metabolism, whilst glucose could be a more restricted, cell-type specific fuel (Rabinowitz and Enerbäck, 2020). In this context, it is important to note that most tissue culture media implement high glucose concentrations as carbon source for cultivated cells, whilst lactate is not included in the formula, which could influence the metabolism of cultured cells in a drastic manner.

A shift of the metabolic preferences towards lactate instead of glucose consumption has been reported as a feature of murine Treg, and is also considered a possible mechanism allowing Treg to better adapt to the TME (Angelin et al., 2017; Watson et al., 2021). Moreover, it has been shown in murine CD4 T cells that the activity of the respiratory chain determined the cytokine responses (Bailis et al., 2019). This raised the possibility that overexpression of LDHB and manipulating cell metabolism could change the differentiation of CD4 T cells and induce a regulatory phenotype. However, the frequency of Treg among the CD4 T cells was not changed by LDHB overexpression, neither in human nor in murine T cells. In addition, the cytokine profile of the human LDHB overexpressing cells was not altered, demonstrating that the differentiation of CD4 T cells was not affected by LDHB overexpression.

Analyzing lactate secretion and the expression of important lactate transporters indicated that LDHB overexpression did not lead to an altered glucose metabolism of T cells. In line, glucose tracing analysis revealed no significant changes after 6 hours.

The most pronounced effect of LDHB overexpression was observed on oxygen consumption upon lactic acid treatment. LDHB overexpressing cells showed an increased respiration directly after addition of 10-15 mM lactic acid, whereas lactic acid treatment suppressed respiration in T cells with normal LDHB expression. The increased respiration did not go along with an increased mitochondrial load of the LDHB overexpressing cells, suggesting a higher mitochondrial activity induced by LDHB overexpression and lactic acid treatment.

Notably, lactic acid treatment did not suppress glucose metabolism to pyruvate, but diminished pyruvate metabolism into lactate and TCA metabolites. This is consistent with our findings in primary stimulated T cells indicating a blockade of both glycolytic activity, mediated by block of the pyruvate reduction, and mitochondrial respiration. Importantly, both involved enzymes,

LDH and pyruvate dehydrogenase (PDH) have a pH optimum around 7.5, explaining their reduced activity upon lactic acid incubation, which causes a drop in intracellular pH below 7.0 (Gay et al., 1968; Pawelczyk and Olson, 1992). Surprisingly, also in the lactic acid metabolic tracing analysis we could not detect substantial changes in the 13C enrichment in TCA metabolites. This could be a consequence of the short observation time. It is possible, that the increased respiration of LDHB cells is caused by increased lactate uptake, which was observed by trend during the 6 h incubation time. After 24 h, this difference was only visible in one of two analyzed donors. Of note, this was congruent with the respiratory profiles, which only showed increased respiratory activity of the donor displaying higher labeled lactate enrichment after 24 h. However, increased respiratory activity of LDHB overexpressing cells could be a consequence from increased glutaminolysis or fatty acid oxidation (Goetzman and Prochownik, 2018). More studies are necessary to elucidate the origin of increased cellular respiration of LDHB cells.

Interestingly, we found by trend an enrichment in m + 3 TCA metabolites. This could either originate from pyruvate metabolism via pyruvate carboxylase (PC) or also through TCA activity when cells can generate unlabeled pyruvate from either lactate or glucose. In the context of lactic acid, this could indicate, that LDHB overexpressing cells might experience a “pyruvate overload” due to increased lactate turnover and upregulate pyruvate carboxylation.

According to published data (Uhlen et al., 2019), pyruvate carboxylase is highest expressed in liver and adipose tissue and is of major importance in the gluconeogenesis (Groen et al., 1986). Cappel and colleagues have shown using PC knockout mice, that PC activity replenishes TCA intermediates in liver and thereby is essential for NAD regeneration (Cappel et al., 2019), which could in turn be used to further fuel glycolysis. Therefore, it would be interesting to study PC expression in LDHB overexpressing T cells in comparison to control cells. However, further analyses are necessary to confirm lactate metabolism by pyruvate carboxylase in T cells and elucidate its interplay with LDHB. These analyses should also involve studies using lactic acid with selectively labeled 13C atoms and focus on labeling of aspartate, which is a known derivative of PC metabolism (Sellers et al., 2015).

Treating LDHB overexpressing cells with lactic acid, we found a higher percentage of cytokine expressing cells among the cells with enhanced LDHB expression compared to those with normal LDHB levels. However, increased intracellular cytokine expression was not reflected by an increased cytokine secretion. This could be reasoned in the acidification of the culture medium by lactic acid. The trafficking of vesicles from the Golgi system to the cell surface and their exocytosis is strongly pH dependent and inhibited by cytosolic acidification (Cosson et al., 1989; Sandvig et al., 1987). Consequently, if the intracellular pH is not increased by LDHB overexpression, the increased intracellular expression of cytokines will not automatically result

in a higher cytokine secretion. In line, when buffering the extracellular pH, we could detect slightly increased cytokine levels in the supernatants of lactic acid treated LDHB overexpressing cells.

Overexpression of Ldhb in murine T cells failed to upregulate respiration or cytokine expression upon lactic acid treatment excluding classical murine tumor models to test the *in vivo* activity of LDHB overexpressing T cells. Therefore, to further test the effects of LDHB overexpression in a physiological model we decided to use spheroid co-culture experiments. Spheroid co-culture experiments using HCT116 spheroids revealed that in two out of three analyzed donors LDHB overexpressing cells preferentially migrated into spheroids and showed higher expression of cytotoxic effector molecules within the spheroids. This suggests, that LDHB overexpression in T cells could be beneficial for their anti-tumor activity and probably improve outcome of ACT treatment approaches. However, this model is based on an allogeneic immune response, which is not entirely reflecting the in-patient situation. Therefore, it would be important to use patient-derived tumor cell lines and T cells to perform spheroid co-culture experiments. Overall, LDHB overexpression seems to represent a promising approach to increase the metabolic fitness of T cells for ACT but might have to be accompanied by additional modifications.

5.1.3. Learning lessons – how immune cells deal with lactic acid

5.1.3.1. How macrophages survive in environments with high lactic acid levels

The sensitivity of immune cells towards lactic acid is different. Whilst T cells and NK cells are affected in both functionality and viability, cells of myeloid origin as dendritic cells and monocytes seem to be more resistant and survive also high lactic acid concentrations (Dietl et al., 2010; Gottfried et al., 2006). As demonstrated in this work, macrophages also survive the treatment with high concentrations of lactic acid. Nevertheless, this lactic acid resistance seems to be donor dependent as in a few donors cells did not survive the lactic acid treatment.

Analysis of the intracellular pH revealed that macrophages are less acidic after lactic acid exposure than T cells. Therefore, we hypothesized that the higher resistance of myeloid cells would be grounded in differences in the pH regulatory system of the cells.

To identify potential target genes related to the higher lactic acid resistance we screened the expression of selected pH-regulatory genes in T cells and myeloid cells using qRT-PCR. In addition, we included natural Treg to this analysis, as it has been reported that they also are more resistant to low-dose lactic acid treatment (Watson et al., 2021). In a general overview, this analysis revealed that indeed macrophages and monocytes as cells from the myeloid lineages express much higher levels of the analyzed pH-regulatory genes compared to T cells.

Surprisingly, this was not true for Treg, suggesting that the lactate resistance of those cells is mainly mediated by an adapted metabolic program and not by their pH regulatory system. However, as most of the studies up to now did not use lactic acid but analyzed the impact of sodium lactate on Treg or used lactic acid in low concentrations not affecting cell viability, it is still not completely clear whether Treg can survive low pH values.

To elucidate more precisely, which part of the pH regulatory system is mediating the lactic acid resistance of macrophages, we applied inhibitors targeting different proteins and protein classes involved in pH regulation and analyzed if this abrogated the lactic acid resistance of macrophages. The obtained results were to a large extent heterogeneous and revealed a high donor dependency of this phenomenon. In most cases, the treatment with a single inhibitor did not completely sensitize the macrophages to lactic acid treatment.

The pH regulatory system of cells is of major importance for their survival even under normal conditions. Because of this, it does not rely on the functionality of one transporter or enzyme class, but rather represents a complex network of connected and cooperating proteins. This is especially well characterized in tumor cells, where the regulation of the intracellular pH is of special importance and even suggested as a potential anti-tumor target (Parks and Pouysségur, 2017; Piasentin et al., 2020). Therefore, it very likely that it is necessary to target several pH regulatory enzymes in parallel to overcome the lactic acid resistance of macrophages.

In our screening approach, we only identified two drugs leading to a complete sensitization of macrophages with a single treatment: Diclofenac and aspirin. Diclofenac, which was described as an MCT inhibitor recently (Renner et al., 2019), was originally developed as a non-steroidal anti-inflammatory drug acting as an inhibitor of cyclooxygenase 1 and 2 (COX-1 and COX-2). Aspirin also acts as a COX inhibitor but does not inhibit lactate secretion or uptake by MCTs. Therefore, the sensitizing of macrophages towards lactic acid cannot be mediated by MCT blockade. Surprisingly, ketoprofen, another COX inhibitor, did not induce macrophage dead upon lactic acid treatment, suggesting that a different mechanism apart from COX inhibition is involved here.

An obscure side effect of NSAIDs is the interference with the intracellular calcium signaling. Ca^{2+} is a versatile intracellular second messenger regulating several cell processes, including cell activation and apoptosis. It has been shown that both diclofenac and high doses aspirin cause an elevation of the intracellular calcium levels when applied to similar concentrations as used in this work (Suzuki et al., 2010; Tanaka et al., 2005). In contrast, according to Tanaka, for ketoprofen the dose required to induce an increase in the cytosolic calcium levels are much higher than those applied here (Tanaka et al., 2005), which would explain that ketoprofen treatment had no impact on macrophage survival. More investigations are needed to confirm

a possible role of Ca^{2+} in regulating cell death upon lactic acid treatment. As Ca^{2+} is a very important messenger in activated lactic acid-susceptible T cells, a link between Ca^{2+} regulation and sensitivity towards lactic acid seems possible.

5.1.3.2. Are T cells themselves the answer?

The response of T cells to lactic acid seems very homogenous at first sight, but taking a closer look, it gets obvious that also here we find differences between different donors and even within one T cell population. Analyzing the bulk T cell population, 15 mM lactic acid leads to a dramatically reduced proliferative capacity and decreased effector functions but using CFSE and flow cytometry it is possible to distinguish T cells that are completely blocked in their proliferation, and another T cell population that still undergoes cell divisions. This raised the question whether the key to restored T cell functions upon lactic acid treatment could be uncovered in this T cell population showing a naturally higher resistance.

Different studies have reported a better response to ACT when specific T cell subsets were transferred. In mice, the transfer of less differentiated naïve, central memory or stem-cell like memory T cells have led to a longer persistence and proliferative capacity of the transferred T cells and enhanced tumor control compared to more differentiated effector and effector memory T cells (Gattinoni et al., 2005; Gattinoni et al., 2009; Klebanoff et al., 2004; Lugli et al., 2013; Sukumar et al., 2013). This could be partially due to a higher ability to withstand the metabolic conditions in the TME. Therefore, we tested whether the distinct memory subsets would differ in their sensitivity towards lactic acid treatment.

We sorted CD4 T cells in naïve, central and effector memory T cells and challenged them with different concentrations of lactic acid. An analysis of the survival probability of the sorted T cells revealed no higher resistance of one T cell subset towards high levels of lactic acid treatment. Yet, one donor was resistant towards lactic acid treatment for 72 h. After 6 d, this resistance was only maintained in EM T cells. Regarding cytokine secretion, effector memory cells seemed slightly more resistant that Tcm and naïve cells when treated with 15 mM lactic acid. Altogether, a clear trend towards a higher resistance of one of the analyzed T cell subsets was not observed in our experiments.

Interestingly, independent of the analyzed subset treatment with 10 mM lactic acid led to a higher cytokine secretion and increased respiration in some the analyzed donors, indicating that lactic acid can serve as a substrate for mitochondrial metabolism and can even sometimes be beneficial. It has been shown that L-lactate can serve as carbon source for TCA cycle activity in human lung tumors (Faubert et al., 2017) and both tumor and healthy tissue in fasted mice (Hui et al., 2017), consistent with the increased respiration of low-dose lactic acid treated

human T cells. In line with the observed increase in cytokine secretion, Wen and colleagues have shown that treatment with high concentrations of sodium lactate increases the cytokine production of T cells *in vitro*. Moreover, injection of tumor bearing mice with sodium lactate leads to better tumor control (Wen et al., 2021), suggesting a link between the increased TCA cycle activity and higher effector functions and underlining the importance of T cell metabolism for T cell functionality. As the uptake of lactate by MCTs is proton dependent, it is likely that the administered lactic acid is taken up more efficiently than sodium lactate and the reported beneficial effect on cytokine secretion and metabolism is achieved at much lower doses.

To gain deeper insights into the factors distinguishing cells with higher lactic acid resistance from those sensitive towards lactic acid we labeled T cells with CFSE, treated them with lactic acid and after one week flow cytometrically sorted for the proliferating and non-proliferating cells according to the CFSE signal.

Hypothesizing that T cells proliferating in the presence of lactic acid might upregulate the necessary genes and pathways to resist lactic acid, we compared proliferating cells with and without lactic acid treatment. We found 376 upregulated genes forming 7 different clusters. Of note, *IL2RA*, encoding for CD25, was one of the differentially regulated genes, in line with the observed upregulation after low dose lactic acid treatment as discussed above. Interestingly, a KEGG enrichment analysis of the upregulated gene revealed an overlap with genes known to be involved in Th17 regulation, in line with reports suggesting a polarization of CD4 T cells towards a Th17 phenotype by lactate treatment (Haas et al., 2015; Pucino et al., 2019). Moreover, the gene signature for pentose phosphate pathway was enriched. This pathway metabolizes glucose to generate NADPH, which is known to be essential for maintenance of cellular redox balance (Ju et al., 2020). As described above, too high ROS levels are detrimental for T cells function, and lactic acid treatment disturbs NADH redox balance and may induce ROS accumulation. Therefore, upregulating pentose phosphate pathway activity could be a compensatory strategy used by T cells upon lactic acid treatment.

Surprisingly, within the genes upregulated by lactic acid treatment in proliferating cells, signature genes of CD14 expressing monocytes were highly enriched. Monocytes belong to the cell types surviving in high lactic acid concentrations (Dietl et al., 2010). On the other side, within the downregulated genes signature genes of NK cells, which are lactic acid sensitive (Brand et al., 2016; Husain et al., 2013) were enriched. Therefore, the susceptibility or resistance of cells towards lactic acid seems to be reflected on a transcriptional level supporting our “learning from macrophages” approach.

5.2. Challenging animal models – Metabolic differences between murine and human T cells

Animal models, especially mice models, are of importance for the development and approval of novel therapeutics, although such studies do not always reflect the in-patient situation due to significant inter-species differences. Nevertheless, in the field of immunometabolism, publications and projects mainly focus on murine T cells and a systematic comparison between the human and murine T cell metabolism has not been performed so far to our knowledge. As the T cell metabolism is of critical importance for the T cell function and therefore for their reaction in the tumor environment, we compared mitochondrial and glycolytic metabolism of human and murine T cells after *in vitro* activation and found major differences between T cells of the different species and minor differences between the analyzed mouse strains.

The regulation of mitochondrial content and glucose uptake was opposite in human and murine cells regardless of the subset analyzed. Quiescent murine T cells showed a higher glucose uptake, but lower mitochondrial content compared to human T cells. Upon stimulation glucose uptake was maintained but mitochondrial content increased in murine T cells, whereas in human T cell populations glucose uptake was significantly elevated but only a slight increase in mitochondrial content was detected. After 72 h of stimulation mitochondrial content was comparable between the species, however glucose uptake was significantly higher in human T cells. Notably, murine T cells start to proliferate already after 24 h whereas human T cells enter the clonal expansion phase beyond 48 h. This might explain the distinct kinetics in glycolysis, as glucose is indispensable for proliferation.

Furthermore, we observed increased basic respiratory activity, respiration related to ATP production and maximum capacity in murine and human T cells upon stimulation, however, more pronounced in human T cell populations. Moreover, human T cells showed an increase in respiratory parameters over the whole observation period, whereas murine T cells displayed maximum respiratory activity after 24 h of stimulation and no further increase or even a decline were observed beyond. As in human T cells the elevated cellular respiration was not accompanied by a significant increase in mitochondrial content, we hypothesized that metabolic fluxes are altered, and the TCA might be more active. Accordingly, human T cells displayed a strong increase in CS activity in the first 48 h of stimulation, in murine T cells CS activity was only increased by trend. However, we have to admit that between 24 h and 48 h of stimulation the size of human T cells is strongly increased, and as mitochondrial content is frequently related to cell size, CS activity might be also increased due to on-blast formation.

The activity of the citrate synthase, a rate-limiting enzyme of the TCA cycle and therefore a measure for mitochondrial activity, reflected the observed kinetics of the analyzed cell types very well and showed a similar regulation. Of note, citrate synthase activity is often used as a

measure for mitochdonrial content but did not match the results observed in the Mitotracker Green measurement. This could be caused by the different analysis time points. Mitotracker Green analysis was carried out after 72 h activation, whilst citrate synthase activity was assessed in a kinetics up to 48 h after initial activations. After 48 h of activation, the cells have not yet divided, but increase the number, length and tightness of the mitochondria cristae (Chao et al., 2017), where the citrate synthase is located, causing a strong increase in the TCA cycle activity and thereby also in the CS activity. More studies are necessary to shed additional lights on the regulation of the mitochondrial dynamics of T cells.

Our analysis revealed that mitochondrial content of murine T cells seems to be comparable to human T cells, but human T cells show higher respiratory activity. This could explain the failure of Ldhb overexpression in murine T cells. It is possible that the mitochondrial biology of human, but not murine T cells allows the increased respiration after Ldhb overexpression.

Strikingly, the most prominent difference between murine and human T cells was found regarding the LDH isoenzyme profile of the T cells. Human T cells express all five isoenzymes before and after activation, but the balance is shifted from a LDHB towards a LDHA based pattern in the course of stimulation, probably to meet the glycolytic demands for proliferation. In contrast, murine T cells express predominantly LDHA and express only little or none of the LDHB containing isoforms. These differences in the LDH isoenzyme distribution could prime the human and murine T cells towards different directions of the glucose flux: Murine T cells towards the production of lactate and probably fueling TCA activity by glutamine metabolism (Carr et al., 2010), human T cells towards a more balanced glucose metabolism of both TCA activity and lactate production.

The observed metabolic differences could be an explanation for discrepancies in the studies regarding the connection of T cell metabolism and function. A closer review of the literature regarding the interconnection of T cell metabolism and function reveals, that studies conducted with murine T cells reveal a glucose dependency of cytokine production, whereas in human T cells only proliferation, but not the cytokine secretion, seems to depend on glucose. Instead, in human T cells, early TCA cycle activity is of critical importance for the development of a cytokine response (Jones et al., 2017; Renner et al., 2015). Our direct comparison revealed a much higher respiratory activity and a higher respiratory reserve of human compared to murine T cells. Moreover, the LDH isoenzyme profile primes murine T cells to a more glycolytic metabolism but might open an alternative way for human T cells to fuel the TCA cycle with lactate as an alternative energy source. In line with the discrepancies observed regarding the glucose dependency of T cells, we also observed a different sensitivity towards LDH inhibition of murine and human T cells. Treatment with NCI-737, an LDH inhibitor targeting both LDHA and LDHB, significantly reduced lactate and cytokine secretion of murine T cells already at low

concentrations, whilst human T cells were less sensitive and affected only by higher concentrations. With regards to the already discussed possible compensation of LDHA by LDHB it is possible, that human T cells might compensate the LDH inhibition by their LDHB expression, whilst murine T cells don't have this option and are stronger affected by LDHi treatment. Accordingly, it has been shown in both murine and human tumor cell lines that the knockout of LDHA alone is not sufficient to completely abrogate the lactate production, indicating a compensatory role of LDHB for lactate production. Cheng and colleagues have reported that phosphorylation of LDHB by overexpressed Aurora-A protein kinase in cancer cells elevates the overall lactate production by the LDH (Cheng et al., 2019). Aurora-A is expressed in both murine and human T cells and has been reported to play an important role in mediating early signals during T cell activation after formation of the immunological synapse (Blas-Rus et al., 2016). Both suggested compensatory mechanisms rely on the expression of LDHB, therefore they would only work in human T cells and not in murine T cells.

To our knowledge, a systematic comparison of the carbon metabolism of murine and human T cells side by side has not yet been performed. Most studies focus either on the comparison of T cell subsets of either species or on one particular aspect of the T cell metabolism. The differences described in this work have major implications for the way, how animal models should be considered. The test of new therapeutic approaches in mice models has a long history and is justifiably an important part of the pre-clinical drug development. But ignoring the important inter-species differences when developing and transferring new strategies could have major implications for the experimental outcome. For example, testing LDH inhibitors in syngeneic mouse models could lead to a failure of this therapeutic approach, as murine T cells are more sensitive towards LDH inhibition, but could succeed in the human situation, as human T cells might still work under this therapy. The other way around, therapeutic approaches could seem promising in mice models, but completely fail in human patients. This dichotomy of on the one side need for animal models to develop and test new therapeutic options without endangering patients and on the other side having a problematic knowledge-transfer situation has led to the development of humanized mice. These are immunodeficient mice equipped with an human immune system and therefore are considered to be closer to the in-patient response, although also these models have limitations (Hahn et al., 2015). In addition, using co-culture models of tumor cell spheroids with human immune cells, as presented in this thesis, may represent a possible strategy. In conclusion, especially in the field of immunometabolism, one should carefully choose and test the model and question your results with respect to the species background.

5.3. Perspectives

The relevance of tumor metabolism for the immune escape is more and more accepted throughout the last years. The present work aimed to develop a strategy, how to enhance the metabolic fitness of T cells in the tumor environment and thereby increase the effectiveness of cell-transfer based therapies.

Immunotherapy, especially the treatment of cancer with re-directed tumor-specific T cells, has become relevant in the past decades. However, whilst being very effective in the treatment of leukemic diseases, the same efficacy has not been achieved in the treatment of solid tumor entities so far (Rad S M et al., 2021).

Regarding the special metabolic conditions in the microenvironment, effective therapy of solid tumors by adoptive cell transfer approaches may require specific additional treatments or modifications of the transferred cells (Abken, 2015; Kosti et al., 2018; Newick et al., 2017). It has been shown, that response of melanoma patients to ACT therapy inversely correlates with the expression of glycolytic genes within the respective tumor (Cascone et al., 2018). Moreover, tumor glycolysis has been associated with a poor prognosis and overall survival, higher incidence of metastasis and worse response to immune checkpoint blockade therapies within different tumor entities (Blatt et al., 2016; Brand et al., 2016; Brizel et al., 2001; Renner et al., 2019; Zhang et al., 2021). In line, lactic acid, thas been shown to inhibit the effector functions of human and murine NK and T cells (Brand et al., 2016; Haas et al., 2015; Husain et al., 2013; Mendler et al., 2012). Here, it has been demonstrated that lactic acid blocks effector function development and cellular metabolism of CD4 T cells.

Different strategies have been tested to enhance the efficacy of ACT therapies. With regards to the tight relationship of the metabolism of T cells and their effector functions, many of them have focused on modulating the mitochondrial function or glycolytic activity of T cells in different manners (reviewed by Jenkins et al., 2021; Rad S M et al., 2021).

The expansion of T cells with cytokines shaping their metabolism towards a higher mitochondrial fitness, as demonstrated for IL-7, IL-15, and IL-21 (Cui et al., 2015; Dwyer et al., 2019; Loschinski et al., 2018), has been suggested to be a promising strategy to enhance CAR T cell function. Furthermore, the expansion of CAR T cells in nutrient restricted media mimicking the metabolic stress in the TME or the application of metabolic inhibitors poses a strategy to allow the CAR T cells to adjust their metabolism accordingly. For instance, expanding T cells in glucose restricted media enriches for cells displaying a Tcm phenotype and augments their killing capacity *in vitro* (Amini and Veraitch, 2019). Besides, inhibition of the glycolysis-promoting PI3K-AKT signaling cascade can promote FAO oxidation and improve CAR T cell function *in vivo* (Crompton et al., 2015; Klebanoff et al., 2017; Perkins et al., 2015).

Similar, applying specific glycolytic inhibitors during expansion has shown to improve the efficacy of transferred T cells (Hermans et al., 2020). The inhibition of the T cell metabolism during the expansion states prevents terminal differentiation of effector T cells, selects for T cells with a Tcm or Tscm phenotype and reduces T cell exhaustion (Jenkins et al., 2021; Rad S M et al., 2021; Rivadeneira and Delgoffe, 2018). However, we found that neither of those strategies increased the lactic acid resistance of T cells, and the memory subset is also not able to cope with tumor-like concentrations of lactic acid. Therefore, additional strategies are needed to enable T cells to survive the hostile conditions in the tumor environment.

One way to increase the resistance of transferred T cells against hostile tumor conditions is to equip them with additional enzymes allowing them to synthesize replenished nutrients or degrade toxic metabolites. This technique is applicable in both patient-derived TILs expanded *in vitro* for re-transfer or manufactured CAR T cells. The development of so-called TRUCKS, CAR T cells with an additional 'playload', allows a stable upgrade of CAR T cells with features increasing their anti-tumor efficacy e.g. release of stimulatory cytokines within the tumor region (Chmielewski and Abken, 2015). Similar, using genetic manipulation to bolster the T cell metabolism has been discovered as a promising strategy in the past decades. Overexpression of arginosuccinate synthase and ornithine transcarbamylase allowed T cells to overcome functional inhibition by arginine restriction and enhanced CAR T cell performance *in vivo* (Fultang et al., 2020). Moreover, downregulation of the adenosine 2a receptor by shRNA or blocking the activation of protein kinase A by expression of a small peptide call RAID (regulatory subunit I anchoring disruptor) increased the resistance of CAR T cells towards inhibition by the other inhibitory tumor metabolites adenosine and PGE2 (Masoumi et al., 2020; Newick et al., 2016). As demonstrated in this work, the overexpression of LDHB could also pose a way to equip CAR T cells with the ability to increase their lactate metabolism and thereby partially overcome the inhibitory effect of lactic acid. However, LDHB overexpression does not solve the problem of tumor acidity. Therefore, one should consider to additionally equip T cells with pH regulatory elements to better cope with low pH values, which should be a subject of further investigation. Furthermore, the closer investigation of lactic acid resistant T cells and macrophages could bring additional tools to further strengthen immunotherapeutic options.

6. Summary

In the 21th century, cancer has become the second leading cause of death worldwide. Novel therapeutic approaches do not only focus on limiting tumor growth or inducing tumor cell death but also include advanced immunotherapeutic approaches. One of the most promising strategies in arming the immune system against tumor diseases are redirected T cells. In 2012, a girl suffering from acute lymphoblastic leukemia was the first patient cured with CAR T cells, which were genetically modified to recognize leukemia cells. In 2017, the first CAR T cell therapy was approved by the federal drug administration. Unfortunately, CAR T cell therapy is to date limited to the treatment of hematological cancer entities and often fails in solid tumors.

The tumor microenvironment has been established as part of the immune evasion machinery of tumor cells in the past decades. It is characterized by low levels of nutrients and high levels of suppressive tumor metabolites negatively affecting the infiltrating immune cells. This directly connects the microenvironment within solid tumors to T cell therapy failure: No matter how specific a T cell is, if it is not able to withstand the suppressive conditions within the tumor environment, it cannot mediate an anti-tumor response. Therefore, finding ways how to increase T cell resistance in the tumor microenvironment is a prerequisite for the development of adoptive T cell transfer therapies (ACTs) for solid tumors.

Lactate is produced by glycolytic tumor cells and exported together with protons, leading to lactate and proton accumulation in the tumor environment. Lactic acid negatively affects survival and effector functions of T cells and NK cells and was found to block T cell metabolism. Decreasing lactate secretion by genetic interference or pharmacological inhibition of lactate transport has demonstrated substantial benefits for the anti-tumor immunity. Thus, in this thesis, different metabolic, pharmacologic and genetic manipulations were investigated in order to increase the resistance of CD4 T cells towards lactic acid.

Lactic acid severely inhibited effector cytokine secretion and proliferation of CD4 T cells and induced apoptosis in higher concentrations. Moreover, lactic acid treatment blocked mitochondrial respiration, inhibited glucose uptake and prevented LDH isoenzyme shift, establishing a link between dampened T cell metabolic activity and effector functions. Buffering of the environmental pH mitigated the lactic acid effects in terms of viability, metabolic inhibition and cytokine secretion, underlining the high pH-dependency of lactic acid meditated inhibition.

One way to increase the lactic acid resistance of T cells could be to modify the culture conditions before adoptive transfer. We hypothesized that glucose limitation would prime the T cells towards a more oxidative metabolism, thereby mitigating the lactic acid impact. Indeed, glucose restricted T cells engaged their cellular respiration. However, glucose restriction did not increase lactic acid resistance of CD4 T cells in our hands.

Pharmacologically, glycolytic inhibition would be an alternative way to increase the mitochondrial respiration of T cells. We compared the influence of two different LDH inhibitors (R-(+)-GNE-140 (GNE) and NCI-737) on T cells. Treatment with NCI-737 led to a more distinct reduction in lactate secretion compared to GNE, but GNE acted stronger in terms of respiratory increase. However, LDH inhibition failed to rescue T cell metabolism upon high dose lactic acid treatment.

Besides modulating culture conditions or pharmacological intervention, genetic modification of T cells offers a way to alter their cellular metabolism.

A key enzyme in lactate metabolism is the lactate dehydrogenase. The adult enzyme is formed by two subunits, LDHA and LDHB, which form homo- and heterodimers and thereby build five isoenzymes. Due to different subset affinities, LDHA is considered to produce, LDHB to consume lactate. Therefore, we hypothesized that by manipulating the balance between LDHA and LDHB we could increase the lactate metabolization of T cells and thereby increase their lactic acid resistance.

In a first attempt, we downregulated LDHA by transfection of T cells with a LDHA-targeted siRNA. This led to a strong downregulation of LDHA for up to 48 h after activation. Surprisingly, LDHA downregulation did not affect lactate secretion or cellular respiration. Moreover, cytokine secretion was not influenced by lack of LDHA. However, the electroporation process was harmful for T cells, as reflected by decreased oxygen consumption and cytokine secretion, and did not increase cytokine secretion or T cell metabolic activity upon lactic acid treatment.

Second, we manipulated the LDH isoenzyme balance by stable overexpression of LDHB through retroviral gene delivery. LDHB overexpression led to a distinct shift in the LDH isoenzyme pattern of T cells. The altered LDH isoenzyme balance did not affect the differentiation or glucose usage of T cells, yet a slight increase in the basic respiratory activity at equal mitochondrial content was observed. Treating T cells with lactic acid, we found an increased cellular respiration and higher cytokine expression upon lactic acid treatment of the LDHB overexpressing cells. Most importantly, a spheroid co-culture experiment revealed higher cytotoxicity and better infiltration of $LDHB^{high}$ T cells.

Surprisingly, when we tried Ldhb overexpression in murine T cells for *in vivo* studies, we could not observe any effects of Ldhb on T cell metabolism and function. Following, we directly compared the mitochondrial and glycolytic metabolism of murine and human T cells and found pronounced differences regarding respiratory activity. Summarized, human T cells showed much higher respiratory activity and respiratory capacity than murine T cells regardless whether CD4 or CD8 T cells were analyzed. The most obvious difference was observed in the

composition of the LDH isoenzymes, which was LDHA based in murine T cells but showed a much more balanced pattern in human T cells.

Lastly, we sought for additional ways to equip T cells with a higher resistance towards lactic acid. Therefore, we tried to learn from cells with the ability to resist high concentrations of lactic acid.

We found that macrophages were able to survive high lactic acid concentrations. With regards to the role of acidity in mediating the lactic acid effects, in first instance we analyzed the expression of key pH regulators in T cells, monocytes, macrophages and Treg. Overall, pH regulators were to a much higher level expressed in macrophages and monocytes compared to T cells, matching the hypothesis of pH regulation being crucial for lactic acid resistance. By applying selective inhibitors, we tried to further elucidate the roles of the different pH regulatory molecules in mediating lactic acid resistance. The obtained results were largely heterogenous, indicating a highly donor dependent and cooperative mechanisms causing better viability upon lactic acid treatment. Only diclofenac and aspirin, both COX inhibitors, induced macrophage dead in combination with lactic acid. However, the COX inhibitor ketoprofen failed to sensitize macrophages towards lactic acid, suggesting a mechanism beyond pH regulation and COX inhibition is responsible the survival ability of macrophages upon lactic acid treatment.

Not only macrophages are more resistant to lactic acid treatment, also within a T cell culture one can find T cells with a higher resistance towards lactic acid.

We wanted to investigate, whether different memory subsets display differential sensitivity towards lactic acid. Therefore, we sorted CD4 T cells in naïve, central memory and effector memory T cells and investigated their reaction on lactic acid treatment. Although slight differences regarding the cellular metabolism, the preservation of cytokine production and viability were observed, no T cell subset displayed a distinctly higher lactic acid resistance.

A CFSE analysis revealed within one bulk T cell culture, that some cells were able to partially preserve their proliferative capacity despite lactic acid treatment. We flow cytometrically sorted for proliferating T cells with and without lactic acid and performed an RNAseq analysis. Within the genes upregulated by lactic acid treatment, we found several genes known to be predominantly expressed by myeloid cells, which was as well reflected in a pathway analysis. Therefore, learning from myeloid cells seems a promising approach for further T cell manipulation.

In this thesis, genetic manipulation of T cells to overexpress the lactate metabolizing enzyme LDHB increased their cytokine secretion and enhanced their functionality in a spheroid co-culture approach. Analyzing macrophages as lactic acid resistant cells opened additional possibilities for further T cell manipulation with regards to pH regulation. However, the

metabolic comparison of murine and human T cells revealed major differences, questioning the reliability of syngeneic mouse models when working with immunometabolic approaches.

7. Zusammenfassung

Krebserkrankungen sind im 21. Jahrhundert die zweithäufigste Todesursache weltweit. Neu entwickelte Therapieverfahren konzentrieren sich mittlerweile jedoch nicht mehr ausschließlich darauf, das Tumorwachstum zu inhibieren oder Tumorzellen abzutöten, sondern beziehen das Immunsystem als Ziel und Mittel möglicher Therapien mit ein. Besonders vielversprechend ist dabei die Verwendung von spezifisch umprogrammierten T Zellen, welche speziell Tumorzellen erkennen und bekämpfen sollen. Im Jahre 2012 wurde erstmalig eine junge Patientin, welche an akuter lymphoblastischer Leukämie litt, unter Verwendung von sogenannten CAR T Zellen geheilt. Diese T Zellen wurden umprogrammiert, um speziell Leukämiezellen zu erkennen. Im Jahr 2017 wurde die erste CAR T Zell basierte Therapie in den USA zugelassen. Jedoch ist die CAR T Zell Therapie bislang auf die Behandlung hämatologischer Krebserkrankungen beschränkt und zeigt bei soliden Tumoren eine deutlich schlechtere Wirkung.

Ein Grund für das Versagen von T Zell Therapien bei soliden Tumoren könnte im Mikromilieu von Tumoren zu finden sein, welches in den vergangenen Jahren als Teil der Immunevasion von Tumoren beschrieben wurde. Es ist charakterisiert durch Depletion von Nährstoffen einerseits und der Akkumulation von inhibierenden Tumormetaboliten andererseits, welche einwandernde Immunzellen negativ beeinflussen. Dies bringt das Tumormilieu direkt mit dem Versagen von T Zell Therapien in Verbindung: Selbst die spezifischste T Zelle kann keine solide anti-Tumor Antwort aufbauen, wenn Sie durch die vorherrschenden Konditionen zu stark negativ beeinflusst wird. Daher ist es für die Weiterentwicklung von T Zell Therapeutika essentiell, Wege zu finden, um die Resistenz von T Zellen gegenüber den Konditionen in der Tumorumgebung zu stärken.

Laktat wird in großer Menge von glykolytischen Tumorzellen produziert und zusammen mit Protonen in die Tumorumgebung sezerniert, wo es als Milchsäure akkumuliert. Milchsäure inhibiert die Effektorfunktionen verschiedener Immunzellen, stört deren zellulären Stoffwechsel und führt darüber hinaus in höheren Konzentrationen zum Zelltod. Durch die Reduktion der Laktatsekretion von Tumorzellen konnte bereits die Immunantwort gegen solide Tumoren deutlich verbessert werden. Daher sollten in der vorliegenden Arbeit pharmakologische, metabolische und genetische Manipulationen von T Zellen untersucht werden hinsichtlich der Fragestellung, ob die Resistenz der Zellen gegenüber Milchsäure dadurch gestärkt werden kann.

Milchsäure beeinträchtigte sowohl die Proliferation als auch die Sekretion von Effektorzytokinen von CD4 T Zellen und induzierte bei höheren Konzentrationen Apoptose. Darüber hinaus wurde unter Behandlung mit Milchsäure eine Blockade der Zellatmung sowie

der LDH Isoenzym-Regulierung und reduzierte Glukoseaufnahme festgestellt, was eine direkte Verbindung des gestörten T Zell Metabolismus und inhibierter Effektorfunktionen nahelegt. Durch Puffern des extrazellulären pHs konnte der Effekt von Milchsäure abgeschwächt werden, was die pH-Abhängigkeit dieses Effekts unterstreicht.

Ein Weg, die Milchsäureresistenz von T Zellen zu erhöhen könnte die Modifikation der Kulturbedingungen vor adoptivem Transfer sein. Wir vermuteten, dass die Kultur von T Zellen unter Glukoserestriktion deren oxidativen Zellmetabolismus verstärken und dabei den Einfluss der Milchsäure reduzieren würde, was jedoch nicht der Fall war.

Ein pharmakologischer Weg, die Zellatmung von T Zellen zu erhöhen, könnte glykolytische Inhibition über Hemmung der Laktatdehydrogenase darstellen. Daher wurde die Wirkung zweier LDH-Inhibitoren (R-(+)-GNE-140 (GNE) und NCI-737) auf T Zellen verglichen. Die Behandlung mit NCI-737 führe zu einer deutlicheren Laktatreduktion, jedoch konnte unter GNE-Behandlung eine bessere Verstärkung der Zellatmung beobachtet werden. Unabhängig davon konnte durch Behandlung mit NCI-737 keine verbesserte Milchsäure-Resistenz erreicht werden.

Neben metabolischen und pharmakologischen Ansatzpunkten biete genetische Modifikation die Möglichkeit, den Metabolismus von T Zellen direkt zu beeinflussen.

Ein Schlüsselenzym im Laktatstoffwechsel ist die Laktatdehydrogenase (LDH), welche in adulten Zellen von den Untereinheiten LDHA und LDHB zusammengesetzt wird. Da diese Untereinheiten verschiedene Substrat-Spezifitäten aufweisen, wird vermutet, dass LDHA eher Laktat produziert, während LDHB eher Laktat verstoffwechselt. Daher versuchten wir, durch Manipulation der Balance zwischen den Isoenzymen die Verstoffwechselung von Laktat in T Zellen zu verstärken und dadurch die Milchsäure-Resistenz zu erhöhen.

In einem ersten Ansatzunkt wurde LDHA durch Elektroporation von T Zellen mit LDHA-spezifischer siRNA reduziert. Dies führte zu einer stark erniedrigten LDHA-Expression bis zu 48 h nach Aktivierung. Zu unserer Überraschung beeinflusste das Fehlen von LDHA die weder die Laktat- noch die Zytokinsekretion. Allerdings konnte durch die Elektroporation eine starke Beeinträchtigung der Zellatmung und der Zytokinsekretion beobachtet werden, und eine Verbesserung der Zellfunktionen unter Milchsäure blieb aus.

In einem weiteren Ansatz versuchten wir, die LDH Isoenzym Balance durch Überexpression von LDHB in T Zellen zu manipulieren. Dies führte zu einer sichtbaren Verschiebung im LDH Isoenzym Muster der Zellen. Überexpression von LDHB hatte keinen Einfluss auf die Differenzierung oder den Glukosemetabolismus der Zellen, obwohl eine leichte Verstärkung der Zellatmung bei unverändertem Mitochondriengehalt feststellbar war. Unter Behandlung mit Milchsäure zeigten die LDHB überexprimierenden Zellen eine verstärkte Zellatmung und eine

verbesserte Zytokinproduktion. In einer Co-Kultur mit Tumor-Sphäroiden zeigten die LDHB überexprimierenden Zellen eine verstärkte Infiltration und bessere Zytotoxizität. Dies unterstreicht das Potential von LDHB überexprimierenden T Zellen in der Tumorbehandlung.

Überraschenderweise konnten die Ergebnisse der LDHB überexprimierenden T Zellen nicht von humanen in murine T Zellen übertragen werden. Daher verglichen wir den Glukose- und mitochondrialen Stoffwechsel von murinen und humanen T Zellen. Dabei stellten wir große Unterschiede in den Stoffwechselaktivitäten der verschiedenen T Zellen fest. Humane T Zellen zeigten eine wesentlich höhere respiratorische Aktivität und Kapazität als murine T Zellen. Am deutlichsten wurde der Unterschied im LDH Isoenzym Profil festgestellt. In murinen T Zellen wurde hauptsächlich die Expression von LDHA mit nur einem geringen Anteil LDHB festgestellt. Dagegen wurde in unstimulierten humanen T Zellen ein LDHB zentriertes Muster gefunden, welches sich unter Stimulation in Richtung LDHA verschob, es wurden jedoch weiter alle LDH Isoenzyme exprimiert.

Um weitere Möglichkeiten zu finden, die Resistenz von T Zellen gegenüber Milchsäure zu erhöhen, wurden Zellen mit einer bestehenden Milchsäureresistenz näher analysiert.

Wir konnten zeigen, dass Makrophagen in der Lage sind, sehr hohe Konzentrationen Milchsäure zu überleben. Mit Bezug zu der Rolle des niedrigen pHs bei der Vermittlung der Inhibition durch Milchsäure wurde in einem ersten Schritt die Expression verschiedener pH regulatorischer Proteine in Makrophagen, Monozyten und T Zellen analysiert. Dabei wurde festgestellt, dass Makrophagen und Monozyten eine höhere Expression dieser pH Regulatoren zeigten. Dies stimmte mit der Vermutung, dass pH Regulation für das Überleben dieser Zellen in Umgebungen mit hohen Konzentrationen Milchsäure essenziell ist, überein. Durch die Verwendung spezifischer Inhibitoren haben wir versucht, die Rolle der verschiedenen pH Regulatoren präziser zu definieren. Die Ergebnisse diesbezüglich waren sehr heterogen und variierten zwischen verschiedenen Spendern, was einen kooperativen Mechanismus, in dem verschiedene pH Regulatoren zur Kompensation der Milchsäure-induzierten Ansäuerung zusammenarbeiten, nahelegt. Lediglich die COX-Inhibitoren Diclofenac und Aspirin induzierten den Zelltod von Makrophagen unter Behandlung mit Milchsäure. Dies legt nahe, dass es einen Mechanismus außerhalb der pH Regulation gibt, der das Überleben von Makrophagen unter Milchsäurebehandlung sichert.

Neben Makrophagen gibt es auch innerhalb einer T Zell Population Zellen, die eine höhere Resistenz gegenüber Milchsäure zeigen.

In einem ersten Schritt untersuchten wir, ob eine der verschiedenen Gedächtnis-Zell-Populationen eine höhere Resistenz gegenüber Milchsäure aufwies. Wir nutzten Durchflusszytometrie, um naive, *Central memory* und *Effector memory* Zellen zu sortieren und

untersuchten deren Reaktionen auf Milchsäure. Obwohl es bezüglich der Atmungsaktivität, Zytokinproduktion und Überleben der Zellen leichte Unterschiede festgestellt wurden, konnte bei keiner der untersuchten Populationen eine erhöhte Milchsäure-Resistenz festgestellt werden.

Unter der Verwendung von CFSE konnten wir feststellen, dass innerhalb einer T Zell Kultur einige Zellen in der Lage waren, ihre Proliferation trotz Behandlung mit Milchsäure zumindest partiell zu erhalten. Wir nutzten CFSE, um proliferierende und nicht proliferierende T Zellen nach Milchsäurebehandlung durchflusszytometrisch zu sortieren und führten eine RNAseq Analyse durch. In den Genen, die durch Milchsäurebehandlung in proliferierenden Zellen induziert wurden, konnte eine Anreicherung der Gensignatur von CD14+ Monozyten festgestellt werden. Dies schlägt eine Brücke zu unserem Versuch, von Makrophagen zu lernen, welche genetische Modifikationen T Zellen zu einer verbesserten Milchsäureresistenz verhelfen könnte.

In der vorliegenden Arbeit konnte gezeigt werden, dass genetische Manipulation von T Zellen zur Überexpression von LDHB die Zytokinsekretion dieser Zellen und deren Funktionalität in einer Spheroid Co-Kultur verbessert. Die Analyse von Makrophagen als milchsäureresistente Zellen eröffnete weitere Manipulationsmöglichkeiten der T Zellen zu Verbesserung der Milchsäureresistenz. Jedoch konnte gezeigt werden, dass der murine und humane T Zell Metabolismus substanziell verschieden sind, was die Zuverlässigkeit von syngenen Mausmodellen bei der Untersuchung immunometabolischer Konzepte in Frage stellt.

References

Abken, H. (2015). Adoptive therapy with CAR redirected T cells: the challenges in targeting solid tumors. Immunotherapy *7*, 535-544.

Aggarwal, M., Boone, C.D., Kondeti, B., and McKenna, R. (2013). Structural annotation of human carbonic anhydrases. Journal of enzyme inhibition and medicinal chemistry *28*, 267-277.

Algarra, I., García-Lora, A., Cabrera, T., Ruiz-Cabello, F., and Garrido, F. (2004). The selection of tumor variants with altered expression of classical and nonclassical MHC class I molecules: implications for tumor immune escape. Cancer immunology, immunotherapy : CII *53*, 904-910.

Amini, A., and Veraitch, F. (2019). Glucose deprivation enriches for central memory T cells during chimeric antigen receptor-T cell expansion. Cytotherapy *21*, S30-S31.

Angelin, A., Gil-de-Gómez, L., Dahiya, S., Jiao, J., Guo, L., Levine, M.H., Wang, Z., Quinn, W.J., Kopinski, P.K., and Wang, L., et al. (2017). Foxp3 Reprograms T Cell Metabolism to Function in Low-Glucose, High-Lactate Environments. Cell Metabolism *25*, 1282-1293.e7.

Antony, P.A., Piccirillo, C.A., Akpinarli, A., Finkelstein, S.E., Speiss, P.J., Surman, D.R., Palmer, D.C., Chan, C.-C., Klebanoff, C.A., and Overwijk, W.W., et al. (2005). CD8+ T cell immunity against a tumor/self-antigen is augmented by CD4+ T helper cells and hindered by naturally occurring T regulatory cells. Journal of immunology (Baltimore, Md. : 1950) *174*, 2591-2601.

Bailis, W., Shyer, J.A., Zhao, J., Canaveras, J.C.G., Al Khazal, F.J., Qu, R., Steach, H.R., Bielecki, P., Khan, O., and Jackson, R., et al. (2019). Distinct modes of mitochondrial metabolism uncouple T cell differentiation and function. Nature *571*, 403-407.

Balmer, M.L., Ma, E.H., Bantug, G.R., Grählert, J., Pfister, S., Glatter, T., Jauch, A., Dimeloe, S., Slack, E., and Dehio, P., et al. (2016). Memory CD8(+) T Cells Require Increased Concentrations of Acetate Induced by Stress for Optimal Function. Immunity *44*, 1312-1324.

Beier, U.H., Angelin, A., Akimova, T., Wang, L., Liu, Y., Xiao, H., Koike, M.A., Hancock, S.A., Bhatti, T.R., and Han, R., et al. (2015). Essential role of mitochondrial energy metabolism in Foxp3^{+} T-regulatory cell function and allograft survival. FASEB journal : official publication of the Federation of American Societies for Experimental Biology *29*, 2315-2326.

Bensinger, S.J., and Christofk, H.R. (2012). New aspects of the Warburg effect in cancer cell biology. Seminars in cell & developmental biology *23*, 352-361.

Bergmeyer, H.U. (1974). Methods of enzymatic analysis (Weinheim: Verl. Chemie).

Bhattacharyya, N.D., and Feng, C.G. (2020). Regulation of T Helper Cell Fate by TCR Signal Strength. Frontiers in immunology *11*, 624.

Blagih, J., Coulombe, F., Vincent, E.E., Dupuy, F., Galicia-Vázquez, G., Yurchenko, E., Raissi, T.C., van der Windt, G.J.W., Viollet, B., and Pearce, E.L., et al. (2015). The energy sensor AMPK regulates T cell metabolic adaptation and effector responses in vivo. Immunity *42*, 41-54.

Blank, C., Brown, I., Peterson, A.C., Spiotto, M., Iwai, Y., Honjo, T., and Gajewski, T.F. (2004). PD-L1/B7H-1 inhibits the effector phase of tumor rejection by T cell receptor (TCR) transgenic CD8+ T cells. Cancer research *64*, 1140-1145.

Blas-Rus, N., Bustos-Morán, E., Pérez de Castro, I., Cárcer, G. de, Borroto, A., Camafeita, E., Jorge, I., Vázquez, J., Alarcón, B., and Malumbres, M., et al. (2016). Aurora A drives early signalling and vesicle dynamics during T-cell activation. Nat Commun *7*, 11389.

Blatt, S., Voelxen, N., Sagheb, K., Pabst, A.M., Walenta, S., Schroeder, T., Mueller-Klieser, W., and Ziebart, T. (2016). Lactate as a predictive marker for tumor recurrence in patients with head and neck squamous cell carcinoma (HNSCC) post radiation: a prospective study over 15 years. Clinical oral investigations *20*, 2097-2104.

Bola, B.M., Chadwick, A.L., Michopoulos, F., Blount, K.G., Telfer, B.A., Williams, K.J., Smith, P.D., Critchlow, S.E., and Stratford, I.J. (2014). Inhibition of monocarboxylate transporter-1 (MCT1) by AZD3965 enhances radiosensitivity by reducing lactate transport. Molecular cancer therapeutics *13*, 2805-2816.

Borst, J., Ahrends, T., Bąbała, N., Melief, C.J.M., and Kastenmüller, W. (2018). CD4+ T cell help in cancer immunology and immunotherapy. Nat Rev Immunol *18*, 635-647.

Bos, R., and Sherman, L.A. (2010). CD4+ T-cell help in the tumor milieu is required for recruitment and cytolytic function of CD8+ T lymphocytes. Cancer Res *70*, 8368-8377.

Bosshart, P.D., Charles, R.-P., Garibsingh, R.-A.A., Schlessinger, A., and Fotiadis, D. (2021). SLC16 Family: From Atomic Structure to Human Disease. Trends in Biochemical Sciences *46*, 28-40.

Boudreau, A., Purkey, H.E., Hitz, A., Robarge, K., Peterson, D., Labadie, S., Kwong, M., Hong, R., Gao, M., and Del Nagro, C., et al. (2016). Metabolic plasticity underpins innate and acquired resistance to LDHA inhibition. Nat Chem Biol *12*, 779-786.

Brand, A., Singer, K., Koehl, G.E., Kolitzus, M., Schoenhammer, G., Thiel, A., Matos, C., Bruss, C., Klobuch, S., and Peter, K., et al. (2016). LDHA-Associated Lactic Acid Production Blunts Tumor Immunosurveillance by T and NK Cells. Cell Metabolism *24*, 657-671.

Brizel, D.M., Schroeder, T., Scher, R.L., Walenta, S., Clough, R.W., Dewhirst, M.W., and Mueller-Klieser, W. (2001). Elevated tumor lactate concentrations predict for an increased risk of metastases in head-and-neck cancer. International Journal of Radiation Oncology*Biology*Physics *51*, 349-353.

Buck, M.D., O'Sullivan, D., Klein Geltink, R.I., Curtis, J.D., Chang, C.-H., Sanin, D.E., Qiu, J., Kretz, O., Braas, D., and van der Windt, G.J.W., et al. (2016). Mitochondrial Dynamics Controls T Cell Fate through Metabolic Programming. Cell *166*, 63-76.

Cachot, A., Bilous, M., Liu, Y.-C., Li, X., Saillard, M., Cenerenti, M., Rockinger, G.A., Wyss, T., Guillaume, P., and Schmidt, J., et al. (2021). Tumor-specific cytolytic CD4 T cells mediate immunity against human cancer. Science advances *7*.

Cairns, R.A., Harris, I.S., and Mak, T.W. (2011). Regulation of cancer cell metabolism. Nature reviews. Cancer *11*, 85-95.

Calcinotto, A., Filipazzi, P., Grioni, M., Iero, M., Milito, A. de, Ricupito, A., Cova, A., Canese, R., Jachetti, E., and Rossetti, M., et al. (2012). Modulation of microenvironment acidity reverses anergy in human and murine tumor-infiltrating T lymphocytes. Cancer research, 2746-2756.

Caligiuri, M.A. (2008). Human natural killer cells. Blood *112*, 461-469.

Camarda, R., Williams, J., and Goga, A. (2017). In vivo Reprogramming of Cancer Metabolism by MYC. Front. Cell Dev. Biol. *5*, 35.

Cao, Y., Rathmell, J.C., and Macintyre, A.N. (2014). Metabolic reprogramming towards aerobic glycolysis correlates with greater proliferative ability and resistance to metabolic inhibition in CD8 versus CD4 T cells. PloS one *9*, e104104.

Cappel, D.A., Deja, S., Duarte, J.A.G., Kucejova, B., Iñigo, M., Fletcher, J.A., Fu, X., Berglund, E.D., Liu, T., and Elmquist, J.K., et al. (2019). Pyruvate-Carboxylase-Mediated Anaplerosis Promotes Antioxidant Capacity by Sustaining TCA Cycle and Redox Metabolism in Liver. Cell metabolism *29*, 1291-1305.e8.

Carr, E.L., Kelman, A., Wu, G.S., Gopaul, R., Senkevitch, E., Aghvanyan, A., Turay, A.M., and Frauwirth, K.A. (2010). Glutamine uptake and metabolism are coordinately regulated by ERK/MAPK during T lymphocyte activation. The Journal of Immunology *185*, 1037-1044.

Cascone, T., McKenzie, J.A., Mbofung, R.M., Punt, S., Wang, Z., Xu, C., Williams, L.J., Wang, Z., Bristow, C.A., and Carugo, A., et al. (2018). Increased Tumor Glycolysis Characterizes Immune Resistance to Adoptive T Cell Therapy. Cell Metabolism *27*, 977-987.e4.

Cham, C.M., Driessens, G., O'Keefe, J.P., and Gajewski, T.F. (2008). Glucose deprivation inhibits multiple key gene expression events and effector functions in CD8+ T cells. European journal of immunology *38*, 2438-2450.

Cham, C.M., and Gajewski, T.F. (2005). Glucose availability regulates IFN-gamma production and p70S6 kinase activation in CD8+ effector T cells. Journal of immunology (Baltimore, Md. : 1950) *174*, 4670-4677.

Chambers, C.A., Kuhns, M.S., Egen, J.G., and Allison, J.P. (2001). CTLA-4-mediated inhibition in regulation of T cell responses: mechanisms and manipulation in tumor immunotherapy. Annual review of immunology *19*, 565-594.

Chang, C.-H., Curtis, J.D., Maggi, L.B., Faubert, B., Villarino, A.V., O'Sullivan, D., Huang, S.C.-C., van der Windt, G.J.W., Blagih, J., and Qiu, J., et al. (2013). Posttranscriptional control of T cell effector function by aerobic glycolysis. Cell *153*, 1239-1251.

Chang, C.-H., and Pearce, E.L. (2016). Emerging concepts of T cell metabolism as a target of immunotherapy. Nat Immunol *17*, 364-368.

Chang, C.-H., Qiu, J., O'Sullivan, D., Buck, M.D., Noguchi, T., Curtis, J.D., Chen, Q., Gindin, M., Gubin, M.M., and van der Windt, G.J.W., et al. (2015). Metabolic Competition in the Tumor Microenvironment Is a Driver of Cancer Progression. Cell *162*, 1229-1241.

Chao, T., Wang, H., and Ho, P.-C. (2017). Mitochondrial Control and Guidance of Cellular Activities of T Cells. Frontiers in immunology *8*, 473.

Chen, E.Y., Tan, C.M., Kou, Y., Duan, Q., Wang, Z., Meirelles, G.V., Clark, N.R., and Ma'ayan, A. (2013). Enrichr: interactive and collaborative HTML5 gene list enrichment analysis tool. BMC bioinformatics *14*, 128.

Cheng, A., Zhang, P., Wang, B., Yang, D., Duan, X., Jiang, Y., Xu, T., Jiang, Y., Shi, J., and Ding, C., et al. (2019). Aurora-A mediated phosphorylation of LDHB promotes glycolysis and tumor progression by relieving the substrate-inhibition effect. Nature communications *10*, 5566.

Chmielewski, M., and Abken, H. (2015). TRUCKs: the fourth generation of CARs. Expert opinion on biological therapy *15*, 1145-1154.

Christofk, H.R., Vander Heiden, M.G., Harris, M.H., Ramanathan, A., Gerszten, R.E., Wei, R., Fleming, M.D., Schreiber, S.L., and Cantley, L.C. (2008). The M2 splice isoform of pyruvate kinase is important for cancer metabolism and tumour growth. Nature *452*, 230-233.

Colegio, O.R., Chu, N.-Q., Szabo, A.L., Chu, T., Rhebergen, A.M., Jairam, V., Cyrus, N., Brokowski, C.E., Eisenbarth, S.C., and Phillips, G.M., et al. (2014). Functional polarization of tumour-associated macrophages by tumour-derived lactic acid. Nature *513*, 559-563.

(2013). Comprehensive molecular characterization of clear cell renal cell carcinoma. Nature *499*, 43-49.

Cooper, E.H., Barkhan, P., and Hale, A.J. (1963). Observations on the proliferation of human leucocytes cultured with phytohaemagglutinin. British journal of haematology *9*, 101-111.

Cosson, P., Curtis, I. de, Pouysségur, J., Griffiths, G., and Davoust, J. (1989). Low cytoplasmic pH inhibits endocytosis and transport from the trans-Golgi network to the cell surface. The Journal of cell biology *108*, 377-387.

Crompton, J.G., Sukumar, M., Roychoudhuri, R., Clever, D., Gros, A., Eil, R.L., Tran, E., Hanada, K., Yu, Z., and Palmer, D.C., et al. (2015). Akt inhibition enhances expansion of potent tumor-specific lymphocytes with memory cell characteristics. Cancer Res *75*, 296-305.

Cui, G., Staron, M.M., Gray, S.M., Ho, P.-C., Amezquita, R.A., Wu, J., and Kaech, S.M. (2015). IL-7-Induced Glycerol Transport and TAG Synthesis Promotes Memory CD8+ T Cell Longevity. Cell *161*, 750-761.

Dang, C.V. (2007). The interplay between MYC and HIF in the Warburg effect. Ernst Schering Foundation symposium proceedings, 35-53.

DeBerardinis, R.J., and Chandel, N.S. (2020). We need to talk about the Warburg effect. Nat Metab *2*, 127-129.

Di Zhang, Tang, Z., Huang, H., Zhou, G., Cui, C., Weng, Y., Liu, W., Kim, S., Lee, S., and Perez-Neut, M., et al. (2019). Metabolic regulation of gene expression by histone lactylation. Nature *574*, 575-580.

Dietl, K., Renner, K., Dettmer, K., Timischl, B., Eberhart, K., Dorn, C., Hellerbrand, C., Kastenberger, M., Kunz-Schughart, L.A., and Oefner, P.J., et al. (2010). Lactic acid and acidification inhibit TNF secretion and glycolysis of human monocytes. The Journal of Immunology *184*, 1200-1209.

Doherty, J.R., Yang, C., Scott, K.E.N., Cameron, M.D., Fallahi, M., Li, W., Hall, M.A., Amelio, A.L., Mishra, J.K., and Li, F., et al. (2014). Blocking lactate export by inhibiting the Myc target MCT1 Disables glycolysis and glutathione synthesis. Cancer research *74*, 908-920.

Dopfer, E.P., Hartl, F.A., Oberg, H.-H., Siegers, G.M., Yousefi, O.S., Kock, S., Fiala, G.J., Garcillán, B., Sandstrom, A., and Alarcón, B., et al. (2014). The CD3 conformational change in the γδ T cell receptor is not triggered by antigens but can be enforced to enhance tumor killing. Cell Reports *7*, 1704-1715.

Dunbar, E.M., Coats, B.S., Shroads, A.L., Langaee, T., Lew, A., Forder, J.R., Shuster, J.J., Wagner, D.A., and Stacpoole, P.W. (2014). Phase 1 trial of dichloroacetate (DCA) in adults with recurrent malignant brain tumors. Investigational new drugs *32*, 452-464.

Dwyer, C.J., Knochelmann, H.M., Smith, A.S., Wyatt, M.M., Rangel Rivera, G.O., Arhontoulis, D.C., Bartee, E., Li, Z., Rubinstein, M.P., and Paulos, C.M. (2019). Fueling Cancer Immunotherapy With Common Gamma Chain Cytokines. Frontiers in immunology *10*, 263.

Ecker, C., Guo, L., Voicu, S., Gil-de-Gómez, L., Medvec, A., Cortina, L., Pajda, J., Andolina, M., Torres-Castillo, M., and Donato, J.L., et al. (2018). Differential Reliance on Lipid Metabolism as a Salvage Pathway Underlies Functional Differences of T Cell Subsets in Poor Nutrient Environments. Cell Reports *23*, 741-755.

Erra Díaz, F., Dantas, E., and Geffner, J. (2018). Unravelling the Interplay between Extracellular Acidosis and Immune Cells. Mediators of inflammation *2018*, 1218297.

Even, S., Lindley, N.D., and Cocaign-Bousquet, M. (2003). Transcriptional, translational and metabolic regulation of glycolysis in Lactococcus lactis subsp. cremoris MG 1363 grown in continuous acidic cultures. Microbiology *149*, 1935-1944.

Faubert, B., Li, K.Y., Cai, L., Hensley, C.T., Kim, J., Zacharias, L.G., Yang, C., Do, Q.N., Doucette, S., and Burguete, D., et al. (2017). Lactate Metabolism in Human Lung Tumors. Cell *171*, 358-371.e9.

Felmlee, M.A., Jones, R.S., Rodriguez-Cruz, V., Follman, K.E., and Morris, M.E. (2020). Monocarboxylate Transporters (SLC16): Function, Regulation, and Role in Health and Disease. Pharmacological Reviews *72*, 466-485.

Fischer, K., Hoffmann, P., Voelkl, S., Meidenbauer, N., Ammer, J., Edinger, M., Gottfried, E., Schwarz, S., Rothe, G., and Hoves, S., et al. (2007). Inhibitory effect of tumor cell-derived lactic acid on human T cells. Blood *109*, 3812-3819.

Frauwirth, K.A., Riley, J.L., Harris, M.H., Parry, R.V., Rathmell, J.C., Plas, D.R., Elstrom, R.L., June, C.H., and Thompson, C.B. (2002). The CD28 Signaling Pathway Regulates Glucose Metabolism. Immunity *16*, 769-777.

Fridman, W.H., Pagès, F., Sautès-Fridman, C., and Galon, J. (2012). The immune contexture in human tumours: impact on clinical outcome. Nature reviews. Cancer *12*, 298-306.

Fultang, L., Booth, S., Yogev, O., Da Martins Costa, B., Tubb, V., Panetti, S., Stavrou, V., Scarpa, U., Jankevics, A., and Lloyd, G., et al. (2020). Metabolic engineering against the arginine microenvironment enhances CAR-T cell proliferation and therapeutic activity. Blood *136*, 1155-1160.

Gatenby, R.A., and Gillies, R.J. (2004). Why do cancers have high aerobic glycolysis? Nature reviews. Cancer *4*, 891-899.

Gattinoni, L., Klebanoff, C.A., Palmer, D.C., Wrzesinski, C., Kerstann, K., Yu, Z., Finkelstein, S.E., Theoret, M.R., Rosenberg, S.A., and Restifo, N.P. (2005). Acquisition of full effector function in vitro paradoxically impairs the in vivo antitumor efficacy of adoptively transferred CD8+ T cells. The Journal of clinical investigation *115*, 1616-1626.

Gattinoni, L., Lugli, E., Ji, Y., Pos, Z., Paulos, C.M., Quigley, M.F., Almeida, J.R., Gostick, E., Yu, Z., and Carpenito, C., et al. (2011). A human memory T cell subset with stem cell-like properties. Nat Med *17*, 1290-1297.

Gattinoni, L., Zhong, X.-S., Palmer, D.C., Ji, Y., Hinrichs, C.S., Yu, Z., Wrzesinski, C., Boni, A., Cassard, L., and Garvin, L.M., et al. (2009). Wnt signaling arrests effector T cell differentiation and generates CD8+ memory stem cells. Nat Med *15*, 808-813.

Gay, R.J., McComb, R.B., and Bowers, G.N. (1968). Optimum Reaction Conditions for Human Lactate Dehydrogenase Isoenzymes as They Affect Total Lactate Dehydrogenase Activity. Clinical Chemistry *14*, 740-753.

Geiger, R., Rieckmann, J.C., Wolf, T., Basso, C., Feng, Y., Fuhrer, T., Kogadeeva, M., Picotti, P., Meissner, F., and Mann, M., et al. (2016). L-Arginine Modulates T Cell Metabolism and Enhances Survival and Anti-tumor Activity. Cell *167*, 829-842.e13.

Gerriets, V.A., Kishton, R.J., Nichols, A.G., Macintyre, A.N., Inoue, M., Ilkayeva, O., Winter, P.S., Liu, X., Priyadharshini, B., and Slawinska, M.E., et al. (2015). Metabolic programming and PDHK1 control CD4+ T cell subsets and inflammation. The Journal of clinical investigation *125*, 194-207.

Gnjatic, S., Atanackovic, D., Jäger, E., Matsuo, M., Selvakumar, A., Altorki, N.K., Maki, R.G., Dupont, B., Ritter, G., and Chen, Y.-T., et al. (2003). Survey of naturally occurring CD4+ T cell responses against NY-ESO-1 in cancer patients: correlation with antibody responses. Proceedings of the National Academy of Sciences *100*, 8862-8867.

Goetzman, E.S., and Prochownik, E.V. (2018). The Role for Myc in Coordinating Glycolysis, Oxidative Phosphorylation, Glutaminolysis, and Fatty Acid Metabolism in Normal and Neoplastic Tissues. Front. Endocrinol. *9*, 129.

Gottfried, E., Kreutz, M., and Mackensen, A. (2012). Tumor metabolism as modulator of immune response and tumor progression. Seminars in cancer biology *22*, 335-341.

Gottfried, E., Kunz-Schughart, L.A., Ebner, S., Mueller-Klieser, W., Hoves, S., Andreesen, R., Mackensen, A., and Kreutz, M. (2006). Tumor-derived lactic acid modulates dendritic cell activation and antigen expression. Blood *107*, 2013-2021.

Groen, A.K., van Roermund, C.W., Vervoorn, R.C., and Tager, J.M. (1986). Control of gluconeogenesis in rat liver cells. Flux control coefficients of the enzymes in the gluconeogenic pathway in the absence and presence of glucagon. Biochem J *237*, 379-389.

Gropper, Y., Feferman, T., Shalit, T., Salame, T.-M., Porat, Z., and Shakhar, G. (2017). Culturing CTLs under Hypoxic Conditions Enhances Their Cytolysis and Improves Their Anti-tumor Function. Cell reports *20*, 2547-2555.

Gubser, P.M., Bantug, G.R., Razik, L., Fischer, M., Dimeloe, S., Hoenger, G., Durovic, B., Jauch, A., and Hess, C. (2013). Rapid effector function of memory CD8+ T cells requires an immediate-early glycolytic switch. Nature immunology *14*, 1064-1072.

Guerra, L., Bonetti, L., and Brenner, D. (2020). Metabolic Modulation of Immunity: A New Concept in Cancer Immunotherapy. Cell Reports *32*, 107848.

Gullino, P.M., Clark, S.H., and Grantham, F.H. (1964). The interstitial fluid of tumors. Cancer research *24*, 780-794.

Haas, R., Smith, J., Rocher-Ros, V., Nadkarni, S., Montero-Melendez, T., D'Acquisto, F., Bland, E.J., Bombardieri, M., Pitzalis, C., and Perretti, M., et al. (2015). Lactate Regulates Metabolic and Pro-inflammatory Circuits in Control of T Cell Migration and Effector Functions. PLoS biology *13*, e1002202.

Hadrup, S., Donia, M., and Thor Straten, P. (2013). Effector CD4 and CD8 T cells and their role in the tumor microenvironment. Cancer microenvironment : official journal of the International Cancer Microenvironment Society *6*, 123-133.

Hahn, S.A., Bellinghausen, I., Trinschek, B., and Becker, C. (2015). Translating Treg Therapy in Humanized Mice. Frontiers in immunology *6*, 623.

Halestrap, A.P. (2012). The monocarboxylate transporter family--Structure and functional characterization. IUBMB Life *64*, 1-9.

Halperin, M.L., Connors, H.P., Relman, A.S., and Karnovsky, M.L. (1969). Factors That Control the Effect of pH on Glycolysis in Leukocytes. The Journal of biological chemistry *244*, 384-390.

Hanahan, D., and Weinberg, R.A. (2011). Hallmarks of cancer: the next generation. Cell *144*, 646-674.

Harmon, C., Robinson, M.W., Hand, F., Almuaili, D., Mentor, K., Houlihan, D.D., Hoti, E., Lynch, L., Geoghegan, J., and O'Farrelly, C. (2019). Lactate-Mediated Acidification of Tumor Microenvironment Induces Apoptosis of Liver-Resident NK Cells in Colorectal Liver Metastasis. Cancer immunology research *7*, 335-346.

Hartmann, F.J., Mrdjen, D., McCaffrey, E., Glass, D.R., Greenwald, N.F., Bharadwaj, A., Khair, Z., Verberk, S.G.S., Baranski, A., and Baskar, R., et al. (2020). Single-cell metabolic profiling of human cytotoxic T cells. Nature biotechnology.

He, S., Kato, K., Jiang, J., Wahl, D.R., Mineishi, S., Fisher, E.M., Murasko, D.M., Glick, G.D., and Zhang, Y. (2011). Characterization of the metabolic phenotype of rapamycin-treated CD8+ T cells with augmented ability to generate long-lasting memory cells. PloS one *6*, e20107.

He, T.-L., Zhang, Y.-J., Jiang, H., Li, X.-H., Zhu, H., and Zheng, K.-L. (2015). The c-Myc-LDHA axis positively regulates aerobic glycolysis and promotes tumor progression in pancreatic cancer. Medical oncology (Northwood, London, England) *32*, 187.

Hermans, D., Gautam, S., García-Cañaveras, J.C., Gromer, D., Mitra, S., Spolski, R., Li, P., Christensen, S., Nguyen, R., and Lin, J.-X., et al. (2020). Lactate dehydrogenase inhibition synergizes with IL-21 to promote CD8+ T cell stemness and antitumor immunity. Proceedings of the National Academy of Sciences of the United States of America *117*, 6047-6055.

Ho, P.-C., Bihuniak, J.D., Macintyre, A.N., Staron, M., Liu, X., Amezquita, R., Tsui, Y.-C., Cui, G., Micevic, G., and Perales, J.C., et al. (2015). Phosphoenolpyruvate Is a Metabolic Checkpoint of Anti-tumor T Cell Responses. Cell *162*, 1217-1228.

Holm, E., Hagmüller, E., Staedt, U., Schlickeiser, G., Günther, H.J., Leweling, H., Tokus, M., and Kollmar, H.B. (1995). Substrate balances across colonic carcinomas in humans. Cancer research *55*, 1373-1378.

Hsieh, J.J., Purdue, M.P., Signoretti, S., Swanton, C., Albiges, L., Schmidinger, M., Heng, D.Y., Larkin, J., and Ficarra, V. (2017). Renal cell carcinoma. Nature Reviews Disease Primers *3*, 17009.

(2019). https://clinicaltrials.gov/ct2/show/NCT02546440. NCT02546440, EudraCT-Number: 2014-000924-11. https://clinicaltrials.gov/ct2/show/NCT02546440. 16.03.2021.

(2021). https://www.clinicaltrials.gov/ct2/show/NCT01791595. https://www.clinicaltrials.gov/ct2/show/NCT01791595. 18.03.2021.

Hui, S., Ghergurovich, J.M., Morscher, R.J., Jang, C., Teng, X., Lu, W., Esparza, L.A., Reya, T., Le Zhan, and Yanxiang Guo, J., et al. (2017). Glucose feeds the TCA cycle via circulating lactate. Nature *551*, 115-118.

Husain, Z., Huang, Y., Seth, P., and Sukhatme, V.P. (2013). Tumor-derived lactate modifies antitumor immune response: effect on myeloid-derived suppressor cells and NK cells. Journal of immunology (Baltimore, Md. : 1950) *191*, 1486-1495.

Ilangumaran, S., Finan, D., La Rose, J., Raine, J., Silverstein, A., Sepulveda, P. de, and Rottapel, R. (2002). A positive regulatory role for suppressor of cytokine signaling 1 in IFN-gamma-induced MHC class II expression in fibroblasts. Journal of immunology (Baltimore, Md. : 1950) *169*, 5010-5020.

Jacobs, S.R., Herman, C.E., Maciver, N.J., Wofford, J.A., Wieman, H.L., Hammen, J.J., and Rathmell, J.C. (2008). Glucose uptake is limiting in T cell activation and requires CD28-mediated Akt-dependent and independent pathways. Journal of immunology (Baltimore, Md. : 1950) *180*, 4476-4486.

Jenkins, Y., Zabkiewicz, J., Ottmann, O., and Jones, N. (2021). Tinkering under the Hood: Metabolic Optimisation of CAR-T Cell Therapy. Antibodies (Basel, Switzerland) *10*.

Jha, M.K., Passero, J.V., Rawat, A., Ament, X.H., Yang, F., Vidensky, S., Collins, S.L., Horton, M.R., Hoke, A., and Rutter, G.A., et al. (2021). Macrophage monocarboxylate

transporter 1 promotes peripheral nerve regeneration after injury in mice. The Journal of clinical investigation *131*.

Johnson, L.A., Morgan, R.A., Dudley, M.E., Cassard, L., Yang, J.C., Hughes, M.S., Kammula, U.S., Royal, R.E., Sherry, R.M., and Wunderlich, J.R., et al. (2009). Gene therapy with human and mouse T-cell receptors mediates cancer regression and targets normal tissues expressing cognate antigen. Blood *114*, 535-546.

Jones, N., Cronin, J.G., Dolton, G., Panetti, S., Schauenburg, A.J., Galloway, S.A.E., Sewell, A.K., Cole, D.K., Thornton, C.A., and Francis, N.J. (2017). Metabolic Adaptation of Human CD4+ and CD8+ T-Cells to T-Cell Receptor-Mediated Stimulation. Frontiers in immunology *8*, 1516.

Jones, R.G., and Thompson, C.B. (2007). Revving the engine: signal transduction fuels T cell activation. Immunity *27*, 173-178.

Ju, H.-Q., Lin, J.-F., Tian, T., Xie, D., and Xu, R.-H. (2020). NADPH homeostasis in cancer: functions, mechanisms and therapeutic implications. Sig Transduct Target Ther *5*, 231.

Justus, C.R., Dong, L., and Yang, L.V. (2013). Acidic tumor microenvironment and pH-sensing G protein-coupled receptors. Frontiers in Physiology *4*, 354.

Kaliamurthi, S., Selvaraj, G., Junaid, M., Khan, A., Gu, K., and Wei, D.-Q. (2018). Cancer Immunoinformatics: A Promising Era in the Development of Peptide Vaccines for Human Papillomavirus-induced Cervical Cancer. CPD *24*, 3791-3817.

Kareva, I., and Hahnfeldt, P. (2013). The emerging "hallmarks" of metabolic reprogramming and immune evasion: distinct or linked? Cancer research *73*, 2737-2742.

Kim, W.Y., and Kaelin, W.G. (2004). Role of VHL gene mutation in human cancer. Journal of clinical oncology : official journal of the American Society of Clinical Oncology *22*, 4991-5004.

Klebanoff, C.A., Crompton, J.G., Leonardi, A.J., Yamamoto, T.N., Chandran, S.S., Eil, R.L., Sukumar, M., Vodnala, S.K., Hu, J., and Ji, Y., et al. (2017). Inhibition of AKT signaling uncouples T cell differentiation from expansion for receptor-engineered adoptive immunotherapy. JCI insight *2*.

Klebanoff, C.A., Finkelstein, S.E., Surman, D.R., Lichtman, M.K., Gattinoni, L., Theoret, M.R., Grewal, N., Spiess, P.J., Antony, P.A., and Palmer, D.C., et al. (2004). IL-15 enhances the in vivo antitumor activity of tumor-reactive CD8+ T cells. Proceedings of the National Academy of Sciences of the United States of America *101*, 1969-1974.

Klein Geltink, R.I., Edwards-Hicks, J., Apostolova, P., O'Sullivan, D., Sanin, D.E., Patterson, A.E., Puleston, D.J., Ligthart, N.A.M., Buescher, J.M., and Grzes, K.M., et al. (2020). Metabolic conditioning of CD8+ effector T cells for adoptive cell therapy. Nature metabolism *2*, 703-716.

Klein Geltink, R.I., O'Sullivan, D., Corrado, M., Bremser, A., Buck, M.D., Buescher, J.M., Firat, E., Zhu, X., Niedermann, G., and Caputa, G., et al. (2017). Mitochondrial Priming by CD28. Cell *171*, 385-397.e11.

Kornberg, M.D., Bhargava, P., Kim, P.M., Putluri, V., Snowman, A.M., Putluri, N., Calabresi, P.A., and Snyder, S.H. (2018). Dimethyl fumarate targets GAPDH and aerobic glycolysis to modulate immunity. Science (New York, N.Y.) *360*, 449-453.

Kosti, P., Maher, J., and Arnold, J.N. (2018). Perspectives on Chimeric Antigen Receptor T-Cell Immunotherapy for Solid Tumors. Frontiers in immunology *9*, 1104.

Krauss, S., Brand, M.D., and Buttgereit, F. (2001). Signaling Takes a Breath – New Quantitative Perspectives on Bioenergetics and Signal Transduction. Immunity *15*, 497-502.

Kuleshov, M.V., Jones, M.R., Rouillard, A.D., Fernandez, N.F., Duan, Q., Wang, Z., Koplev, S., Jenkins, S.L., Jagodnik, K.M., and Lachmann, A., et al. (2016). Enrichr: a comprehensive gene set enrichment analysis web server 2016 update. Nucleic Acids Res *44*, W90-7.

Ledderose, C., Bao, Y., Lidicky, M., Zipperle, J., Li, L., Strasser, K., Shapiro, N.I., and Junger, W.G. (2014). Mitochondria are gate-keepers of T cell function by producing the ATP that drives purinergic signaling. J. Biol. Chem. *289*, 25936-25945.

Leone, R.D., and Powell, J.D. (2020). Metabolism of immune cells in cancer. Nature reviews. Cancer *20*, 516-531.

Li, S.S. (1989). Lactate dehydrogenase isoenzymes A (muscle), B (heart) and C (testis) of mammals and the genes coding for these enzymes. Biochemical Society transactions *17*, 304-307.

Liu, M., Wang, X., Wang, L., Ma, X., Gong, Z., Zhang, S., and Li, Y. (2018). Targeting the IDO1 pathway in cancer: from bench to bedside. Journal of hematology & oncology *11*, 100.

Liu, Y., Lin, P., Zhao, Y., Wu, L.-Y., Wu, Y., Peng, J., He, Y., and Yang, H. (2021). Pan-cancer analysis of clinical significance and associated molecular features of glycolysis. Bioengineered *12*, 4233-4246.

Loschinski, R., Böttcher, M., Stoll, A., Bruns, H., Mackensen, A., and Mougiakakos, D. (2018). IL-21 modulates memory and exhaustion phenotype of T-cells in a fatty acid oxidation-dependent manner. Oncotarget *9*, 13125-13138.

Lu, H., Forbes, R.A., and Verma, A. (2002). Hypoxia-inducible factor 1 activation by aerobic glycolysis implicates the Warburg effect in carcinogenesis. The Journal of biological chemistry *277*, 23111-23115.

Luengo, A., Li, Z., Gui, D.Y., Sullivan, L.B., Zagorulya, M., Do, B.T., Ferreira, R., Naamati, A., Ali, A., and Lewis, C.A., et al. (2021). Increased demand for NAD+ relative to ATP drives aerobic glycolysis. Molecular Cell *81*, 691-707.e6.

Lugli, E., Dominguez, M.H., Gattinoni, L., Chattopadhyay, P.K., Bolton, D.L., Song, K., Klatt, N.R., Brenchley, J.M., Vaccari, M., and Gostick, E., et al. (2013). Superior T memory stem cell persistence supports long-lived T cell memory. The Journal of clinical investigation *123*, 594-599.

Macintyre, A.N., Gerriets, V.A., Nichols, A.G., Michalek, R.D., Rudolph, M.C., Deoliveira, D., Anderson, S.M., Abel, E.D., Chen, B.J., and Hale, L.P., et al. (2014). The glucose transporter Glut1 is selectively essential for CD4 T cell activation and effector function. Cell Metabolism *20*, 61-72.

Mack, N., Mazzio, E.A., Bauer, D., Flores-Rozas, H., and Soliman, K.F.A. (2017). Stable shRNA Silencing of Lactate Dehydrogenase A (LDHA) in Human MDA-MB-231 Breast Cancer Cells Fails to Alter Lactic Acid Production, Glycolytic Activity, ATP or Survival. Anticancer research *37*, 1205-1212.

Marinkovic, D., Marinkovic, T., Kokai, E., Barth, T., Möller, P., and Wirth, T. (2004). Identification of novel Myc target genes with a potential role in lymphomagenesis. Nucleic Acids Res *32*, 5368-5378.

Markert, C.L., Shaklee, J.B., and Whitt, G.S. (1975). Evolution of a gene. Science (New York, N.Y.) *189*, 102-114.

Marshall, O.J. (2004). PerlPrimer: cross-platform, graphical primer design for standard, bisulphite and real-time PCR. Bioinformatics (Oxford, England) *20*, 2471-2472.

Masoumi, E., Jafarzadeh, L., Mirzaei, H.R., Alishah, K., Fallah-Mehrjardi, K., Rostamian, H., Khakpoor-Koosheh, M., Meshkani, R., Noorbakhsh, F., and Hadjati, J. (2020). Genetic and pharmacological targeting of A2a receptor improves function of anti-mesothelin CAR T cells. J Exp Clin Cancer Res *39*, 49.

Matoba, S., Kang, J.-G., Patino, W.D., Wragg, A., Boehm, M., Gavrilova, O., Hurley, P.J., Bunz, F., and Hwang, P.M. (2006). p53 regulates mitochondrial respiration. Science (New York, N.Y.) *312*, 1650-1653.

Mehta, M.M., Weinberg, S.E., and Chandel, N.S. (2017). Mitochondrial control of immunity: beyond ATP. Nat Rev Immunol *17*, 608-620.

Mekhail, K., Gunaratnam, L., Bonicalzi, M.-E., and Lee, S. (2004). HIF activation by pH-dependent nucleolar sequestration of VHL. Nature cell biology *6*, 642-647.

Mendler, A.N., Hu, B., Prinz, P.U., Kreutz, M., Gottfried, E., and Noessner, E. (2012). Tumor lactic acidosis suppresses CTL function by inhibition of p38 and JNK/c-Jun activation. International journal of cancer *131*, 633-640.

Menk, A.V., Scharping, N.E., Moreci, R.S., Zeng, X., Guy, C., Salvatore, S., Bae, H., Xie, J., Young, H.A., and Wendell, S.G., et al. (2018). Early TCR Signaling Induces Rapid Aerobic Glycolysis Enabling Distinct Acute T Cell Effector Functions. Cell reports *22*, 1509-1521.

Menkin, V. (1956). Biology of inflammation; chemical mediators and cellular injury. Science (New York, N.Y.) *123*, 527-534.

Met, Ö., Jensen, K.M., Chamberlain, C.A., Donia, M., and Svane, I.M. (2019). Principles of adoptive T cell therapy in cancer. Semin Immunopathol *41*, 49-58.

Michalek, R.D., Gerriets, V.A., Jacobs, S.R., Macintyre, A.N., Maciver, N.J., Mason, E.F., Sullivan, S.A., Nichols, A.G., and Rathmell, J.C. (2011). Cutting edge: distinct glycolytic and lipid oxidative metabolic programs are essential for effector and regulatory CD4+ T cell subsets. The Journal of Immunology *186*, 3299-3303.

Monroe, G.R., van Eerde, A.M., Tessadori, F., Duran, K.J., Savelberg, S.M.C., van Alfen, J.C., Terhal, P.A., van der Crabben, S.N., Lichtenbelt, K.D., and Fuchs, S.A., et al. (2019). Identification of human D lactate dehydrogenase deficiency. Nat Commun *10*, 1477.

Morgan, R.A., Dudley, M.E., Wunderlich, J.R., Hughes, M.S., Yang, J.C., Sherry, R.M., Royal, R.E., Topalian, S.L., Kammula, U.S., and Restifo, N.P., et al. (2006). Cancer regression in patients after transfer of genetically engineered lymphocytes. Science *314*, 126-129.

Moss, P.A., Rosenberg, W.M., and Bell, J.I. (1992). The human T cell receptor in health and disease. Annual review of immunology *10*, 71-96.

Mullard, A. (2021). FDA approves fourth CAR-T cell therapy. Nature reviews. Drug discovery *20*, 166.

Murphy, K.M., and Weaver, C. (2017). Janeway's immunobiology (New York, London: GS Garland Science Taylor & Francis Group).

Nakajima, T., Schulte, S., Warrington, K.J., Kopecky, S.L., Frye, R.L., Goronzy, J.J., and Weyand, C.M. (2002). T-cell-mediated lysis of endothelial cells in acute coronary syndromes. Circulation *105*, 570-575.

Newick, K., O'Brien, S., Moon, E., and Albelda, S.M. (2017). CAR T Cell Therapy for Solid Tumors. Annual review of medicine *68*, 139-152.

Newick, K., O'Brien, S., Sun, J., Kapoor, V., Maceyko, S., Lo, A., Puré, E., Moon, E., and Albelda, S.M. (2016). Augmentation of CAR T-cell Trafficking and Antitumor Efficacy by Blocking Protein Kinase A Localization. Cancer Immunol Res *4*, 541-551.

Obre, E., and Rossignol, R. (2015). Emerging concepts in bioenergetics and cancer research: metabolic flexibility, coupling, symbiosis, switch, oxidative tumors, metabolic remodeling, signaling and bioenergetic therapy. The international journal of biochemistry & cell biology *59*, 167-181.

Ohashi, T., Aoki, M., Tomita, H., Akazawa, T., Sato, K., Kuze, B., Mizuta, K., Hara, A., Nagaoka, H., and Inoue, N., et al. (2017). M2-like macrophage polarization in high lactic acid-producing head and neck cancer. Cancer science *108*, 1128-1134.

Okamura, H., Kashiwamura, S., Tsutsui, H., Yoshimoto, T., and Nakanishi, K. (1998). Regulation of interferon-γ production by IL-12 and IL-18. Current Opinion in Immunology *10*, 259-264.

Ossendorp, F., Mengedé, E., Camps, M., Filius, R., and Melief, C.J. (1998). Specific T helper cell requirement for optimal induction of cytotoxic T lymphocytes against major histocompatibility complex class II negative tumors. The Journal of experimental medicine *187*, 693-702.

Osthus, R.C., Shim, H., Kim, S., Li, Q., Reddy, R., Mukherjee, M., Xu, Y., Wonsey, D., Lee, L.A., and Dang, C.V. (2000). Deregulation of glucose transporter 1 and glycolytic gene expression by c-Myc. The Journal of biological chemistry *275*, 21797-21800.

O'Sullivan, D., and Pearce, E.L. (2015). Targeting T cell metabolism for therapy. Trends in immunology *36*, 71-80.

O'Sullivan, D., van der Windt, G.J.W., Huang, S.C.-C., Curtis, J.D., Chang, C.-H., Buck, M.D., Qiu, J., Smith, A.M., Lam, W.Y., and DiPlato, L.M., et al. (2014). Memory CD8(+) T cells use cell-intrinsic lipolysis to support the metabolic programming necessary for development. Immunity *41*, 75-88.

Ottensmeier, C.H., Perry, K.L., Harden, E.L., Stasakova, J., Jenei, V., Fleming, J., Wood, O., Woo, J., Woelk, C.H., and Thomas, G.J., et al. (2016). Upregulated Glucose Metabolism Correlates Inversely with CD8+ T-cell Infiltration and Survival in Squamous Cell Carcinoma. Cancer research *76*, 4136-4148.

Parkin, J., and Cohen, B. (2001). An overview of the immune system. The Lancet *357*, 1777-1789.

Parks, S.K., and Pouysségur, J. (2017). Targeting pH regulating proteins for cancer therapy-Progress and limitations. Seminars in cancer biology *43*, 66-73.

Pawelczyk, T., and Olson, M.S. (1992). Regulation of pyruvate dehydrogenase kinase activity from pig kidney cortex. Biochem J *288 (Pt 2)*, 369-373.

Pearce, E.L., Walsh, M.C., Cejas, P.J., Harms, G.M., Shen, H., Wang, L.-S., Jones, R.G., and Choi, Y. (2009). Enhancing CD8 T-cell memory by modulating fatty acid metabolism. Nature *460*, 103-107.

Peng, M., Yin, N., Chhangawala, S., Xu, K., Leslie, C.S., and Li, M.O. (2016). Aerobic glycolysis promotes T helper 1 cell differentiation through an epigenetic mechanism. Science (New York, N.Y.) *354*, 481-484.

Perkins, M.R., Grande, S., Hamel, A., Horton, H.M., Garrett, T.E., Miller, S.M., Latimer, H.J., Horvath, C.J., Kuczewski, M., and Friedman, K.M., et al. (2015). Manufacturing an Enhanced CAR T Cell Product By Inhibition of the PI3K/Akt Pathway During T Cell Expansion Results in Improved In Vivo Efficacy of Anti-BCMA CAR T Cells. Blood *126*, 1893.

Piasentin, N., Milotti, E., and Chignola, R. (2020). The control of acidity in tumor cells: a biophysical model. Sci Rep *10*, 13613.

Pilon-Thomas, S., Kodumudi, K.N., El-Kenawi, A.E., Russell, S., Weber, A.M., Luddy, K., Damaghi, M., Wojtkowiak, J.W., Mulé, J.J., and Ibrahim-Hashim, A., et al. (2016). Neutralization of Tumor Acidity Improves Antitumor Responses to Immunotherapy. Cancer research, 1381-1390.

Pollizzi, K.N., Patel, C.H., Sun, I.-H., Oh, M.-H., Waickman, A.T., Wen, J., Delgoffe, G.M., and Powell, J.D. (2015). mTORC1 and mTORC2 selectively regulate $CD8^+$ T cell differentiation. The Journal of clinical investigation *125*, 2090-2108.

Porporato, P.E., Dhup, S., Dadhich, R.K., Copetti, T., and Sonveaux, P. (2011). Anticancer targets in the glycolytic metabolism of tumors: a comprehensive review. Frontiers in pharmacology *2*, 49.

Propper, D.J., Chao, D., Braybrooke, J.P., Bahl, P., Thavasu, P., Balkwill, F., Turley, H., Dobbs, N., Gatter, K., and Talbot, D.C., et al. (2003). Low-dose IFN-gamma induces tumor MHC expression in metastatic malignant melanoma. Clin Cancer Res *9*, 84-92.

Pucino, V., Certo, M., Bulusu, V., Cucchi, D., Goldmann, K., Pontarini, E., Haas, R., Smith, J., Headland, S.E., and Blighe, K., et al. (2019). Lactate Buildup at the Site of Chronic Inflammation Promotes Disease by Inducing CD4+ T Cell Metabolic Rewiring. Cell Metabolism *30*, 1055-1074.e8.

Quezada, S.A., Simpson, T.R., Peggs, K.S., Merghoub, T., Vider, J., Fan, X., Blasberg, R., Yagita, H., Muranski, P., and Antony, P.A., et al. (2010). Tumor-reactive CD4(+) T cells develop cytotoxic activity and eradicate large established melanoma after transfer into lymphopenic hosts. The Journal of experimental medicine *207*, 637-650.

Quinn, W.J., Jiao, J., TeSlaa, T., Stadanlick, J., Wang, Z., Wang, L., Akimova, T., Angelin, A., Schäfer, P.M., and Cully, M.D., et al. (2020). Lactate Limits T Cell Proliferation via the NAD(H) Redox State. Cell Reports *33*, 108500.

Rabinowitz, J.D., and Enerbäck, S. (2020). Lactate: the ugly duckling of energy metabolism. Nat Metab *2*, 566-571.

Rad S M, A.H., Halpin, J.C., Mollaei, M., Smith Bell, S.W.J., Hirankarn, N., and McLellan, A.D. (2021). Metabolic and Mitochondrial Functioning in Chimeric Antigen Receptor (CAR)-T Cells. Cancers *13*, 1229.

Rao, R.R., Li, Q., Odunsi, K., and Shrikant, P.A. (2010). The mTOR kinase determines effector versus memory CD8+ T cell fate by regulating the expression of transcription factors T-bet and Eomesodermin. Immunity *32*, 67-78.

Raphael, I., Joern, R.R., and Forsthuber, T.G. (2020). Memory CD4+ T Cells in Immunity and Autoimmune Diseases. Cells *9*.

Rapoport, A.P., Stadtmauer, E.A., Binder-Scholl, G.K., Goloubeva, O., Vogl, D.T., Lacey, S.F., Badros, A.Z., Garfall, A., Weiss, B., and Finklestein, J., et al. (2015). NY-ESO-1-specific TCR-engineered T cells mediate sustained antigen-specific antitumor effects in myeloma. Nat Med *21*, 914-921.

Raud, B., Roy, D.G., Divakaruni, A.S., Tarasenko, T.N., Franke, R., Ma, E.H., Samborska, B., Hsieh, W.Y., Wong, A.H., and Stüve, P., et al. (2018). Etomoxir Actions on Regulatory and Memory T Cells Are Independent of Cpt1a-Mediated Fatty Acid Oxidation. Cell Metabolism *28*, 504-515.e7.

Reed, C.M., Cresce, N.D., Mauldin, I.S., Slingluff, C.L., and Olson, W.C. (2015). Vaccination with Melanoma Helper Peptides Induces Antibody Responses Associated with Improved Overall Survival. Clin Cancer Res *21*, 3879-3887.

Renner, K., Bruss, C., Schnell, A., Koehl, G., Becker, H.M., Fante, M., Menevse, A.-N., Kauer, N., Blazquez, R., and Hacker, L., et al. (2019). Restricting Glycolysis Preserves T Cell Effector Functions and Augments Checkpoint Therapy. Cell reports *29*, 135-150.e9.

Renner, K., Geiselhöringer, A.-L., Fante, M., Bruss, C., Färber, S., Schönhammer, G., Peter, K., Singer, K., Andreesen, R., and Hoffmann, P., et al. (2015). Metabolic plasticity of human T cells: Preserved cytokine production under glucose deprivation or mitochondrial restriction, but 2-deoxy-glucose affects effector functions. European journal of immunology *45*, 2504-2516.

Renner, K., Singer, K., Koehl, G.E., Geissler, E.K., Peter, K., Siska, P.J., and Kreutz, M. (2017). Metabolic Hallmarks of Tumor and Immune Cells in the Tumor Microenvironment. Frontiers in immunology *8*, 248.

Rivadeneira, D.B., and Delgoffe, G.M. (2018). Antitumor T-cell Reconditioning: Improving Metabolic Fitness for Optimal Cancer Immunotherapy. Clin Cancer Res *24*, 2473-2481.

Robbins, P.F., Morgan, R.A., Feldman, S.A., Yang, J.C., Sherry, R.M., Dudley, M.E., Wunderlich, J.R., Nahvi, A.V., Helman, L.J., and Mackall, C.L., et al. (2011). Tumor regression in patients with metastatic synovial cell sarcoma and melanoma using genetically engineered lymphocytes reactive with NY-ESO-1. Journal of clinical oncology : official journal of the American Society of Clinical Oncology *29*, 917-924.

Rohwer, N., Dame, C., Haugstetter, A., Wiedenmann, B., Detjen, K., Schmitt, C.A., and Cramer, T. (2010). Hypoxia-inducible factor 1alpha determines gastric cancer chemosensitivity via modulation of p53 and NF-kappaB. PloS one *5*, e12038.

Safinia, N., Scotta, C., Vaikunthanathan, T., Lechler, R.I., and Lombardi, G. (2015). Regulatory T Cells: Serious Contenders in the Promise for Immunological Tolerance in Transplantation. Frontiers in immunology *6*, 438.

Salerno, F., Guislain, A., Cansever, D., and Wolkers, M.C. (2016). TLR-Mediated Innate Production of IFN-γ by CD8+ T Cells Is Independent of Glycolysis. The Journal of Immunology *196*, 3695-3705.

Sanchez, J., Jackson, I., Flaherty, K.R., Muliaditan, T., and Schurich, A. (2020). Divergent Impact of Glucose Availability on Human Virus-Specific and Generically Activated CD8 T Cells. Metabolites *10*.

Sandvig, K., Olsnes, S., Petersen, O.W., and van Deurs, B. (1987). Acidification of the cytosol inhibits endocytosis from coated pits. The Journal of cell biology *105*, 679-689.

Sanford Health (2020). Phase II Study of DCA (Dichloroacetate) in Combination With Cisplatin and Definitive Radiation in Stage III-IV Squamous Cell Carcinoma of the Head and Neck. NCT01386632, DCA 2010. https://clinicaltrials.gov/ct2/show/NCT01386632. 16.03.2021.

San-Millán, I., and Brooks, G.A. (2017). Reexamining cancer metabolism: lactate production for carcinogenesis could be the purpose and explanation of the Warburg Effect. Carcinogenesis *38*, 119-133.

Scharping, N.E., Menk, A.V., Moreci, R.S., Whetstone, R.D., Dadey, R.E., Watkins, S.C., Ferris, R.L., and Delgoffe, G.M. (2016). The Tumor Microenvironment Represses T Cell Mitochondrial Biogenesis to Drive Intratumoral T Cell Metabolic Insufficiency and Dysfunction. Immunity *45*, 374-388.

Sellers, K., Fox, M.P., Bousamra, M., Slone, S.P., Higashi, R.M., Miller, D.M., Wang, Y., Yan, J., Yuneva, M.O., and Deshpande, R., et al. (2015). Pyruvate carboxylase is critical for non-small-cell lung cancer proliferation. The Journal of clinical investigation *125*, 687-698.

Semenza, G.L. (2002). HIF-1 and tumor progression: pathophysiology and therapeutics. Trends in Molecular Medicine *8*, S62-S67.

Semenza, G.L. (2008). Tumor metabolism: cancer cells give and take lactate. The Journal of clinical investigation *118*, 3835-3837.

Semenza, G.L. (2009). Regulation of oxygen homeostasis by hypoxia-inducible factor 1. Physiology (Bethesda, Md.) *24*, 97-106.

Semenza, G.L. (2010). Oxygen homeostasis. Wiley interdisciplinary reviews. Systems biology and medicine *2*, 336-361.

Sena, L.A., Li, S., Jairaman, A., Prakriya, M., Ezponda, T., Hildeman, D.A., Wang, C.-R., Schumacker, P.T., Licht, J.D., and Perlman, H., et al. (2013). Mitochondria are required for antigen-specific T cell activation through reactive oxygen species signaling. Immunity *38*, 225-236.

Shim, H., Dolde, C., Lewis, B.C., Wu, C.S., Dang, G., Jungmann, R.A., Dalla-Favera, R., and Dang, C.V. (1997). c-Myc transactivation of LDH-A: implications for tumor metabolism and growth. Proceedings of the National Academy of Sciences *94*, 6658-6663.

Shime, H., Yabu, M., Akazawa, T., Kodama, K., Matsumoto, M., Seya, T., and Inoue, N. (2008). Tumor-secreted lactic acid promotes IL-23/IL-17 proinflammatory pathway. Journal of immunology (Baltimore, Md. : 1950) *180*, 7175-7183.

Singer, K., Gottfried, E., Kreutz, M., and Mackensen, A. (2011). Suppression of T-cell responses by tumor metabolites. Cancer immunology, immunotherapy : CII *60*, 425-431.

Siska, P.J., Beckermann, K.E., Mason, F.M., Andrejeva, G., Greenplate, A.R., Sendor, A.B., Chiang, Y.-C.J., Corona, A.L., Gemta, L.F., and Vincent, B.G., et al. (2017). Mitochondrial dysregulation and glycolytic insufficiency functionally impair CD8 T cells infiltrating human renal cell carcinoma. JCI insight *2*.

Siska, P.J., Decking, S.-M., Babl, N., Matos, C., Bruss, C., Singer, K., Klitzke, J., Schön, M., Simeth, J., and Köstler, J., et al. (2021). Metabolic imbalance of T cells in COVID-19 is hallmarked by basigin and mitigated by dexamethasone. The Journal of clinical investigation *131*.

Sojka, D.K., Huang, Y.-H., and Fowell, D.J. (2008). Mechanisms of regulatory T-cell suppression - a diverse arsenal for a moving target. Immunology *124*, 13-22.

Song, J., Lee, K., Park, S.W., Chung, H., Jung, D., Na, Y.R., Quan, H., Cho, C.S., Che, J.-H., and Kim, J.H., et al. (2018). Lactic Acid Upregulates VEGF Expression in Macrophages and Facilitates Choroidal Neovascularization. Invest. Ophthalmol. Vis. Sci. *59*, 3747-3754.

Sonveaux, P., Copetti, T., Saedeleer, C.J. de, Végran, F., Verrax, J., Kennedy, K.M., Moon, E.J., Dhup, S., Danhier, P., and Frérart, F., et al. (2012). Targeting the lactate transporter MCT1 in endothelial cells inhibits lactate-induced HIF-1 activation and tumor angiogenesis. PloS one *7*, e33418.

Steinman, R.M., and Banchereau, J. (2007). Taking dendritic cells into medicine. Nature *449*, 419-426.

Sukumar, M., Liu, J., Ji, Y., Subramanian, M., Crompton, J.G., Yu, Z., Roychoudhuri, R., Palmer, D.C., Muranski, P., and Karoly, E.D., et al. (2013). Inhibiting glycolytic metabolism

enhances CD8+ T cell memory and antitumor function. The Journal of clinical investigation *123*, 4479-4488.

Suzuki, Y., Inoue, T., and Ra, C. (2010). NSAIDs, Mitochondria and Calcium Signaling: Special Focus on Aspirin/Salicylates. Pharmaceuticals (Basel, Switzerland) *3*, 1594-1613.

Szabo, P.A., Miron, M., and Farber, D.L. (2019). Location, location, location: Tissue resident memory T cells in mice and humans. Science immunology *4*.

Tan, H., Yang, K., Li, Y., Shaw, T.I., Wang, Y., Blanco, D.B., Wang, X., Cho, J.-H., Wang, H., and Rankin, S., et al. (2017). Integrative Proteomics and Phosphoproteomics Profiling Reveals Dynamic Signaling Networks and Bioenergetics Pathways Underlying T Cell Activation. Immunity *46*, 488-503.

Tan, Z., Xie, N., Banerjee, S., Cui, H., Fu, M., Thannickal, V.J., and Liu, G. (2015). The monocarboxylate transporter 4 is required for glycolytic reprogramming and inflammatory response in macrophages. J. Biol. Chem. *290*, 46-55.

Tanaka, K., Tomisato, W., Hoshino, T., Ishihara, T., Namba, T., Aburaya, M., Katsu, T., Suzuki, K., Tsutsumi, S., and Mizushima, T. (2005). Involvement of intracellular Ca2+ levels in nonsteroidal anti-inflammatory drug-induced apoptosis. The Journal of biological chemistry *280*, 31059-31067.

Tang, P., Xu, J., Oliveira, C.L., Li, Z.J., and Liu, S. (2017). A mechanistic kinetic description of lactate dehydrogenase elucidating cancer diagnosis and inhibitor evaluation. Journal of enzyme inhibition and medicinal chemistry *32*, 564-571.

Tay, R.E., Richardson, E.K., and Toh, H.C. (2021). Revisiting the role of CD4+ T cells in cancer immunotherapy-new insights into old paradigms. Cancer Gene Ther *28*, 5-17.

Teixeira, J., Basit, F., Swarts, H.G., Forkink, M., Oliveira, P.J., Willems, P.H.G.M., and Koopman, W.J.H. (2018). Extracellular acidification induces ROS- and mPTP-mediated death in HEK293 cells. Redox Biology *15*, 394-404.

Toes, R.E., Ossendorp, F., Offringa, R., and Melief, C.J. (1999). CD4 T cells and their role in antitumor immune responses. The Journal of experimental medicine *189*, 753-756.

Tran, E., Turcotte, S., Gros, A., Robbins, P.F., Lu, Y.-C., Dudley, M.E., Wunderlich, J.R., Somerville, R.P., Hogan, K., and Hinrichs, C.S., et al. (2014). Cancer immunotherapy based on mutation-specific CD4+ T cells in a patient with epithelial cancer. Science *344*, 641-645.

Trapani, J.A., and Smyth, M.J. (2002). Functional significance of the perforin/granzyme cell death pathway. Nature reviews. Immunology *2*, 735-747.

Turvey, S.E., and Broide, D.H. (2010). Innate immunity. The Journal of allergy and clinical immunology *125*, S24-32.

Uhl, F.M., Chen, S., O'Sullivan, D., Edwards-Hicks, J., Richter, G., Haring, E., Andrieux, G., Halbach, S., Apostolova, P., and Büscher, J., et al. (2020). Metabolic reprogramming of donor T cells enhances graft-versus-leukemia effects in mice and humans. Sci. Transl. Med. *12*.

Uhlen, M., Karlsson, M.J., Zhong, W., Tebani, A., Pou, C., Mikes, J., Lakshmikanth, T., Forsström, B., Edfors, F., and Odeberg, J., et al. (2019). A genome-wide transcriptomic analysis of protein-coding genes in human blood cells. Science *366*, eaax9198.

Unruh, A., Ressel, A., Mohamed, H.G., Johnson, R.S., Nadrowitz, R., Richter, E., Katschinski, D.M., and Wenger, R.H. (2003). The hypoxia-inducible factor-1 alpha is a negative factor for tumor therapy. Oncogene *22*, 3213-3220.

van Bruggen, J.A.C., Martens, A.W.J., Fraietta, J.A., Hofland, T., Tonino, S.H., Eldering, E., Levin, M.-D., Siska, P.J., Endstra, S., and Rathmell, J.C., et al. (2019). Chronic lymphocytic leukemia cells impair mitochondrial fitness in CD8+ T cells and impede CAR T-cell efficacy. Blood *134*, 44-58.

van der Windt, G.J.W., Everts, B., Chang, C.-H., Curtis, J.D., Freitas, T.C., Amiel, E., Pearce, E.J., and Pearce, E.L. (2012). Mitochondrial respiratory capacity is a critical regulator of CD8+ T cell memory development. Immunity *36*, 68-78.

van der Windt, G.J.W., O'Sullivan, D., Everts, B., Huang, S.C.-C., Buck, M.D., Curtis, J.D., Chang, C.-H., Smith, A.M., Ai, T., and Faubert, B., et al. (2013). CD8 memory T cells have a bioenergetic advantage that underlies their rapid recall ability. Proceedings of the National Academy of Sciences of the United States of America *110*, 14336-14341.

van Leemputte, F., Vanthienen, W., Wijnants, S., van Zeebroeck, G., and Thevelein, J.M. (2020). Aberrant Intracellular pH Regulation Limiting Glyceraldehyde-3-Phosphate Dehydrogenase Activity in the Glucose-Sensitive Yeast tps1Δ Mutant. mBio *11*.

Vesell, E.S. (1965). Lactate dehydrogenase Isozymes: substrate inhibition in various human tissues. Science (New York, N.Y.) *150*, 1590-1593.

Walenta, S., and Mueller-Klieser, W.F. (2004). Lactate: mirror and motor of tumor malignancy. Seminars in radiation oncology *14*, 267-274.

Walenta, S., Salameh, A., Lyng, H., Evensen, J.F., Mitze, M., Rofstad, E.K., and Mueller-Klieser, W. (1997). Correlation of high lactate levels in head and neck tumors with incidence of metastasis. The American Journal of Pathology *150*, 409-415.

Walenta, S., Wetterling, M., Lehrke, M., Schwickert, G., Sundfør, K., Rofstad, E.K., and Mueller-Klieser, W. (2000). High lactate levels predict likelihood of metastases, tumor recurrence, and restricted patient survival in human cervical cancers. Cancer research *60*, 916-921.

Wang, R., Dillon, C.P., Shi, L.Z., Milasta, S., Carter, R., Finkelstein, D., McCormick, L.L., Fitzgerald, P., Chi, H., and Munger, J., et al. (2011). The transcription factor Myc controls metabolic reprogramming upon T lymphocyte activation. Immunity *35*, 871-882.

Warburg, O., Wind, F., and Negelein, E. (1927). The metabolism of tumors in the body. The Journal of General Physiology, 519-530.

Ward, F.J., Dahal, L.N., Wijesekera, S.K., Abdul-Jawad, S.K., Kaewarpai, T., Xu, H., Vickers, M.A., and Barker, R.N. (2013). The soluble isoform of CTLA-4 as a regulator of T-cell responses. European journal of immunology *43*, 1274-1285.

Waring, P., and Müllbacher, A. (1999). Cell death induced by the Fas/Fas ligand pathway and its role in pathology. Immunology and cell biology *77*, 312-317.

Watson, M.J., Vignali, P.D.A., Mullett, S.J., Overacre-Delgoffe, A.E., Peralta, R.M., Grebinoski, S., Menk, A.V., Rittenhouse, N.L., DePeaux, K., and Whetstone, R.D., et al. (2021). Metabolic support of tumour-infiltrating regulatory T cells by lactic acid. Nature *591*, 645-651.

Wen, J., Cheng, S., Zhang, Y., Wang, R., Xu, J., Ling, Z., Ma, L., Ai, X., and Sun, B. (2021). Lactate anions participate in T cell cytokine production and function. Science China. Life sciences.

Wieczorek, M., Abualrous, E.T., Sticht, J., Álvaro-Benito, M., Stolzenberg, S., Noé, F., and Freund, C. (2017). Major Histocompatibility Complex (MHC) Class I and MHC Class II Proteins: Conformational Plasticity in Antigen Presentation. Frontiers in immunology *8*, 292.

Wieman, H.L., Wofford, J.A., and Rathmell, J.C. (2007). Cytokine stimulation promotes glucose uptake via phosphatidylinositol-3 kinase/Akt regulation of Glut1 activity and trafficking. Molecular biology of the cell *18*, 1437-1446.

Wilson, C.B., Rowell, E., and Sekimata, M. (2009). Epigenetic control of T-helper-cell differentiation. Nature reviews. Immunology *9*, 91-105.

Wu, H., Estrella, V., Beatty, M., Abrahams, D., El-Kenawi, A., Russell, S., Ibrahim-Hashim, A., Longo, D.L., Reshetnyak, Y.K., and Moshnikova, A., et al. (2020). T-cells produce acidic niches in lymph nodes to suppress their own effector functions. Nat Commun *11*, 4113.

Xie, H., Hanai, J.-I., Ren, J.-G., Kats, L., Burgess, K., Bhargava, P., Signoretti, S., Billiard, J., Duffy, K.J., and Grant, A., et al. (2014). Targeting lactate dehydrogenase--a inhibits tumorigenesis and tumor progression in mouse models of lung cancer and impacts tumor-initiating cells. Cell Metabolism *19*, 795-809.

Xie, Y., Shi, X., Sheng, K., Han, G., Li, W., Zhao, Q., Jiang, B., Feng, J., Li, J., and Gu, Y. (2019). PI3K/Akt signaling transduction pathway, erythropoiesis and glycolysis in hypoxia (Review). Molecular medicine reports *19*, 783-791.

Xie, Z., Bailey, A., Kuleshov, M.V., Clarke, D.J.B., Evangelista, J.E., Jenkins, S.L., Lachmann, A., Wojciechowicz, M.L., Kropiwnicki, E., and Jagodnik, K.M., et al. (2021). Gene Set Knowledge Discovery with Enrichr. Current protocols *1*, e90.

Xu, K., Yin, N., Peng, M., Stamatiades, E.G., Shyu, A., Li, P., Zhang, X., Do, M.H., Wang, Z., and Capistrano, K.J., et al. (2021). Glycolysis fuels phosphoinositide 3-kinase signaling to bolster T cell immunity. Science (New York, N.Y.) *371*, 405-410.

Yang, L., Pang, Y., and Moses, H.L. (2010). TGF-beta and immune cells: an important regulatory axis in the tumor microenvironment and progression. Trends in immunology *31*, 220-227.

Yang, L., Sanderlin, E., Justus, C., and Krewson, E. (2015). Emerging roles for the pH-sensing G protein-coupled receptors in response to acidotic stress. CHC, 99.

Yeung, C., Gibson, A.E., Issaq, S.H., Oshima, N., Baumgart, J.T., Edessa, L.D., Rai, G., Urban, D.J., Johnson, M.S., and Benavides, G.A., et al. (2019). Targeting Glycolysis through Inhibition of Lactate Dehydrogenase Impairs Tumor Growth in Preclinical Models of Ewing Sarcoma. Cancer research *79*, 5060-5073.

Younes, S.-A., Talla, A., Pereira Ribeiro, S., Saidakova, E.V., Korolevskaya, L.B., Shmagel, K.V., Shive, C.L., Freeman, M.L., Panigrahi, S., and Zweig, S., et al. (2018). Cycling CD4+ T cells in HIV-infected immune nonresponders have mitochondrial dysfunction. The Journal of clinical investigation *128*, 5083-5094.

Ždralević, M., Brand, A., Di Ianni, L., Dettmer, K., Reinders, J., Singer, K., Peter, K., Schnell, A., Bruss, C., and Decking, S.-M., et al. (2018). Double genetic disruption of lactate dehydrogenases A and B is required to ablate the "Warburg effect" restricting tumor growth to oxidative metabolism. J. Biol. Chem. *293*, 15947-15961.

Zeng, X., Liu, L., Zheng, M., Sun, H., Xiao, J., Lu, T., Huang, G., Chen, P., Zhang, J., and Zhu, F., et al. (2016). Pantoprazole, an FDA-approved proton-pump inhibitor, suppresses colorectal cancer growth by targeting T-cell-originated protein kinase. Oncotarget *7*, 22460-22473.

Zhang, L., Li, Y., Dai, Y., Wang, D., Wang, X., Cao, Y., Liu, W., and Tao, Z. (2021). Glycolysis-related gene expression profiling serves as a novel prognosis risk predictor for human hepatocellular carcinoma. Sci Rep *11*, 18875.

Zhang, Y., Kurupati, R., Liu, L., Zhou, X.Y., Zhang, G., Hudaihed, A., Filisio, F., Giles-Davis, W., Xu, X., and Karakousis, G.C., et al. (2017). Enhancing CD8+ T Cell Fatty Acid Catabolism within a Metabolically Challenging Tumor Microenvironment Increases the Efficacy of Melanoma Immunotherapy. Cancer cell *32*, 377-391.e9.

Zhang, Y.-X., Zhao, Y.-Y., Shen, J., Sun, X., Liu, Y., Liu, H., Wang, Y., and Wang, J. (2019). Nanoenabled Modulation of Acidic Tumor Microenvironment Reverses Anergy of Infiltrating T Cells and Potentiates Anti-PD-1 Therapy. Nano letters, 2774-2783.

Zhang, Z., Zi, Z., Lee, E.E., Zhao, J., Contreras, D.C., South, A.P., Abel, E.D., Chong, B.F., Vandergriff, T., and Hosler, G.A., et al. (2018). Differential glucose requirement in skin homeostasis and injury identifies a therapeutic target for psoriasis. Nature medicine *24*, 617-627.

Zhao, E., Maj, T., Kryczek, I., Li, W., Wu, K., Zhao, L., Wei, S., Crespo, J., Wan, S., and Vatan, L., et al. (2016). Cancer mediates effector T cell dysfunction by targeting microRNAs and EZH2 via glycolysis restriction. Nat Immunol *17*, 95-103.

Zhu, J., and Paul, W.E. (2008). CD4 T cells: fates, functions, and faults. Blood *112*, 1557-1569.

Publications

Ždralević, Maša; Brand, Almut; Di Ianni, Lorenza; Dettmer, Katja; Reinders, Jörg; Singer, Katrin; Peter, Katrin; Schnell, Annette; Bruss, Christina; **Decking, Sonja-Maria**; Koehl, Gudrun; Felipe-Abrio, Blanca; Durivault, Jérôme; Bayer, Pascale; Evangelista, Marie; O'Brien, Thomas; Oefner, Peter J.; Renner, Kathrin; Pouysségur, Jacques; Kreutz, Marina (2018): Double genetic disruption of lactate dehydrogenases A and B is required to ablate the "Warburg effect" restricting tumor growth to oxidative metabolism. In: The Journal of biological chemistry 293 (41), S. 15947–15961. DOI: 10.1074/jbc.RA118.004180.

Renner, Kathrin; Seilbeck, Anton; Kauer, Nathalie; Ugele, Ines; Siska, Peter J.; Brummer, Christina; Bruss, Christina; **Decking, Sonja-Maria**; Fante, Matthias; Schmidt, Astrid; Hammon, Kathrin; Singer, Katrin; Klobuch, Sebastian; Thomas, Simone; Gottfried, Eva; Peter, Katrin; Kreutz, Marina (2018): Combined Metabolic Targeting with Metformin and the NSAIDs Diflunisal and Diclofenac Induces Apoptosis in Acute Myeloid Leukemia Cells. In: Frontiers in pharmacology 9, S. 1258. DOI: 10.3389/fphar.2018.01258.

Renner, Kathrin; Bruss, Christina; Schnell, Annette; Koehl, Gudrun; Becker, Holger M.; Fante, Matthias; Menevse, Ayse-Nur; Kauer, Nathalie; Blazquez, Raquel; Hacker, Lisa; **Decking, Sonja-Maria**; Bohn, Toszka; Faerber, Stephanie; Evert, Katja; Aigle, Lisa; Amslinger, Sabine; Landa, Maria; Krijgsman, Oscar; Rozeman, Elisa A.; Brummer, Christina; Siska, Peter J.; Singer, Katrin; Pektor, Stefanie; Miederer, Matthias; Peter, Katrin; Gottfried, Eva; Herr, Wolfgang; Marchiq, Ibtisam; Pouyssegur, Jacques; Roush, William R.; Ong, SuFey; Warren, Sarah; Pukrop, Tobias; Beckhove, Philipp; Lang, Sven A.; Bopp, Tobias; Blank, Christian U.; Cleveland, John L.; Oefner, Peter J.; Dettmer, Katja; Selby, Mark; Kreutz, Marina (2019): Restricting Glycolysis Preserves T Cell Effector Functions and Augments Checkpoint Therapy. In: Cell reports 29 (1), 135-150.e9. DOI: 10.1016/j.celrep.2019.08.068.

Fante, Matthias A.; **Decking, Sonja-Maria**; Bruss, Christina; Schreml, Stephan; Siska, Peter J.; Kreutz, Marina; Renner, Kathrin (2021): Heat-Inactivation of Human Serum Destroys C1 Inhibitor, Pro-motes Immune Complex Formation, and Improves Human T Cell Function. In: IJMS 22 (5), S. 2646. DOI: 10.3390/ijms22052646.

Siska, Peter J.; **Decking, Sonja-Maria**; Babl, Nathalie; Matos, Carina; Bruss, Christina; Singer, Katrin; Klitzke, Jana; Schön, Marian; Simeth, Jakob; Köstler, Josef; Siegmund, Heiko; Ugele, Ines; Paulus, Michael; Dietl, Alexander; Kolodova, Kristina; Steines, Louisa; Freitag, Katharina; Peuker, Alice; Schönhammer, Gabriele; Raithel, Johanna; Graf, Bernhard; Geismann, Florian; Lubnow, Matthias; Mack, Matthias; Hau, Peter; Bohr, Christopher; Burkhardt, Ralph; Gessner, Andre; Salzberger, Bernd; Wagner, Ralf; Hanses, Frank; Hitzenbichler, Florian; Heudobler, Daniel; Lüke, Florian; Pukrop, Tobias; Herr, Wolfgang; Wolff, Daniel; Spang, Rainer; Poeck, Hendrik; Hoffmann, Petra; Jantsch, Jonathan; Brochhausen, Christoph; Lunz, Dirk; Rehli, Michael; Kreutz, Marina; Renner, Kathrin (2021): Metabolic imbalance of T cells in COVID-19 is hallmarked by basigin and mitigated by dexamethasone. In: *The Journal of clinical investigation* 131 (22). DOI: 10.1172/JCI148225.

Hofbauer, Joshua; Hauck, Andreas; Matos, Carina; **Decking, Sonja-Maria**; Rechenmacher, Michael; Schulz, Christian; Regotta, Sabine; Mickler, Marion; Haferkamp, Sebastian; Herr, Wolfgang; Kreutz, Marina; Schnell, Annette (2021): Predictive Myeloid Subsets and Metabolic Markers in Immunotherapy. (Submitted)

Matos, Carina; Peter, Katrin; Weich, Laura; Peuker, Alice; Schoenhammer, Gabriele; Roider, Tobias; Ghimire, Sakhila; Babl, Nathalie; **Decking, Sonja-Maria**; Hammon, Kathrin; Herr, Wolfgang; Stark, Klaus; Heid, Iris M; Renner, Kathrin; Holler, Ernst; Kreutz, Marina (2021): Anti-thymocyte globulin treatment augments 1,25-Dihydroxyvitamin D3 serum levels in patients undergoing hematopoietic stem cell transplantation. In: *Frontiers in immunology*. (Submitted)

Acknowledgement

Ich möchte mich herzlich bei allen Personen bedanken, dich mich bei der Anfertigung dieser Arbeit begleitet und unterstützt haben.

An erster Stelle geht der Dank natürlich an **Prof. Marina Kreutz** und **PD Kathrin Renner-Sattler**. Als ich am Ende meines Studiums bei euch im Büro saß, war ich mir sehr sicher, dass ich nach meinem Masterabschluss nie wieder etwas mit Forschung zu tun haben möchte. Ihr habt es geschafft, meine Begeisterung und Faszination für die Wissenschaft neu zu wecken. Vielen Dank für euer Vertrauen, eure Geduld und die Zeit, die ihr in meine Betreuung investiert habt. Ich konnte bei euch nicht nur fachlich, sondern auch persönlich wachsen und würde die Entscheidung für eine Promotion unter eurer Betreuung jederzeit wieder treffen.

Frau **PD Dr. Friederike Berberich-Siebelt** und Herrn **Prof. Richard Warth** danke ich für Übernahme de Mentorats meiner Doktorarbeit und die zahlreichen konstruktiven Ratschläge im Rahmen meiner ‚Research Reports'.

Vielen Dank an **Prof. Philipp Beckhove** und **Prof. Wolfgang Herr**, die die Anfertigung dieser Dissertation am Regensburger Zentrum für Interventionelle Immunologie im Rahmen einer klinischen Kooperationsgruppe mit der Inneren Medizin III des Universitätsklinikums Regensburg ermöglicht haben.

Ein großer Dank geht an **Prof. Dr. Simone Thomas** und ihre Arbeitsgruppe, die uns bei unseren ersten Gehversuchen mit der retroviralen Transduktion von humanen T Zellen unterstützt haben. Vielen Dank, **Carina, Regina** und **Kathrin**, für jedes Mal DNA ausleihen und eure Geduld beim Beantworten meiner zahlreichen Fragen.

Weiterhin geht ein großer Dank an **Prof. Markus Feuerer**, **Dr. Sebastian Bittner** und **Brigitte Ruhland** für die Unterstützung bei der Etablierung der Transduktion von murinen T Zellen.

PD Dr. Petra Hoffmann danke ich für ihre Unterstützung bei der Etablierung der Sort-Strategie und für ihre Ratschläge in Sachen FACS. Ein großes Danke gilt darüber hinaus noch dem Team der RCI FACS Core Facility, **Irina**, **Rüdiger** und **Jaqui**, für die am Sorter verbrachten Stunden.

Vielen Dank an **PD Dr. Katja Dettmer-Wilde** und **Prof. Peter Öfner** für die Messung, Auswertung und Hilfestellung bei der Interpretation der Metabolomics-Experimente.

Danke an **Prof. Michael Rehli**, **Dr. Claudia Gebhard**, **Dr. Nicholas Strieder** und dem gesamten Team der NGS Core Facility für die Unterstützung bei der Durchführung und Auswertung der RNAseq Experimente. Vielen Dank, **Johanna** und **Hanna**, nicht nur für die

praktische Arbeit im Labor, sondern auch für angenehme Atmosphäre und die vielen (schönen) Stunden im H1 und im D5.

Vielen Dank auch an alle Bewohner der (ehemaligen) „Baracke H1“ für den besonderen Zusammenhalt.

Ein herzlicher Dank geht an alle aktuellen und ehemaligen Mitglieder der AG Kreutz, die mich auf diesem Weg begleitet haben. Ein Team mit einem besseren Zusammenhalt und tollerer Atmosphäre hätte ich mir nicht wünschen können.

Danke, **Alice**, für alle ELISAs, FACS Färbungen und sonstige Arbeiten, bei denen du mich immer wieder unterstützt hast, und für deinen unendlichen Erfahrungsschatz.

Thank you, **Carina**, for always having a helping hand, an open ear for every small and big problem and for your advice in so many FACS and personal questions. And for sharing coffee and cookies in difficult times!

Vielen Dank liebe **Moni**, für dein Engagement, deine unglaublich liebevolle Art, dein Einfühlungsvermögen, dein Verständnis und deine bedingungslose Hilfsbereitschaft.

Liebe **Tina**, vielen Dank für alles, was ich von dir lernen durfte, für jede Unterstützung und deine absolute Hilfsbereitschaft.

Danke an **Marcus**, der immer seine Hilfe angeboten hat, und an **Peter**, für die hilfreichen Ratschläge im Laborseminar.

Ein besonderer Dank geht an **Gabriele Schönhammer** und **Nathalie Babl**.

Gabi, du hast mir mit deiner offenen und liebevollen Art den Start in der AG Kreutz wirklich leicht gemacht. Vielen Dank für deine Geduld, deine Unterstützung mit der Nemesis aller Zellkulturen, viele lustige Stunden an der Sterilbank, die ungezählten Zymogramme und PCR-Platten, so manchen gewaschenen Western-Blot und auch die ruhigen Stunden mit vertrauensvollen Gesprächen. Und auch für den ein oder anderen liebevollen Stups in die richtige Richtung…

Dir, liebe **Nathalie**, möchte ich für die unzähligen, zum Teil recht erheiternden (und mehr oder weniger chaotischen) Situationen danken – ob jetzt im Labor während einer gemeinsamen Spätschicht oder beim Kuchen backen, es gab eigentlich immer irgendwas, worüber wir gemeinsam lachen konnten. Ich bin unendlich froh, dass du dich damals zum Bleiben entschieden hast und möchte unsere gemeinsame Zeit und vor allem die daraus gewachsene Freundschaft auf keinen Fall mehr missen. Vielen Dank für alles, was ich von und mit dir lernen durfte, sei es nun die Entwicklung eines gewissen Selbstbewusstseins oder die Pflege von

Mäusen oder Sphäroiden. Ich hätte mir keine bessere Mitdoktorandin wünschen können und hoffe inständig, dass wir auch in 10 Jahren noch als Freunde gemeinsam auf diese Zeit zurückblicken!

Zu guter Letzt möchte ich meiner Familie danken. Meinen Eltern, **Hildegard** und **Lutz Decking**, die mich in jeder erdenklichen Weise unterstützt haben. Sie haben mich stets motiviert, mich angetrieben und bei Problemen jeglicher Art stets ein offenes Ohr gehabt, auch wenn uns hunderte Kilometer trennten. Und meinem Partner, **Kilian Paede**, der stets an meiner Seite stand. Vielen Dank fürs Bestärken, Aufmuntern, bisweilen auch Aushalten und die vielen schönen Stunden – mögen ihnen noch viel Schönere folgen!